

# **Determination of toxic elements, rare earth elements and radionuclides in coal fly ash, products and waste**

By

Chuks Paul Eze

Department of Chemistry, University of the Western Cape



Dr. O. O. Fatoba

A thesis submitted in fulfilment of the requirements for the degree of  
Doctor of Philosophy in Chemistry in the Department of Chemistry  
Faculty of Science  
University of the Western Cape

December 2014

## Abstract

---

Coal fly ash has been studied extensively to understand the environmental impacts associated with its disposal, management and reuse. Although several beneficiation processes have been proposed, there has been little or no emphasis on the environmental safety of such processes, products and wastes. Elemental analysis has revealed that toxic elements and radionuclides are present in coal fly ash. Rare earth elements (REE) such as La, Ce and Y are also present in significant amounts in coal fly ash. The aims of this study were to determine the total elemental composition of coal fly ash using different analytical techniques; to validate the application potentials of fly ash beneficiation processes in terms of their environmental safety; and to valorise coal fly ash with a view of recovering REE either by concentrating or leaching the REE in the coal fly ash, products or waste from the beneficiation processes. The beneficiation processes studied were treatment of acid mine drainage (AMD) with fly ash; and the synthesis of geopolymer from fly ash. The fresh fly ash sample used in this study was collected directly from the hoppers at Matla power station and the AMD sample was collected from Carletonville goldmine. A total of 54 major, trace and REE were accurately determined in the ash using different analytical techniques. It was shown that the elemental content of Matla fly ash was of the same order as the SRM NIST coal fly ash 1633b. The comparative study of the four analytical techniques established that ENAA can accurately determine the major, minor and trace elements; that XRF is best suited for the determination of the major and minor elements, whilst the LA ICP-MS is reliable for trace elements determination. The solid residue (AMD/FA) resulting from the AMD interaction with fly ash was characterized with fly ash and the results compared. The results revealed that the amounts of La ( $141.09 \pm 3.85$  mg/kg), Ce ( $27.45 \pm 2.04$  mg/kg), and Nd ( $63.73 \pm 0.05$  mg/kg) in AMD/FA residue was considerably higher than their average abundance in the earth crust that varies from 66 mg/kg in Ce and 40 mg/kg in Nd to 35 mg/kg in La. The results also showed that the AMD/FA residue contained As ( $11.39 \pm 1.21$  mg/kg), Cd ( $3.77 \pm 0.02$  mg/kg), Cr ( $72.43 \pm 1.27$  mg/kg), Hg ( $10.50 \pm 0.85$  mg/kg), Ni ( $124.15 \pm 1.6$  mg/kg) and Pb ( $22.46 \pm 1.43$  mg/kg) which are potentially harmful if leached in to the environment in excessive amounts. The activity concentrations of  $^{238}\text{U}$  and  $^{232}\text{Th}$  in Matla fly ash

## Abstract

---

were ( $140.1 \pm 5.2$  Bq/L and  $163.3 \pm 1.1$  Bq/L, respectively) while, in the AMD/FA residue the activity concentrations of  $^{238}\text{U}$  and  $^{232}\text{Th}$  were ( $357.8 \pm 21.2$  Bq/L and  $173.0 \pm 2.6$  Bq/L, respectively). These values were higher than the world-wide average concentrations. Analysis of DIN-S4 leachate of Matla fly ash and AMD/FA, revealed that Pb, Mo, Ba, U, Al, Ca, Mg, Na, K, Hg, As, Pb, Fe, Cr, Co, Sr, U, Zn and Si were mobile in Matla fly ash and AMD/FA residue at L/S 10:1 and that higher amounts of U (0.68 %) leached from the AMD/FA residue at L/S ratio 10:1 than from Matla fly ash (0.10 %). The presence of these toxic elements in AMD/FA residue raises concern over its safety with regard to its disposal. The Matla fly ash and synthesized geopolymer were characterised and the results were compared. The gamma spectrometric analysis revealed that the activity of radionuclides:  $^{238}\text{U}$  ( $93.7 \pm 9.7$  Bq/L)  $^{226}\text{Ra}$  ( $92.5 \pm 2.3$  Bq/L)  $^{232}\text{Th}$  ( $108.4 \pm 1.0$  Bq/L)  $^{40}\text{K}$  ( $120.5 \pm 3.3$  Bq/L) in the synthesised geopolymer were lower than that of the Matla fly ash  $^{238}\text{U}$  ( $140.1 \pm 5.2$  Bq/L)  $^{226}\text{Ra}$  ( $138.2 \pm 2$  Bq/L)  $^{232}\text{Th}$  ( $163.3 \pm 1.1$  Bq/L)  $^{40}\text{K}$  ( $175.0 \pm 3.5$  Bq/L) and meets the requirements as a building material in terms of radioactivity. The DIN-S4 leaching test showed that Zn ( $0.10 \pm 0.003$  mg/kg), V ( $0.15 \pm 0.0012$  mg/kg), Ni ( $0.02 \pm 0.002$  mg/kg), Pb ( $0.014 \pm 0.0002$  mg/kg), and Hg ( $0.024 \pm 0.004$  mg/kg) were leached from the synthesised geopolymer. In comparison, the following amounts of Zn ( $0.03 \pm 0.002$  mg/kg), V ( $0.03 \pm 0.0009$  mg/kg), Ni ( $0.02 \pm 0.0018$  mg/kg), and Pb ( $0.002 \pm 0.0001$  mg/kg), were leached from Matla fly ash. This showed that geopolymerisation had no effect on the mobility of these elements. Although elements such as Fe ( $9.76 \pm 0.19$  mg/kg), Mn ( $4.18 \pm 0.08$  mg/kg), As ( $0.069 \pm 0.009$  mg/kg) and the radionuclide U ( $0.01 \pm 0.0025$  mg/kg) were detected in Matla fly ash leachates they were below detection limit in the synthesised geopolymer leachate indicating that these species were immobilized in the synthesised geopolymer. The leachates and solid residues from the sequential leaching of the non-magnetic fraction of Matla fly ash with 8 M NaOH, 5 M  $\text{H}_2\text{SO}_4$ , 3 M HCl and 7 M  $\text{HNO}_3$  were also analysed to determine if the major elements (Si, Al, Fe, Ca, Mg, Na and K) were extracted and if the REE were concentrating up in the solid residues or leachates. The results revealed that  $36.99 \pm 4.80$  %,  $39.45 \pm 5.06$  %,  $53.02 \pm 0.84$  %, and  $45.08 \pm 0.03$  % of Si were

## Abstract

---

retained in the non-magnetic fraction of the Matla fly ash residue after leaching with 8 M NaOH, 5 M H<sub>2</sub>SO<sub>4</sub>, 3 M HCl, and 7 M HNO<sub>3</sub>, respectively. For Al, the residues from the four leaching steps were 27.95 ± 0.84 %; 22.61 ± 1.71 %; 27.42 ± 0.95 % and 26.05 ± 0.03 %, respectively. The leaching efficiency of Si and Al with respect to each of the reagents can be ordered as: NaOH>H<sub>2</sub>SO<sub>4</sub>>HNO<sub>3</sub>>HCl and H<sub>2</sub>SO<sub>4</sub>>HNO<sub>3</sub>>HCl>NaOH, respectively. The ICP=MS analyses of the leachates obtained after the sequential leaching of the non-magnetic fraction of Matla fly ash revealed that HCl leached 85.54 % of Yb, 79.35 % of Er, 78.09 % of Ce, 52.60 % of La, 54.17 % of Pr, 49.73 % of Eu, 41.03 % of Nd and 38.47 %. For the REE the leaching efficiency with respect to each of the reagents can be ordered as: HCl >H<sub>2</sub>SO<sub>4</sub>>HNO<sub>3</sub>>NaOH. This showed that the REE are better leached from the non-magnetic fraction of the Matla fly ash with acids (low pH) rather than with base (high pH). This study has proved that XRF and LA ICP-MS are reliable for the determination of the major and trace elements, respectively in fly ash and equivalent to ENAA; that the AMD/FA residue was enriched in REE, toxic elements and radionuclides which were carried over from AMD to the waste residue; that the geopolymerisation process immobilized U and that the synthesised geopolymer is safe in terms of radiological hazard to be used as construction material; finally, that REE Yb, Er, Ce, La, Pr, Eu, Nd and Tb are recoverable from fly ash.



## Keywords

---

Coal fly ash

Major and trace elements

Radionuclides

Rare earth elements

Mineralogy

Acid mine drainage

Jet loop reactor

Solid residue

Geopolymer

Leachates

Leaching behaviour

Sequential leaching



## Declaration

---

I declare that “Determination of toxic elements, rare earth elements and radionuclides in coal fly ash, products and waste” is my own work, has not been submitted before for any degree or examination in any other university, and that all the sources I have used or quoted have been indicated and acknowledged as complete references.

Full Name: Chuks Paul Eze

December 2014



Signed.....



## Dedication

---

To Chukwuma, Isioma and Chukwuwatem, for inspiring me



## Acknowledgements

---

I would like to express my special appreciation and thanks to my supervisor Professor Leslie Petrik, you have been a tremendous mentor to me. I would like to thank you for encouraging my studies and for allowing me to grow as a research scientist. Your advice on both research as well as on other aspects of life have been priceless. I would also like to thank my co-supervisor, Dr Olanrewaju Fatoba for your contributions, support, assistance and guidance to this work.

I would like to acknowledge Dr P.P. Maleka, Research Scientist in the Environmental Radioactivity Laboratory at iThemba Labs and Prof R. Lindsay in the Physics Department, University of the Western Cape for the vast knowledge they shared with me in terms of radioactivity analysis. I would also like to acknowledge Professor Marina Frontasyeva and Professor Alexander Nechaev of the Joint Institute for Nuclear Research (JINR), Dubna, Russia for their advice and support on Instrumental epithermal neutron activation analysis (ENAA). I am grateful to Ms. I. Wells for the IC and ICP analysis and Dr Olushola Ayanda for his advice and support on this project. I am also grateful to A. Abbott, V. Kellerman and my colleagues at the Environmental Nanoscience Group for their assistance, encouragement, advice and suggestions for my work. I would like to express my gratitude to the South African National Research Fund (NRF) and Department of Science and technology (DST) for their financial assistance.

Special thanks goes to my siblings for their prayers, advice, assistance, encouragement and support; my friends that have become my brothers and sisters; for all their support; and my wife and children for inspiring me. Finally I thank my God, my good Father, for letting me through all the difficulties. I have experienced His love and guidance everyday which made it possible for me to complete this study. I will keep on trusting and believing you for my future. Thank you, Lord.

## List of Abbreviations

---

ASTM	American Society for Testing and Materials
EC	Electrical Conductivity
TDS	Total Dissolved Solids
IC	Ion Chromatography
ENAA	Epithermal neutron activation analysis
FT-IR	Fourier-transform infrared spectroscopy
ICP-OES	Inductively Coupled Plasma-Optical Emission Spectrometry
ICP-MS	Inductively Coupled Plasma- mass Spectrometry
LA ICP-MS	Laser ablation inductively coupled plasma - mass spectrometer
XRF	X-ray Fluorescence
XRD	X-ray Diffraction
HR-SEM/EDS	High resolution scanning electron microscope and energy dispersive X-ray spectrometry (HR-SEM/EDS)
LOI	Loss on ignition
SRM	Standard reference material
AMD	Acid mine drainage
REE	Rare earth elements
AMD/FA	Acid mine drainage/fly ash
NORMS	Naturally occurring radionuclides
TWQR	Target water quality range
WHO	World Health Organisation
JINR	Joint Institute for Nuclear Research

# Table of Contents

---

## Chapter One: Introduction

<b>1</b>	<b>Introduction.....</b>	<b>1</b>
1.1	Background .....	1
1.2	Problem statement .....	6
1.3	Aim and objectives .....	7
1.4	Research Question.....	8
1.5	Research Approach.....	9
1.6	Scope and delimitation .....	10
1.7	Outline of the subsequent chapters.....	11

## Chapter Two: Literature review

<b>2</b>	<b>Introduction.....</b>	<b>14</b>
2.1	Fly ash classification .....	15
2.2	Properties of fly ash.....	17
2.2.1	Fly Ash Morphology.....	17
2.2.2	Particle Size Distribution and Surface Area.....	19
2.3	Chemical properties of fly ash.....	20
2.3.1	Chemical composition of fly ash .....	20
2.4	Mineralogy of fly ash .....	30
2.5	The pH and of chemistry fly ash .....	32
2.6	Leaching Process of Fly Ash.....	33
2.7	Mobility of Species in Fly Ash.....	37
2.8	Disposal and Environmental Effect of Fly ash.....	39
2.9	Beneficial Application of Fly Ash.....	40
2.9.1	Cement and Construction Industry .....	40
2.9.2	Removal of Heavy Metals in Water Treatment .....	41
2.9.3	Soil Amendment .....	42

## Table of Contents

---

2.9.4	Synthesis of zeolites .....	43
2.10	Acid mine drainage (AMD).....	44
2.10.1	Treatment technologies of acid mine drainage .....	46
2.10.2	Treatment of acid mine drainage with coal fly ash .....	49
2.11	Geopolymer .....	50
2.11.1	Geopolymerisation .....	52
2.11.2	Properties and applications of geopolymers .....	53
2.12	Extraction of metals from coal fly ash .....	54
2.12.1	Recovery of rare earth elements from coal fly ash .....	56
2.13	Determination of the elemental composition of coal fly ash.....	57
2.13.1	X-ray Fluorescence (XRF).....	58
2.13.2	Inductively coupled plasma - optical emission spectrometer (ICP-OES) .....	59
2.13.3	Laser Ablation Inductively Coupled Plasma Mass Spectrometry (LA-ICP-MS).....	59
2.13.4	Neutron activation analysis (NAA).....	60
2.13.5	Matrix effect.....	61
2.13.6	Accuracy and precision .....	62
2.14	Characterisation techniques.....	63
2.14.1	Mineralogical analysis (XRD) .....	64
2.14.2	Fourier Transform Infrared Spectroscopy (FT-IR).....	64
2.14.3	Morphological Analysis (SEM).....	66
2.14.4	Gamma ray spectrometry .....	67
2.15	Ion Chromatography (IC) .....	68
2.16	Conclusion.....	70

## Table of Contents

---

### Chapter Three: Methodology

<b>3</b>	Introduction.....	<b>73</b>
3.1	Sampling of Fly ash from Matla power station .....	73
3.2	Sampling of AMD from Carletonville goldmine .....	73
3.3	Storage of Samples .....	74
3.4	Characterisation of coal fly ash .....	74
3.4.1	Epithermal Neutron Activation Analysis .....	75
3.4.2	X-Ray Fluorescence Spectroscopy .....	75
3.4.3	Inductively-Coupled Plasma-Optical Emission Spectroscopy.....	76
3.4.4	Laser Ablation Inductively Coupled Plasma-Mass Spectrometry ..	76
3.4.5	Gamma ray spectrometry .....	77
3.4.6	Fourier Transform Infrared Spectroscopy .....	78
3.4.7	Mineralogical characterization by X-ray Diffraction Spectroscopy	78
3.4.8	Scanning Electron Microscopy .....	79
3.5	Characterization of mine water .....	79
3.5.1	Ion chromatography (IC) .....	80
3.5.2	pH, electrical conductivity and total dissolved solids measurements 80	
3.6	Methodology .....	81
3.6.1	DIN-S4 Leaching Test .....	82
3.6.2	Treatment of AMD with fly ash.....	83
3.6.3	Standardised synthesis of foamed geopolymers .....	84
3.6.4	Sequential extraction of major components of coal fly ash .....	85

### Chapter Four: Comparison of analytical techniques

<b>4</b>	Introduction.....	<b>90</b>
4.1	ENAA:Quality Assurance .....	90



## Table of Contents

---

4.2	Major and minor elements.....	94
4.3	Trace elements.....	97
4.4	REE .....	99
4.5	Summary .....	101

### **Chapter Five: Applications of fly ash for AMD treatment**

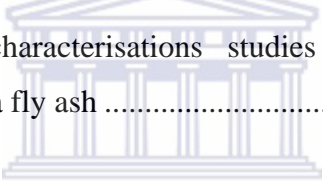
<b>5</b>	<b>Introduction.....</b>	<b>103</b>
5.1	Overview .....	104
5.2	Materials and methods.....	106
5.3	Results and discussion of the characterisation of the Carletonville goldmine AMD before and after treatment with Matla fly ash.....	107
5.4	Results of the characterisation of AMD/FA residue .....	110
5.4.1	FT-IR analysis of geopolymer from Matla fly ash.....	110
5.4.2	Morphological analysis .....	112
5.4.3	Mineralogical analysis .....	116
5.4.4	Bulk Chemical Composition Analysis .....	118
5.5	Radioactivity .....	128
5.5.1	Activity of Carletonville goldmine water .....	129
5.5.2	Activity of Matla fly ash and AMD/FA residue .....	131
5.6	DIN-S4 Leaching test.....	132
5.6.1	pH and EC.....	133
5.6.2	Results of DIN-S4 Leachate.....	135
5.7	Summary of characterisation of the Matla fly ash Carletonville AMD before and after treatment and AMD/FA residue .....	139

### **Chapter Six: Geopolymer from fly ash**

<b>6</b>	<b>Introduction.....</b>	<b>143</b>
----------	--------------------------	------------

## Table of Contents

---

6.1	Overview .....	144
6.2	Materials and methods.....	145
6.3	Results of the characterisation of geopolymer .....	146
6.3.1	FT-IR analysis of geopolymer from Matla fly ash.....	146
6.3.2	Morphological analysis of geopolymer from Matla fly ash.....	148
6.3.3	Mineralogical analysis of geopolymer from Matla fly ash .....	151
6.3.4	Bulk Chemical Composition Analysis.....	153
6.4	Activity of the synthesised geopolymer .....	159
6.5	Leaching .....	161
6.5.1	pH and EC.....	161
6.5.2	Results of DIN-S4 Leachate.....	164
6.6	Summary of characterisations studies of the foamed geopolymer synthesised from Matla fly ash .....	168
		
<b>Chapter Seven: Possibility of Rare earth recovery from fly ash</b>		
<b>7</b>	<b>Introduction.....</b>	<b>171</b>
7.1	Overview .....	171
7.2	Materials and methods.....	173
7.3	The results of the magnetic separation of Fe from Matla fly ash.....	174
7.3.1	Elemental composition of the fractions produced during the extraction of iron oxide from Matla fly ash .....	175
7.3.2	REE composition of Matla fly ash, the non-magnetic fraction and magnetic fraction.....	176
7.3.3	Mineralogical analysis of Matla fly ash, the magnetic and non-magnetic fractions .....	178
7.4	The results of the sequential leaching of non-magnetic fraction of Matla fly ash.....	179

## Table of Contents

---

7.4.1	Composition of the major element in the solid residue produced during the sequential leaching of the non-magnetic fraction of Matla fly ash	179
7.4.2	Elemental composition of the REE in the solid residue produced during the sequential leaching of the non-magnetic fraction of Matla fly ash	182
7.4.3	Elemental composition of the REE in the leachate (supernatant) produced during the sequential leaching of the non-magnetic fraction of Matla fly ash.....	185
7.4.4	Mineralogical analysis of the solid residues from the leaching of the non-magnetic fraction of Matla fly .....	189
7.5	Summary of the sequential leaching studies of the non-magnetic fraction of Matla fly ash .....	191
<b>Chapter Eight: Conclusions and Recommendation</b>		
8	Introduction.....	<b>193</b>
8.1	Overview .....	193
8.2	Summary on the elemental composition of Matla fly ash using nuclear and related analytical techniques .....	193
8.3	Summary of the applications of fly ash for AMD treatment.....	194
8.4	Summary of the application of Matla fly ash in the synthesis of foamed geopolymer.....	197
8.5	Summary of the sequential leaching of REE from Matla fly ash.....	199
8.6	Significance of the study .....	201
8.7	Recommendations .....	202

## List of Figures

---

Figure 3.1: Map showing the mine water and FA sampling sites	74
Figure 3.2: Schematic of the sequential extraction procedure	86
Figure 4.1: Concentrations of major elements in Matla fly ash determined by ENAA, ICP- OES, and XRF [number of determinations = 3]	95
Figure 4.2: Concentrations of trace elements in Matla fly ash determined by ENAA, ICP- OES, LA ICP – MS, and XRF [number of determinations = 3]	98
Figure 4.3: Concentrations of REE in Matla fly ash determined by ENAA, LA ICP – MS, ICP- OES, and XRF [number of determinations = 3]	100
Figure 5.1: FT-IR spectra of the Matla fly ash and the fly ash/ AMD residue	111
Figure 5.2: SEM Micrograph of Matla fly ash and AMD/FA residue showing the area chosen for EDS analysis	113
Figure 5.3: XRD patterns for Matla fly ash sample and the AMD/FA residue [G = Gypsum; E = Etringitte; H = Hematite; M = mullite; Q = Quartz; L = Lime]	116
Figure 5.4: Concentrations of major elements in Matla fly ash (MFA), AMD fly ash residue (AMD/FA) determined by XRF spectroscopy [number of determinations = 3]	120
Figure 5.5: Concentrations of trace elements in Matla fly ash (MFA) and AMD fly ash residue (AMD/FA) as determined by LA ICP-MS [number of determinations for LA ICP-MS = 3]	124
Figure 5.6: Concentrations of REE in Matla fly ash (MFA) and AMD/FA residue (AMD/FA) determined by LA ICP-MS [number of determinations for LA ICP-MS n = 3]	127
Figure 5.7: pH of Matla fly ash, AMD/FA residue and the synthesised geopolymer using different L/S ratios [number of determination = 3]	133
Figure 5.8: EC profile of Matla fly ash and AMD/FA residue using different L/S ratios [number of determination = 3]	134
Figure 6.1: FTIR spectra of the Matla fly ash compared to the synthesised geopolymer	146
Figure 6.2: SEM Micrograph of Matla ash and the synthesised geopolymer showing the area chosen for EDS analysis	149
Figure 6.3: XRD patterns for Matla fly ash sample and the synthesised geopolymer [M = Mullite; Q = Quartz; S = Sodalite; Ha = Halite; L= Lime; H = Hematite]	151

## List of Figures

---

Figure 6.4: Concentrations of major elements in Matla fly ash and the synthesised geopolymer determined by XRF spectroscopy [number of determinations = 3]	154
Figure 6.5: Concentrations of trace elements in Matla fly ash and the synthesised geopolymer determined by LA ICP-MS [number of determinations = 3].....	156
Figure 6.6: Concentrations of REE in Matla fly ash) and the synthesised geopolymer determined by LA ICP-MS [number of determinations = 3].....	158
Figure 6.7: pH of leachates of Matla fly ash and the synthesised geopolymer using different L/S ratios [number of determinations = 3] .....	162
Figure 6.8: EC profile of leachates of Matla fly ash and the synthesised geopolymer using different L/S ratios [number of determinations = 3] .....	163
Figure 7.1: XRD patterns of the extracted Magnetic and non-magnetic fraction and Matla fly ash. (H = hematite, L = lime, M = mullite, Ma = magnetite, and Q = quartz.....	178
Figure 7.2: Percentage composition of the major components major components that remained in the solid residue after the sequential leaching the non-magnetic fraction of Matla fly ash with NaOH, H <sub>2</sub> SO <sub>4</sub> , HCL and HNO <sub>3</sub> .....	180
Figure 7.3: REE composition (mg/kg) in the solid residue after the sequential leaching the non-magnetic fraction of Matla fly ash with NaOH, H <sub>2</sub> SO <sub>4</sub> , HCL and HNO <sub>3</sub> .....	183
Figure 7.4: Elemental composition of the REE in the leachate (supernatant) produced during the sequential leaching of the non-magnetic fraction of Matla fly after the sequential leaching with NaOH, H <sub>2</sub> SO <sub>4</sub> , HCL and HNO <sub>3</sub> .....	186
Figure 7.5: XRD patterns of the extracted Magnetic and non-magnetic fraction and Matla fly ash. (G = gypsum, L = lime, M = mullite, Mg = magnetite, Q = quartz and S = sodalite).....	189

## List of Tables

---

Table 2:1: ASTM standards classification of fly ash (ASTM C 618, 1993) .....	16
Table 2:2: Normal range of chemical composition for fly ash produced from different coal ranks (expressed as weight %) ( <a href="http://cementconsultant.org/flyash.pdf">http://cementconsultant.org/flyash.pdf</a> ) .....	22
Table 2:3: Average trace element composition for fly ash (El-Mogazi et al., 1988) .....	23
Table 2:4: Comparative levels of radioactivity in fly ash and coal (Baxter, M. 1996) .....	26
Table 2:5: The running costs and possible income that can be generated from the products of the various technology proposed by the Inter-ministerial Committee on acid mine drainage (Coetzee et al., 2010).....	49
Table 3:1: XRD operating parameters .....	78
Table 3:2: Composition of the Dionex SEVEN ANION certified standard .....	80
Table 3:3 List of reagents used .....	81
Table 4:1: Elemental concentration in the NIST SRM 1633b determined by ENAA in Dubna and the certified values (NIST, 2008) .....	91
Table 4:2: Elemental concentrations in the NIST SRM 1633b (noncertified values (NIST, 2008)).....	93
Table 5:1: The physicochemical parameters of the Carletonville goldmine AMD Carletonville goldmine AMD before and after treatment with Matla fly ash (TDS and concentrations are in mg/L).....	108
Table 5:2: EDS analysis of the chosen areas (atomic %) of Matla fly ashes and AMD/FA residue.....	115
Table 5:3: Activity concentrations (Bq/l) of radionuclides found in Carletonville goldmine Water samples (n=3) .....	130
Table 5:4: Activity concentrations of radionuclides found in AMD/FA residue compared to the activity of Matla fly ash and Carletonville goldmine AMD (n=2) .....	131
Table 6:1: SEM-EDS (atomic %) of the synthesised geopolymer compared to Matla fly ash n = 3 .....	150
Table 6:2: Activity concentrations of radionuclides found in the synthesised geopolymer compared to the activity of Matla fly ash .....	159

## List of Tables

---

Table 6:3: Radiological hazard indices of the synthesized geopolymer and Matla fly ash.....	160
Table 6:4: Comparison of total elemental content and amount leached out in DIN-S4 from Matla fly ash and synthesised geopolymer at L/S 10:1 (n=3).....	165
Table 6:5; Comparison of total elemental content and amount leached out in DIN-S4 from Matla fly ash and synthesised geopolymer at L/S 20:1 (n=3).....	166
Table 7:1: Major element composition of Matla fly ash, the non-magnetic fraction and magnetic fraction.....	175
Table 7:2: REE composition of Matla fly ash, the non-magnetic fraction and magnetic fraction.....	177



## Chapter 1: Introduction

### 1 Introduction

The chapter deals with the introduction to the study. The background provides a brief overview of coal fly ash; its origin, composition, properties and beneficiation in sections 1.1. Details of the problem statement, research aims and objectives, research questions, research approach and the research scope and delimitation are also presented in this chapter (sections 1.2 to 1.6). The chapter ends with a preview of the subsequent chapters in this thesis in section 1.7.

#### 1.1 Background

Coal is one of the world's major important and abundant energy sources and is mostly combusted to generate electrical power. Approximately 42 % of the world's electricity is fuelled by coal (World Energy Council, 2013). South Africa is endowed with significant coal deposits and the country's power generation depends heavily on coal combustion, which accounts for 93% of its electricity (Eberhard, 2011).

The solid materials resulting from the coal combustion process are fly ash, bottom ash, boiler slag, and flue gas desulphurization (FGD) materials. Fly ash is the bulk residue produced from the combustion of coal, and constitutes approximately 70% of the solid residue (Jala and Goyal 2006). Fly ash is a particulate matter which travels with the flue gas that must be removed prior to releasing it via the stack and into the atmosphere, to avoid pollution. The fly ash is removed from the flue gas either by electrostatic precipitators or bag filters and collected in hoppers.

The properties of fly ash depend on the physical and chemical properties of the coal of origin, the coal particle size, the combustion process, and the type of ash collector used (Adriano et al., 1980). Although the chemical composition of fly ash from different sources varies in concentrations, it still consists of the same basic chemical constituents. The main constituents of fly ash are silica,



## Chapter One: Introduction

---

aluminium, iron and calcium with smaller amounts of sulphur, magnesium, alkalis, and traces of many other elements such as Co, Cd, As, Se, Zn, Mo, Pb, B, Cu and Ni (Cho et al., 2005).

Several studies on the mineral phases of fly ash show that it consists mainly of aluminosilicate glass matrix in addition to crystalline mullite and quartz as the major mineral phases (Mattigod et al., 1990). Elements such as As, Na, Mg, K, Sr, B and Mo occur as part of the crystalline phases within the aluminosilicate glass. They also exist as coatings deposited on the surfaces of the individual particles by the condensation of elements liberated from the coal into the furnace gases during combustion. The majority of the elements in fly ash have a prevailing link to some minerals and phases in the parent coal.

Fly ash disposal is of major concern globally because of the enormous quantity that is generated and the environmental issues arising from the disposal methods that are currently employed. In South Africa, millions of tons of fly ash are produced annually from the combustion of pulverized coal to generate electricity in coal-fired power plants. Fly ash is mainly disposed of by either dry or wet disposal methods. In dry disposal, the fly ash is conditioned with brine and then transported by truck, chute or conveyor to the site and disposed by constructing a dry embankment; the ash heap is then irrigated with waste water for dust suppression. In wet disposal, the fly ash is transported as slurry through pipes and disposed in impoundments that are called ash ponds or dams.

Coal fly ash is considered a highly contaminating medium because the toxic trace elements in coal are accumulated in higher concentrations in the combustion by product (Hansen et al., 2002; Petrik et al., 2003; Gitari et al., 2008). Thus, various environmental risks are associated with fly ash disposal; these include air pollution, loss of arable land, surface and ground water contamination due to the leaching and mobilization of non-degradable toxic metals, and other chemical species from the ash dump by rainfall or groundwater (Dellantonio et al., 2008; Senapati, 2011; Neupane and Donahoe, 2013).

## Chapter One: Introduction

---

In spite of the numerous environmental problems related with coal combustion, it will continue to be a major source of electrical power generation for many years to come. Hence in the management of this combustion by-product the focus is not only on the prevention of environmental pollution, but also on methods that can be used to utilize the fly ash so that it can become a valuable source of raw material. This can be achieved through precisely defining and controlling physical and chemical characteristics of fly ash; so that a uniform and reproducible material can be supplied for reuse (Foner et al., 1998) without generating a secondary hazard.

Some of the valuable uses of fly ash are in the making of cement or concrete due to its cementitious and pozzolanic properties which improves the workability, durability and strength in hardened concrete. The use of fly ash has been proposed in the treatment of acid mine drainage (AMD) because it contains relative high concentrations of CaO, which is considered as a liming agent to neutralise acid mine drainage (Somerset et al., 2005). Another proposed beneficial use of fly ash is in agriculture as a soil amendment, in composting and as a source of nutrients for plants because it contains almost all the necessary plant nutrients (Kishor et al., 2010). Ash is also used as a low-cost adsorbent for the removal of heavy metal such as Ni, Cr, Pb, As, Cu, Cd and Hg from wastewaters due to the high surface area of the fly ash particles (Cetin and Pehlivan, 2006). Furthermore fly ash can be considered as a cheap source material in the synthesis of zeolites and geopolymers because of its high aluminosilicate content (Álvarez-Ayuso et al., 2008).

Coal fly ash has been studied extensively to understand the environmental impacts associated with its disposal, management and reuse (Adriano et al., 1980; Asokan et al., 2005; Sushil and Batra., 2006 and Blissett, and. Rowson, 2012). Research of coal fly ash compositions has revealed that toxic elements (Davison et al., 1974; McNally et al, 2012) and naturally occurring radionuclides (NORMS) (Parami et al, 2010) are present in coal fly ash. Toxic elements in fly ash include

## Chapter One: Introduction

---

arsenic (As), chromium (Cr), cadmium (Cd), lead (Pb) and mercury (Hg) while the NORMS include uranium ( $^{238}\text{U}$ ), thorium ( $^{232}\text{Th}$ ), and their numerous decay products, including radium ( $^{226}\text{Ra}$ ) and also potassium ( $^{40}\text{K}$ ). The presence of these toxic elements in fly ash raises concern over its safety with regard to its disposal and beneficiations because these elements are likely to cause harmful effects on the environment (Bailey et al., 1998). Pb, As, Cr and Hg are the elements usually regard as the most toxic to humans and animals due to their neurotoxic and carcinogenic actions. Various health effects are linked to the exposure to these elements even at low concentrations.

Also, characterisation of coal fly ash (Fatoba, 2008; Akinyemi, 2010; Smolka-Danielowska, 2010; Eze, 2011; Kashiwakura et al, 2013), has shown that rare earth elements (REE) such as lanthanum (La), cerium (Ce), neodymium (Nd) and yttrium (Y) are present in this solid waste. REE are a set of seventeen chemical elements in the periodic table. These are the fifteen lanthanides together with Sc and Y. Scandium and yttrium are considered as REE because they usually occur in the same ore deposits as the lanthanides and exhibit similar chemical properties (Kempe and Wolf, 2006; Makreski et al., 2011). The unsaturated 4f electronic structure of REE gives them unique physical and chemical properties that have led to the increase in their demand as a result of their growing importance in advanced technology (Kubota et al., 2001; Jiang et al., 2006).

REE have been widely used in automotive catalytic converters, fluid cracking catalysts in petroleum refining, phosphors in colour television and flat panel displays, (cell phones, portable DVDs, and laptops), permanent magnets and rechargeable batteries for hybrid and electric vehicles, and generators for wind turbines, and numerous medical devices. REE are also used in jet fighter engines, missile guidance systems, antimissile defence, and space-based satellites and communication systems. China is currently the dominant producer of REE and is believed to be responsible for over 97 % of the world mine production on a rare earth oxide equivalent basis (USGS, 2012). Other countries with notable production in 2009 were: Brazil, India, Kyrgyzstan and Malaysia. Minor

## Chapter One: Introduction

---

production may have occurred in Indonesia, Commonwealth of Independent States, Nigeria, North Korea and Vietnam (USGS, 2011). China is also the major consumer of REE, used mainly in manufacturing electronics products for domestic and export markets. Japan and the United States are the second and third largest consumers of rare earth materials.

Owing to their unique physical and chemical properties, REE are now of growing importance as novel materials for creating specific functions in advanced technology. But many applications are held back by the cost of these elements (Zhang et al., 2007; Uda et al., 2000). Hence, there is an ever-increasing demand for REE in the international markets, with emphasis on identifying new resources to ensure adequate supply for present and future use. Coal fly ash can be considered as a potential already mined source for extraction of REE for industrial use. The ability to extract the REE present in coal fly ash is important in terms of economic and environmental issues because the procedure can be used to produce value-added products from stored coal fly ash.

Several studies have being carried out on the beneficiation of coal fly ash by the Environmental and Nano Science research group (ENS) of the Department of Chemistry in the University of the Western Cape, South Africa in order to produce or manufacture value-added products from stored fly ash. These studies include the synthesis of zeolites (Musyoka, 2012), treatment of AMD and neutral mine drainage (NMD) (Madzivire, 2013), synthesis of foamed geopolymers (Boke et al., 2014), synthesis of nano-iron (Gilbert, 2014) and CO<sub>2</sub> sequestration (Muriithi, 2013). Extensive research of coal fly ash derived from South African power generation (Fatoba, 2008; Akinyemi, 2011; Eze, 2012; Madivire, 2013), has shown that toxic elements such as As, Cd, Cr, Pb and Se; and radionuclides such as Th, U, Ra and radio isotopes of K and Pb are present in this solid waste. Although several reuse processes of fly ash have being proposed, however there has been little or no emphasis on the environmental safety of such processes, products and wastes. This study will investigate some of the ash reuse process in order to ascertain the environmental safety of the fly ash reuse process products

and waste. This will be accomplished through accounting for the toxic elements, REE and radionuclides in coal fly ash, fly ash based products and waste. The fly ash beneficiation processes that will be examined are the treatment of AMD with fly ash, and the synthesis of geopolymer

### 1.2 Problem statement

Worldwide huge amounts of coal fly ash are generated in order to meet energy demands and about 70 % of fly ash is disposed as waste (Haynes, 2009). Currently in South Africa, Eskom generated nearly 25 million tons of fly ash annually from coal combustion, of which only 1.2 million tons was utilised beneficially (Eskom, 2013). Thus a significant amount is still disposed as waste. One way of combating the problems caused by the enormous volume of fly ash is by optimizing the uses of fly ash so that it could become a valuable raw material.

Research on the beneficiation of fly ash has industrial interest and environmental importance due to the huge amount that is generated worldwide from coal combustion in order to meet energy demands. Several reuse processes of fly ash have been proposed with little or no emphasis on the environmental safety of such processes, products and wastes. Elemental analysis of coal fly ash has revealed that it is contaminated with a range of toxic elements and radionuclides. The study of the environmental safety of fly ash reuse products and wastes is highly significant because of the toxic and potentially toxic elements that are present in coal fly ash. Hence the fly ash beneficiation processes, products and wastes or disposal sites should be investigated for the fate and ultimate location of the accumulated toxic components.

Currently, 97% of the REE used in commerce come from mines in China, about 2% from India, and about one-half percent or less each from Brazil, Malaysia, and the USA and this precarious situation does not augur well for the technological future of mankind (Gschneidner, 2011). This production monopoly of REE by China is an unreasonable and unhealthy situation that has to be changed in order

to avert a repeat of the 1978 cobalt crises due to the political unrest in Zaire (now Democratic Republic of Congo) that controlled 48% of the world cobalt supply (Alonso et al., 2012).

With the ever-increasing demand for REE and their compounds, there is a need to explore new resources to ensure sufficient supply for present and future use. Thereby reducing cost and opening up further opportunities for applications of these unique elements. REE, such as lanthanum (La), cerium (Ce), and yttrium (Y) are present in significant amounts in South African coal fly ash (Eze et al., 2014). However, there has been very little in the literature to investigate REE recovery from such secondary resources. Hence this study will attempt to develop a sequential leaching scheme and systematically leach the major elements/REE in coal fly ash in order to have a residue or leachate that is concentrated with the REE in the fly ash. This may facilitate the extraction and recovery of the REE from the residue or leachate.

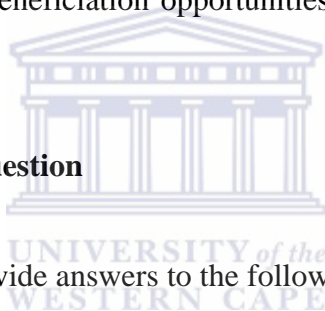
### 1.3 Aim and objectives

The aim of this study is to investigate and validate the application potentials of fly ash beneficiation processes in terms of their environmental safety. This study will determine quantitatively, the full elemental composition of coal fly ash using different analytical techniques. The study will then focus on determining hazardous element partitioning in the waste remaining after: 1) the treatment of AMD with fly ash; 2) the partitioning of hazardous elements in geopolymer synthesised from fly ash. The study also seeks to develop a sequential leaching scheme with a view of pre-concentrating or leaching of the REE in the coal fly ash.

Hence the specific objectives of this study are as follows:

- To determine the analytical technique best suited for accurate qualitative and quantitative determination of the different types of elements that are contained in coal fly ash
- To determine if any toxic or valuable elements are concentrating up in any of the ash reuse processes or products or waste residue and effluents
- To determine if these toxic elements accumulate enough during any process steps, product or waste, to constitute an environmental hazard or a valuable feedstock
- To determine if any of the processes are unsustainable because of the damage that may arise from the processes or unsafe levels of contaminants in the products
- To determine that the reuse processes are not wasting valuable resources
- To explore any beneficiation opportunities arising from the current reuse processes

### 1.4 Research Question



This study intends to provide answers to the following questions

- Which analytical techniques are best suited for determining and quantifying the different categories of elements that are contained in coal fly ash?
- Which REE, toxic heavy metals or radionuclides are present in fly ash, the fly ash reuse process or products, and in what concentrations?
- Are these elements present in sufficient concentration to warrant extraction and recovery or to cause concern in any effluent or residue generated during processing?
- Do these elements remain in the reuse process or products/waste or leach out?
- Are they highly soluble or insoluble and what is their environmental mobility?

### 1.5 Research Approach

Several experiments involving spectroscopic analysis, chemical characterizations and solvent extraction procedures were carried out in order to achieve the objectives of this research. The research was approached using the following specific techniques:

- The treatment of AMD with coal fly ash following the same procedure reported by Madzivire, 2013
- Geopolymer synthesised from coal fly ash following the protocols and optimized conditions reported by Boko et al 2014

Characterisation of the fly ash and the reuse products and all waste streams originating from reuse process was carried out to determine the physical characteristics and chemical compositions using the following methods:

- Fourier transform infrared spectroscopy (FTIR) was used to determine the molecular structure and chemical bonding of the synthesised geopolymer and fly ash samples
- Epithermal Neutron Activation Analysis (ENAA) was used in determining the total elemental composition of the fly ash
- X-ray fluorescence (XRF) analysis was used in determining the composition of the major elements in the fly ash, fly ash/AMD residue and synthesised geopolymers samples.
- X-ray Diffraction (XRD) analysis was used for the study of mineralogical phases and composition of the fly ash, fly ash/AMD residue and synthesised geopolymers samples.
- High Resolution Scanning Electron Microscope and Energy Dispersive X-ray spectrometry (HR-SEM/EDS) was used to present detailed imaging



information about the morphology and surface texture of individual particles, as well as elemental composition of the sample. It was used to characterize the morphological features of the fly ash, fly ash/AMD residue and synthesised geopolymer samples.

- Gamma spectroscopy was used to analyse for radionuclides in the geopolymers, fly ash and AMD before and after treatment. This analytical method was used to measure the radioactivity in the samples.
- The inductively coupled plasma - mass spectrometer (ICP-MS) was used to determine the concentrations of the trace elements in the AMD before and after treatment with fly ash.
- Laser ablation inductively coupled plasma - mass spectrometer (LA ICP-MS) was used to analyse for the trace elements in the fly ash, fly ash/AMD residue and synthesised geopolymers.
- Leaching test was carried out to determine the stability and leachability/solubility of the chemical species in the geopolymers.
- The leaching test that was used is the DINS-4. The method is intended to represent materials coming into contact with fresh rain water or ground water. The leaching procedure was carried out by adding to the required sample weight, a volume of deionised water to give a 10:1 ratio of water to dry sample.
- A Sequential leaching procedure was designed to extract the major components of fly ash in order to pre-concentrate or leach out the REE in the fly ash.

### 1.6 Scope and delimitation

The research utilized fly ash from Matla power station (Matla fly ash), as the base material for the beneficiation processes that were investigated. The procedures that were used in synthesising the geopolymers and in the treatment of the AMD were those recommended in previous studies carried out at the ENS research group at the Chemistry Department of the University of the Western Cape. The characterization of the fly ash beneficiation products and wastes in comparison

## Chapter One: Introduction

---

with Matla fly ash (feed stock) were therefore investigated. The leaching experiments were conducted on the solid products, waste and fly ash (feed stock) samples to determine the leachability/solubility of the toxic chemical species that could be easily released when the products or wastes get into contact with water. Furthermore the sequential extraction scheme used in this study was designed from the different extraction experiments that have been used in the extraction of major elements such as silicon, aluminium and iron; zeolite and hydrotalcite synthesis from coal fly ash. The limitation of this study is the inability to study all the beneficiation processes that have been conducted on fly ash by the ENS group with fly ashes from different power stations due to lack of funds and time.

### 1.7 Outline of the subsequent chapters

Besides this introductory chapter this thesis will also consist of the following chapters:

Chapter 2: Literature review

Chapter two will contain the reviews of different literature focusing on the source, physical and chemical properties, disposal, environmental impact and beneficiation of coal fly ash. The literature of REE, geopolymers and AMD was reviewed. The principles behind the analytical techniques used in this study were also reviewed.

Chapter 3: Sampling, experimental and analytical methods

The outline of sampling protocol, analytical procedures and experimental methods used in this study to address the research objectives will be presented in chapter 3. A detailed outline of the procedures used for the synthesis of foamed geopolymer from fly ash and the AMD treatment with fly ash will also be covered in this chapter. Furthermore the methods that were used in the characterisation, leaching

## Chapter One: Introduction

---

and analysis of the fly ash samples, fly ash reuse products and waste will be presented in this chapter.

### Chapter 4: Comparison of analytical techniques

Chapter 4 presents and discusses the results obtained in the elemental analysis of the Matla fly ash as. In this chapter the results are presented of ENAA, XRF, ICP-OES and LA ICP-MS analysis of the fly ash samples. The results will be discussed in order to understand the method that is best suited for determining the different categories of elements that are contained in coal fly ash.

### Chapter 5: Application of fly ash for AMD treatment

In chapter 5 the use of coal fly ash in the treatment of AMD as specified in chapter 3 will be presented and discussed. The results obtained from the characterisation of the fly ash sample, the AMD before and after treatment with fly ash and the resulting AMD/FA residue will be presented. The results were used to determine the toxicity of the treated AMD and AMD/FA residue. The results were discussed and compared to that reported in literature and significant findings were highlighted.

### Chapter 6: Application of fly ash in synthesis of geopolymers

In this chapter the use of fly ash in the synthesis of geopolymers is presented and discussed. The results obtained from the characterisation of the fly ash and synthesised geopolymer samples are presented and compared in order to understand the changes in the elemental composition, morphology, mineralogical content of the feedstock and product. The results obtained from the DIN-S4 leaching test and the gamma ray spectroscopy was used to determine the leachability and radioactivity of the synthesised geopolymer with respect to environmental safety.

## Chapter One: Introduction

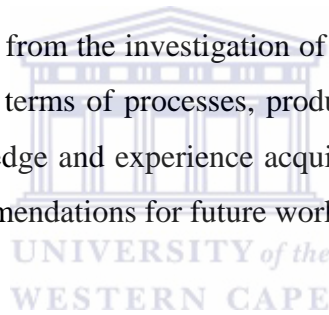
---

### Chapter 7: Possibility of REE recovery from fly ash

The results of the sequential leaching experiments will be presented and discussed in this chapter. The chapter will focus on determining where the REE are concentrating during the sequential extraction scheme. The results and findings were used to assess the overall efficiency of the process as well as the environmental implications of the process, products and wastes.

### Chapter 8: Conclusion and recommendations

The conclusions reached from the investigation of the environmental safety of the fly ash beneficiations in terms of processes, products and waste are presented in this chapter. The knowledge and experience acquired from this study are used to make appropriate recommendations for future work.



### Chapter Two

#### 2 Introduction

Chapter two contains the review of different literature focusing on the source, physical and chemical properties, disposal, environmental impact and beneficiation of coal fly ash in sections 2.1 to 2.10. The geopolymer literature will also be reviewed in section 2.11 in order to understand the synthesis methods, the physical, chemical properties and applications. The literature of AMD will also be reviewed with focus on its origin, characterisation and treatment methods in Section 2.12. Furthermore, the literature of the analytical techniques used in this study is also reviewed in sections 2.14 to 2.16. The chapter ends with a summary of the major findings from the review of the literature.

Coal fly ash is the major component of the waste material produced from the combustion of coal. It is produced as a waste product from the combustion of pulverised coal to generate electricity in power plants and steam generating plants. Fly ash is formed when pulverized coal and air are blown into the boiler's combustion chamber where it instantly ignites, the combustion generates heat and produces a molten mineral residue. Boiler tubes remove heat from the boiler resulting in the cooling of the flue gas and hardening of the molten mineral residue to form ash. Bottom ash or slag (which are coarse ash particles), fall to the bottom of the combustion chamber, while the lighter fine ash particles (fly ash), remain suspended in the flue gas. To prevent the release of fly ash into the atmosphere, the fly ash is removed by particulate emission control devices, such as electrostatic precipitators or filter fabric baghouses. About 80 % of the solid residue from the pulverised coal combustion is released as fly ash ([www.fhwa.dot.gov](http://www.fhwa.dot.gov)).

The properties of fly ash depend on the physical and chemical properties of the coal source, the coal particle size, the combustion process, and the type of ash collector used. Fly ash usually consists of spheres composed of crystalline matter and some residual carbon. Although in bulk, fly ash is considered as

homogeneous agglomerate consisting mainly of spherical particles ranging from a micron up to tens of microns in diameter. The individual particles vary in size, morphology, mineralogy and chemical composition. The variable physical and chemical properties of fly ashes are attributed to the influence of the coal source, particle size, type of combustion process and moisture content (Jankowski et al., 2006; Vassilev and Vassileva, 2007; Sočo and Kalembkiewicz, 2009).

Fly ash is deemed to be highly contaminating because of the high surface area of the particles. This high surface area gives rise to the enrichment of potentially toxic elements which condense during cooling of combustion gases (Querol et al., 1996). Hence the disposal of fly ash is of major concern globally because of the enormous quantity that is generated and the environmental issues arising from the disposal methods that are currently employed. Worldwide huge amounts of coal fly ash are generated in order to meet energy demands and about 70 % of fly ash is disposed as waste (Haynes, 2009). In 2009, China generated over 375 million tons of coal ash (Greenpeace, 2010). In 2008, the coal-fuelled electric power industry generated approximately 72.4 million tons of coal fly ash, in the USA (www.epa.). India was predicted to generate about 170 million tonnes per annum (Sushil, and Batra, 2006). In South Africa, Eskom generated nearly 36.7 million tons of fly ash in 2009 from coal combustion, of which only 5.7% was utilised beneficially (www.eskom.co.za) while Sasol produced about 4 million tonnes annually (Mahlaba et al., 2011). Thus management of this combustion waste is of major concern. In the management of this combustion by-product the focus should not only be on the prevention of environmental pollution, but also on methods that can be used to produce or manufacture value-added products from stored fly ash

### **2.1 Fly ash classification**

Fly ash is usually classified into two types, class F (low lime) and class C (high lime) (ASTM C618), based on their silica, alumina and iron oxide content. Class F fly ash is produced by the combustion of anthracite and bituminous coal and class F has > 70% total of SiO<sub>2</sub>, Al<sub>2</sub>O<sub>3</sub>, Fe<sub>2</sub>O<sub>3</sub>. Class F is pozzolanic in nature

## Chapter Two: Literature review

---

(hardening when reacted with  $\text{Ca}(\text{OH})_2$  and water). Class F fly ashes usually contain less than 5 % CaO. Combustion of sub bituminous and lignite coal typically produces class C fly ash. Class C fly ash has a higher alkali and sulphate content than class F. Class C has a sum of  $\text{SiO}_2$ ,  $\text{Al}_2\text{O}_3$ , and  $\text{Fe}_2\text{O}_3$  in the range of 50 – 70%, and contains a large proportion of CaO (10–35%). Also class C is both cementitious (self-hardening when reacted with water) and pozzolanic (Vassilev and Vassileva, 2006). Table 2.1 below presents the ASTM parameters for the classification of fly ash based on the composition of the fly ash.

Table 2:1: ASTM standards classification of fly ash (ASTM C 618, 1993)

	Class F	Class C
$\text{SiO}_2 + \text{Al}_2\text{O}_3 + \text{Fe}_2\text{O}_3$ , min %	70	50
$\text{SO}_3$ , max %	5	5
Moisture content, max %	3	3
LOI, max %	6	6
Available alkalis, as $\text{Na}_2\text{O}$ , max %	1.5	1.5

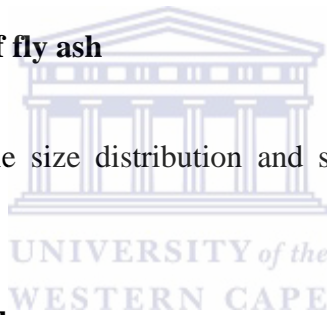
The combustion of high rank bituminous and anthracite coals produces low calcium class F fly ashes that have pozzolanic properties. In contrast the combustion of low rank lignite and sub-bituminous coals produces high calcium class C fly ashes that are self-cementing and pozzolanic (Mattigod et al., 1990). Other chemical and physical requirements in this classification include content of  $\text{SO}_3$  ( $\geq 5.0\%$ ), moisture ( $\geq 3.0\%$ ),  $\text{Na}_2\text{O}$  ( $\geq 1.5\%$  optional), particle size ( $\geq 34\% \pm 5\%$  on average value retained on  $45 \mu\text{m}$ ), and loss on ignition (LOI) ( $\geq 6.0\%$  and up to 12% for Class F fly ashes based on performance) (Vassilev and Vassileva, 2007).

The classification of fly ashes into four chemical groups with respect to certain chemical and physical properties was recommended by the subcommittee of ‘‘Fly Ash Utilization’’ at the United Nations. The classifications are based on the  $\text{SiO}_2/\text{Al}_2\text{O}_3$  ratio, on the granulometry and Blaine specific surface area (SSA) and

on the content of free CaO of the fly ash. Based on the  $\text{SiO}_2/\text{Al}_2\text{O}_3$  ratio the fly ash are categorised as: (1) Group I – silico-aluminate fly ashes with  $\text{SiO}_2/\text{Al}_2\text{O}_3$  ratio  $\geq 2$  and CaO  $< 15\%$ ; (2) Group II – alumino-silicate fly ashes with  $\text{SiO}_2/\text{Al}_2\text{O}_3$  ratio  $< 2$ , CaO  $< 15\%$ , and  $\text{SO}_3 < 3\%$ ; (3) Group III – limesulphate fly ashes with CaO  $> 15\%$  and  $\text{SO}_3 > 3\%$ ; and (4) Group IV – basic fly ashes with CaO  $> 15\%$  and  $\text{SO}_3 < 3\%$ . Based on the granulometry and Blaine specific surface area (SSA), fly ashes were divided into (1) fine-grained fly ashes ( $< 25\%$  are  $> 75 \mu\text{m}$  and SSA of  $> 3.0 \text{ m}^2 \text{ g}^{-1}$ ); (2) medium-grained fly ashes (40– 75% are  $< 75 \mu\text{m}$  and SSA of  $1.5\text{--}3.0 \text{ m}^2 \text{ g}^{-1}$ ); (3) coarse-grained fly ashes ( $< 40\%$  are  $< 75 \mu\text{m}$  and SSA of  $< 1.5 \text{ m}^2 \text{ g}^{-1}$ ). According to the content of free CaO, fly ashes were specified into: (1) inactive or very slightly active ( $< 3.5\%$ ); (2) slightly active (3.5–7%); (3) active (7.0–14.0%); and (4) very active ( $> 14\%$ ), (Vassilev and Vassileva, 2007).

### 2.2 Properties of fly ash

The morphology, particle size distribution and surface area of the fly ash are covered in this section.



#### 2.2.1 Fly Ash Morphology

The morphology of fly ash particle describes the size, shape, or structure and surface properties of the particle which is determined by combustion temperature and cooling rate in the power plant (Kutchko and Kim, 2006). The study of the fly ash particle morphology is important in understanding its physical, chemical and leaching behaviour in terms of applications, toxicology and environmental studies (Singh et al., 2007; Wang et al., 2007). The surfaces of particles are generally smooth in fly ash that has not weathered and are assumed to be mainly aluminosilicate structures. While in weathered fly ash the particle surfaces have features such as encrustations, corrosions and etching which may have resulted from leaching or formation of new mineral phases as a result of weathering (Praharaj et al., 2001; Yeheyis et al., 2009).



## Chapter Two: Literature review

---

Fisher et al., (1978) used light microscopy to analyse fly ash particle morphology which they classified into eleven major categories based on opacity, shape and type of inclusions. According to the authors the opaqueness is determined by the composition of the particle such as iron oxides content whereas non opaque particles are mostly silicates that originated from clays and siltstones associated with the coal. The different characteristic shapes of the particles were attributed to combustion exposure time and temperature. They also stated that the relative abundances of the eleven morphological particle categories within each size regime seem to rely on particle size. The majority of the particles in the finer fractions are spherical, glassy and mostly non-opaque showing complete melting of the silicate minerals in the coal particle. The minor opaque spheres are usually iron oxide particles like magnetite. Kutcho and Kim, (2006) also reported that the fly ash samples were comprised of over 50 % amorphous alumino-silicate spheres and a lower quantity of iron-rich spheres. The finest fraction is made up of 87 % non-opaque solid spheres and 7.9 % cenospheres whereas the coarsest fraction comprises of 26 % non-opaque solid spheres and 41 % cenospheres.

Various morphological studies are in tune with these findings and shows that fly ash consists of a range of spherical and irregularly shaped particles of different sizes ranging from  $<1\mu\text{m}$  to  $>200\mu\text{m}$  formed from the various physical and chemical reactions that occur during the coal combustion process. The combustion heat causes the inorganic minerals in coal to fluidise or volatilise or to react with oxygen; which during cooling, may form crystalline solids, spherical amorphous particles or condense as coating on particles. Agglomerated particles are produced due to high temperature sintering reactions; spherical amorphous particles are formed from the fast cooling in the post-combustion zone; hollow cenospheres result from the expansion of trapped volatile matter that can cause the particle to expand while plerospheres are hollow spheres incorporating fly ash spheres (Fisher et al., 1978; Cho et al., 2005; Kutcho and Kim, 2006; Saikia et al., 2006). Morphological studies have also shown the range of spherical and irregular shaped particles of different sizes that make up the fly ash. The alumino-silicate iron-rich spherical particles are usually small in size (between  $0.1\mu\text{m}$  and

100  $\mu\text{m}$ ) whereas the irregular shaped particles which consist mostly of unburned carbon are larger ( $<1\mu\text{m} - >200\mu\text{m}$ ) (Styszko-Grochowiak et al., 2004; Potgieter-Vermaak et al., 2005; Cho et al., 2005).

Fly ash colour is highly influenced by the mineral phase and is mostly determined by two components. The unburned carbon resulting from incomplete combustion of coal is responsible for the grey and black colour; while iron oxide with its characteristics colour depending on the oxidation state of iron is another important component in determining the colour of fly ash. Trivalent iron (i.e.  $\text{Fe}^{3+}$ ) is brown, red, or yellow, while bivalent iron (i.e.  $\text{Fe}^{2+}$ ) is grey or grey with a bluish tinge. Magnetite which contains both  $\text{Fe}^{3+}$  and  $\text{Fe}^{2+}$  is black and can be brown when finely dispersed (Raclavska et al., 2009) The influence of iron in determining the colour of fly ash again agrees with findings of Fisher et al., (1978).

### 2.2.2 Particle Size Distribution and Surface Area

A number of related factors such as the size distribution of the coal particle and the accessory minerals, combustion conditions and the particulate emission control devices determine the particle size distribution of fly ash (Fisher, 1983). The size and distribution of these particles is the most important characteristic determining its reactivity. The smaller particles have greater specific surface area making a larger area susceptible to hydrolysis. The particle size distribution is important during interaction of fly ash with different solutions because it affects the mobilisation of any trace element on the surface (Mattigod et al., 1990; Iyer, 2002; Jankowski et al., 2006). The particle size distribution also plays a role in the concentrations of some elements in fly ash. Fisher et al., (1983) reported that the concentrations of some elements are dependent on particle size while some are independent of particle size. The highest size dependence is exhibited by the most volatile elements (Cd, Zn, Se, As, Sb, W, Mo, Ga, Pb and V) or their oxides while the least volatile elements do not exhibit significant particle size dependence. Extension of vapour-phase condensation to the sub-micrometre regime and

homogeneous nucleation were attributed to the particle size dependence of the trace elements in fly ash.

The particle size of a material can be important in understanding the physical and chemical properties of fly ash and plays a very important role in the utilization and disposal of fly ash. If fly ash is to be considered as a partial replacement for cement a low bulk density is required to make it ideal as a lightweight building material (Ural, 2005). The particle-size distribution of fly ashes is also a vital factor for their use as pozzolans. ASTM 618C requires that 34% of the ash must remain on a 45 mm sieve on wet sieving.

### 2.3 Chemical properties of fly ash

The chemical composition of fly ash, the mineralogy, the pH and chemistry are reviewed in this section.

#### 2.3.1 Chemical composition of fly ash

The elemental composition of fly ash can be determined with X-ray fluorescence spectrometry (XRF), instrumental neutron activation analysis (INAA), inductive coupled plasma-optical emission spectroscopy (ICP-OES/MS) and laser ablation inductive coupled plasma-mass spectrometry (LA ICP-MS). The chemical composition of fly ash comprises major (>1wt %), minor (1–0.1wt %), and trace (<0.1wt %) elements (Vassilev and Vassileva, 1996). The proportions of the major elements are usually determined by XRF, while the minor and trace elements proportions are determined with ICP-OES or ICP-MS. Fly ashes from the four coal ranks (anthracite, bituminous, sub-bituminous, and lignite coals) differ in chemical composition as a result of the difference in their coal heating values, chemical composition, ash content, and geological origin. Thus the chemical constituents of fly ash mostly depend on the chemical composition of the coal, the combustion conditions and removal effectiveness of air pollution

## Chapter Two: Literature review

---

control device (electrostatic precipitators or bag filters) used (Adriano et al., 1980; Goodarzi, 2006; Vassilev and Vassileva, 2007).

Although the chemical composition of fly ash varies, elemental composition analysis of fly ash shows most sources of fly ash still consist of the same fundamental chemical elements but in different concentrations. The knowledge of how elements are partitioned in fly ash is important because the particle enriched surface almost dominates the chemical contents of its core. The surface layer of the particle seems to define most of the important characteristics such as pH, leaching and mobilization properties of the fly ash. As stated earlier the surface area of the fly ash particle increases as its size decreases thus the particles have an unusually large surface area that are enriched with elements that are volatilized during coal combustion and are condensed at lower temperature on the fly ash particles. The partitioning of elements and their surface association in fly ash is controlled by the extent of vaporisation during the coal combustion process (Choi et al., 2002).

Table 2.2 compares the chemical composition range of the major and minor elements reported as oxides for bituminous, sub-bituminous, and lignite coal fly ashes. Sub-bituminous, and lignite fly ashes have higher CaO and lower LOI (loss on ignition) than bituminous fly ash.

## Chapter Two: Literature review

Table 2:2: Normal range of chemical composition for fly ash produced from different coal ranks (expressed as weight %) (<http://cementconsultant.org/flyash.pdf>)

Component	Bituminous	Sub-bituminous	Lignite
SiO <sub>2</sub>	20-60	40-60	15-45
Al <sub>2</sub> O <sub>3</sub>	5-35	20-30	10-25
Fe <sub>2</sub> O <sub>3</sub>	10-40	4-10	4-15
CaO	1-12	5-30	15-40
MgO	0-5	1-6	3-10
SO <sub>3</sub>	0-4	0-2	0-10
Na <sub>2</sub> O	0-4	0-2	0-10
K <sub>2</sub> O	0-3	0-4	0-4
LOI	0-15	0-3	0-5

Table 2.2 compares the chemical composition range of the major and minor elements reported as oxides for bituminous, sub-bituminous, and lignite coal fly ashes. Sub-bituminous, and lignite fly ashes have higher CaO and lower LOI (loss on ignition) than bituminous fly ash. As shown in the table, silica, alumina, iron and calcium oxide are the principal constituents of typical fly ash samples. The effects of these elements on the fly ash properties in terms of the classification and morphology have been reviewed and discussed in sections 2.1 and 2.2.1 respectively. The impact of these elements on the fly ash mineralogy, pH and chemistry will be discussed in sections 2.4 and 2.5 respectively.

Table 2.3 presents the average trace element composition in fly ash. The concentrations of these elements are higher in the fly ash than the original coal due to the volatilization and condensation during and following the coal combustion process. A high concentration of these trace elements creates environmental problems in the utilization and disposal of fly ash. These elements may leach out and contaminate the soil, surface and ground water (Sushil, and Batra, 2006).

## Chapter Two: Literature review

Table 2:3: Average trace element composition for fly ash (El-Mogazi et al., 1988)

Elements	Concentrations (mg/kg)	Elements	Concentrations (mg/kg)
As	23-312	Pb	31-241
B	10-600	Mo	6.6-41
Cd	02-3.9	Ni	1.8-15
Cu	45-259	Se	1.2-17
Cr	43-259	Zn	15-406

From Table 2.3 above, it is noticed that fly ash consists of trace elements such as Pb, As, Cd, Cr, Ni, Se and Zn. Globally analysis of fly ash has shown that a broad range of heavy metals exist in fly ash (Adriano et al., 1980; Asokan et al., 2005; Dutta et al, 2009; Izquierdo and Querol, 2012; Blissett, and. Rowson, 2012; Eze et al, 2013). Fly ash also contains radionuclides such as U, Th, and isotopes of Pb and K (Parami et al, 2010; Madzivire, 2013). Studies of coal fly ashes have also shown that REE such as lanthanum, cerium, neodymium and yttrium are present in this solid waste (Fatoba, 2008; Smolka-Danielowska, 2010; Akinyemi, 2010; Eze, 2011; Kashiwakura et al, 2013). Thus fly ashes also have potential for REE valorisation.

A brief overview of toxic metals, radionuclides and REE will be are covered in section 2.3.11, 2.3.12 and 2.3.1.3 respectively.

### 2.3.1.1 Heavy metal

The term heavy metal usually denotes any metallic chemical element with a specific density greater than  $5 \text{ g/cm}^3$  which is harmful or toxic at low concentrations (Järup, L. 2003). Heavy metals include lead (Pb), cadmium (Cd), zinc (Zn), mercury (Hg), arsenic (As), chromium (Cr), copper (Cu), iron (Fe), and the platinum group elements. Constant exposure to heavy metals may result in adverse health effects because they are not biodegradable and have the tendency to accumulate in living organisms (Bailey et al, 1998). Human exposure to heavy

## Chapter Two: Literature review

---

metals occurs through several processes such as the intake of contaminated air and food; also through contact with contaminated soil or industrial waste. Heavy metals enter the environment by natural processes such as weathering or anthropogenic means such as mining, emissions, solid or liquid waste discharge. The anthropogenic source of heavy metals has been identified as the main source of heavy metal pollution of the environment (Cheng, S. 2003).

According to Järup, (2003) adverse health effects of these heavy metals in humans may occur at lower exposure levels than previously anticipated. Fly ash usually contains harmful toxic heavy metals such as Hg, As, Pb and Cd (Griepink et al., 1983). Other heavy metals such as Ba, Co, Fe, Mg, Mn, Cu, Ga, Pb, Sb, S, Zn, La, Rb, Nd, Eu, Sm, Ta, Tb, Lu, W, Se, U, Mo, and Sc have also been identified in fly ashes (Griepink et al., 1983; Xu et al, 2003; Smołka-Danielowska, 2006; Goodarzi, 2006). Generally these elements may be toxic although their compositions in fly ash may differ depending on the coal source (Adriano et al., 1980). The presence of these elements in fly ash raises concern over its safety with regards to its disposal and beneficiation since studies has shown that these elements may leach out of fly ash (Wang et al., 1999). Hence this study will attempt to determine the fate of these elements during the fly ash reuse process, products and wastes.

Arsenic is present in coal ash and can leach from ash (Pandey et al., 2011) and may contaminate surface- or/and ground water. Polluted drinking water is a key route of arsenic exposure which generates a range of harmful health effects and consumption of high quantities can result in death (Singh et al., 2007). Constant exposure to arsenic in drinking water can cause several types of cancer such as skin cancer, bladder cancer, lung cancer and kidney cancer (Smith et al., 1992).

Elemental analysis and leaching studies have revealed the presence of cadmium (Cd) in coal fly ash which is readily mobilized (Fernfindez-Turiel et al., 1994). Cd poses as an environmental threat because it can form aqueous complexes due to its solubility and permeate river sediments which may pose an environmental

## Chapter Two: Literature review

---

threat (Wu et al., 2013). Cd exposure occurs via the food chain and through inhalation. Chronic exposure may result in kidney disease, increased blood pressure and skeletal damage (Järup, L. 2003).

Chromium is a toxic metal that is frequently found in coal ash (Smółka-Danielowska, 2006) and has the potential to leach out (Jankowski et al., 2006). Cr exists in a trivalent form ( $\text{Cr}^{3+}$ ) and hexavalent form ( $\text{Cr}^{6+}$ ) and mainly enters the soil and aquatic environment via dumped waste. Chronic exposure to Cr through ingestion of contaminated water or via inhalation of large doses can have an adverse effect on humans because  $\text{Cr}^{6+}$  is a known carcinogen (Rowbotham et al., 2000).

Lead is a highly toxic heavy metal that has been known for hundreds of years (Lidsky and Schneider, 2003) and is also present in coal fly ash (Adriano et al., 1980; Smółka-Danielowska, 2006). Lead exposure occurs via coal ash contaminated soils, drinking water contaminated by coal ash and from inhalation of fly ash. It is a potent neurotoxin that affects body organs such as kidneys, red blood cells and the nervous system (Hsiang and Díaz, 2011).

Mercury is present in fly ash derived from the combustion of coal that contains mercury. It is a toxic heavy metal with the tendency to bio-accumulate (Wang et al., 2007). Mercury may leach from fly ash into soil or water where it is converted into the toxic methylmercury ( $\text{CH}_3\text{Hg}^+$ ), by anaerobic organisms. This  $\text{CH}_3\text{Hg}^+$  is absorbed by small organisms and the larger organisms that feed on them. The concentration of the  $\text{CH}_3\text{Hg}^+$  increases as it progresses up the food chain (Guimaraes et al. 2000). Human exposure is usually through the consumption of fish and sea food from contaminated ecosystem (Trasande et al., 2005). Adults, children, and developing foetuses are at risk from ingestion and the developing nervous system of the foetus may be more vulnerable to methylmercury than the adult nervous system (Bose-O'Reilly et al., 2011). Symptoms of methylmercury poisoning may include; impairment of the peripheral vision; disturbances in



## Chapter Two: Literature review

sensations; lack of coordination of movements; impairment of speech, hearing, walking; and muscle weakness.

### 2.3.1.2 Radionuclide and radioactivity in coal fly ash

Radionuclides are elements with atoms that have an unstable nucleus such as U, Th and R. In order to achieve stability these atoms undergo radioactive decay, a process that is usually accompanied by the release of beta particles, neutrons or gamma rays. Radionuclides such as U, Th and their decay products, including radium (Ra) and radon (Rn) occur naturally in coal (Tadmor, J., 1986; Charro and Peña, 2012). During combustion of coal most of the radionuclides and their decay products are released from the coal and are divided between the gas phase and solid phase of the combustion products. The partitioning between the gas and solid phase is governed by the volatility and chemistry of the individual elements (Baxter, M. 1993). The less volatile elements such as Th, U, and the majority of their decay products are almost entirely retained in the solid combustion wastes. The concentration of most radioactive elements (radionuclides) in solid combustion wastes is approximately 10 times the concentration in the original coal. Almost 100 % of the radon gas contained in the feed coal is transferred to the gas phase and is lost in stack emissions (USGS, 1997).

In Table 2.4 below some characteristic data for radionuclides in coal and fly-ash are presented.

Table 2:4: Comparative levels of radioactivity in fly ash and coal (Baxter, M. 1996)

Activity content in becquerels per kilogram (Bq/kg)								
	$K^{40}$	$U^{235}$	$Rn^{226}$	$Pb^{210}$	$Po^{210}$	$Th^{232}$	$Th^{238}$	$Ra^{238}$
Coal	50	20	20	20	20	20	20	20
Fly ash	265	200	240	930	1700	70	110	130

## Chapter Two: Literature review

---

Table 2.4 shows that during coal combustion enrichment from five-fold to two orders of magnitude occur in the radioactivity of the resultant fly ash radioactivity. These enhanced concentrations of radionuclides and their decay daughters in fly ash emit alpha particles, beta particles, and gamma rays, and may radiologically affect the environment (Tadmor, J., 1986; Nisnevich et al., 2008; Janković et al., 2011). The radioactive decay for  $U^{238}$  occurs through a long chain of 13 different radionuclides before terminating as a stable state in  $Pb^{206}$ . Similarly  $Th^{232}$  undergoes radioactive decay via a series of radionuclides and ends with a stable isotope of  $Pb^{208}$ . These  $U^{238}$  and  $Th^{232}$  offspring radionuclides (Rn, Ra and Po) are also radioactive and emit alpha or beta radiation and gamma rays that may be dangerous to the environment (Eckerman and Ryman 1993; MacKenzie, A., 2000).

Radionuclides in fly ash may leach and contaminate the environment (Mljac and Krigman, 1996). The radioactivity of South African coal fly ashes is an important factor that has to be investigated if fly ash is to be used for water treatment or geopolymerisation. It is important to evaluate and understand the radioactivity and leachability of the radionuclides present in the fly ash. This will help in ascertaining that the radioactivity from the fly ash will not be transferred into the product water. Likewise the use of fly ash in the making of geopolymers for the construction industries needs to be carried out properly to avoid excessive radioactive emissions from the final structures.

The radiological hazard due to the use of the materials has been calculated using some indices such as radium equivalent index (Beretka and Matthew 1985), external hazard index (Xinwei 2004) and activity index or gamma index (EC 1999). Radium equivalent index  $Ra_{Eq}$  index in Bq/kg is a useful guide to compare the specific activities in materials. It is defined based on the assumption that 10 Bq/kg of  $^{226}Ra$ , 7 Bq/kg of  $^{232}Th$  and  $^{130}Bq/kg$  of  $^{40}K$  produce the same gamma dose rate. It is calculated using the following equation:

$$Ra_{eq} = C_{Ra} + 1.43C_{Th} + 0.077C_K$$

## Chapter Two: Literature review

---

Where,  $C_{Ra}$ ,  $C_{Th}$  and  $C_K$  are the specific activities (Bq/kg dry weight) of  $^{226}Ra$ ,  $^{232}Th$  and  $^{40}K$ , respectively (Beretka and Mathew, 1985). The maximum value of  $Ra_{eq}$  in building materials must be less than 370 Bq/kg in order to keep the gamma-ray dose below  $1.5 \text{ mSv y}^{-1}$  (UNSCEAR 2000).

The gamma-rays emanating from building materials can pose a health hazard and is normally given in terms of the external hazard index,  $H_{ex}$  (Xinwei 2004); The  $H_{ex}$  is calculated as follows:

$$H_{ex} = \frac{C_{Ra}}{370} + \frac{C_{Th}}{259} + \frac{C_K}{4810}$$

Where,  $C_{Ra}$ ,  $C_{Th}$  and  $C_K$  are the specific activities (Bq/kg dry weight) of  $^{226}Ra$ ,  $^{232}Th$  and  $^{40}K$ , respectively. The value of this index must be less than 1 for the radiation hazard to be considered negligible.

The restriction on building materials for gamma radiation is based on a dose range of  $0.3$  to  $1 \text{ mSv y}^{-1}$  (EC 1999, STUK 2003). To establish whether a building material meets this requirement, the activity index or gamma index  $I_\gamma$  of the samples is calculated from the following equation (EC 1999, STUK 2003, Kovler 2000):

$$I_\gamma = \frac{C_{Ra}}{300} + \frac{C_{Th}}{200} + \frac{C_K}{3000}$$

$I_\gamma$  is a dimensionless quantity because the numerical quantities in the denominator of the equation are also in units of Bq/kg. The material can be used as building material without restriction in terms of radioactivity, if the activity index  $I_\gamma$  is  $1$  or  $< 1$ .

### 2.3.1.3 Rare earth elements (REE)

REE are a collection of 17 elements namely the lanthanides, yttrium (Y, atomic number 39) and scandium (Sc, atomic number 21). The lanthanides consist of 15 elements in the periodic table with atomic numbers 57 to 71 namely: lanthanum (La), cerium (Ce), praseodymium (Pr), neodymium (Nd), promethium (Pm),

## Chapter Two: Literature review

---

samarium (Sm), europium (Eu), gadolinium (Gd), terbium (Tb), dysprosium (Dy), holmium (Ho), erbium (Er), thulium (Tm), ytterbium (Yb), and lutetium (Lu). Scandium (Sc) and yttrium (Y) are considered as REE because they usually occur in the same ore deposits as the lanthanides and exhibit similar chemical properties (Kempe and Wolf, 2006; Makreski et al., 2011).

REE are in great demand due to their unique physical and chemical properties best suited for the development and manufacturing of advanced materials for high-technology devices (Zhang et al., 2007). The unsaturated 4f electronic structure of REE gives them their unique physical and chemical properties (Chakhmouradian and Wall, 2012; Massari and Ruberti, 2013). These properties such as high density, high melting point, high conductivity and high thermal conductance have led to the increase in their demand as a result of their growing importance in advanced technology (Kubota et al., 2000; Jiang et al., 2005; Rademaker et al., 2013). While many important properties are shared by all the REE, others are specific to particular elements (Jordens et al., 2013). REE are widely used in almost every product that forms part of our daily lives such as mobile phones, plasma, LCD and LED screens, portable DVDs, laptop computers, disk drives and rechargeable batteries for appliances (Chakhmouradian and Wall, 2012). They are also used in automotive catalytic converters, fluid cracking catalysts in petroleum refining, in permanent magnets and rechargeable batteries for hybrid and electric vehicles, and generators for wind turbines, and numerous medical devices (Binnemans et al., 2013; Massari and Ruberti, 2013; Rademaker et al., 2013). Furthermore there are important defence applications, such as jet fighter engines, missile guidance systems, antimissile defence, and space-based satellites and communication systems (Massari and Ruberti, 2013).

REE are certain to have an incessant, unique and vital impact on our lives, especially in the industrial age of the 21st century due to the discovery of new applications for these little known materials in our increasingly high-tech world through research and development. Hence there is an ever-increasing demand for

REE in the international markets, with emphasis on identifying new resources to ensure adequate supply for present and future use.

Studies of coal fly ash (Fatoba, 2008; Akinyemi, 2010; Eze, 2011), has shown that REE, such as lanthanum (La), cerium (Ce), and yttrium (Y) are present in significant amounts in South African coal fly ash. However, there has been very little in the literature to investigate REE recovery from fly ash. This study will attempt to pre-concentrate the REE in South African coal fly ash in order to explore its recovery potential.

### 2.4 Mineralogy of fly ash

The phase and mineral composition of coal fly ash generally consists of inorganic (90 %-99 %), organic (1 %-9 %) and fluid (<0.5 %) components (Vassilev and Vassileva, 2005). The inorganic component is mostly comprised of amorphous glassy (non-crystalline) matter (34% - 80%) and crystalline matter (17% - 63%) characterised by various major (1–10%), minor (0.1–1%) or accessory (<0.1%) mineral phases. The organic part is made up of the unburnt coal components characterised by marginally altered, semi-coked and coked coal particles. The fluid component comprises of liquid, gas and gas-liquid inclusions that were associated with both inorganic and organic matter (Vassilev and Vassileva, 1996; Vassilev and Vassileva, 2005). The percentage amorphous (glass) or crystalline content of the fly ash particles depends on the rate of cooling of the fluidized coal minerals in the post combustion area. Rapid cooling of the fluidized minerals results in spherical glassy particles whereas crystalline structures are formed when the fluidized minerals cool gradually (Kim, 2002).

The chemical reactions occurring during fly ash utilisation (cement and concrete or zeolite or geopolymer synthesis) and disposal (weathering) can be attributed to the amorphous (glass) components in fly ash. Due to its large quantity and the disorderly character of the atoms involved, it is also the main matrix in the ash for adsorbed trace elements that may be released from the fly ash during its leaching

## Chapter Two: Literature review

---

(Ward and French, 2006). The mineral components of coal fly ash have natural or technogenic origin and can be categorised into primary, secondary and tertiary minerals or phases. The primary minerals or phases are original coal minerals or phases that have not undergone phase transformations during coal combustion. The secondary minerals and phases are new mineral phases formed during coal combustion. The tertiary mineral phases are new minerals or phases formed during fly ash transport and storage (Vassilev and Vassileva, 1996).

Global studies of the mineralogical composition of coal fly ashes, showed that aluminosilicate glass, mullite ( $\text{Al}_6\text{Si}_2\text{O}_{13}$ ), quartz ( $\text{SiO}_2$ ), magnetite ( $\text{Fe}_3\text{O}_4$ ), anorthite/albite ( $(\text{Ca},\text{Na})(\text{Al},\text{Si})_4\text{O}_8$ ), anhydrite ( $\text{CaSO}_4$ ), ettringite ( $3\text{CaO} \cdot \text{Al}_2\text{O}_3 \cdot 3\text{CaSO}_4 \cdot 32\text{H}_2\text{O}$ ), opaline ( $\text{SiO}_2$ ), hematite ( $\text{Fe}_2\text{O}_3$ ) and lime ( $\text{CaO}$ ), were the major mineral phases present in coal fly ashes from some power plants in Europe (Moreno et al., (2005). In India, Praharaj et al., (2002) reported that quartz, mullite, hematite and magnetite were the major phases. Ilmenite and anorthite were observed as likely minor phases in coal fly ashes from India. In the case of fresh and weathered fly ash studied in Australia (Ward et al., 2009), the major phases reported were quartz, mullite, magnetite, and hematite together with a large fraction of glass and amorphous phases. Also probable traces of gypsum ( $\text{CaSO}_4 \cdot 2\text{H}_2\text{O}$ ) are shown in the fresh fly ash. Choi et al., (2002) in their studies of Korean fly ashes reported that the major phases present were mullite, quartz and iron oxide (hematite and magnetite). South African fly ash mineralogy was found to contain mullite ( $\text{Al}_6\text{Si}_2\text{O}_{13}$ ) amorphous Fe-Al silicates, lime ( $\text{CaO}$ ), quartz ( $\text{SiO}_2$ ), portlandite ( $\text{Ca}(\text{OH})_2$ ), anorthite ( $\text{Ca}_2\text{Al}_2\text{Si}_2\text{O}_8$ ), hematite ( $\text{Fe}_2\text{O}_3$ ), magnetite ( $\text{Fe}_3\text{O}_4$ ) and anatase ( $\text{TiO}_2$ ) (Nathan et al.,1999).

The mineralogical studies of the various fly ashes reported by the various authors above, shows that although the major phases are similar, the different minerals indicate the variation in the fly ashes and their chemical compositions. The prominent major phases reported in all the studies are glass, mullite, quartz, magnetite and hematite. Quartz is a major crystalline phase in fly ash. It exists as a hard mineral commonly found as cell and pore infillings in the organic matter of

coal and is usually a primary mineral because it is mostly unaltered by the combustion process due to its high fusion temperature (Ward, 2009). Mullite is a secondary mineral because it does not exist in coal but is formed from the decomposition of kaolinite an aluminosilicate mineral in the coal (Koukouzas et al., 2009, White and Case, 1990). Magnetite and hematite are also secondary minerals. They are formed from the oxidation of pyrite and other iron bearing minerals in the coal (Hurley and Schobert, 1993).

### 2.5 The pH and of chemistry fly ash

The pH of fly ash is either acidic or alkaline depending on its chemical constituents. The amounts of acidic and alkaline components in a soluble fraction of the fly ash determine the pH. According to Ward et al (2009) the pH developed in fly ash relates to the equilibrium between the alkaline earth metals (CaO and MgO) content and the potentially acid producing  $\text{SO}_4^{2-}$  and  $\text{PO}_4^{2-}$ . Acidic fly ashes have low concentrations of CaO and MgO in relation to the sulphate content whilst alkaline fly ashes have significant CaO and MgO concentrations in relation to the  $\text{SO}_4^{2-}$  and  $\text{PO}_4^{2-}$ . Roy and Griffin (1984) after studying fly ash from bituminous coal attributed the acidity of fly ash to sulphuric acid content in the ash samples. Furthermore acidic fly ash is more likely to occur when the ash is exposed for longer periods to exhaust gases due to condensation of sulphuric acid from the gas stream onto particle surfaces (Roy and Berger, 2011). While the initial reaction of coal ash with water may produce an acidic or alkaline solution, it has been observed that the pH of ash-water systems can change with time, Roy and Berger, (2011) attributed this change in pH to geochemical buffers. According to them the pH of acidic fly ash may be transitory due to the neutralisation of the fly ash acidity with time, by the hydration of metal oxides through a reaction path that is eventually buffered by  $\text{CO}_2$ . The decrease in the pH of alkaline fly ash with time resulted from the interaction of the alkaline components of the fly ash with atmospheric  $\text{CO}_2$  (Eze et al, 2013).



When fly ash comes into contact with an aqueous media some components will dissolve to a greater or lesser degree and become mobile, the outcome of this interaction is known as the leachate (Zandi and Russell, 2007). Although fly ashes vary in terms of physical and chemical characteristics, they usually consist of aluminosilicate glassy particles with surfaces that are enriched with toxic trace elements such as As, B, Cr and Sr as a result of condensation reactions during combustion. Elements such as K, Pb and many of the other trace elements are distributed throughout the particle and are not preferentially concentrated (Zandi and Russell, 2007). The surface associated fraction might dominate the leachate chemistry during the early stage of fly ash/water interaction. However, as leaching progresses, further weathering of the aluminosilicate glass matrix would release the elements incorporated within the glass particle (Choi et al., 2002).

The leaching and mobility of these trace elements contained in fly ash is of major concern and should be properly understood in terms of environmental performance when utilising fly ash as a raw material. Studies have shown that the pH of fly ash plays a major role in aqueous media and influences the dissolution and leaching of mobile species from fly ash. Analysis of leachate water from ash ponds reveals that alkalinity and acidity controlled the extractability of elements such as As, B, Be, Cd, Cr, Cu, F, Mo, Se, V and Zn. Aqueous extracts of an acidic fly ash contained concentrations of Cd, Co, Cu, Mn, Ni, Zn, As, B, Be, Cd, F, Mo, Se and V (Ward et al., 2009, Iyer, 2002). Understanding the leaching and mobility of the species in fly ash is vital in predicting the environmental impact associated with fly ash disposal/storage, reuse and beneficiations (Bhattacharyya et al., 2009; Praharaj et al., 2002).

### **2.6 Leaching of Fly Ash**

Fly ash is a complex mixture of various minerals that are associated with high amount of toxic elements which may be leached during disposal or utilisation in different environmental conditions (Kim et al., 2003). Leaching is a process that involves the loss of soluble components from a solid matrix by the action of a



## Chapter Two: Literature review

---

percolating liquid. The main aqueous media in contact with disposed fly ashes are the infiltrating rainwater (Praharaj et al., 2002), the slurry water used to transport the fly ash from the plant to the dam, and the waste water used for dust control of the ash dump.

Some chemical species in coal fly ash are likely to be released from the disposed or stored ash, the beneficiation processes, products, or waste when the ash comes in contact with water. The risk associated with coal fly ash leaching could result in the transfer of toxic elements from the fly ash to the environment (Ugurlu, 2004). These toxic elements such as the heavy metal and radionuclides in coal fly ash are mostly in trace quantities (Izquierdo and Querol, 2012). The trace elements in coal fly ash are prone to leaching due to the transformations that occur in the coal mineral matter during high temperature combustion (Jones, 1995). The distribution of trace elements in fly ash particles depends on their volatility during the coal combustion process (Clarke & Sloss, 1992).

The elements Mn, Ba, V, Co, Cr, Ni, Ln, Ga, Nd, As, Sb, Sn, Br, Zn, Se, Pb, Hg and S in the coal are volatile to a significant extent in the combustion process, whereas, elements such as Mg, Na, K, Mo, Ce, Rb, Cs and Nb seem to have lesser portion volatilized during combustion. On the other hand, Si, Fe, Ca, Sr, La, Sm, Eu, Tb, Py, Yb, Y, Se, Zr, Ta, Na, Ag, and Zn are either not volatilized or only show slight trends associated with the geochemistry of the associated mineral matter (Iyer, 2002). The trace metals are usually volatilized during the combustion and consequently concentrated on the surface layer of the fly ash particles (Steenari et al., 1999). The surface associated elements usually dominate the leachate chemistry during the early stage of fly ash in contact with water (Iyer, 2002). However, as leaching progresses, further weathering of the aluminosilicate glass matrix would release the elements incorporated within the glassy matrix (Choi et al., 2002).

The leaching behaviour of major and trace elements in fly ash varies with the properties of the fly ash such as temperature, pH, composition, mineralogy,

## Chapter Two: Literature review

---

morphology, particle size distribution and the methods employed in studying the leaching process. Also the mineral phases with which these elements are associated and their distribution in the fly ash can influence their leachability (Baba et al., 2008; Saikia et al., 2006; Jankowski et al., 2006; Wang et al., 1999). According to Gitari et al., (2009) neutralization and chemical weathering has been identified as the main leaching processes of coal fly ash.

The rate of dissolution and leaching of elements from fly ash is influenced by the pH of the leachate which depends on the elemental composition of the coal fly ash and the extent of weathering. The pH value of solutions developed during the leaching process appears to be related to the acidity or alkalinity of the original fly ash which in turn depends on the CaO or MgO content of the ash. Baba et al., (2008) reported that the effects of pH on leachability has been studied and documented but the effect of temperature has not yet been fully studied, though pH and temperature have a great influence on the seepage of heavy metal into water resources. They studied the transfer of heavy metals from fresh (unweathered) fly ash to water with standard experimental methods at different pH and temperature conditions and found that metals leach from coal fly ash at concentrations inversely proportional to the leachate pH and temperatures. They concluded that the metal leaching (As, Cd, Co, total Cr, Cr<sup>6+</sup>, Cu, Ni, Pb, Se and Zn) increased with decreasing pH. Temperatures beyond 30 °C stabilise elemental concentrations of Cd, Cr, Pb, As and Cr (VI) irrespective of the pH of the system.

The leaching of the elements in coal fly ash is also influenced by the fly ash mineralogical compositions (Saikia et al., 2006; Zandi and Russell, 2007). The liberation of species from coal fly ash in aqueous medium depends on the mineralogy of the species present in the fly ash. Usually the toxic elements occur as part of a solid phase in coal fly ash (Saikia et al., 2006) and leaching behaviour of these elements mainly depends on their host phases. The potentially toxic elements are mainly contained in the amorphous (glass) phase and magnetic fractions in coal fly ash (Hulett et al., 1980; Yan and Neretnieks, 1995).

## Chapter Two: Literature review

---

The morphology of the coal fly ash particles has an effect on its leachability. The occurrence of a non-porous uninterrupted outer surface and a dense particle interior can limit heavy metal leachability from the coal fly ash (Ramesh and Koziński, 2001). Particle size distributions in conjunction with specific surface area of the coal fly ash particles also provide information on potential interactions between the fly ash and the aqueous media (Sukandar et al., 2006). The major chemical processes involved in fly ash leaching are: constituent solubility; metal complexation; sorption; dissolution of primary solids and precipitation of secondary solids; redox, sorption and hydrolysis reactions (Zandi and Russell, 2007; Jankowski et al., 2006).

An understanding of the chemical behaviour of the coal fly ash elements when in contact with water, and their interactions with other components in the system is required to evaluate the impacts of environmental conditions on the release of trace elements. Although the chemical composition of coal fly ash can give an idea about the pollutants passing into water, however to quantify these phenomena it is necessary to carry out leaching tests. The leaching tests usually entail the contacting of the fly ash with a liquid in order to establish which element will be leached by the liquid and released to the environment. The leaching tests are important in predicting the environmental impact associated with fly ash disposal techniques and beneficiations (Bhattacharyya et al., 2007; Praharaaj et al., 2002).

Laboratory leaching tests are the general methods used to evaluate the amount of constituents that may be released out of a waste/solid material. The procedures are usually designed to determine the parameters that control the release of constituents and to estimate the leachability of toxic components. Leaching tests entail contacting the waste/solid material with a liquid to determine the components that will be leached by the liquid and released to the environment. Most of the leaching tests available include agitated extraction tests, serial batch tests, flow-through tests, flow-around tests, etc. These different tests are used to address different aspects of leaching such as the physical mechanisms involved, chemical interactions between the waste and the leaching fluid, the kinetics of

leaching, leaching as a function of time, etc. (Sorini and Jackson, 1988). However many leaching tests use more aggressive leaching media than those which would occur in a natural environment (Yan, 1998).

Leaching tests are usually categorised as extraction or batch leaching tests and dynamic or column leaching tests. Extraction or batch leaching test involves mixing a specific quantity of the solid material, and the leachant (extraction liquid) for a particular period of time. The product of the combination (leachate) is then filtered and the supernatant stored away for further investigation or analysis. The dynamic or column test involves constant streaming of the leachant over the solid material (Harwell, 1999; Kim, 2005; van der Sloot, 2008). Examples of some leaching tests are the DIN-S4 (German leach test), acid neutralization capacity test (ANC), toxicity characteristic leaching protocol (TCLP), serial batch leaching procedure (SBLP), synthetic groundwater leaching procedure (SGLP), mine water leaching procedure (MWLP), 3TIER integrated framework leaching protocol (3TIER) (Fatoba, 2008; Kim and Hesbach, 2009). In the prediction of the environmental impacts of coal fly ash reuse products and wastes the leaching behaviour of the fly ash materials in aqueous and weakly acidic solutions are the most important. The weakly acidic solution is similar to some natural leaching media, such as acid rain and some of these leaching tests would be applicable to testing products made out of fly ash.

### 2.7 Mobility of Species in Fly Ash

The mobility of potential pollutants (chemical species) due to ash leaching has been the focus of extensive study. An understanding of the factors that determine environmental mobility of species from coal fly ash is important in evaluating the potential impacts of fly ash on the environment and developing novel methods to control the species leaching from fly ash. Elemental analysis of coal fly ash has shown that apart from Si, Al and Fe, fly ash may also be rich in potentially mobile major cations such as Ca, Mg, Na and K, and in minor elements, such as P and B. A number of metals and metalloids (such as Cd, As, Se, Pb, Ni, Cu, Cr, Co, Mo,

## Chapter Two: Literature review

---

Be) that are present as carbonates, oxides, hydroxides and sulphates, may also occur in trace concentrations (Gómez et al., 2007).

A significant factor in the mobility of particular elements in emplaced ashes is the pH developed within the relevant ash-water system. Fly ash, especially ash with an alkaline pH, also has a relatively strong buffering capacity, and tends to retain its natural pH value to a significant extent even if placed in a contrasting pH environment (Jankowski et al., 2006). Studies have shown that the mobility of many species in fly ash also varies with the ash disposal method and that the difference in species mobility is largely attributed to the changes in the pH of the ash water system. Analysis of leachate water from ash ponds reveals that alkalinity and acidity controlled the extractability of elements like As, B, Be, Cd, Cr, Cu, F, Mo, Se, V and Zn. Aqueous extracts of an acidic fly ash contained concentrations of Cd, Co, Cu, Mn, Ni, Zn, As, B, Be, Cd, F, Mo, Se and V (Ward et al., 2009; Iyer, 2002).

The mobility of trace elements from coal fly ashes also depends on the elemental concentration and mode of occurrence. Studies have shown (Alboréset al., 2000; Sočo et al., 2008) that mobility and biological availability of trace metals in solid waste materials like coal fly ash depend not only on their total concentration but also on the physicochemical forms in which they occur. It is now widely recognized that the toxicity and the mobility of these pollutants depend strongly on their specific chemical forms and on their binding state (Gleyzes et al., 2002). Hence, identification of the main binding states and phase associations of trace elements in solid waste samples helps in understanding geochemical processes in order to evaluate the remobilization potential and the risks induced (Gleyzes et al., 2002).

Leaching tests are used to determine the mobility of certain elements in soils, industrial wastes and other materials, as well as their ionic speciation (Querol et al., 1996). Speciation which provides information about the chemical association of a certain metal is often needed in the modelling and prediction of dissolution

processes. Chemical speciation can be defined as the process of determining and recognizing specific chemical species or binding forms; it allows discernment of the availability and mobility of metals in solid waste samples in order to understand their chemical behaviour and fate. Thus, some useful environmental guidelines for handling potential toxic hazards can be developed. Chemical speciation is of interest in environmental analytical chemistry because the behaviour of trace elements in natural systems depends on the forms, as well as the amounts, which are present (Sočo et al., 2008).

### 2.8 Disposal and Environmental Effect of Fly ash

Fly ash is mainly disposed through either dry or wet disposal methods. In dry disposal, the fly ash is conveyed by truck, chute or conveyor to the disposal site and disposed by building a dry embankment (Bhat, and Lovell, 1996). The ash heap may then be irrigated with water for dust suppression. In wet disposal, the fly ash is mixed with water and transported as slurry through pipes and disposed in ash ponds or dams where over time the water is allowed to drain away. Various environmental risks such as air, surface water and groundwater pollution may be linked to disposed coal fly ash.

Air pollution results from wind-blown ash dust from the ash dump (Dellantonio et al., 2009). Deposition of the air borne particulate material on surface water or soil may lead to the contamination of the surface water or soil. The other serious problems that arise from both ash disposal methods include the need for a large area of land for the construction of the dump or dam which will lead to reduction in arable land over time. Also the construction of new dams and dumps to replace the old ones that are filled up is done at a great cost and further loss of arable land. Another problem is the vast amounts of water that is needed to turn the ash into slurry. The fly ash disposal or storage sites should be monitored for accumulation of species because after combustion the toxic trace elements in coal are left behind in higher concentrations in the coal fly ash (Gitari et al., 2003). Also interaction with water used in the wet disposal method or from the atmosphere may result in

the leaching of toxic metals which may also contaminate the underlying soil and ultimately the groundwater.

### 2.9 Beneficial Application of Fly Ash

The beneficiation of fly ash has been the focus of various studies in order to help with the management of the enormous amount that is generated during coal combustion and disposed as waste (Ahmaruzzaman, 2010). Thus the uses of coal fly ash has been investigated in construction, agriculture, acid mine drainage (AMD) treatment, removal of heavy metals in water treatment and in the synthesis of zeolite and geopolymers (Madzivire et al., 2013; Gitari et al., 2008). Some of these applications are discussed in the following sections and the treatment of AMD with fly ash; its use for geopolymers production and as a feed stock for metal recovery will be covered in more detail since this study is focused on the three processes.

#### 2.9.1 Cement and Construction Industry

The cementitious and pozzolanic properties of coal fly ash allow it to be used by the construction industry in the making of cement or concrete. The cementitious and pozzolanic properties improve the workability, durability and strength of hardened concrete (Jaturapitakkul et al., 2004). Also another significant property of coal fly ash is the loss on ignition (LOI), which is a measure of the amount of unburned carbon remaining in the fly ash (Styszko-Grochowiak et al., 2004). The LOI is as an indicator of the suitability of coal fly ash for use as a cement replacement in concrete. According to ASTM C618, a loss-on-ignition (LOI) greater than 6 % renders fly ash unusable for cement or concrete manufacture, because the presence of carbon can influence air entrainment which is an important property of concrete. Surfactants, or air entraining admixtures that are normally used in the formulation of concrete, can be adsorbed onto the surfaces of the porous residual carbon particles resulting in a reduced resistance of the concrete to freeze and thaw (Senneca, 2008).



Fly ash can certainly be beneficially used in the concrete and construction industries. It is used as a partial replacement for Portland cement in concrete manufacture (Ahmaruzzaman, 2010) and used as a sand supplement in the manufacture of building bricks, blocks and pavers (Manz, 1997). It is also used as a replacement for the fine aggregate (sea sand or machine-ground sand) in concretes and mortars. In addition it is also used as a constituent of light-weight aerated concrete, especially for construction of insulating building blocks. These uses of fly ash could replace many of the low fines concrete blocks used presently. Furthermore it is used as a constituent of “flowable fill” for filling trenches, and surrounding insulation in building basements, shelters, foundations etc (Foner et al., 1999).

### 2.9.2 Ash Absorbent to Remove Heavy Metals in Water Treatment

Heavy metals are among the most important pollutants in wastewater, and are becoming a severe public health problem due to the toxicity of some heavy metals. Removal of heavy metals and metalloids from aqueous solutions is usually carried out by a number of processes such as, chemical precipitation, solvent extraction, ion exchange, reverse osmosis or adsorption etc. Among these processes, the adsorption process may be a simple and effective technique for the removal of heavy metals from wastewater. Fly ash has been widely used as a low-cost adsorbent for the removal of heavy metals such as Ni, Cr, Pb, As, Cu, Cd and Hg from wastewaters. The major chemical composition of fly ash (alumina, silica, ferric oxide, calcium oxide, magnesium oxide and carbon), and its physical properties such as porosity, particle size distribution and surface, highlights its potential as an adsorbent in waste water treatment (Cetin and Pehlivan, 2006).

Heavy metal adsorption on fly ash depends on the initial concentration of the heavy metal, contact time and pH. The initial concentration of heavy metal has a strong effect on the adsorption capacity of the fly ash. The adsorption capacity of fly ash depends on the surface activities, such as specific surface area available for



solute surface interaction. In a certain pH range, most metal adsorption increased with increased pH up to a certain value, and then decreased with a further increase in pH (Krishnan and Anirudhan, 2003). Fly ash can be regenerated after the adsorption, using suitable reagents. Batabyal et al., (1995) reported the regeneration of the used saturated fly ash with 2% aqueous H<sub>2</sub>O<sub>2</sub> solution. The regenerated fly ash was dried, cooled and used for further adsorption. The adsorption rate and equilibrium time were found to be the same as the fresh fly ash particles.

### 2.9.3 Soil Amendment

Fly ash is also used in agriculture as a soil amendment, in composting and as a source of nutrients for plants based on its chemical compositions and physical properties. Fly ash contains almost all the necessary plant nutrients i.e., macronutrients including P, K, Ca, Mg and S and micronutrients like Fe, Mn, Zn, Cu, Co, B and Mo, except organic carbon and nitrogen. It can replace lime, a costly amendment for acid soils; agricultural lime application contributes to global warming through emission of CO<sub>2</sub> to the atmosphere. Use of fly-ash instead of lime as soil ameliorant can reduce net CO<sub>2</sub> emission and thereby lower global warming (Basu et al., 2007). According to Kishor et al., (2010), the beneficial and harmful effects of fly ash application to soil are as follows:

#### Beneficial effects

(1) Improvement in soil texture; (2) reduction in the bulk density of soil; (3) improvement in the water holding capacity of the soil; (4) optimization of the soil pH value; (5) increases the soil buffering capacity; (6) improvement in the soil aeration, percolation and water retention in the treated zone (due to dominance of silt-size particles in fly ash); (7) reduction in crust formation; (8) provision of micro-nutrients like Fe, Zn, Cu, Mo, B etc.; (9) provision of macro-nutrients like K, P, Ca, etc.; (10) reduction in the consumption of soil ameliorants (fertilizers, lime); (11) fly ash can also be used for insecticidal purposes and (12) decreases the metal mobility and availability in soil, due to an increased pH.

### Harmful effects

(1) High pH results in the reduction in bioavailability of some nutrients (generally from 8 to 12); (2) high salinity and (3) high content of phytotoxic elements, especially boron.

Fly ash may be suitable for use on agricultural land where food crops are produced, although potential trace element enrichment in plants from certain types of fly ash may make it more suitable for non-food chain end uses (Punshon et al., 2002).

### 2.9.4 Synthesis of zeolites

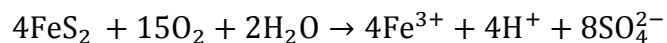
Zeolites are natural or synthetic aluminosilicates that consist of systematic arrangements of  $\text{SiO}_4$  and  $\text{AlO}_4$  tetrahedra. The corresponding substitution of silicon (Si) by aluminium (Al) gives rise to an overall negative charge (Brönsted acid site) that is balanced by cations such as  $\text{Na}^+$ ,  $\text{K}^+$ ,  $\text{Ca}^{2+}$  and  $\text{Mg}^{2+}$ , affording zeolites the property of cationic exchange (Bailey et al., 1999). Synthetic zeolites possess vital and remarkable benefits over their natural equivalents because they can be made in an identical, pure-phase state. Also, appropriate zeolite structures that do not occur in nature can be produced, which has resulted in the classification of more than 200 synthetic zeolite structures (Rayalu et al., 2001). Synthetic zeolites are widely used in separation and refinery industries as catalysts, adsorbents and ion exchangers due to their meso and microporous structures. The significant catalytic activity and selectivity of zeolite materials are attributed to their large internal surface area and highly distributed active Brönsted acid sites that are accessible through their uniform pore sizes, high thermal resistance, chemical inertness and high mechanical strength (Bayati et al., 2008).

Coal fly ash has been confirmed to be a good as starting materials for the synthesis of zeolites due to its high content of aluminosilicate glass, mullite ( $\text{Al}_6\text{Si}_2\text{O}_{13}$ ) and quartz ( $\text{SiO}_2$ ). By applying different synthesis methods, many researchers have synthesized various types of zeolites from fly ash, such as zeolite Na-P1 (Inada et al., 2005), zeolite A (Murayama et al., 2002, Rayalu et al., 2001), and zeolite ZSM-5 (Chareonpanich et al., 2004).

### 2.10 Acid mine drainage (AMD)

Globally, South Africa occupies a prominent position in the mineral markets due to its vast mineral resources which have created outstanding infrastructures and a vibrant economy. However, mining activities have also created a serious environmental threat to the country and AMD has been reported in the different mining sites in South Africa such as the Witwatersrand (Coetzee et al., 2010). AMD refers to the seepage of polluted acidic water ( $\text{pH} < 5.0$ ), loaded with iron, sulphate and other metals. AMD is produced when sulphur-bearing minerals are exposed to oxygen and water (Akcil and Koldas, 2006). It occurs both as a natural process during rock weathering and from activities associated with earth intrusion such as mining (Gaikwad and Gupta, 2007). The latter is the major source of AMD which occurs mostly in abandoned mines but can also occur in active mines and mineralized areas with exposed rocks rich in pyrites ( $\text{FeS}_2$ ) (McCarthy, 2011).

The chemical reactions that occur during the formation of AMD can be summarized as this overall reaction:





A stream destroyed by acid mine drainage in Krugersdorp Game Reserve, South Africa ([www.earthlife.org.za](http://www.earthlife.org.za))

AMD is usually characterised by low pH, high salt content (generally made up of  $\text{SO}_4^{2-}$ ), and high levels of metals – mostly Fe (giving it the characteristic red-orange colour). Depending on the area, the water may contain heavy metals such as Fe, Mn, Al, Cu, Ca, Pb, Mg, Na, Ni and radioactive species Th and U (Taylor et al., 2005; Akcil and Koldas, 2006; Gitari et al 2011).

AMD is a global problem and has been categorised as the biggest distinct environmental challenge confronting the mining industry, due to its persistence and cost. It also most likely to continue to create a problem after the mines have stopped operating. AMD can pollute soil and water supplies as it spreads underground or decants and flows into streams and rivers. AMD pollution may result in the contamination of drinking water and disrupted growth and reproduction of aquatic plants and animals. Thus AMD must be treated to prevent environmental pollution and the costs of treatment vary by several orders of

magnitude depending on site conditions, volume of the AMD, and the chemical nature of the AMD.

### 2.10.1 Treatment technologies of acid mine drainage

The production of alkalinity is the fundamental process in the treatment of AMD (Madzivire, 2013). This causes the metals and sulphates to precipitate or to be reduced and produces a stream of water free of most impurities. Although the general treatment mechanisms may incorporate chemical and/or physical and/or biological processes, the main purpose is to reduce acidity and toxic metal concentrations, increase pH and often lower sulphate concentrations and salinity (Taylor et al., 2005). Acid mine drainage treatment falls under two broad categories, active and passive. Active treatment requires continuous input of a neutralizing agent to the source of the AMD or directly to the stream that has been impacted to maintain the process. Active treatment can be very successful; however, it requires a long-term and continuous commitment to treatment, being an end of pipe treatment technology. Passive treatment involves a variety of techniques to raise the pH and reduce metal loadings through a constructed treatment or containment project. It entails relatively little resource input when in operation but can involve some periodic maintenance. Currently there are several techniques available to remediate AMD, which may be grouped as those that utilise either chemical or biological mechanisms to neutralise AMD and remove metals from solution. Both abiotic and biological techniques comprise those that are classified as active or passive treatment (Johnson and Hallberg, 2005).

AMD can be treated with current techniques if adequate measures are used for specific situations. However, the cost and the environmental impacts of technologies are the major limiting factors (Madzivire, 2013). The current treatments of acid mine drainage in South Africa are not economically sustainable to the South African government hence innovative treatment technologies have been developed in recent years to find more economical ways to treat acid mine drainage in South Africa (Coetzee, 2010). Examples of innovative technologies

## Chapter Two: Literature review

---

developed in South Africa that could be considered for the treatment of AMD (REF) include:

1. The CSIR ABC (Alkali-Barium-Calcium) Process developed by the Council for Scientific and Industrial Research (CSIR). This is a precipitation process that utilizes barium to precipitate dissolved sulphate from mine water. The sludge produced by the process has potential as a source of sulphur and lime making it a cost effective process. However, the pilot studies on the thermal stage have not been successfully completed.

2. SAVMIN was developed by Mintek a research and development organisation in South Africa to treat AMD. The process relies on the selective precipitation of insoluble complexes at different stages during the treatment process and the recycling of some of the reagents used in the process. This also results in the production of potable water and valorisable by-products.

3. High Pressure Reverse Osmosis (HiPRO) Process developed by South African turnkey project house Keyplan and is in use at Anglo Coal mines in Mpumalanga. The process transforms water with a high acidity and sulphate concentration into superior-quality drinking water for use by local communities.

4. Slurry Precipitation and Recycle Reverse Osmosis (SPARRO). A variation of the membrane desalination process was developed to treat AMD in South Africa. The concept of the SPARRO process is based on the protection of the membrane surfaces by providing a slurry suspension onto which the precipitation products can form. High water recoveries were achieved by a demonstration scale plant (Pulles et al., 1992).

5. Environmental and Remedial Technology Holdings (EARTH Ion Exchange). This process is an ion exchange based process that was developed by Environmental and Remedial Technology Holdings (Earth) (Pty) Ltd for the purification of mine water for discharge or re-use as agricultural, process,

## Chapter Two: Literature review

---

industrial or potable water . The process was designed to produce potable water and useful and saleable products waste such as ammonium sulphate solution and mixed metal nitrate solution (Howard et al, 2009). The viability of this technology depends on stable prices and available markets for the products.

6. The Rhodes BioSURE process was developed by the Environmental Biotechnology Group (EBRU) of Rhodes University in the early 1990s. The bio-process takes out acidic sulphate from AMD by utilizing free waste feedstock, such as sewage sludge, in place of expensive carbon and electron donor sources (ethanol and hydrogen). BioSURE has been used at Grootvlei by ERWAT (the East Rand Water Care Company).

The Inter-ministerial Committee on acid mine drainage of South Africa studied several of the current and possible treatment methods that were developed to be used as a solution for active remediation of AMD in the country. The study summarised that AMD treatment has proven to be very costly in South Africa as all of the treatment methods listed above are not sustainable. This is because the difference of the running costs and the income that can be generated from the products from the treatment process is negative as shown in Table 2.5. below.



## Chapter Two: Literature review

Table 2:5: The running costs and possible income that can be generated from the products of the various technology proposed by the Inter-ministerial Committee on acid mine drainage (Coetzee et al., 2010).

Technology	Running costs (R.m <sup>-3</sup> )	Income (R.m <sup>-3</sup> )	Difference (R.m <sup>-3</sup> )
Alkali Barium calcium	4.04	3.56	-0.49
HDS HiPRO	9.12	3.35	-5.78
SPARRO	12.79	4.29	-8.51
SAVMIN	11.3	3.84	-7.46
EARTH ion exchange	12.95	10.7	-2.25
BioSURE	3.8	0	-3.8
Lime treatment	5.5	0.7	-4.8

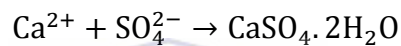
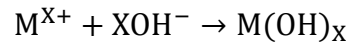
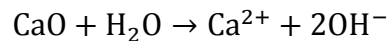
### 2.10.2 Treatment of acid mine drainage with coal fly ash

Acid mine drainage treatment with coal fly ash is of one the innovative technologies being studied for sustainable treatment of acid mine drainage in South Africa. The utilisation of fly ash as a possible treatment agent for AMD has been the focus of several research studies (Abbott et al., 2001; Xenidis et al., 2002; Pérez-López et al., 2007a-c; Gitari et al., 2010). The outcome of these research investigations has established that fly ash can be used as an alternative, cheap and economically viable agent compared to the conventional alkaline agents such as limestone and lime. The treatment of AMD with coal fly ash is cheap because fly ash is found close to the coal mines since most coal power station are built close to the coal mines. This means low transport costs of fly ash to the treatment facility. Also because fly ash is a waste material; using it for water treatment will go a long way in achieving zero effluent discharge in coal mines and coal fired power stations.

The treatment of mine water with fly ash takes advantage of the available CaO in the fly ash to neutralize the mine water. Extensive study of the AMD remediation



with coal fly ash (Madzivire, 2010; Madzivire, 2012) revealed that fly ash can neutralize AMD when mixed together due to the dissolution of CaO from the fly ash which raises the pH of the AMD. This increase in the pH leads to the precipitation of heavy metals in the form of hydroxides, and sulphates in the form of gypsum. This result's not only in the removal of heavy metals and sulphates but also of some trace elements in mine water due to sorption capabilities of the surface of metals hydroxides precipitated (Gitari, et al., 2011).



Research also demonstrated that the use of high energy mixing devices such as a jet loop reactor increased the dissolution of fly ash matrix and increased the kinetics of the reactions during treatment as well as reduced the amount of fly ash used in the treatment (Madzivire, 2010).

The chemistry of the treatment of acid mine drainage treatment with coal fly ash is now well understood. However, this treatment option also leads to generation of solid waste (AMD/FA residue) that requires disposal. Various heavy metals (As, Cd, Hg, and Pb) and radionuclides (U and Th) are present in AMD and fly ash as revealed by the elemental analysis of AMD and coal fly ash. This study will investigate the treated water and the AMD/FA residue in order to determine where the toxic heavy metals and radionuclides end up.

### 2.11 Geopolymer

Geopolymer is a term introduced by Davidovits in 1979, to designate a class of amorphous to semi-crystalline three-dimensional silico-aluminate materials that he developed. These materials that could be considered as a new binder or new

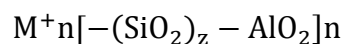
## Chapter Two: Literature review

---

cement for concrete resulted from his quest to develop non-flammable and non-combustible plastic materials in the aftermath of the catastrophic fires in France between 1970 and 1972 which involved common organic plastic. Presently the term geopolymer is generically used to describe the amorphous to crystalline products that are formed in the reaction of aluminosilicate with alkali hydroxide/alkali silicate solution (Duxson et al., 2005). Research has shown that materials containing large amounts of silica and alumina that are partially dissolved in alkaline solutions may be used as reagents for the synthesis of geopolymers. These include natural minerals such as kaolinite, feldspar, albite and stilbite. Treated minerals can also be used such as metakaolinite and waste materials such as building waste, blast furnace slag and fly ash (Xu and Van Deventer 2002; Álvarez-Ayuso et al., 2008), thus making them cheap to produce.

Geopolymers comprise of a Si–O–Al structure with alternating SiO<sub>4</sub> and AlO<sub>4</sub> tetrahedral linked together in three dimensional by sharing all the oxygen atoms. Positive ions such as Na<sup>+</sup>, K<sup>+</sup> and Ca<sup>2+</sup>, must be present as charge balancing cations in the framework cavities to balance the negative charge of Al<sup>3+</sup> in IV fold coordination (Izquierdo et al., 2009). Thus, in order to appropriately designate the geopolymeric structures, a terminology “poly(sialate)” was proposed. The sialate is an abbreviation for silicon-oxo-aluminate: Polysialates are chain and ring polymers with Si<sup>4+</sup> and Al<sup>3+</sup> in IV-fold coordination with oxygen and are of the types: poly(sialate) (-Si-O-Al-O) (Si:Al = 1); poly(sialate-siloxo) (-Si-O-Al-O-Si-O-) (Si:Al = 2) and poly(sialatedisiloxo) (-Si-O-Al-O-Si-O-Si-O-) (Si:Al = 3) (Davidovits 1991; Komnitsas and Zaharaki, 2007).

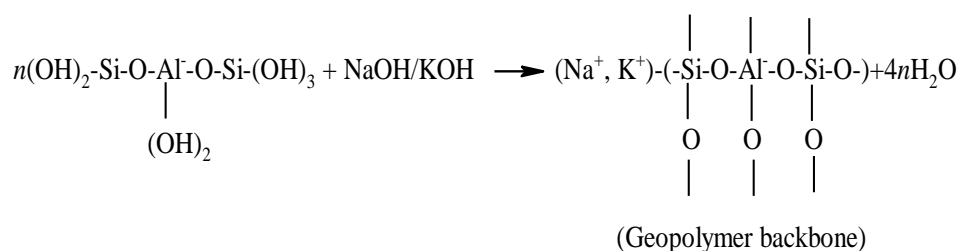
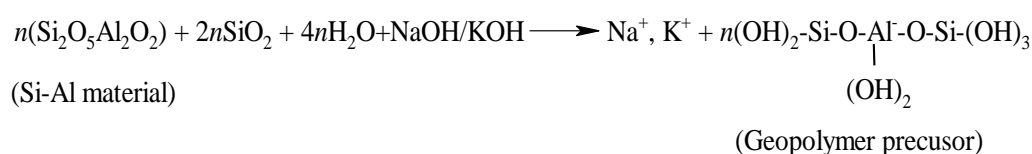
The general formula to describe the chemical composition of polymers is:



Where z (Si/Al ratio) is 1, 2 or 3, M is an alkali cation (such as K<sup>+</sup> or Na<sup>+</sup>) (Davidovits 1991; Álvarez-Ayuso et al., 2008).

### 2.11.1 Geopolymerisation

Geopolymerisation is a term that describes the process involving the formation of geopolymers. It is based on an intricate heterogeneous reaction that occurs between a solid material rich in aluminosilicate oxides and an alkali metal silicate solution under highly alkaline conditions. The geopolymerisation reaction is exothermic and carried out under atmospheric pressure at temperatures below 100° C. The process involves four main steps that can overlap with each other and occur almost simultaneously. The first is the generation of reactive species or alkali activation, which is the dissolution of amorphous phases (e.g., aluminosilicates) by alkali to produce small reactive monomeric or dimeric silica and alumina. The second step is the reorientation, which is the transportation or orientation or condensation of precursor ions into oligomers. The third step is the actual setting reaction, which is the polycondensation process leading to the formation of amorphous to semi-crystalline aluminosilicate polymers. The last stage involves the bonding of the undissolved solid particles into the geopolymeric framework and hardening of the whole geopolymeric system (Buchwald et al. 2004; Duxson et al. 2005, 2007). However, these three steps can overlap with each other and occur almost simultaneously, thus making it difficult to isolate and examine each of them separately (Palomo et al. 1999). Geopolymerisation may be presented schematically as follows:



### 2.11.2 Properties and applications of geopolymers

Geopolymers have good physiochemical and mechanical properties such as low density, micro- or nano-porosity, small shrinkage, high strength, great surface hardness and significant thermal stability, heat and fire resistance, chemical resistance, and high compressive strength. The starting raw materials play a vital role in the geopolymerisation reaction and control the chemical composition and microstructure of the final geopolymeric products (Van Jaarseveld et al. 2003; Duxson et al. 2007). Varying the silica to alumina and alkaline to silica ratio results in geopolymers with different physiochemical and mechanical properties. Owing to these properties, geopolymers are considered as alternative materials for certain industrial applications in the areas of civil engineering, plastics industries, automobile and aerospace, mining and metallurgy (Davidovits 1991).

Several studies have been focused on the utilization of coal fly ash in the development of geopolymers as a replacement for cement in the construction industry (Duxson et al. 2007; Lloyd et al., 2010). The production of ordinary Portland cement (OPC) pollutes the environment due to the huge amount of CO<sub>2</sub> that is emitted by the cement plant into the atmosphere during lime kilning. The CO<sub>2</sub> results from the burning of large amount of fuel and the decomposition of limestone and cement plants may emit up to 1.5 billion tons of CO<sub>2</sub> into the atmosphere annually (Al Bakri et al., 2012). The interest in the use of fly ash for geopolymer production globally, is due to the abundance of this industrial waste that is rich in Si and Al (Van Jaarseveld et al. 2003). Another major advantage for the use of fly ash is its cementitious properties. Furthermore geopolymer can be synthesised from fly ash and high alkaline solution at room temperature (Srinivasan and Sivakumar, 2013). In this study geopolymer synthesised from coal fly ash will be investigated in order to determine if the toxic elements in the fly ash based geopolymer are locked up in the geopolymer matrix or the extent to which these elements are leached out when the geopolymer concrete comes into contact with water.

### 2.12 Extraction of metals from coal fly ash

It is well-known that coal fly ash contains elements such as aluminium, iron, and titanium, as well as trace amounts of other valuable metals such as the REEs. The review of literature has revealed several methods and techniques to accomplish the extraction of various valuable elements from coal fly ash (Iyer and Scott, 2001; Matjie et al., 2005). Some methods are aimed at extraction and recovery of elements of interest such as aluminium and iron present in coal fly ash, (Prakash et al., 2001; Bai, et al., 2010). The others techniques are focused on methods of purifying the extracted element of interest by the removal of other elements (Shuangqing Su et al., 2011). Some methods have also investigated the extraction of minor and trace elements in fly ash (Mohapatra and Rao, 2001; Font et al., 2007). Potential methods that have been applied in the recovery of valuable resources from coal fly ash include physical and chemical treatments.

The magnetic separation method has been applied in the removal of the iron oxide present in coal fly ash (Prakash et al., 2001). It has also been utilised in several studies as a pre-stage before the main operations of ash treatment (Shin et al., 1995; Scott et al., 2001). The Fe material obtained from this process has found useful applications as source of nano Fe (Gilbert, 2014). Coal ash usually consists of 4-10% Fe (as  $\text{Fe}_2\text{O}_3$ ). The possibility of recovering the magnetic fraction from South African fly ash and its classified fractions has been studied. It was reported that the total Fe (as  $\text{Fe}_2\text{O}_3$ ) in Hedrina coal fly ash determined by XRF was  $4.52 \pm 0.06\%$ . The magnetic fraction obtained after fly ash magnetic separation was rich in Fe ( $93.15 \pm 2.12\%$  as  $\text{Fe}_2\text{O}_3$ ). The non-magnetic residue was depleted of Fe and contained  $1.56 \pm 0.06\%$  Fe as  $\text{Fe}_2\text{O}_3$  (Gilbert, 2014).

Almost all of the world's aluminium is produced using alumina generated from the Bayer process. This is the most economic means of obtaining alumina from bauxite and was developed by Karl Bayer in the late 19th century (Habashi, 1995). Three major steps are involved in the Bayer process namely: extraction, precipitation, and calcination (Hind et al., 1999). The extraction stage, involves

## Chapter Two: Literature review

---

the digestion of bauxite with a solution of NaOH to yield aluminate liquor, containing alumina in the form of  $\text{Al}(\text{OH})_4$ . In the precipitation step, crystalline alumina trihydrate, (gibbsite,  $\text{Al}_2\text{O}_3 \cdot 3\text{H}_2\text{O}$ ) is precipitated from the digested aluminate liquor by hydrolysis. Finally, in the calcination process water is driven off from the crystalline gibbsite,  $\text{Al}_2\text{O}_3 \cdot 3\text{H}_2\text{O}$  to form alumina ( $\text{Al}_2\text{O}_3$ ).

The uses of aluminium are enormous and diverse, ranging from consumer packaging to automobile parts, paints, cosmetics, and even pharmaceuticals. Coal fly ash contains a substantial amount of aluminium oxide (20-30 wt. %) and a high level of silica (40-65 wt. %). However, a large amount of aluminium of the coal fly ash exists as components of mullite ( $\text{Al}_6\text{Si}_2\text{O}_{13}$ ) which makes it impossible to recover through the Bayer method (Yao et al., 2014). The mullite phase in coal fly ash is a secondary mineral that results from the thermal chemical reactions between alumina and silica (kaolinite) in the course of the coal combustion.. To achieve the greatest aluminium extraction from coal fly ash, these mullite surfaced spheres have to be broken down or disintegrated to free the alumina confined as well as aluminium bonded within mullite (Bai, et al., 2010). Although hydrofluoric acid can effectively decompose the mullite in coal fly ash, its industrial application is limited due to high cost and toxicity that makes it an environmental hazard.

The techniques used for the extraction of aluminium from coal fly ash are generally categorised into acidic, alkali and acidic-alkali method. The acidic method entails acid-resistant and air-tight processing equipment. The acidic-alkali method is an intricate process with a sequence of procedures, which involves sintering, silica-alumina separation, purification, precipitation, etc. In order to avoid high energy calcination, the alkali dissolution method is promising. A two-step alkali dissolution process has been used in preparing ultrafine  $\text{Al}(\text{OH})_3$  product from coal fly ash. The first step was to desilicate the fly ash in order to increase the Al/Si ratio. The second step was the extraction of  $\text{Al}(\text{OH})_3$  with a 89% recovery (Shuangqing Su et al., 2011).

### 2.12.1 Recovery of rare earth elements from coal fly ash

Studies on coal fly ash, derived from South African power generation (Fatoba, 2008; Akinyemi, 2010; Eze, 2011) have shown that rare earth elements such as La, Ce, Nd and Y are present in this solid waste. There is an increasing demand for REE in international markets because of their applications in advanced technologies such as satellite communications, wind turbines, permanent magnets and appliances such as cell phones, flat screen television and hybrid cars that form part of our everyday life. This has prompted identifying new mineral sources to ensure adequate supply for present and future use.

REE are not as "rare" as their name implies but are enriched in the earth's crust and usually occur together naturally due to their similar ionic radii and oxidation state. This similarity in ionic radii and oxidation states of the REE allow for easy replacement of the REE for each other into various crystal lattices. This replacement accounts for their wide distribution in the earth's crust and the characteristic multiple occurrences of REE within a single mineral. REE are moderately abundant in the earth's crust, some even more abundant than copper, lead, gold, and platinum (Moldoveanu and Papangelakis, 2012). While some are more abundant than many other minerals, most REE are not concentrated enough to make them easily exploitable economically. Most REE throughout the world are located in deposits of the minerals bastnaesite and monazite (Jiang et al., 2005; Nasab et al., 2011; USGS, 2011).

There is considerable variation in the mining and processing methods employed in the exploitation of REE deposits due to the diversity of their mineral deposits.

Hydrometallurgy processes have been used in the extraction of REE from waste material such as spent optical glass (Jiang et al., 2005). The technique is becoming a well-established and efficient method of recovering metals from raw materials and secondary sources. This is because hydrometallurgical processes, using selective leaching technology, can often chemically beneficiate mineral ores that are difficult to separate using conventional mineral processes (Habashi, 2005).



Hydrometallurgy is a field of chemical technology concerned with the production of metals from their ores and secondary sources. Hydrometallurgical processes include leaching, transferring desirable components into solution using acids or halides as leaching agents; concentration of the leach solution as well as metal recovery from the solution (Kamberović et al., 2009).

The extraction separation and purification of REE from ores have gained considerable attention because of the ever-increasing demand for REE. The high cost of these processes results in the high cost and relative scarcity of REE. Hence, the advantage of recovering REE from fly ash over minerals is in the availability of fly ash as an already mined fine powder that can be readily processed chemically. Thereby eliminating the cost of excavation, pulverization, and grinding of the minerals to a fine powder necessary for chemical processing. The ability to extract REE from coal fly ash is important in terms of economic and environmental issues because the procedure can be used to produce value-added products from stored coal fly ash. One of the objectives of this investigation is to develop a practical method to leach out the REE in coal fly ash. This will involve systematically extracting major fly ash components such as Fe, Si, Al and Ca in order to pre-concentrate or leach out the trace constituent such as REE.

### **2.13 Determination of the elemental composition of coal fly ash**

Globally, coal fly ash has been studied extensively to understand the environmental impacts associated with its reuse, disposal and management. Research of coal fly ash derived from South African power generation (Fatoba, 2008; Akinyemi, 2011; Eze, 2012; Madivire, 2013), has shown that REE such as La, Ce, Nd and Y; toxic elements such as As, Cd, Cr, Pb and Se; and radionuclides such as Th, U, Ra and radio isotopes of K and Pb are present in this solid waste. These elements have economic and toxic potential, hence an accurate method of determining the total elemental content of fly ash is fundamental in the qualitative and quantitative analysis of the elements of toxicity and value in fly ash. The analytical methods widely used in determining the elemental



compositions of fly ash are X-ray Fluorescence (XRF) spectroscopy (Adriano et al., 1980; Dogan et al 2001); inductively coupled plasma - optical emission spectrometer/Mass Spectrometry (ICP-OES/MS) (Parami et al, 2010; McNally et al, 2012); Laser Ablation Inductively Coupled Plasma Mass Spectrometry (LA-ICP-MS) (Spears, D. 2004) and instrumental neutron activation analysis (INAA) (Smolka-Danielowska, 2010).

### 2.13.1 X-ray Fluorescence (XRF)

X-ray Fluorescence (XRF) spectroscopy is generally used for the qualitative and quantitative elemental analysis of major elements in solid environmental, geological, biological, industrial and other samples. It has been used extensively for the qualitative and quantitative elemental analysis of fly ash (Smith et al., 1979; Vijayan et al., 1997; Adriano et al., 1980). The XRF spectrometer works on the principle of bombarding atoms with X-rays which knock out inner shell electrons thus creating vacancies. These vacancies are then filled up when outer shell electrons fall back from higher energy levels. This phenomenon emits fluorescence energy and wavelength spectra, which are characteristic of atoms of specific elements thus enabling the estimation of their relative abundances (Weltje & Tjallingii, 2008).

XRF offers a major advantage in that it is non-destructive, fast, cost-effective (Czichos et al., 2006). It can analyse many elements in the periodic table ranging from beryllium (Be) with atomic number 4 to uranium (U) with atomic number 92 at trace levels (ppm). Its disadvantages are that analyses are normally limited to elements heavier than fluorine (Djingova et al., 1998) and that a large amount of sample is required for analysis due to the sample preparation method (Richardson et al., 1995). Furthermore the XRF technique cannot compete in accuracy with other well established techniques for trace element analysis (Misra, 2011).

### 2.13.2 Inductively coupled plasma - optical emission spectrometer (ICP-OES)

The inductively coupled plasma - optical emission spectrometer (ICP-OES) is one of the Inductively Coupled Plasma (ICP) spectroscopic techniques that are used to determine concentrations of a wide range of elements in solution. ICP-OES makes use of the fact that the atoms of elements can take up energy from an inductively coupled plasma, are thereby excited, and fall back into their ground state again emitting a characteristic radiation (Meynen et al. 2009). The identification of this radiation permits the qualitative analysis of a sample.

ICP-OES is a robust analytical method capable of providing analyses for a wide range of elements in a diversity of sample matrices. According to Olesik et al., (1991), the precision of ICP-OES ranges between 0.2 - 0.5 % for liquid samples or dissolved solids while accuracy ranges from 10% using simple, pure aqueous standards, to 0.5% using more elaborate calibration techniques. The sensitivity of ICP-OES ranges from sub-ppb to 100 ppb (Holloway & Vaidyanathan, 2009).

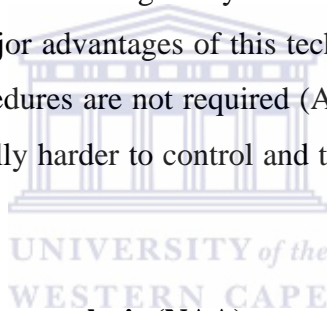
The ICP-OES/MS technique has been used in determining the concentration of elements in fly ash and its main disadvantage is that the fly ash has to be digested before analysis (Hou and Jones, 2000; Chen and Ma, 2001). An acid digestion required for the ICP-OES analysis of fly ash may result in contamination of the sample from the acid and the subsequent dilution technique (Hannaker et al., 1984; Brown and Milton, 2005). Acid digestion also enhances matrix effect which has a huge impact on the quantification of the elements determined by ICP-OES.

### 2.13.3 Laser Ablation Inductively Coupled Plasma Mass Spectrometry (LA-ICP-MS)

The Laser Ablation Inductively Coupled Plasma Mass Spectrometry (LA-ICP-MS) technique is a versatile and strong analytical method that can be used for the

direct analysis of solid samples (Günther, 2002). The LA-ICP-MS technique involves the direct ablating of the sample material to create aerosols that are transported into the core of inductively coupled argon plasma (ICP) (Spears, 2004), which generates temperature of approximately 8000°C. The plasma in ICP-MS is used to generate ions that are then introduced to the mass analyser. These ions are then separated and collected according to their mass to charge ratios.

The applicability of LA-ICP-MS has been demonstrated on a wide variety of samples, where major, minor, and trace element concentrations or isotope ratio determinations have been of interest. The major advantages of this technique are that sample-size and sample preparation procedures are not required (Alexander, et al, 1998). Also any type of solid sample can be ablated for analysis and the technique is capable of determining many trace elements down to low ppm or even ppb levels. The major advantages of this technique are that sample-size and sample preparation procedures are not required (Alexander, et al, 1998). Though, sample aliquots are usually harder to control and to assess accurately (Brown and Milton, 2005).

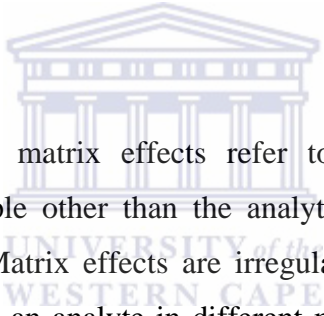


#### 2.13.4 Neutron activation analysis (NAA)

Neutron activation analysis (NAA) is a valuable technique for qualitative and quantitative identification of the major, minor, and trace elements in a sample. NAA is one of the most accurate techniques for identifying elemental abundances known. In this analytical technique the sample is bombarded with neutrons to produce radioactive atoms whose emissions are indicative of the elements present. The basic requirements for NAA include the detailed understanding of the reactions that occur when neutrons interact with the target nuclei. Also required are a source of neutrons and an instrument that can detect gamma rays accurately. NAA is widely performed in many different fields of science because of its sensitivity and precision. This technique is able to detect all the elements in a sample, irrespective of their chemical form or oxidation state (Hibstie, et al, 2013).

Instrumentation neutron activation analysis (INAA) is regarded as a very consistent and accurate technique for trace element certification and as a reference method when other analytical techniques provide illogical results (Orvini and Speziali, 1998). INAA is a valuable technique for qualitative and quantitative identification of the major, minor, and trace elements in a sample (Araripe et al, 2006). INAA is one of the most accurate techniques for identifying elemental abundances known (Hibstie, et. al, 2013). The XRF, ICP-OES and LA ICP-MS are competitive with INAA in terms of sensitivity, selectivity, and multi element capability. However, INAA still maintains a unique position in the analytical circle due to its capacity for blank-free and matrix-independent multi element determinations which makes it an excellent reference technique (Ehmann and Vance 1989; Brown and Milton, 2005).

### 2.13.5 Matrix effects



In analytical chemistry, matrix effects refer to the combined effect of all components of the sample other than the analyte, on the measurement of the quantity (Patel, 2011). Matrix effects are irregularities in analyte response that occur when investigating an analyte in different material matrices (Windom and Hahn, 2009). Matrix effects may considerably affect method performance parameters such as limit of detection (LOD), limit of quantification (LOQ), linearity, accuracy and precision (Patel, 2011). Thus influencing the ability of an analytical method to qualitatively identify and quantitatively measure target compounds in environmental and other samples by indirectly affecting the intensity and resolution of observed signals. The XRF, ICP-OES and LA ICP-MS techniques are prone to matrix effect.

In the ICP-OES maintaining accuracy and precision is generally limited by matrix effects (Boss and Fredeen, 1999). Matrix effects are caused by the major elements in the samples (e.g. easily ionisable elements (EIEs) such as Na, K, Li) (Todoli et al. 2002) or reagents used for sample digestion and solution storage (e.g. mineral acids such as HNO<sub>3</sub>, H<sub>2</sub>SO<sub>4</sub>, HCl) (Todoli and Mermet 1999). It is a fundamental

problem with accuracy of the quantitative elemental analysis of coal fly ash using ICP-OES because excess acid from acid digestion can be a source of error in the analysis (Eze et al., 2014).

Matrix effects include the following: atomization and volatilization interference, nebulisation interference, transfer and desolvation interferences, chemical interference and ionization interference. Matrix effects result in the suppression or enhancement of analyte signal and are usually caused by the changes in the energy transfer between the plasma and sample (during the processes of atomization, excitation and ionization) and the changes in the efficiency of sample aerosol formation, transport and filtration (Kola and Perämäki 2004). In the case of elemental matrix effects, there is no satisfactory study explaining the causes and mechanism of these interferences due to the complexity of the processes related to these effects. As explained by Lehn et al. (2003) this could be because of the differences in the behaviours of the elements and although a hypothesis can be used to explain the effects for the most of the elements, there is usually at least one element that does not follow the observed trend.

UNIVERSITY of the  
WESTERN CAPE

### 2.13.6 Accuracy and precision

In this study the elemental content of Matla fly ash will be fully determined using XRF, ICP-OES, LA ICP-MS and NAA. The results obtained will be compared in order to establish the analytical technique that is most cost effective and accurate thus best suited for determining the different categories of elements that are contained in fly ash.


The key points that will be considered in selecting any analytical technique are accuracy and precision. Accuracy is the measurement of how close an experimental value is to the true value. It is realized by use of control samples with known compositions, which are treated in the same way as routine samples. Control samples allow monitoring of the performance of the whole analytical procedure, including all sample preparation steps. In order to demonstrate

## Chapter Two: Literature review

---

accuracy of the method, analysis of (standard, certified) reference materials (RMs) is the most commonly used. Another way to confirm accuracy of the method of interest is to compare results with those obtained with well established (reference) and independent procedures (Welna et al., 2011).

Precision (reproducibility) is the degree to which further measurements or calculations show the same or similar results. It is expressed by means of relative standard deviation of measurements (RSD). The smaller RSD value, the higher precision is obtained. The XRF, ICP-OES and LA ICP-MS are generally based on analysing standards with known concentrations and comparing them to the concentrations in the analysed sample for identification and quantification. The relative standard deviations (RSD) obtained from the concentrations of the elements in the certified standards used to calibrate the instruments is calculated as follows:


$$\frac{\text{Expected value} - \text{Analytical value}}{\text{Expected value}} \times 100\%$$

UNIVERSITY of the  
West Indies

Expected value = value of the certified standard; Analytical value = value obtained when certified was analysed.

The percentage RSD calculated is used as a measure of accuracy and precision of the instrument/analytical technique and reported results should have significant figures that fall within the standard deviations of the techniques.

### 2.14 Characterisation techniques

The other analytical methods used in this study in the characterisation of the Matla fly ash, MFA/AMD residue and synthesised geopolymer are X-ray diffraction (XRD), which is used in determining the mineral phases present in the samples. The Fourier Transform Infrared spectroscopy (FT-IR) will be used to analyse the functional group that are presents in the samples. Morphological

analysis will be carried out with scanning electron microscopy (SEM)-EDS and gamma spectroscopy will be used to measure radioactivity.

### 2.14.1 Mineralogical analysis (XRD)

X-ray diffraction (XRD) is an analytical technique which uses the diffraction pattern produced by bombarding a single crystal with X-rays to determine the phase identity and crystal structure. The diffraction pattern is recorded and then analysed or "solved" to reveal the nature of the crystal (Wicks et al., 1995). This technique is widely used in chemistry and biochemistry to determine the structures of an immense variety of molecules, including inorganic compounds, DNA, and proteins. When single crystals are not available, related techniques such as powder diffraction or thin film x-ray diffraction coupled with lattice refinement algorithms such as Rietveld refinement may be used to extract similar, though less complete, information about the nature of the crystal. The atomic spacing in the crystal lattice can be determined using Bragg's law ( $n\lambda=2d\sin\theta$ ) (Scrivener et al. 2004). The electrons that surround the atoms, rather than the atomic nuclei themselves, are the entities that physically interact with the incoming X-ray photons. If the angles of incidence ( $\theta$ ) and the wavelength ( $\lambda$ ) are known, the spacing  $d$  of the reflecting atomic planes can be determined using the above equation. The lattice spacing is characteristic of the mineral, thus, the X-ray diffraction method can be used for the identification of minerals and for the analysis of mixtures of minerals.

### 2.14.2 Fourier Transform Infrared Spectroscopy (FT-IR)

The Fourier transform infrared (FT-IR) spectrometer is the most common type of infrared (IR) spectrometer. IR spectroscopy is the study of the interaction of IR light with matter and the technique can be used for identifying and analysing chemical compounds. The technique measures the range of wavelengths in the IR region that are absorbed by a sample when irradiated with an infrared source. Absorption in the IR region gives rise to changes in vibrational and rotational



## Chapter Two: Literature review

---

position of the molecules in the sample. The absorption frequency relies on the vibrational frequency of the molecules, while the absorption intensity relies on how well the IR photon energy can be passed on to the molecule. This depends on the change in the dipole moment that arises due to molecular vibration. Thus, a molecule will absorb IR light only if the absorption causes a change in the dipole moment. Consequently, every compound except for elemental diatomic gases such as N<sub>2</sub>, H<sub>2</sub> and O<sub>2</sub>, have IR spectra (Åmand, and Tullin, 1999). The patterns of absorption bands at the different wavelengths throughout the IR region are distinctive to each molecule and are used to identify molecular components and structures.

Absorption bands in the range of 4000 - 1500 wavenumbers (cm<sup>-1</sup>) are usually due to functional groups such as -OH, C=O, N-H, CH<sub>3</sub>, etc. The region between 1500 - 400 wavenumbers is referred to as the fingerprint region (Cooke, 2005). Absorption bands in this region are mostly due to intra-molecular phenomena, and are very specific for each substance. These highly specific signals are decrypted and interpreted using a mathematical technique called Fourier transformation. This process creates a computer-generated mapping of the spectral information. The resulting graph is used to search against reference libraries for identification of the sample.

A major advantage of IR spectroscopy is its capability as an analytical technique to acquire spectra from a very wide range of solids, liquids and gaseous samples. However, in most cases some form of sample preparation is required and it is the most challenging aspects of IR analyses (Hsu, 1997). This is due to the opacity of some samples to IR radiation; these types of samples must be dissolved or diluted in a transparent matrix in order to obtain good quality spectra. Attenuated Total Reflectance (ATR) is the most widely used IR sampling tool. ATR normally permits qualitative or quantitative analysis of samples with little or no sample preparation, which significantly improves sample analysis. The advantages of ATR-FTIR are that it is relatively fast, and that through the use of different accessories, single and multiple internal reflections can be used in characterization



of highly IR absorbent materials such as rubbers and polymers. These qualities make ATR-FTIR a popular tool for structural elucidation and compound identification.

The main goal of IR spectroscopic analysis in this study is to determine the chemical functional groups in the sample. This will enable the comparative study of the fly ash and the reuse products and wastes in order to understand the structural changes arising from the beneficiation processes and to identify any new compound formed during the processes.

### 2.14.3 Morphological Analysis (SEM)

The scanning electron microscope (SEM) is a type of electron microscope capable of producing high-resolution images of a sample surface. The SEM uses a focused beam of high-energy electrons to generate a variety of signals at the surface of solid specimens. The signals that are derived from electron-sample interactions reveal information about the sample (Thomas and Gai, 2004). Due to the manner in which the image is created, SEM images have a characteristic three-dimensional appearance and are useful for judging the surface structure and morphology (texture), and crystalline structure and orientation of materials making up the sample. The SEM is routinely used to generate high-resolution images of shapes of objects and to show spatial variations in chemical compositions. It is also widely used to identify phases based on qualitative chemical analysis and/or crystalline structure. Precise measurement of very small features and objects down to 50 nm in size is also accomplished using the SEM. Specimen preparation includes drying the sample in the oven at 100 °C and making it conductive, if it is not already. Photographs are taken at a very slow rate of scan in order to capture greater resolution. SEM is typically used to examine the external structure of objects that are as varied as biological specimens, rocks, metals, ceramics and almost anything that can be observed in a dissecting light microscope (<http://mcc.lsu.edu/More%20about%20SEM.html>). Scanning electron microscopy examines structure by bombarding the specimen with a scanning

beam of electrons and then collecting slow moving secondary electrons that the specimen generates (Thomas and Gai, 2004). These are collected, amplified, and displayed on a cathode ray tube. The electron beam and the cathode ray tube scan synchronously so that an image of the surface of the specimen is formed.

### Detection of secondary electrons

The most common imaging mode monitors low energy (<50 eV) secondary electrons. Due to their low energy, these electrons originate within a few nanometres from the surface. The electrons are detected by a scintillator-photomultiplier device and the resulting signal is rendered into a two-dimensional intensity distribution that can be viewed and saved as a digital image. This process relies on a raster-scanned primary beam. The brightness of the signal depends on the number of secondary electrons reaching the detector. If the beam enters the sample perpendicular to the surface, then the activated region is uniform about the axis of the beam and a certain number of electrons escape from within the sample. As the angle of incidence increases, the "escape" distance of one side of the beam will decrease, and more secondary electrons will be emitted. Thus steep surfaces and edges tend to be brighter than flat surfaces, which results in images with a well-defined, three-dimensional appearance. Using this technique, resolutions less than 1 nm are possible.

#### 2.14.4 Gamma ray spectrometry

Gamma ray spectroscopy is an analytical technique for detecting and identifying and determining gamma emitting radioactive materials. It is a powerful non-destructive analytical method used for the qualitative and quantitative determination of gamma emitters in soil, waste, environmental samples etc. (Ebaid, 2010; Muhammad, et al., 2010). The analytical technique is the same whether the radioactivity is natural or laboratory induced. Hence both in-situ and laboratory gamma spectroscopy are frequently used for monitoring and evaluating radioactivity and radiation dose rates in the environment resulting from both

## Chapter Two: Literature review

---

natural and anthropogenic sources (Muhammad, et al., 2010). Currently, gamma ray spectroscopy is used in many areas in determining the types and quantities of radioactive nuclides induced in various materials (Ashbaugh, 1992). Gamma-ray spectroscopy is a viable analytical tool because each radioactive nuclide has a unique radiation signature that separates it from all other radionuclides. Generally, radionuclides decay by gamma ray emission, the emitted radiation (gamma rays) and the energy or energy distribution of that radiation identifies each nuclide or isotopes present (Browne et al., 1986).

Gamma rays are produced when nuclei of a radioactive element of higher energy decay to nuclei of lower energy. Gamma radiation is an electromagnetic radiation like x-ray, visible light, radio waves, and ultraviolet light. This electromagnetic radiation differs only in the amount of energy it possesses and gamma photons have no mass and no electrical charge. Gamma ray spectroscopy measures electromagnetic radiation in the gamma ray spectrum of radioactive sources through counting and measuring the energy of individual photons emitted from elements. The measured energy of a gamma ray relates to the type of element and its isotope, while the number of counts corresponds to the abundance of the radioactive source.

The process of measuring a gamma ray begins at the radioactive source, which emits high energy photons during its unstable decay. Once one of the photons gets absorbed by a detector, there is a reaction that causes the electrons to get excited and exude energy. This energy given off by the electrons is then recorded by electronic sensors as an analog signal. After processing and often amplifying the analog signal are changed by convertors to digital signals that can be translated by a computer. Finally, the computer records the energy level of each pulse and adds up all of the pulses onto a histogram.

### 2.15 Ion Chromatography (IC)

## Chapter Two: Literature review

---

Ion chromatography is a form of liquid chromatography that uses ion-exchange resins to separate atomic or molecular ions based on their interaction with the resin. Its greatest utility is for analysis of anions for which there are no other rapid analytical methods. It is used for water chemistry analysis. Ion chromatographs are able to measure concentrations of major anions, such as fluoride, chloride, nitrate, nitrite, and sulphate, as well as major cations such as lithium, sodium, ammonium, potassium, calcium, and magnesium in the parts-per-billion (ppb) range depending on column condition. Concentrations of organic acids can also be measured through ion chromatography. Most ion-exchange separations are done with pumps and metal columns. The column packings for ion chromatography consist of ion-exchange functional groups bonded to inert polymeric particles. For cation separation the cation-exchange resin is usually a sulfonic or carboxylic acid, and for anion separation the anion-exchange resin is usually a quaternary ammonium group.

Ion chromatography, measures concentrations of ionic species by separating them based on their interaction with a resin. Ionic species separate differently depending on species type and size ([www.lycos.com/info/ion.html](http://www.lycos.com/info/ion.html)). Sample solutions pass through a pressurized chromatographic column where ions are absorbed by column constituents. As an ion extraction liquid, known as eluent, runs through the column, the absorbed ions begin separating from the column. The retention time of different species determines the ionic concentrations in the sample. Total concentration of ions in solution can be detected qualitatively by measuring the conductivity of the solution.

In ion chromatography, the mobile phase contains ions that create a background conductivity, making it difficult to measure the conductivity due only to the analyte ions as they exit the column. This problem can be greatly reduced by selectively removing the mobile phase ions after the analytical column and before the detector. This is done by converting the mobile phase ions to a neutral form or removing them with an eluent suppressor, which consists of an ion-exchange column or membrane ([www.files.chem.vt.edu/chem-ed/sep/lc/ion-chro.html](http://www.files.chem.vt.edu/chem-ed/sep/lc/ion-chro.html)). For

cation analysis, the mobile phase is often HCl or HNO<sub>3</sub>, which can be neutralized by an eluent suppressor that supplies OH<sup>-</sup>. The Cl<sup>-</sup> or NO<sub>3</sub><sup>-</sup> is either retained or removed by the suppressor column or membrane. The same principle holds for anion analysis. The mobile phase is often NaOH or NaHCO<sub>3</sub>, and the eluent suppressor supplies H<sup>+</sup> to neutralize the anion and retain or remove the Na<sup>+</sup>.

Some typical applications of ion chromatography include drinking water analysis for pollution and other constituents; determination of water chemistries in aquatic ecosystems; determination of sugar and salt content in foods; Isolation of select proteins ([www.lycos.com/info/ion.html](http://www.lycos.com/info/ion.html)).

### 2.16 Conclusion

Coal fly ash is a particulate waste product that results from the combustion of pulverised coal to generate electrical power. The bulk of the fly ash produced globally is disposed as waste and only a minor fraction are beneficially reused. The management of this combustion waste is of major concern due to the enormous amount that is generated and disposed of as waste. Various environmental risks are associated with fly ash disposal, these include air pollution, loss of arable land and surface and ground water contamination due to the leaching and mobilization of non-degradable toxic metals, and other chemical species from the ash dump by rainfall or groundwater. One way of combating the problems caused by the huge volume of disposed fly ash is by optimizing the uses of fly ash so that it could become a valuable raw material. Thus the uses of coal fly ash in construction, agriculture, AMD treatment, removal of heavy metals in water treatment and in the synthesis of zeolite and geopolymer.

Coal fly ash has been studied extensively and elemental analysis has revealed that rare earth elements, toxic elements and radionuclides are present in this combustion waste. The presence of toxic elements in fly ash raises concern over its safety with regard to its disposal and beneficiations since studies have shown that these elements may leach out of fly ash. Hence it is important to attempt to

## Chapter Two: Literature review

---

determine the fate of the toxic elements in the fly ash reuse process, products and wastes. In order to achieve these objectives an accurate method of determining the chemical composition of fly ash is fundamental in the qualitative and quantitative analysis of the elements of toxicity and value in fly ash. The analytical methods widely used in determining the elemental compositions of fly ash are X-ray Fluorescence (XRF) spectroscopy; inductively coupled plasma – optical emission spectrometer/Mass Spectrometry (ICP-OES/MS); Laser Ablation Inductively Coupled Plasma Mass Spectrometry (LA-ICP-MS) and instrumental neutron activation analysis (INAA). These analytical techniques have different advantages and disadvantages hence it is important to establish the analytical technique that is best suited for determining the different categories of elements that are contained in fly ash.

This study will focus on the environmental safety of fly ash utilization in terms of AMD treatment and synthesis of geopolymer. The radioactivity of South African coal fly ashes is an important factor that has to be investigated if it is to be used for water treatment or geopolymerisation. It is important to evaluate and understand the radioactivity and leachability of the radionuclides present in the fly ash. Hence the radiological hazard of the use of the synthesized geopolymer and the AMD/FA residue needs to be determined. The utilisation of fly ash as a possible treatment agent for AMD has been established by several research studies. The treatment of mine water with fly ash takes advantage of the available CaO in the fly ash to neutralize the mine water. The chemistry of the treatment of acid mine drainage treatment with coal fly ash is now well understood. However, no attention has been given to the solid waste resulting from the process. Hence this study will investigate the treated water and the waste residue produced in order to determine where the toxic heavy metals and radionuclides in the fly ash and AMD end up. Fly ash can be used as a cheap source material for making geopolymers because its high aluminosilicate content produces geopolymers with very high strengths that can be used as a light weight construction materials. In this study geopolymer synthesised from coal fly ash will be investigated in order to determine if the toxic elements in the fly ash are locked up in the geopolymer

## Chapter Two: Literature review

---

matrix or are leached out when the geopolymer concrete come in contact with water.

Coal fly ash studies have shown that significant amounts REE, such as lanthanum (La), cerium (Ce), and yttrium (Y) are present in South African coal fly ash. However, there have been very little studies in investigating the recovery of REE from fly ash. This study will also attempt to concentrate the REE in South African coal fly ash by attempting to come up with a sequential leaching scheme that can be used in pre-concentrating the REE in the coal fly ash.



### Chapter Three: Methodology

#### 3 Introduction

The previous chapter reviewed the literature concerning coal fly ash with a specific focus on chemical composition and valorisation. This chapter describes the sampling methods used in this study in sections 3.1 and 3.2. The characterisation techniques used in this study are presented in Sections 3.4 and 3.5 respectively. The experimental methodology used in this study are discussed in Section 3.6

##### 3.1 Sampling of Fly ash from Matla power station

The fresh fly ash samples used in this study were collected directly from the hoppers at Matla power station located in Mpumalanga province of South Africa indicated by the red peg in the map below (Figure 3.1.1). The power stations are usually located within close proximity to the coal mines in South Africa. The fly ash samples were kept in plastic containers which were tightly closed to prevent ingress of air, and stored at room temperature for subsequent analysis.

##### 3.2 Sampling of AMD from Carletonville goldmine

The AMD samples used in this study was collected from a goldmine in Carletonville situated in the Western basin of the Witwatersrand of South Africa (Figure 3.1.1). The goldmine where the water was sampled is still active and is indicated by the yellow peg in the map below. The AMD was pumped into 25 L plastic containers, sealed and stored at room temperature for characterisation.



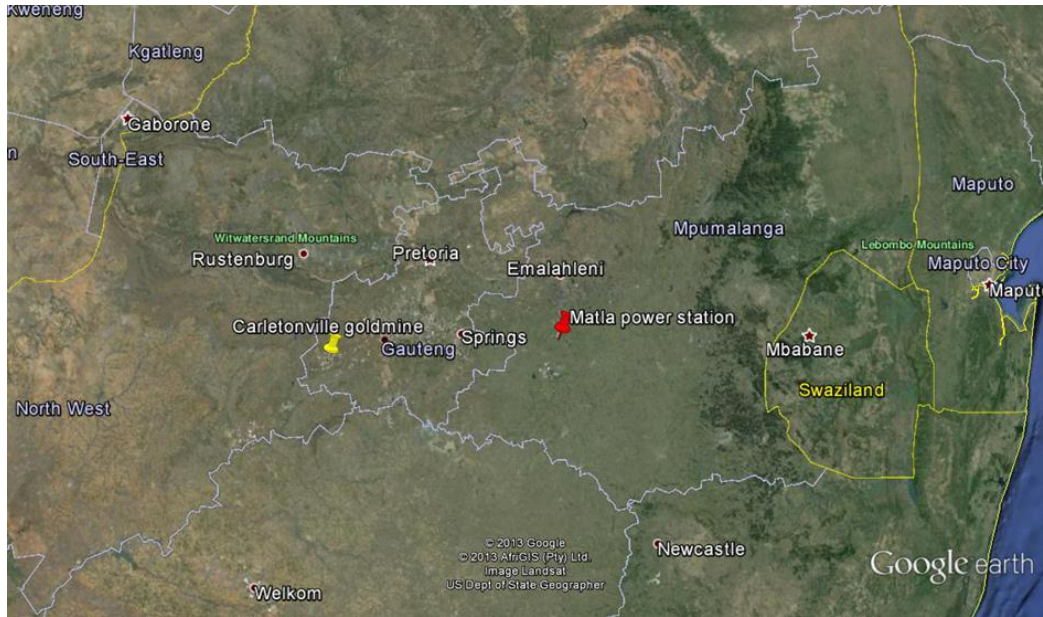


Figure 3.1: Map showing the mine water and FA sampling sites

### 3.3 Storage of Samples

The fly ash samples obtained from Matla power station were stored in sealed plastic containers that were labelled accordingly, in a dark cool cupboard away from any heat source, direct sunlight and fluctuating temperatures. The AMD was also stored in plastic containers under similar conditions to the Matla fly ash samples.

### 3.4 Characterisation of coal fly ash

ENAA, XRF, ICP-OES and LA ICP-MS were used to determine the elemental composition of the Matla fly ash sample. Gamma ray spectroscopy was also used to measure the activity content of the Matla fly ash. The FA ash/AMD residue resulting from the treatment of the Carletonville goldmine AMD with Matla fly ash and the geopolymer synthesised from Matla fly ash were also subjected to all the above mentioned analytical techniques for comparative studies.

### 3.4.1 Epithermal Neutron Activation Analysis

The epithermal neutron activation analysis (ENAA) was carried out at the reactor IBR-2 in Frank Laboratory of Neutron Physics (FLNP), Joint Institute for Nuclear Research (JINR), Dubna. For short irradiation, 100 mg of the Matla fly ash sample was heat-sealed in polyethylene bags. For long irradiation, the same amount of the Matla fly ash was packed in aluminum cups. To determine short-lived isotopes, the Matla fly ash samples were irradiated for 60 sec. After irradiation two gamma-spectrometric measurements were performed; the first one for 3 minutes after 2-3 minutes of decay, and the second for 15 minutes after 9-10 minutes decay. Long-lived isotopes were determined after irradiation for 100 hours in the cadmium-screened channel 1. After irradiation samples were re-packed into clean containers and measured after 4-5 and 20-23 days for 30 minutes and for 1.5 hours, respectively. Gamma spectra were registered as described elsewhere (Dmitriev et al., 2013). The elemental content of a NIST Certified Reference Material 1633 b was also determined by ENAA. The results obtained were then compared to the certified values (NIST, 2008).

### 3.4.2 X-Ray Fluorescence Spectroscopy

The Matla fly ash samples were crushed into a fine powder (particle size < 100  $\mu\text{m}$ ) with a jaw crusher and milled in a tungsten zirconium mill (to prevent contamination from trace and REE) prior to the preparation of a fused disc for major element and trace analysis. The jaw crusher and mill were cleaned with uncontaminated quartz after analysing each sample to avoid cross contamination. Pressed powder pellets were prepared for XRF analysis using 8 g of the sample and a few drops of MOVIOL (a brand of poly vinyl alcohol) was added for binding. The composition was then determined by XRF spectrometry on a Philips 1404 Wavelength Dispersive spectrometer. The spectrometer was fitted with an Rh tube and with the following analysing crystals: LIF200, LIF220, LIF420, PE, TLAP and PX1. The instrument is fitted with a gas-flow proportional counter and a scintillation detector. The gas-flow proportional counter uses 90 % argon and 10 % methane

gas mixture. Trace elements were analysed on a pressed powder pellet at various kV and mA tube operating conditions, depending on the analysed element. Matrix effects in the samples were corrected for by applying theoretical alpha factors and measured line overlap factors to the raw intensities measured with the SuperQ Philips software. Control standards that were used in the calibration procedures were NIM-G (Granite from the Council for Mineral Technology, South Africa) and BHVO-1 (Basalt from the United States Geological Survey, Reston). The XRF technique reports concentration as % oxides for major elements and ppm (mg/kg) for minor and trace elements. The elements reported as mass % oxides were converted to ppm of the elements using element conversion software downloaded at [www.marscigrp.org/elconv.html](http://www.marscigrp.org/elconv.html)

### 3.4.3 Inductively-Coupled Plasma-Optical Emission Spectroscopy

The aqueous samples taken in this study were filtered through a 0.45  $\mu\text{m}$  membrane filter to remove suspended solids and then diluted with de-mineralized water to obtain EC values of between 50 and 100  $\mu\text{Scm}^{-1}$ . The sample was introduced through a high sensitivity glass, single-pass cyclone spray chamber and conical nebulizer using argon gas. It was then passed through axially oriented plasma. The wavelength released by different analytes was detected with a charge-coupled device (CCD) detector and auto integrated using ICP Expert II software. The ICP-OES instrument was calibrated before analysis. The accuracy of the instrument was checked using certified standards. Three replicates were run for each sample in order to check the reproducibility of the analysis.

### 3.4.4 Laser Ablation Inductively Coupled Plasma-Mass Spectrometry

The laser Ablation Inductively Coupled Plasma-Mass Spectrometry LA ICP-MS instrument was set by connecting a 213 nm laser ablation system to an Agilent 7500ce ICP-MS. The fly ash sample was coarsely crushed and fusion disks were made by an automatic Claisse M4 Gas Fusion instrument and ultrapure Claisse Flux. A chip of sample was mounted in a 2.4 cm round resin disk. The mounted

sample was then polished for analysis. The Matla fly ash sample was ablated using He gas and then mixed with Ar after coming out of the ablation cell. The sample was then passed through a mixing chamber before being introduced into the ICP-MS. Trace elements were quantified using National Institute of Standards and Technology (NIST) 612 for calibration method and  $^{29}\text{Si}$  as internal standard. Three replicate measurements were made on each sample. The calibration standard was run after every 12 samples. A quality control standard was run in the beginning of the sequence as well as with the calibration standards throughout. Both basaltic glass, BCR-2 or BHVO 2G were certified reference standards produced by USGS (Dr Steve Wilson, Denver, CO 80225) that were used for this purpose. A fusion control standard from certified basaltic reference material (BCR-2, also from USGS) was also analysed in the beginning of a sequence to verify ablation on fused material. Data was processed using Glitter software.

### 3.4.5 Gamma ray spectrometry

The Matla fly ash sample was measured by means of gamma ray spectrometry at the environmental radioactivity laboratory (ERL), iThemba LABS. The Matla fly ash was transferred into a 1.3 L (polypropylene) Marinelli beaker and filled up to the 1L mark, closed and sealed. A copper lid of ~2 mm thickness was used as an extra lid by placing it on top of the sand sample inside the Marinelli and sealing it with a silicone sealant, so as to eliminate the leakage of radon ( $^{222}\text{Rn}$  produced in the  $^{238}\text{U}$  decay series). The Marinelli beaker which contained the Matla fly ash was kept for 21 days in order to achieve radioactive secular equilibrium between  $^{238}\text{U}$  and  $^{232}\text{Th}$  decay series and their respective progeny.

The HPGe detector at iThemba LABS (ERL) is a closed-end coaxial Canberra p-type detector (model GC4520) with a built-in preamplifier. This detector has a crystal diameter of 62.5 mm and a length of 59.5 mm and has 45% relative efficiency at 1.33 MeV with 2.1 keV Full Width-at-Half Maximum (FWHM) energy resolution at 1332 keV. The cool-down time is 6 hours and it has a cryostat liquid nitrogen consumption rate of < 1.8 litres per day.

### 3.4.6 Fourier Transform Infrared Spectroscopy

Fourier Transform Infrared spectroscopy (FT-IR) was used to monitor evolution of crystallinity during synthesis and also provide information about molecular structure. The Matla fly ash, AMD/FA residue and the synthesised geopolymer were analysed using the FT-IR. Approximately 15 mg of the sample to be analysed was placed on the Attenuated Total Reflectance (ATR) sample holder of a Perkin Elmer spectrum 100 FT-IR spectrometer. The sample was recorded in the range of  $1800 - 250 \text{ cm}^{-1}$ , baseline was corrected and the spectra smoothed. The use of diamond cells with beam condenser or microscope allowed adjustment of the thickness of a sample by squeezing which enables analysis of microgram samples to be performed.

### 3.4.7 Mineralogical characterization by X-ray Diffraction Spectroscopy

The fly ash, AMD/FA and synthesized geopolymer (after being ground to a fine powder) were placed in sample holder and the crystalline phases were characterised using a Philips X-ray diffractometer with Cu-K $\alpha$  radiation. The XRD instrument operating conditions were as given in Table 3.1.

Table 3:1: XRD operating parameters

Parameter	Settings
Radiation source	Cu-K $\alpha$
Radiation wavelength ( $\lambda$ )	1.542 Å
Range	104
Time constant	1 s
Preset	1000 counts/s
Voltage	40 kV
Current	25 mA
$2\theta$ range	$40 < 2\theta < 60^\circ$
$2\theta$ /step	$0.1^\circ$
Anti-scatter slit	$1^\circ$

## Chapter Three: Methodology

---

The phase identification was performed by searching and matching obtained spectra with the powder diffraction file data base originating from JCPDS (Joint committee of powder diffraction standards) files for inorganic compounds.

### 3.4.8 Scanning Electron Microscopy

The morphology of the fly ash, FA/AMD and synthesised geopolymer were investigated using the Auriga high resolution scanning electron microscope (HRSEM) equipped with a CDU-lead detector at 3.00 kV. The fly ash samples were oven-dried at 105 °C for 12 hours in preparation for the analysis. The dried samples were sprinkled on a carbon adhesive tape attached onto an aluminium stub. Since the samples that were analysed were poor electromagnetic conductors, the aluminium stubs were carbon coated using argon gas on Sputter Coater S150B. The carbon coating was done under vacuum. Each sample was then mounted into specimen holders and the morphology (texture) and chemistry of the samples were analysed from backscattered electron as well as secondary electron images.

### 3.5 Characterization of mine water

After collection, the AMD was manually filtered through a 0.45 µm pore filter. The filtered samples were then divided into two portions for cation or anion analysis. The portions reserved for cation analysis were preserved with 3 drops of concentrated nitric acid (HNO<sub>3</sub>) for approximately 100 mL of each AMD sample. Analysis of anions was done using ion chromatography (IC) (section 3.5.1) and cations using ICP-OES (as outlined in section 3.4.3.). Along with the analytical techniques and gamma ray spectrometry as explained in Section 3.4.5, the AMD sample was also subjected to physical analyses such as determination of pH, electrical conductivity (EC) and total dissolved solids (TDS), as per the procedure set out in Section 3.5.2. The product water recovered after treatment of the AMD with fly ash was also subjected to all the above mentioned analytical techniques for comparative studies.



### 3.5.1 Ion chromatography (IC)

The concentration of the anions in the AMD was determined by ion chromatography (IC). The AMD was filtered through a 0.45  $\mu\text{m}$  membrane filter to remove suspended solids and then diluted with de-mineralized water to obtain EC values of between 50 and 100  $\mu\text{S}/\text{cm}$ .  $\text{SO}_4^{2-}$ ,  $\text{Cl}^-$ ,  $\text{NO}_3^-$  and  $\text{PO}_4^{3-}$  were analysed in the leachates using a Dionex ICS-16000 ion chromatograph with an Ion Pac AS14A column and AG14-4 mm guard column. A Dionex SEVEN ANION certified standard was used to check the efficiency of the IC machine. The SEVEN ANION was made up of the composition as shown in Table 3.2 below.

Table 3.2: Composition of the Dionex SEVEN ANION certified standard

Anion	Certified concentration (mg/L)
$\text{F}^-$	20
$\text{Cl}^-$	30
$\text{NO}_2^-$	100
$\text{Br}^-$	100
$\text{NO}_3^-$	100
$\text{PO}_4^{3-}$	150
$\text{SO}_4^{2-}$	150

### 3.5.2 pH, electrical conductivity and total dissolved solids measurements

pH, electrical conductivity (EC) and total dissolved solids (TDS) are parameters used in measuring water quality. The pH of a solution is a measure of the hydrogen ion  $[\text{H}^+]$  concentration in the solution which defines the acidity or alkalinity of the solution. The EC is a measure of the conductivity of the test sample solution and can be used to determine the concentration of inorganic compounds present in water. TDS is the measurement of the combined content of all inorganic and organic substances contained in a liquid which are present in a molecular, ionized or micro-granular (colloidal) suspended form.

## Chapter Three: Methodology

The pH, EC and TDS of the samples in this study were measured, using a Hanna 991 301 pH meter with portable pH/EC/TDS/Temperature probe. The instrument was calibrated before use with buffer solutions of pH 4.0 and 7.0 and a standard of 12.88 mS/cm at room temperature. Triplicate measurements of the samples were taken.

### 3.6 Methodology

There are several standard experimental methods employed in this study in order to investigate and validate the application potentials of fly ash in the treatment of AMD and as a source of REE. These experimental procedures include: (1) the treatment of the AMD from Carletonville goldmine with Matla fly ash. (2); the synthesis of light weight geopolymer from Matla fly ash. (3) The pre-concentration of the REE in Matla fly ash. The list of reagents used is given in Table 3.3

List of reagents used

Table 3.3 below presents the name, source, catalogue number and purity of the reagents that were used in this study.

Table 3:3 List of reagents used

Reagent	Name	Source	Catalogue No	%Purity
HF	Hydrofluoric acid	Merck	100334	48
HNO <sub>3</sub>	Nitric acid	Merck	100443	65
HCl	Hydrochloric acid	Merck	101514	32
H <sub>2</sub> SO <sub>4</sub>	Sulphuric acid	Merck	100731	95-97
NaOH	Sodium hydroxide	Kimex		98
NaOCl	Sodium hypochlorite	Kimex		12
H <sub>2</sub> BO <sub>3</sub>	Boric acid	Merck	100162	99.5



### 3.6.1 Total Acid Digestion

The digestant for total acid digestion of the solid Matla fly ash sample selected included hydrofluoric acid (HF) and aqua regia (HCl and HNO<sub>3</sub> mixed in the ratio of 3:1 respectively). The digestion was carried out according to (Jackson and Miller, 1998). 0.25 g of the Matla fly ash sample was weighed into a Teflon cup. 2 mL of concentrated HF and 5 ml aqua regia were added. The Teflon cup was put in a digestion vessel (Parr bomb), sealed and heated to 200°C for 2 hours in an oven. The Parr bomb was removed from the oven and allowed to cool down. 25 mL of H<sub>3</sub>BO<sub>3</sub> was added to the sample in order to prevent the formation of sparingly soluble fluorides in the sample. The digestate was filtered through 0.45 µm membrane filter and made up to 100 mL with ultra-pure water (ELGA Pure lab UHQ). The procedure was triplicated.

### 3.6.2 DIN-S4 Leaching Test

This leaching test provides information about the behaviour of a fly ash when it comes in contact with water. The DIN-S4 method is an agitated extraction test which involves shaking for a period of 24h and uses a wide range of water to solid material ratio (10:1) (Institut fur Normung, 1984). Triplicates samples of each fly ash batch were made using the above liquid to solid ratios.

10g and 5g of each of Matla fly ash and the synthesised geopolymer were placed in 250 ml plastic bottles and each mixed with 100 ml of ultrapure water. The bottles were then shaken for 24 hours under room temperature in an orbital shaker at 150 rpm. The supernatants are decanted and filtered through a 0.45µm membrane filter after the leaching test. The pH, EC and TDS of the filtered leachates are measured and recorded and acidified with HNO<sub>3</sub> for cation analysis. The filtered leachates were stored in the refrigerator at 4°C until the samples were analysed for cations using ICP-MS.

### 3.6.3 Treatment of AMD with fly ash

The AMD from Carletonville goldmine was treated in an 80 L pilot plant as shown in Figure 3.2 below using the protocol developed by Madzivire et al. (2013). The pilot plant was composed of an 80 L tank, a centrifugal pump, a motor and a jet loop reactor. The pilot plant was supplied by Mr G. Nieuwoudt of Biofuelson. 80 L of the Carletonville goldmine mine AMD was mixed with 16 kg of Matla coal FA, 200 g of lime using a jet loop reactor, after 30 min of mixing 344.95 g of  $\text{Al}(\text{OH})_3$  was added according to Madzivire et al. (2013). The temperature, pH and EC were measured after every 15 min. Aliquot samples were collected after every 30 min and filtered using a 0.45  $\mu\text{m}$  membrane filter. The samples to be analysed for cations using ICP-OES were preserved by adding 2 drops of concentrated  $\text{HNO}_3$  while the samples to be analysed for anions using IC were analysed. All the samples were preserved at 4 °C.



Figure 3.2: The setup of the 80 L pilot plant for the treatment of AMD

### 3.6.4 Standardised synthesis of foamed geopolymers

The foamed geopolymer was synthesised by the method proposed by (Boke et al., 2014). All sodium hydroxide was analytical grade (98%). All sodium hypochlorite solution was 12% supplied by Merck. The fresh fly ash samples collected from Matla power station was used as feedstock to prepare the geopolymer.

100 g of sodium hypochlorite solution was added to the 200 g fly ash in a 1000 ml polypropylene beaker and mixed together for 10 minutes using a flat blade impeller to form a slurry. The beaker was immersed in a cooling bath of ice. While still mixing, after the first 10 minutes, 40 g of NaOH pellets was added a teaspoonful at a time to the slurry. Since the dissolution of NaOH is exothermic, the temperature of the slurry was always monitored and kept below 35°C. According to the increase or decrease in slurry temperature, more NaOH pellets were added so as to complete the addition of all NaOH within a time of 50 minutes. After the addition of all the NaOH, the stirring was continued for a further 30 minutes to form homogenous slurry. The slurry was immediately poured into moulds having a lid that seals over the mould. 100 g samples of slurry were poured into small polypropylene moulds. The sealed moulds were further sealed by placing them into zip-lock polyethylene bags. The purpose of sealing was to ensure minimal loss of water or moisture during the subsequent hydrothermal treatment. It was necessary to limit the absorption of atmospheric water vapour and carbon dioxide by the NaOH solution in the slurry. The zip-lock bags with moulds were directly placed into a lab oven set at 30°C. The moulds were left in the oven and the oven adjusted as follows. 24 hours at 30°C, then 24 hours at 60°C, and then 24 hrs at 90°C. The samples were then allowed to cool, the seals removed, and then the samples were left exposed to dry in the oven at 30°C for another 24 hrs. After completion of drying, each foamed geopolymer sample was afterwards kept in its sealed container.

### 3.6.5 Sequential extraction of major components of coal fly ash

In overview, the sequential extraction procedures used in this study were adopted from the extraction techniques that have been used in several studies of the extraction and recovery of different components from fly ash. These methods included the separation of iron from fly ash (Gilbert, 2014) followed by the extraction of Si and Al and other components from coal fly ash. First, a wet chemical method was employed in the extraction of the Fe. The second step involved NaOH leaching of the fly ash residue in order to extract Si (Su et al, 2011). The third step was the H<sub>2</sub>SO<sub>4</sub> leaching of the desilicated fly ash residue to extract Al (Bai et al, 2011). The fourth step was the treatment of HCl to remove Si and Al (Muriithi G., 2012) and the final step was the HNO<sub>3</sub> treatment to remove trace elements from the fly ash (Stas et al., 2007). The extracted components was analysed using ICP-MS. The fly ash residue in each step was analysed using LA ICP-MS for elemental composition and XRD studies were also carried out on the extracted Fe and resulting fly ash residue from each step. A schematic of the sequential extraction procedure is shown below.

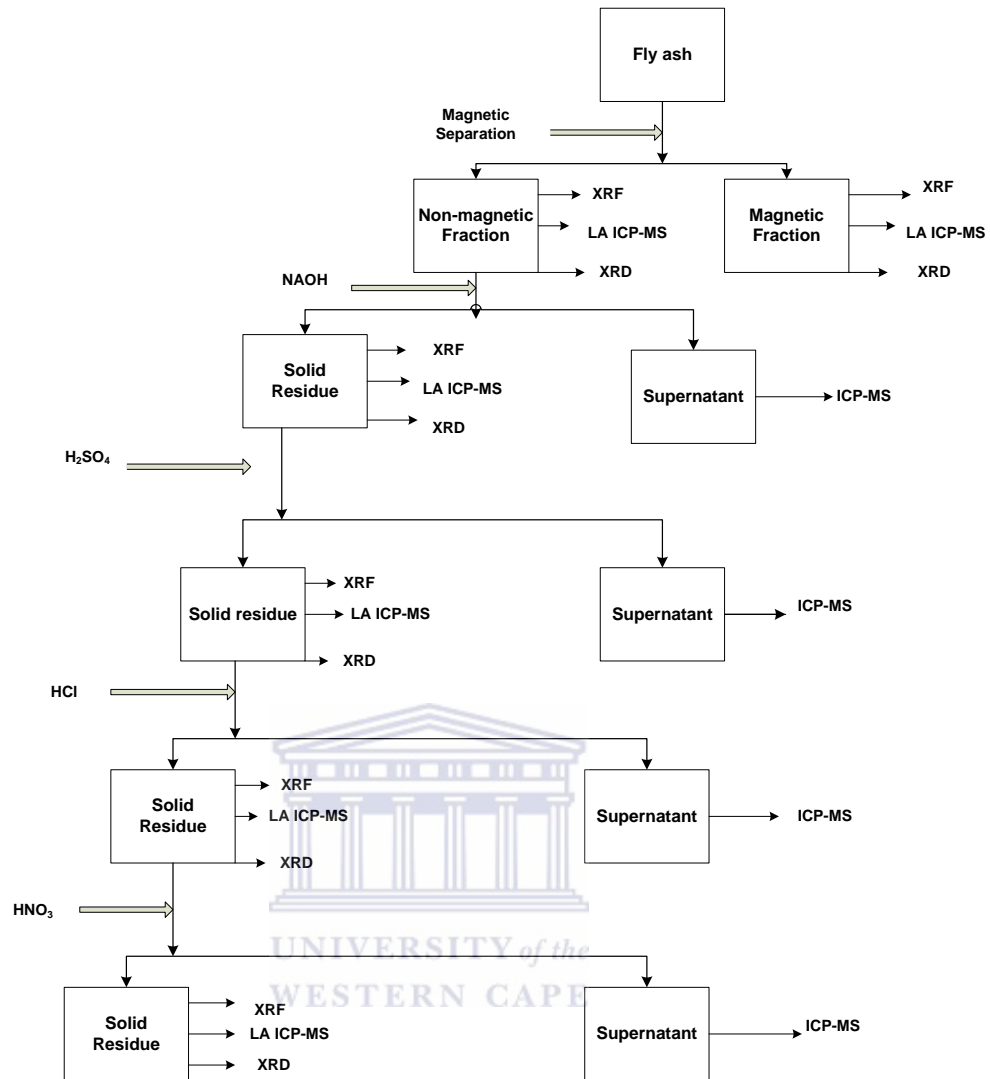


Figure 3.3: Schematic of the sequential extraction procedure

Figure 3.3 shows the steps involved in the sequential extraction scheme for the removal of the major components of the fly ash. The aim of this scheme was to progressively remove the major elements in the fly ash in order to have a residue with elevated concentrations of the REE. The Fly ash treatment with NaOH, H<sub>2</sub>SO<sub>4</sub>, HCl and HNO<sub>3</sub> were carried out in a reflux flask shown in Figure 3.4 below followed by detailed explanations of the procedures.



Figure 3.4: Set up of the sequential leaching of fly ash

i. Magnetic separation of iron from fly ash

The extraction of iron from Matla fly ash involved using a wet magnetic separation step. The method involved measuring 100 g of fly ash into a plastic beaker, to which 200 mL of ultra-pure water was then added. A rod was used to initiate the mixing of the slurry, after which a magnetic stirring bar was introduced into the beaker. The slurry of fly ash and water was then stirred using a magnetic stirrer set at a constant speed of 250 rpm. This was essential to create homogeneity. Once a stirring time of two hours had elapsed, the beaker was

removed from the magnetic stirrer and a bar magnet was used to attract and remove the iron that had been liberated from the fly ash. The solid residue which was essentially the non-magnetic fraction of the fly ash was collected on a 0.45 filter paper by vacuum filtration using a Buchner funnel; while the filtrate or supernatant was collected in the flask. The magnetically separated iron fraction was then washed several times using portions of deionised water, after which it was dried in an oven at 70 °C for 24 hours. The iron and solid residue were then subjected to LA ICP-MS, XRD and XRF.

### ii. NaOH leaching

The non-magnetic fraction of the fly ash was mixed with 8M NaOH solution in a reflux flask. The L/S ratio of the NaOH to fly ash residue was 3:1. The mixture was stirred at 500 rpm at 95°C for 120 minutes. The NaOH/fly ash solution was then filtered and the clear supernatant was analysed using ICP-OES. The desilicated residue obtained was washed with distilled water. 5 g of was collected and analysed by LA ICP-MS, XRD and XRF while the supernatant was analysed using ICP-MS.

### iii. H<sub>2</sub>SO<sub>4</sub> Leaching

The residue from the NaOH leaching was washed and treated with 5M H<sub>2</sub>SO<sub>4</sub>. The L/S ratio of the H<sub>2</sub>SO<sub>4</sub> to NaOH residue was 2:1. The mixture was placed in an open beaker and the H<sub>2</sub>SO<sub>4</sub> evaporated off by heating at 150 °C. Six part of water was added to the residue and it was stirred at 500 rpm for 30 minutes at 90 °C. The solution was then filtered using a 0.45 filter paper to collect the solid residue and the filtrate analysed using ICP-OES. The residue was rinsed with boiling water and subjected to LA ICP-MS, XRD and XRF while the supernatant was analysed using ICP-MS.

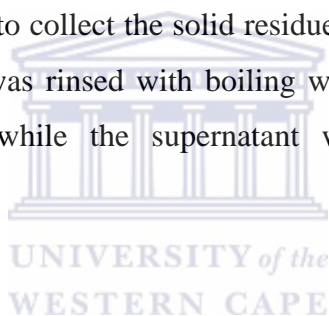


iv. HCl leaching

10 g of the residue after H<sub>2</sub>SO<sub>4</sub> leaching was dissolved in 200 ml of 3M HCl; the temperature was set to 100 °C and stirred for 2 hr to fully pectize the silica component of fly ash. The obtained suspension was filtered to separate and remove the silica gel from the leachate containing other elements. The residue was rinsed with boiling water and subjected to LA ICP-MS, XRD and XRF while the supernatant was analysed using ICP-MS.

v. HNO<sub>3</sub> leaching

10 g of the residue after HCl leaching was dissolved in 100 ml of 7M HNO<sub>3</sub>; the temperature was set to 100 °C and stirred for 4 hr. The solution was then filtered using a 0.45 filter paper to collect the solid residue and the filtrate analysed using ICP-OES. The residue was rinsed with boiling water and subjected to LA ICP-MS, XRD and XRF while the supernatant was analysed using ICP-MS.





### Chapter Four: Comparison of analytical techniques

#### 4 Introduction

The results obtained on determining the elemental content in Matla fly ash using ENAA, ICP-OES, LA ICP-MS, and XRF as described in chapter three are presented and discussed in this chapter. The results will be used to determine the analytical technique that is best suited in determining the different elements in fly ash. To demonstrate the accuracy and reliability of ENAA as the most powerful primary analytical technique (Bode et al., 2009), NIST Standard Reference Material 1633b (bituminous coal fly ash) was used. The results are given in Tables 4.1 and 4.2, subdivided according to the level of certification (certified and non-certified values). A total of 54 elements were determined using ENAA, ICP-OES, LA ICP-MS, and XRF, these elements are categorised into major, trace and REE and presented in three tables (Figures 4.3 to 4.5). The major elements in the Matla fly ash with concentrations  $> 1$  wt. % are presented in Table 3, whilst the minor ( $1-0.1$  wt. %), and trace ( $< 0.1$  wt. %) elements (Vassilev and Vassileva, 2006) are presented with the REE in Table 4 and the other trace elements in Table 5. The techniques and principles on which these analytical methods are based are different and each of these techniques has its own merits and demerits which may affect the outcome of the Matla fly ash analysis. The composition of the elements in the Matla fly ash sample shows that it is Class F since the sum of  $\text{SiO}_2$ ,  $\text{Fe}_2\text{O}_3$  and  $\text{Al}_2\text{O}_3$  is greater than 70% (ASTM, 1994; McCarthy, 1987). Class F is produced from the burning of bituminous coal and anthracites. Thus the elemental composition of the Matla fly ash can be compared to the given concentrations of the elements in SRM 1633b-NIST (bituminous).

#### 4.1 ENAA: Quality Assurance

To assure the quality of ENAA the NIST Certified Reference Material 1633b was used. The concentrations of the elements in the NIST SRM 1633b determined by ENAA in Dubna (present value) are compared to the known concentrations of the NIST SRM 1633b (certified value).

## Chapter Four: Comparison of analytical techniques

Table 4:1: Elemental concentration in the NIST SRM 1633b determined by ENAA in Dubna and the certified values (NIST, 2008)

Element	NIST certified value, (mg/kg)	ENAA Present value (mg/kg)	Minimum detection limit (mg/kg)	RSD %
Al	150500	151000	179	-0.33
As	136.2	133	0.507	2.35
Ba	709	708	21.4	0.14
Ca	15100	15100	691	0.00
Cr	198.2	198	33.3	0.10
Cu	112.8	71.9	662	36.26
Fe	77800	77700	518	0.13
K	19500	20400	4910	-4.62
Mg	4820	4810	176	0.21
Mn	131.8	132	2.8	-0.15
Na	2010	2090	38.5	-3.98
Ni	120.6	121	23.4	-0.33
Se	10.26	9.83	1.39	4.19
Si	230200	230000	334000	0.09
Sr	1041	1040	32.4	0.10
Th	25.7	27.4	0.108	-6.61
U	8.79	8.49	0.286	3.41
V	295.7	312	14.4	-5.51

It can be seen from Table 4.1 that there is a strong agreement between the results obtained by ENAA of the NIST SRM 1633b and the certified values of this standard. Except Cu (36.26%) the RSD% values of the analysed certified SRM were below  $\pm 10\%$ . The RSD is used to test for the accuracy of the instrument in order to determine the reliability of the instrument in the analysis of each element. The acceptable range for RSD value is about  $\pm 10\%$ . The RSD % was calculated as follows:

## Chapter Four: Comparison of analytical techniques

---

$$\frac{\text{Expected value} - \text{Analytical value}}{\text{Expected value}} \times 100\%$$

Expected value = value of the certified standard; Analytical value = value obtained when certified was analysed.

In Table 4.2, the noncertified values of some elements in the NIST SRM 1633b are compared to the amounts determined by ENAA in Dubna. Except for Gd (–109.23%) and Zn (–107.62%), there is a good agreement between the two values. The RSD% of the analysis is also below  $\pm 10\%$ , however the RSD% values Gd (–109.23%) and Zn (–107.62%) clearly shows that their determined amounts in the NIST SRM 1633b are inaccurate and unreliable.



## Chapter Four: Comparison of analytical techniques

Table 4:2: Elemental concentrations in the NIST SRM 1633b (noncertified values (NIST, 2008))

<b>Element</b>	<b>NIST Non Certified value, (mg/kg)</b>	<b>ENAA Present value (mg/kg)</b>	<b>Minimum detection limit (mg/kg)</b>	<b>RSD %</b>
Br	2.9	2.72	0.454	6.21
Ce	190	190	8.16	0.00
Co	50	47.7	0.326	4.60
Cs	11	11	0.17	0.00
Dy	17	16.2	4.85	4.71
Eu	4.1	4.1	0.776	0.00
Gd	13	27.2	0.718	-109.23
Hf	6.8	8	0.414	-17.65
La	94	92.3	1.43	1.81
Nd	85	157	36.6	-84.71
Rb	140	140	1.84	0.00
Sb	6	5.26	0.0519	12.33
Sc	41	41	0.198	0.00
Sm	20	20	0.0907	0.00
Ta	1.8	1.84	0.038	-2.22
Tb	2.6	2.6	0.0651	0.00
Ti	7910	7920	1760	-0.13
Tm	2.1	1.98	0.353	5.71
Yb	7.6	7.61	1.03	-0.13
Zn	210	436	9.27	-107.62

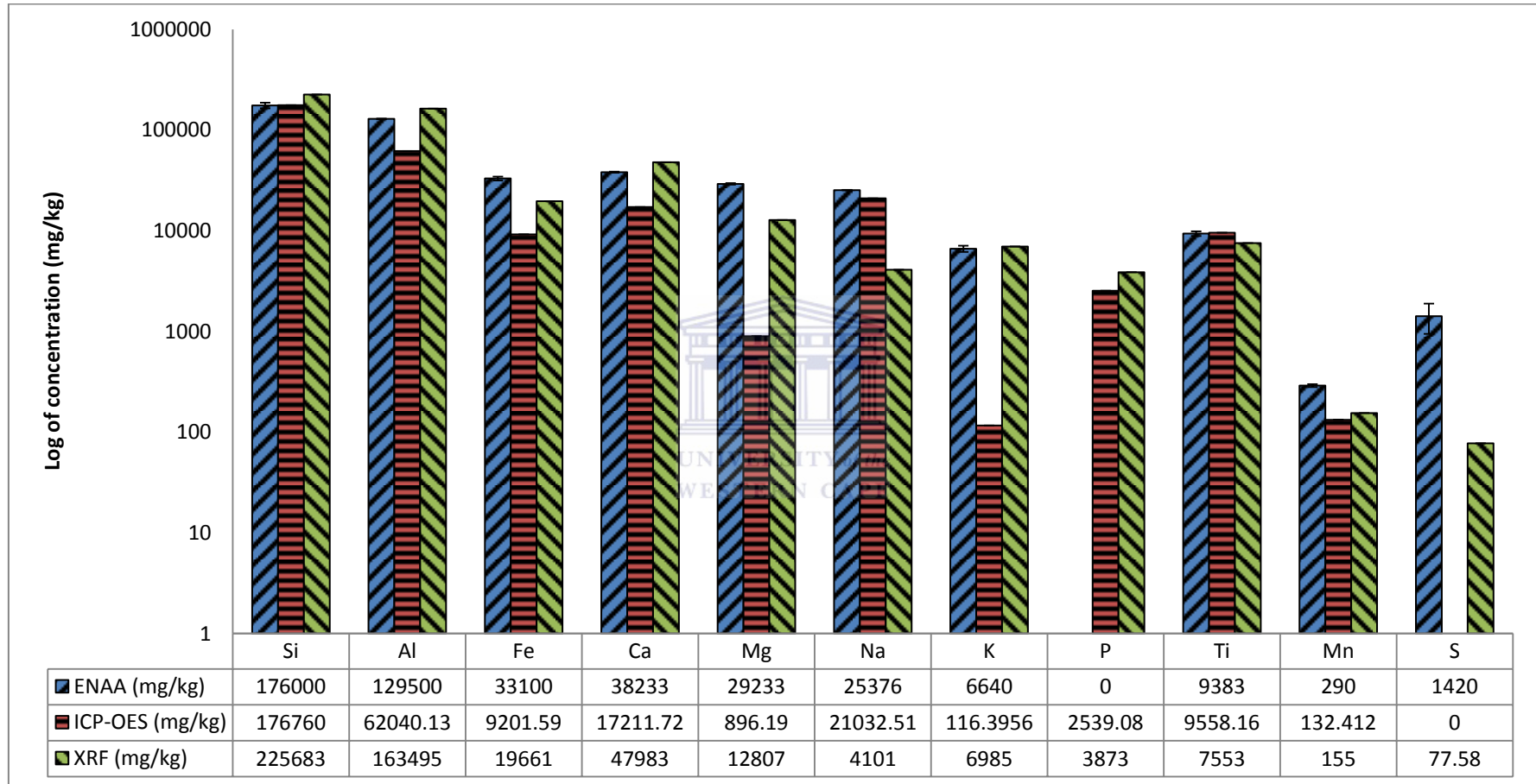
In Table 4.2, the noncertified values of some elements in the NIST SRM 1633b are compared to the amounts determined by ENAA in Dubna. Except Gd (-109.23%) and Zn (-107.62%), there is a good agreement between the two values. The RSD% of the analysis is also below  $\pm 10\%$ , however the RSD% values Gd (-109.23%) and Zn (-107.62%) clearly shows that their determined amounts in the NIST SRM 1633b are inaccurate and unreliable.

### 4.2 Major and minor elements

The concentrations of the major elements in the Matla fly ash determined by the concentration in Matla fly ash determined by ENAA, ICP-OES and XRF are presented and discussed below



## Chapter Four: Comparison of analytical techniques



0 = Not detected

Figure 4.1: Concentrations of major elements in Matla fly ash determined by ENAA, ICP- OES, and XRF [number of determinations = 3]

## Chapter Four: Comparison of analytical techniques

---

Figure 4.1 presents the concentrations of major elements in the Matla fly ash determined by ICP-OES, XRF, and ENAA. The composition of the elements in the Matla fly ash sample shows that it is Class F since the sum of  $\text{SiO}_2$ ,  $\text{Fe}_2\text{O}_3$  and  $\text{Al}_2\text{O}_3$  is greater than 70% (ASTM, 1994; McCarthy, 1987). Class F is produced from the burning of bituminous coal and anthracites. Thus the elemental composition of the Matla fly ash can be compared to the given concentrations of the elements in SRM 1633b-NIST (bituminous). The major elements were not determined by the LA ICP-MS technique due to unavailability of suitable standards. The results revealed that the major elements analysed in the Matla fly ash were Si, Al, Fe, Ca, Mg, Na, K, P, Ti, Mn and S while Sr and Ba were present as minor elements. The ENAA technique did not report the concentration of P. From Table 3, the concentration of the major elements in the Matla fly ash obtained using XRF and ENAA were in better agreement when compared to the certified SRM (1633b-NIST) in Table 1. Also, from Figure 3 it was observed that the concentrations of the major elements (Al, Fe, Mg, and K) in the Matla fly ash obtained using ICP-OES were more than an order of magnitude lower than the concentrations obtained using XRF and ENAA whereas XRF results of Na were two orders of magnitude lower than ICP-OES and ENAA. However the elemental abundances of these elements seemed to be proportional. The lower concentrations determined by ICP-OES might be attributed to the sample preparation involved in the technique or matrix effects. The ICP-OES/MS is mostly used in determining the concentration of elements in fly ash. However, its main disadvantage is that the fly ash has to be digested before analysis (Hou and Jones, 2000; Chen and Ma, 2001; Enamorado-Báez et al., 2013). An acid digestion required for ICP-OES of fly ash may result in either loss or contamination of the sample from the acid and the subsequent dilution technique (Hannaker et al., 1984; Brown and Milton, 2005; Zhang et al., 2007). The Matla fly ash was digested prior to ICP-OES and that process may have resulted in the lower elemental concentrations detected in the Matla fly ash (Iwashita et al, 2005).

## Chapter Four: Comparison of analytical techniques

---

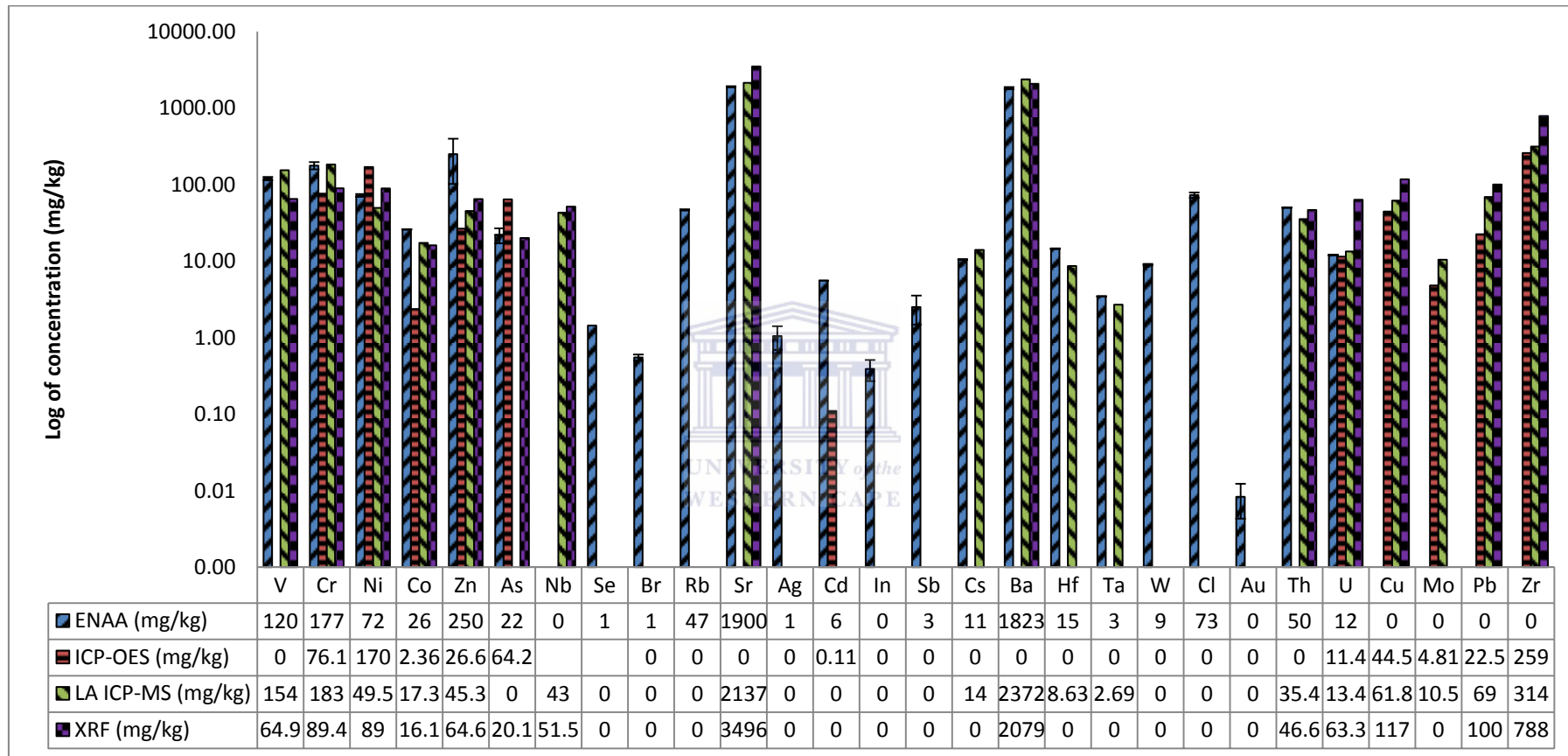
### 4.3 Trace elements

The concentrations of the trace elements in the Matla fly ash determined by the concentration in Matla fly ash determined by ENAA, ICP-OES and XRF are presented and discussed below





## Chapter Four: Comparison of analytical techniques



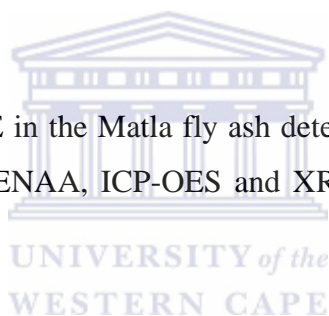
0 = not detected

Figure 4.2: Concentrations of trace elements in Matla fly ash determined by ENAA, ICP- OES, LA ICP – MS, and XRF [number of determinations = 3]

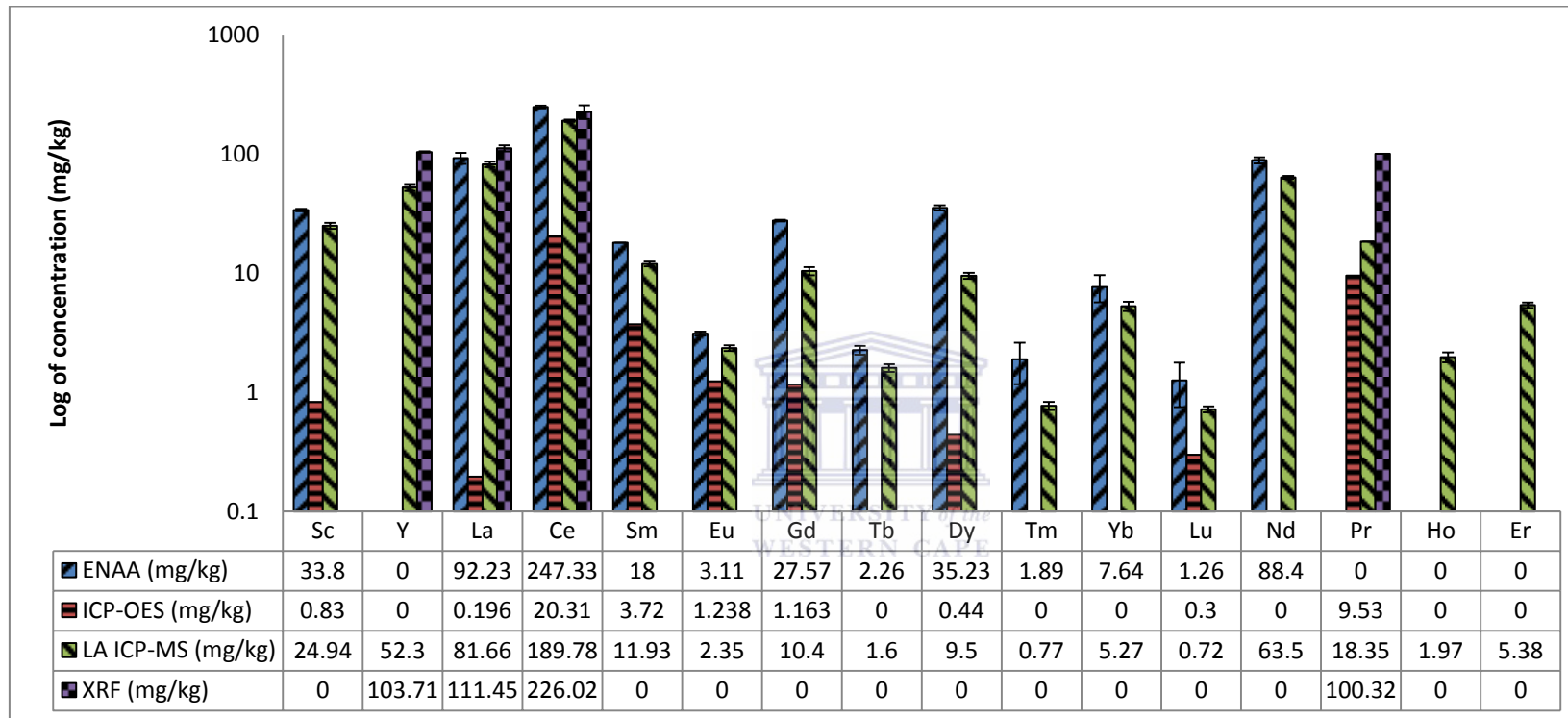
The trace element composition of the Matla fly ash determined by ENAA, ICP-OES, LA-ICP-MS and XRF is presented in Figure 4.2. The ICP-OES and XRF techniques reported 15 trace elements in the analysis of the Matla fly ash while 17 and 23 trace elements were reported by the LA-ICP-MS and ENAA techniques, respectively. Cd was not determined by XRF analysis. Also, As and Cd were not obtained by LA ICP-MS, while it is impossible to determine Pb by ENAA because no suitable nuclides exists. However As, Cd, Pb were obtained by ICP-OES. These elements are of major environmental concern due to their toxicity. The amounts of the trace elements in the Matla fly ash obtained using the LA-ICP-MS and ENAA were in better agreement in abundance when compared to the certified SRM (1633b-NIST).

#### 4.4 REE

The concentrations of the REE in the Matla fly ash determined by the concentration in Matla fly ash determined by ENAA, ICP-OES and XRF are presented and discussed below.



## Chapter Four: Comparison of analytical techniques



0 = Not detected

Figure 4.3: Concentrations of REE in Matla fly ash determined by ENAA, LA ICP – MS, ICP- OES, and XRF [number of determinations = 3]

In Figure 4.3 the REE composition of the Matla fly ash determined by ENAA, ICP-OES, LA-ICP-MS and XRF are presented. Ten REE were determined by ICP-OES, whilst only three REE were determined by XRF technique. LA-ICP-OES and ENAA allowed determination of 16 and 12 REE, respectively. Sc, La, and Ce were the only REE determined by XRF technique due to unavailability of a suitable standard for calibrating the REE. Moreover, the XRF cannot compete with other well established techniques such as INAA and ICP-MS (Misra, 2011). The concentrations of the REE in the Matla fly ash obtained by ICP-OES were also much lower compared to the REE concentrations obtained when the Matla fly ash was analysed using XRF, LA-ICP-OES and ENAA. This lower concentration of REE may also be attributed to the sample preparation used for the ICP-OES as it was observed for the major element concentrations. The concentration of the REE in the Matla fly ash samples obtained by LA-ICP-MS and ENAA are proportional to the given concentrations of REE in the SRM. Hence LA-ICP-MS and ENAA may be considered as better techniques than ICP-OES or XRF analysis in determining the REE concentrations in coal fly ash.

### 4.5 Summary

ENAA along with ICP-OES, LA ICP-MS, and XRF were used to determine the elemental composition of coal fly ash from the Malta coal power station in the Mpumalanga province of South Africa. The aim of this chapter was to determine the analytical technique that was best suited in determining the different elements in fly ash. For the first time a total of 54 major, trace and rare earth elements were accurately determined in Matla fly ash by the four analytical techniques. It was shown that the elemental content of this particular coal fly ash was of the same order as the NIST standard reference material Coal Fly Ash 1633b. The concentration of the major elements in the Matla fly ash as determined by ENAA and XRF was very similar, apart from Na and correlate well with that of the certified SRM NIST 1633b. Determination of trace and REE content obtained by the ENAA and LA ICP-MS techniques was more reliable than their determination by the XRF or ICP-OES techniques. Coal fly ash can thus be considered as a

## Chapter Four: Comparison of analytical techniques

---

potential source for extraction of REE for industrial use. The hazardous impact of heavy metals such as Cd, Pb, As, Sr, U, Th, in particular, observed in the studied coal fly ash should be monitored in the reuse of fly ash in agriculture and construction materials. Although ENAA is a sensitive and accurate method for the determination of many trace elements, this method has some shortcomings. Pb cannot be determined because of its nuclear characteristics. Moreover the ENAA technique is not readily available in South Africa compared to XRF and LA ICP-MS making it difficult to use the method for routine application. Thus this study will focus on the use of XRF spectroscopy for the determination of the major and minor elements whilst the LA ICP-MS will be used for trace elements and REE determination. Also the reliability of the XRF and LA ICP-MS has been confirmed by the results presented in this study



### Chapter 5: Applications of fly ash for AMD treatment

#### 5 Introduction

This chapter presents and discusses the use of coal fly ash in the treatment of AMD. It includes the results of the IC and ICP-OES employed in determining the chemical composition of Carletonville AMD before and after treatment with fly ash. The physical and chemical characterisation of Matla fly ash and the resulting solid (AMD/FA residue) after the AMD treatment was carried out using different analytical techniques such as LA ICP-MS, XRF, XRD, SEM-EDS and FTIR. This chapter also presents and discusses the results of the Gamma Spectroscopy of the Carletonville AMD before and after treatment, Matla fly ash and AMD/FA residue in order to determine the radioactivity of the process feedstock, product and waste. Furthermore the results of the leaching tests (DIN-S4) of the Matla fly ash and the AMD/FA residue carried out in order to determine the solubility and leachability of the toxic components are also presented and discussed. Section 5.1 gives an overview of AMD treatment with coal fly and the aim and objectives of this chapter. Whilst a brief descriptions of the materials and methods used are given in section 5.2. The results and discussions of this chapter are divided into four (4) sections (5.3, 5.4, 5.5, and 5.6). Section 5.3 presents and compares the results of the characterisation of the Carletonville goldmine AMD before and after treatment with Matla fly ash. The characterisation of Matla fly ash and the AMD/FA residue are presented and compared in section 5.4. The results from the gamma spectrum analysis and the DIN-S4 leaching test will be presented and discussed in section 5.5 and 5.6 respectively. This chapter will end with a summary of the major findings from the use of Matla fly ash in the treatment of Carletonville goldmine AMD. The results of the use of fly ash in the synthesis of foamed geopolymer will be presented and discussed in chapter six.

### 5.1 Overview

Acid mine drainage (AMD) is formed when sulphide minerals, such as pyrite, found in association with the coal or overburden come into contact with oxygen and water during mining and oxidize. Sulphide minerals undergo further bacterially-catalysed oxidation reactions which accelerate acidity generation and increase iron and sulphate concentrations in recipient water bodies. Acid mine drainage is characterized by high acidity (pH 2–4), high sulphate concentrations (1–20 g/L) and high concentration of heavy metals such as Fe, Mn, Al, Cu, Ca, Pb, Mg, Na and Ni (Gitari et al., 2008). The major sources of AMD include drainage from underground mine shafts, runoff and discharge from open pits and mine waste dumps, tailings and ore stockpiles. AMD is a global problem and has been categorised as the biggest distinct environmental challenge confronting the mining industry. This is because AMD causes ground and surface water pollution as it spreads underground and flows into surface streams and rivers near active and abandoned mines (Dutta et al., 2009). Hence AMD should be treated to avoid environmental pollution. There are various available treatment techniques to remediate AMD. These are technologies using either chemical or biological to neutralise AMD (Johnson and Hallberg, 2005). AMD treatment technologies are generally categorized as active and passive treatment technologies. Active treatment requires continuous inputs of resources to sustain the process while passive treatment requires relatively little resource input once in operation. Microbial and chemical reagents, whether natural or non-natural, are the main strategies in the treatment of AMD along with technologies that could enhance their effectiveness and remove suspended solids in the solution. Fundamentally, production of alkalinity is the main process in the treatment of AMD (Madzivire, 2009). This causes the metals and sulphates to precipitate or to be reduced and produce a stream of water free of most impurities. Although mine water can be treated with current techniques if adequate measures are used for a specific situation, the cost and the environmental impacts of technologies are the major limiting factors (Madzivire, 2009).

## Chapter Five: Applications of fly ash for AMD treatment

---

The current treatments of acid mine drainage are not economically sustainable to the South African government hence innovative treatment technologies have been developed in recent years to find more economical treatments for acid mine drainage in South Africa (Coetzee et al., 2010). AMD treatment with coal fly ash is one of the innovative technologies being studied for sustainable treatment of acid mine drainage in South Africa. Fly ash can be used in the treatment of acid mine drainage because it contains a relative high concentration of CaO, which is considered as a liming agent to neutralise acid mine drainage. The neutralisation of acid mine drainage is usually attained by the addition of chemicals such as CaO, Ca(OH)<sub>2</sub>, CaCO<sub>3</sub>, NaOH and Na<sub>2</sub>CO<sub>3</sub>. The use of fly ash for acid mine drainage neutralisation, involves a process whereby the pH of the acid mine drainage is increased from pH 2–3 up to a neutral pH of 7, or even over pH 10. Fly ash contains considerable amounts of total alkalinity in the form of CaO, MgO, K<sub>2</sub>O and Na<sub>2</sub>O, thus increasing the neutralisation potential of fly ash. Calcium oxide (CaO) is formed in fly ash by the oxidation of calcium during coal combustion process in a coal-fired power station. Fly ash may therefore be a substitute for limestone or lime treatment in the neutralisation and removal of sulphates from AMD (Somerset et al., 2005).

Several studies have been carried out on the treatment of AMD with fly ash and the chemistry of the process is well understood but few have paid any attention to the resulting solid after the treatment which may be used for backfill or may prove to be an environmental burden. Hence the aim of this chapter is to evaluate and understand the toxicity of treated AMD and solid waste residue generated from the AMD treatment with fly ash. The objectives of this chapter are a) to determine if any toxic elements are concentrating up in the treated AMD or the AMD/fly ash waste residue that may then constitute an environmental hazard; b) to determine if any valuable elements accumulate enough in the AMD/fly ash waste residue that can be exploited; and c) to determine if the processes is unsustainable because of the damage that may arise from the leaching of contaminants from the AMD/fly ash waste residue.



### 5.2 Materials and methods

The AMD was collected from Carletonville goldmine situated in the Western basin of Witwatersrand Goldfields, South Africa. The pH, EC and total dissolved solids (TDS) were measured in the laboratory as described in Chapter 3, Section 3.5.2. The chemical composition of the samples were also analysed using IC and ICP-OES as outlined in Chapter 3, Section 3.4.3 and 3.5.1 respectively. The Carletonville goldmine AMD was treated with Matla fly ash in a jet loop reactor as described in chapter 3, Section 3.6.1. The treated Carletonville goldmine AMD was also characterised for anions and cations using IC and ICP-OES respectively. The pH, EC and total dissolved solids (TDS) were also measured. The Matla fly ash samples used in this study were collected directly from the hoppers at Matla power station located in Mpumalanga province of South Africa. The Matla fly ash and the solid residue generated after the AMD treatment with the fly ash in the jet loop reactor (AMD/FA residue) were characterised using different analytical techniques such as LA ICP-MS and XRF for determination of chemical composition; FTIR for structural analysis; XRD for analysis of the mineral phase composition; and SEM-EDS for morphological and elemental composition. The procedures for these analytical processes are detailed in Chapter 3 sections 3.4.2, 3.4.4, 3.4.6, 3.4.7 and 3.4.7 respectively. The activity measurement of Matla fly ash, the Carletonville gold mine AMD before and after treatment with Matla fly ash in the jet loop reactor; and the produced waste (AMD/FA residue) were undertaken using gamma spectrometric analysis as explained in Chapter 3, section 3.4.5. The DIN-S4 leaching test was carried out to assess the concentrations of toxic elements in the water soluble fraction of the Matla fly ash and AMD/FA residue according to the method specified in section 3.6.1.

### **5.3 Results and discussion of the characterisation of the Carletonville goldmine AMD before and after treatment with Matla fly ash.**

The results of the physiochemical parameters of the Carletonville goldmine water before and after treatment with the Matla fly ash in the jet reactor were obtained using pH, EC, IC and ICP-OES. The results obtained are compared to each other and the target water quality range (TWQR) recommended by the World Health Organisation, (WHO) and are presented in Table 5.1 below



## Chapter Five: Applications of fly ash for AMD treatment

Table 5:1: The physicochemical parameters of the Carletonville goldmine AMD Carletonville goldmine AMD before and after treatment with Matla fly ash (TDS and concentrations are in mg/L)

Parameter	AMD	Treated water	TWQR	Parameter	AMD	Treated water	TWQR
pH	2.26 ± 0.03	9.49 ± 0.94	6-9	Ce	3.32 ± 0.27	0.06 ± 0.03	NA
EC (mS/cm)	6.3 ± 0.10	3.33 ± 0.25	0-700	B	3.21 ± 1.04	Nd	0-2.4
TDS	3.23 ± 0.06	2.59 ± 0.0-16	NA	Y	1.75 ± 0.07	Nd	NA
SO <sub>4</sub> <sup>2-</sup>	4943.53 ± 63.70	482.22 ± 3.03	200-500	Sr	1.11 ± 0.06	0.01 ± 0.0	NA
Cl <sup>-</sup>	83.21 ± 5.01	1.71 ± 0.08	0-250	Cr	0.69 ± 0.26	Nd	0-0.05
Ca	1002.98 ± 31.64	0.41 ± 0.52	0-32	Th	0.23 ± 0.11	0.15 ± 0.04	NA
Al	658.65 ± 28.32	0.37 ± 0.10	0-0.2	Cd	0.07 ± 0.02	Nd	0-0.003
Fe	374.04 ± 25.83	Nd	0-0.3	Ba	0.06 ± 0.03	Nd	0-0.7
Mg	274.54 ± 12.56	Nd	0-30	Be	0.04 ± 0	0.01 ± 0.0	0-0.012
Na	226.50 ± 17.86	3.85 ± 0.56	0-2.4	Se	Nd	0.28 ± 0.02	0-0.04
K	74.91 ± 5.80	35.43 ± 1.99	0-50	P	0.019 ± 0.001	0.26 ± 0.02	NA
Mn	71.74 ± 4.12	Nd	0-0.1	As	Nd	0.12 ± 0.03	0-0.01
Si	39.61 ± 4.38	Nd	NA	Pb	Nd	0.08 ± 0.05	0-0.01
Zn	23.87 ± 1.50	Nd	0-3	Rb	0.14 ± 0.06	0.05 ± 0.01	NA
Ni	20.93 ± 1.03	Nd	NA	Y	7.15 ± 0.07	0.02 ± 0.0	NA
Co	10.35 ± 0.56	0.05 ± 0.01	NA	Zr	Nd	0.02 ± 0.0	NA
Hg	4.79 ± 0.81	Nd	0-0.006	Cu	3.90 ± 0.19	0.02 ± 0.01	0-2
Cu	3.90 ± 0.19	Nd	0-2	Nb	Nd	0.01 ± 0.0	NA
U	3.65 ± 0.36	1.40 ± 0.24	0-0.3	Ti	0.03 ± 0.01	0.01 ± 0.0	NA

NA = Not available, Nd = Not detected

## Chapter Five: Applications of fly ash for AMD treatment

---

Table 5.1 presents the physiochemical parameters of the Carletonville goldmine water before and after treatment with Matla fly ash. From the table it was observed that the natural pH of the Carletonville goldmine water before treatment with Matla fly ash was  $2.26 \pm 0.03$  which was not within the target water quality range (TWQR) of 6-9 mg/L as recommended by the World Health Organisation (WHO). The natural pH of Carletonville goldmine water makes it unsuitable for domestic, agricultural and industrial use (WHO, 2011). According to Morin and Hutt (1997), mine water having  $\text{pH} > 6$  can be classified as acid mine drainage (AMD). Hence the Carletonville goldmine water can be classified as AMD. The EC and TDS of the Carletonville goldmine AMD before treatment with Matla fly ash were  $6.3 \pm 0.10$  mS/cm and  $3.23 \pm 0.06$  mg/L respectively. Usually ionic species from salts are responsible for high EC and TDS readings. AMD usually has a high concentration of dissolved heavy metals and sulphate (Feng et al., 2000).

From Table 5.1 it is also apparent that the Carletonville goldmine water before treatment with Matla fly ash contained high concentration of Ca ( $702.98 \pm 31.64$  mg/L), Al ( $658.65 \pm 28.32$  mg/L), Fe ( $574.04 \pm 25.83$  mg/L), Mg ( $274.54 \pm 12.56$  mg/L), Na ( $226.50 \pm 17.86$  mg/L) and Mn ( $71.74 \pm 4.12$  mg/L) as well as high concentration of  $\text{SO}_4^{2-}$  ( $4943.53 \pm 63.70$  mg/L). Also, the Carletonville goldmine water before treatment with Matla fly ash sample also contained higher levels of toxic metals (B, Cd, Cr, Hg, and Zn) and radionuclides (Th and U). These elements were above the TWQR for potable water set by World Health Organization (WHO) as shown in Table 5.1 (WHO, 2011) The presence of these elements in the acidic Carletonville goldmine mine water is due to the effect of sulphuric acid which dissolves and mobilizes the elements from the surrounding rocks as it flows around or beyond the mining area. The chemical composition of the generated acidic mine water has been reported to be mainly influenced by the geology of the bedrock in the coal mine (Madzivire et al., 2010).

From Table 5.1 it can also be observed that the jet loop treatment of the Carletonville goldmine AMD (80L) with 16 kg of Matla coal fly ash, 200g of

$\text{Ca(OH)}_2$  and 344.95 g of  $\text{Al(OH)}_3$  resulted in the removal of sulphate ions to within the TWQR for potable water (WHO, 2011). However, the product water did not conform to drinking water requirements with respect to eight parameters. These were pH ( $9.49 \pm 0.94$ ) and the concentration of K, Na, Al, U, Se, As, and Pb. These parameter values were higher than the TWQR values. The higher amount of As and Pb, which are toxic heavy metals and U, a radionuclide, in the product water is of major concern. Thus the product water requires further treatment to reduce the pH and remove K, Na, Al, U, Se, As, and Pb. It was observed that Se, As and Pb were not detected in the Carletonville AMD but were determined in the treated water. As and Pb are heavy metals that are harmful or toxic at low concentrations. The As and Pb detected in the treated AMD is likely to have leached out of Matla fly ash into the treated water as the elements were not detected in the AMD..

### 5.4 Results of the characterisation of AMD/FA residue

#### 5.4.1 FT-IR analysis of geopolymer from Matla fly ash

The solid residue (AMD/FA) that was produced from the treatment of the Carletonville goldmine water with Matla fly ash was characterised using the FT-IR technique in order to obtain information about the configuration of the AMD/FA residue sample. Figure 5.1 compares the FT-IR spectrum of the AMD/FA residue and Matla fly ash.

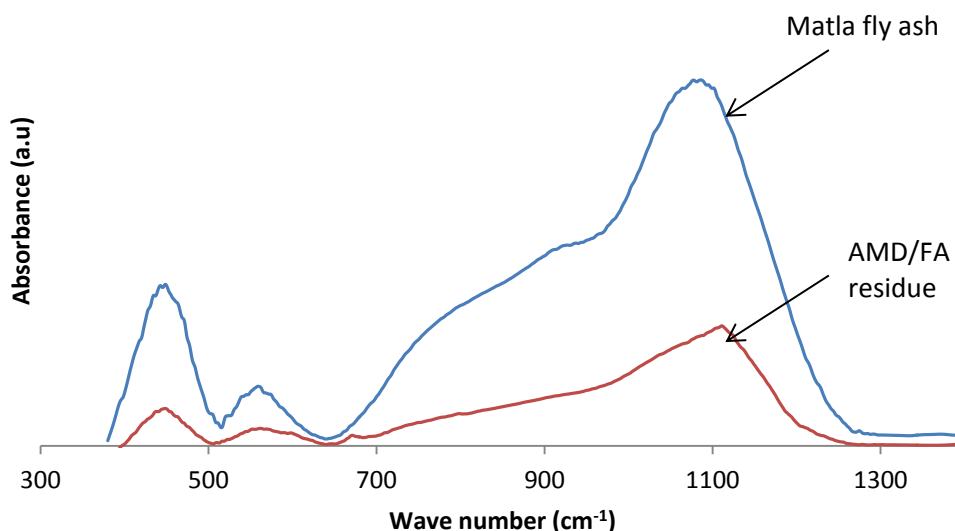


Figure 5.1: FT-IR spectra of the Matla fly ash and the fly ash/ AMD residue

Figure 5.1 shows the FT-IR spectrum of the Matla fly ash compared to the residue after the treatment of the AMD with Matla fly ash in a jet loop reactor. The FT-IR spectra of the Matla fly ash and the AMD/FA residue shows a broad band around  $1104\text{ cm}^{-1}$  attributed to the asymmetric stretching vibrations of Si-O-Si and Al-O-Si at around  $1104\text{ cm}^{-1}$  (Mohan and Gandhimathi, 2009). Another band located  $445\text{ cm}^{-1}$  is ascribed to Si atom in the fourfold coordinated (O-Si-O) bending modes of  $\text{SiO}_4$  tetrahedra (Fernández-Jiménez, and. Palomo, 2005). The only difference observed when the FT-IR spectrum of the Matla fly ash was compared to that of the AMD residue was the lower intensity of the spectrum of the AMD/FA residue. This may be due to decrease in crystalline quartz content of AMD as result of the jetloop effect on the mineral phases in the fly ash. The absence of new peaks in the spectrum of the fly ash and AMD residue compared to the Matla fly ash is an indication that the fly ash and AMD interaction in the jet loop reactor did not result in the formation of new functional groups in the AMD/FA residue.

### 5.4.2 Morphological analysis

The scanning electron micrographs showing the surface morphology of the Matla fly ash and the AMD/FA residue are shown in Figure 5.9 below. The morphological characteristics of Matla fly and AMD/FA residue samples were visualized using a SEM as outlined in section 3.4.8. The elemental compositions of the Matla fly ash sample, and AMD/FA residue based on EDS analysis (Atomic %) were also determined and the areas chosen for EDS analysis are also presented in Figure 5.2 below. The methodology is specified in Section 3.4.8. The major advantage of EDS analysis is for the qualitative verification of the elements that are present and their relative abundance in the Matla fly ash.



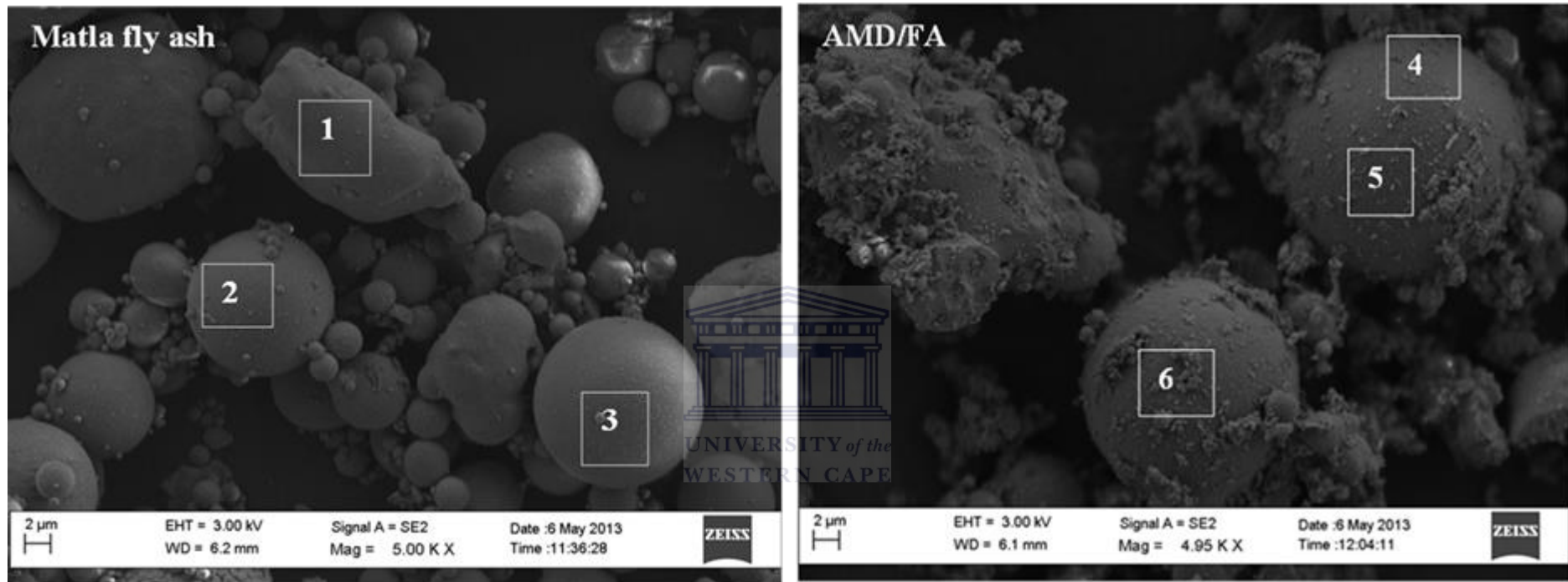


Figure 5.2: SEM Micrograph of Matla fly ash and AMD/FA residue showing the area chosen for EDS analysis



## Chapter Five: Applications of fly ash for AMD treatment

---

Figure 5.2 compares the SEM micrograph of the Matla fly ash to the SEM micrograph of the AMD/FA residue. The SEM micrograph shows that the Matla fly ash consisted of irregular as well as spherically shaped particles. Some agglomerated particles were also observed in the fly ash sample and the outer surfaces of the spherical Matla ash particles were smooth. Whilst the SEM micrograph of the AMD/FA residue shows that the AMD/FA residue as well as the Matla fly ash consists of irregular as well as spherically shaped particles. Some agglomerated particles were also observed in the AMD/FA residue. The outer surfaces of the AMD/FA residue particles appeared encrusted.

According to Seames (2003), the smooth outer surfaces of fly ash particles are assumed to be mainly aluminosilicate structures. The spherical shapes and the agglomeration observed in the fly ash sample could be attributed to the high temperature and conditions during the coal combustion process (Kutchko and Kim, 2006). The spherical shape of the ash is an indication that the particles were formed under un-crowded free fall conditions and a relatively sudden cooling, which helps to maintain the spherical shape; while the agglomerated nature of some particles is an indication that the particles were produced due to high temperature sintering reactions (Saikia et al., 2006). The occurrence of irregular shapes in the fly ash sample could be the consequence of fragmentation mechanisms relating to particle inflation, cracking, and cenosphere fracture within the coal particles or through the formation and shedding of partially melted attachment or mineral inclusions during char combustion (Seames, 2003). The encrustations observed on the outer surfaces of the AMD/FA residue particles can be attributed to the leaching (Eze et al, 2013) and formation of new mineral phases in the fly ash (Yeheyis et al., 2009) during the acid mine drainage and fly ash interaction in the jet loop react

The elemental composition of the Matla fly ash and AMD/FA residue, based on EDS analysis (Atomic %) are presented in Table 5.2. The methodology is specified in Section 3.4.8. The major advantage of EDS analysis is for the qualitative verification of the elements that are present and their relative

## Chapter Five: Applications of fly ash for AMD treatment

abundance in the Matla fly ash and AMD/FA residue. EDS analysis is not an appropriate technique for the quantitative determination of the chemical compositions of a fly ash sample due to the large variations in the elemental compositions of the very small area of analysed spots (Fatoba, 2008). This is because of the inhomogeneity at the micron level. Thus XRF and LA ICP-MS were performed to confirm the quantitative composition and the results are presented in section 5.4.3. Table 5.2 below presents the elements detected in the area analysed (determined by EDS) on the Matla fly ash sample and AMD/FA residue.

Table 5:2: EDS analysis of the chosen areas (atomic %) of Matla fly ashes and AMD/FA residue

Element	Analysed spots on Matla fly ash			Analysed spots on AMD/FA residue		
	1	2	3	4	5	6
Al	18.50	5.27	45.22	25.02	36.82	36.26
Si	30.69	12.40	48.45	22.53	51.18	49.78
K	Nd	Nd	1.02	Nd	0.90	Nd
Ca	5.43	3.83	1.29	23.64	4.76	7.46
Ti	3.60	Nd	2.35	2.00	1.66	1.75
Fe	41.77	78.50	1.67	4.90	2.81	2.31
Mg	Nd	Nd	Nd	2.30	1.89	2.48
S	Nd	Nd	Nd	19.61	Nd	Nd
Total	100	100	100	100	100	100

Nd = Not detected

Generally the predominant elements present, were, Si, Al, Ca and Fe in the six areas analysed, in the Matla fly ash and AMD/FA sample. While S was detected in one spot of the three analysed spots of the AMD/FA residue, Mg was detected in the three analysed spots in AMD/FA residue analysis but not detected in any of the analysed spots in the Matla fly ash. K was only detected in one spot of the three analysed spots of the Matla fly ash, and similarly in the AMD/FA residue. The atomic % of Si and Al detected in the Matla fly ash and Matla AMD analysis

were observed to be higher than the atomic % of Ca detected in both analysed samples. In the elemental analysis of coal fly ash from different regions of the world Si and Al have been shown to be the predominant elements (Blissett and Rowson, 2012). The inconsistency of S, Mg and K shows the inhomogeneity of the Matla fly and AMD/FA residue samples. It also highlights the fact that elemental determination using EDS technique is mainly qualitative and not appropriate for elemental quantitative analysis.

### 5.4.3 Mineralogical analysis

Figure 5.3 shows the XRD patterns of the Matla fly ash and the AMD/FA residue. The results compare the mineralogical phases present in Matla fly ash with the AMD/FA residue in order to observe if there are any changes in mineral phases resulting from the interaction between the AMD and the Matla fly ash in the jet loop reactor.

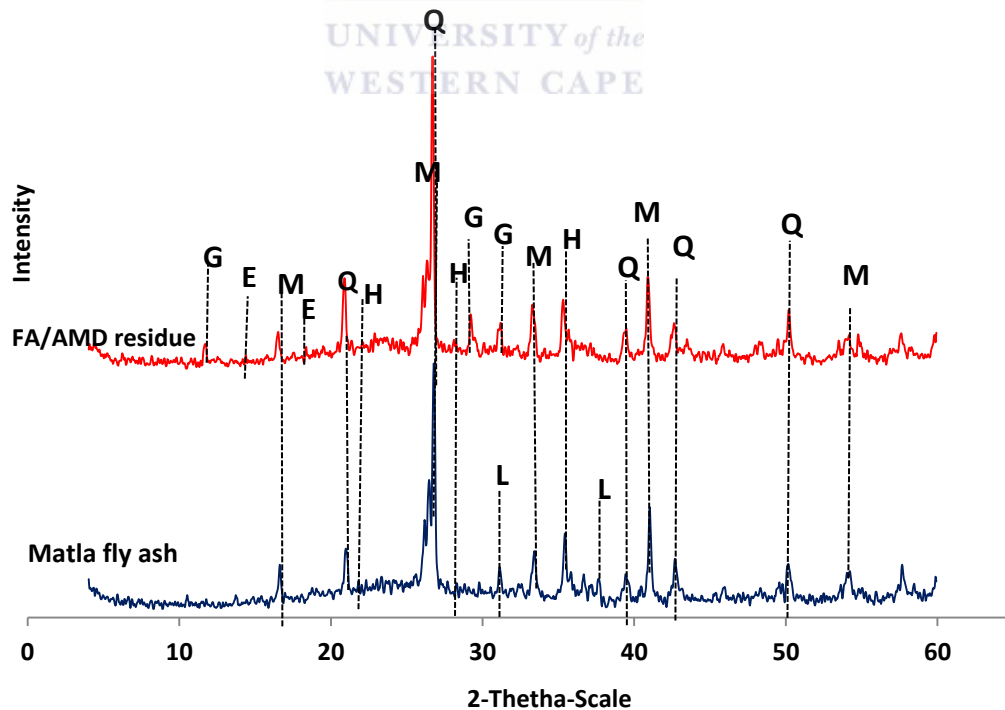


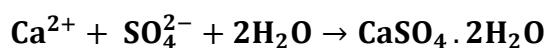
Figure 5.3: XRD patterns for Matla fly ash sample and the AMD/FA residue [G = Gypsum; E = Etringite; H = Hematite; M = mullite; Q = Quartz; L = Lime]

## Chapter Five: Applications of fly ash for AMD treatment

Fig 5.3 compares the qualitative XRD result of Matla fly ash to the AMD/FA residue. The XRD results revealed that the major crystalline mineral phases for the Matla fly ash samples and AMD/FA residue were quartz (SiO<sub>2</sub>) and mullite (Al<sub>6</sub>Si<sub>2</sub>O<sub>13</sub>). Hematite (Fe<sub>2</sub>O<sub>3</sub>) was also identified in the Matla fly ash sample and AMD/FA residue sample. In comparison lime (CaO) was identified in the Matla fly ash sample but was not identified in the AMD/FA residue sample. These identified mineral phases (hematite and lime) were present in low amounts as can be seen from their relatively minor peaks when compared to those of quartz and mullite. Whilst gypsum (CaSO<sub>4</sub>•2H<sub>2</sub>O) and ettringite (Ca<sub>6</sub>Al<sub>2</sub>(SO<sub>4</sub>)<sub>3</sub>(OH)<sub>12</sub>•26H<sub>2</sub>O) were present as new formed secondary mineral phases in the AMD/FA residue.

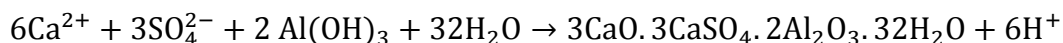
According to Singh and Kolay (2002) quartz and mullite are the major crystalline constituents of coal fly ashes. Quartz is a hard mineral commonly found as cell and pore infillings in the organic matter of coal and is regarded as a primary mineral. It is basically considered as non-reactive in combustion processes due to its high fusion temperature (Ward, 2002). Mullite is a secondary mineral that is assumed to be formed during the thermal decomposition of kaolinite, an aluminosilicate mineral in the coal (Koukouzas et al., 2009, White and Case, 1990). Lime, which is also a secondary mineral may have resulted from the decomposition of calcite or dolomite during, which are the most important and common calcium-bearing minerals in coal.

The gypsum and ettringite mineral phases detected in the AMD/FA residue resulted from the interaction between the AMD and the fly ash in the jet loop reactor. The AMD treatment with fly ash proceeds via the formation of gypsum and ettringite resulting in the reduction of the high SO<sub>4</sub><sup>2-</sup> content in the AMD. The gypsum is formed through the following reaction:



## Chapter Five: Applications of fly ash for AMD treatment

According to Madzivire, (2011), ettringite may form when  $\text{Al}(\text{OH})_3$  is added to the AMD and fly ash mixture in the jet loop reactor as shown in Equation: 5.2 below.



The XRD helps to interpret the SEM results of the AMD/FA in section 5.4.1 which showed encrustation on the surfaces of the particles when compared to the smooth surfaces of the Matla fly ash particle. These encrustations can be attributed to the formation of new mineral phases (gypsum and ettringite). EDS analysis of the encrustation on the AMD/FA residue (Figure 5.2, spot 4) detected Ca and S which are the elements present in gypsum and ettringite the observed new mineral phases. The existence of these Ca mineral phases in the AMD/FA residue is of environmental importance. This is because ettringite and other secondary Ca-hydrated phases in fly ash are likely to encompass and render insoluble elements of environmental concern such as Cr or Se and to some extent will control the leachability of these elements from the AMD/FA residue (Izquierdo and Querol, 2012).

### 5.4.4 Bulk Chemical Composition Analysis

The results obtained for the quantitative elemental composition of Matla fly ash and AMD/FA residue, using XRF and LA ICP-MS are presented in Figures 5.4, 5.5 and 5.6. The choice of techniques used for analysis was based on the findings from the study of the accuracy of different analytical methods in elemental analysis of Matla fly ash discussed in chapter four. XRF spectroscopy was used in the determination of the major elements in the samples while The LA ICP-MS was used in the elemental determination of the trace elements and REEs in the samples. The major elements in fly ash with concentrations  $> 1$  wt. % and the minor (1–0.1 wt. %) are presented in Figure 5.4, whilst the trace ( $<0.1$  wt. %) elements (Vassilev and Vassileva, 1996) are presented in Figure 5.5 and the REEs are presented in Figure 5.6.

### 5.4.4.1 Major Elements

The results of the concentration of the major and minor elements in the AMD/FA residue sample determined using XRF spectroscopy is presented in Figure 5.4 below. The compositions of the elements are reported as weight percentage (wt. %) and are compared to the concentration of the elements in Matla fly ash sample.



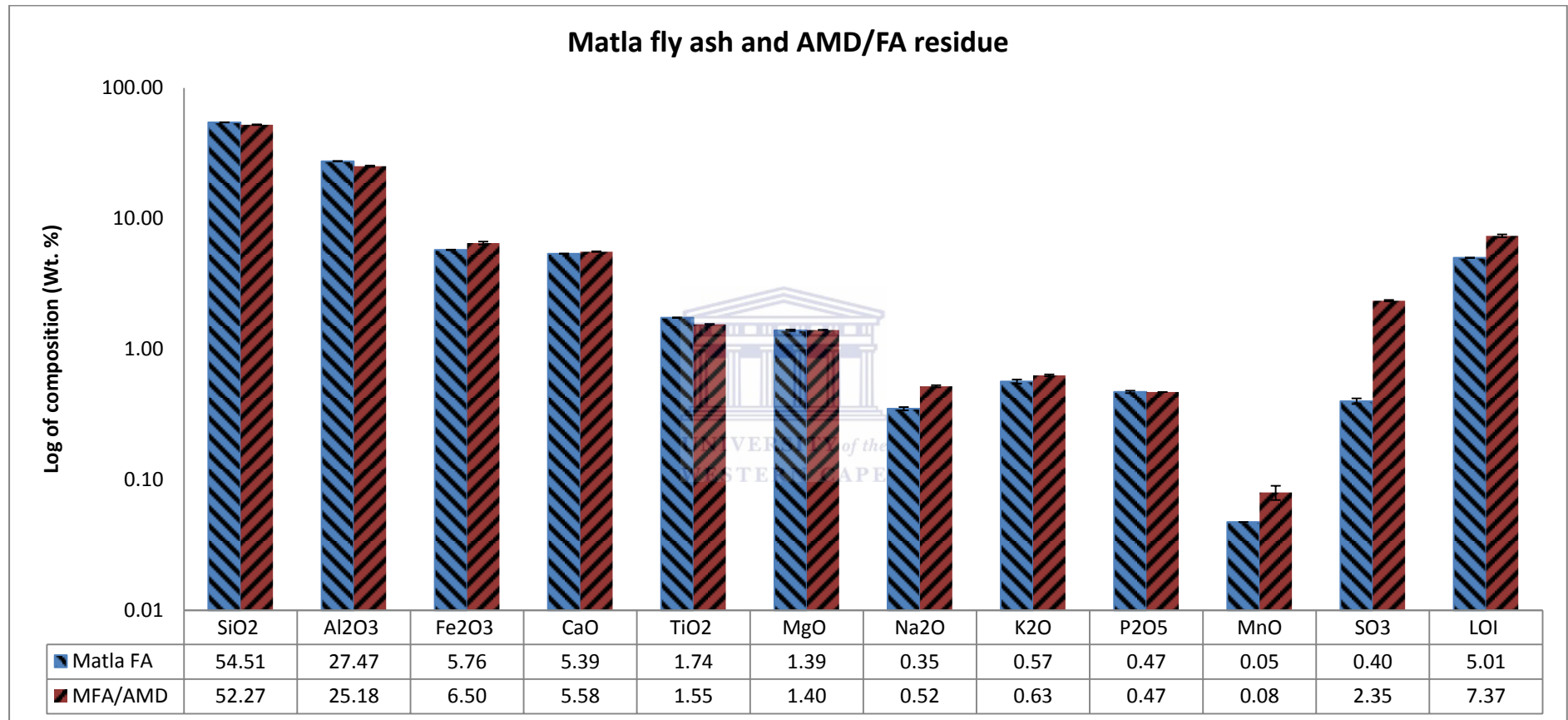


Figure 5.4: Concentrations of major elements in Matla fly ash (MFA), AMD fly ash residue (AMD/FA) determined by XRF spectroscopy [number of determinations = 3]

## Chapter Five: Applications of fly ash for AMD treatment

---

The results using XRF, giving the quantitative composition of the major and minor elements in AMD/FA residue and Matla fly ash are presented and compared in Figure 5.4. The results show that the composition of the major elements in the AMD/FA had the same qualitative trend as the major elemental composition of the Matla fly ash. Also it was noted that the major elemental composition of the Matla fly ash was similar to the reported composition of major elements in fly ash from other South African power stations and other regions of the world as reported by Gitari et al., (2008) and Blissett and Rowson, (2012) respectively.

The sum of the weight % of  $\text{SiO}_2$ ,  $\text{Al}_2\text{O}_3$  and  $\text{Fe}_2\text{O}_3$  was 87.74 % and 83.95 % for the Matla fly ash and AMD/FA residue respectively. Thus the Matla fly ash can be classified as class F. According to the American Society for Testing and Materials (ASTM C 618-92a), fly ash can be classified as class F or C based on the sum of the oxides of aluminium, silicon and iron in the fly ash. Class F fly ash are characterised by (i) the sum of  $\text{SiO}_2$ ,  $\text{Al}_2\text{O}_3$ ,  $\text{Fe}_2\text{O}_3 > 70$  %, (ii)  $\text{SO}_3 < 5$  %, (iii) moisture content  $< 3$  % and (iv) loss on ignition (LOI)  $< 6$  %. (v)  $\text{CaO} < 20$  %. The Matla fly ash contained 5.39 % CaO which is in the mid-range among Class F fly ashes that usually have low calcium content (Vassilev and Vassileva, 2007). Class F ash is regarded as a pozzolanic material. A pozzolan is a siliceous, or a siliceous and aluminous, material that has no inherent cementitious property. In a very finely divided form however, it will chemically react with  $\text{Ca}(\text{OH})_2$  at ordinary temperatures and in the presence of  $\text{H}_2\text{O}$  to form compounds exhibiting cementitious properties (Blissett and Rowson, 2012). In comparison the AMD/FA residue also meets up with all the requirements of class F fly ash classification except for the higher LOI (7.73 %). The loss on ignition (LOI) is an indication of volatiles, unburnt carbon or organic content. The higher LOI observed for the AMD/FA residue compared to the Matla fly ash could indicate higher organic content in the AMD/FA residue because of the interaction with AMD. It is more likely that the enriched LOI of the AMD/FA residue was due to the structural incorporation of  $\text{H}_2\text{O}$  into secondary mineral phases formed in the in the AMD/FA (Yeheyis et al., 2009) during the AMD treatment in the jet loop reactor.



## Chapter Five: Applications of fly ash for AMD treatment

---

The results of the SEM and XRD analysis in sections 5.4.1 and 5.4.2 respectively corroborate the formation of new secondary hydrated mineral phases (gypsum ( $\text{CaSO}_4 \cdot 2\text{H}_2\text{O}$ ) and ettringite ( $\text{Ca}_6\text{Al}_2(\text{SO}_4)_3(\text{OH})_{12} \cdot 26\text{H}_2\text{O}$ )).

The amounts of Si (54.51 %) and Al (27.47 %) in the Matla fly ash were observed to be higher than their concentrations in the AMD/FA residue, Si (52.27 %) and Al (25.18 %). However, elemental analysis of the Carletonville AMD and treated water in Table 5.1 shows that the concentration of Al was reduced from  $658.65 \pm 28.32$  mg/L in the Carletonville goldmine to  $0.37 \pm 0.10$  mg/L in the treated water. While Si with a concentration of  $39.61 \pm 4.38$  mg/L in the Carletonville goldmine was not detected in the treated water. Therefore one would expect a slight increase in the concentration of Al and Si in the AMD/FA residue. The observed slight decrease in the concentrations of Al and Si in the AMD/FA residue in Figure 5.3 could be attributed to dilution because of the increase in the concentrations of the other species in the residue such as  $\text{Fe}_2\text{O}_3$ , MnO,  $\text{SO}_3$  originating from the AMD and LOI; or sample loss during jet looping; or inhomogeneity of the AMD/FA residue as a result of the difficulty in taking a proper representative sample due to the large amount of the residue.

An increase in the concentrations of Fe (increased by 0.74 %), Ca (increased by 0.19 %), S (increased by 1.95 %), Mn (increased by 0.03 %) and Mg (increased by 0.01 %) was observed in the AMD/FA residue compared to the Matla fly ash. This increase in the concentrations of Fe, Ca, S Mn and Mg in the AMD/FA residue resulted from the interaction of the AMD and fly ash in the jet loop reactor. Table 5.1 revealed that species such as Fe, Ca, Sulphate, Mn and Mg were detected in high concentrations in AMD but were present in lower concentrations or not detected in the treated water. Research on AMD and fly ash interaction has established that AMD neutralisation occurs due to an increase in pH that results from the dissolution of lime (CaO) in the fly ash. The increase in pH of the AMD leads to the precipitation of heavy metals in the form of hydroxides and of sulphates as gypsum (Gitari, et al., 2008). Thus, the Ca detected in Matla fly ash and from AMD/FA residue are from lime and gypsum, respectively. This is

## Chapter Five: Applications of fly ash for AMD treatment

---

supported by the SEM analysis of the AMD/FA particle (Figure 5.2) that revealed encrustations on the surface of the particles indicating the formation of new mineral phases during the Carletonville goldmine AMD interaction with Matla fly ash. This was further corroborated by the XRD analysis (Figure 5.3) of the AMD/FA residue that identified gypsum as a secondary mineral phase formed during the interaction.

### 5.4.4.2 Trace elements

The comparison of the concentrations of the trace elements in the Matla fly ash and AMD/FA residue samples determined by LA ICP-MS are presented in Figure 5.13 below. The compositions of the trace elements are reported in mg/kg.



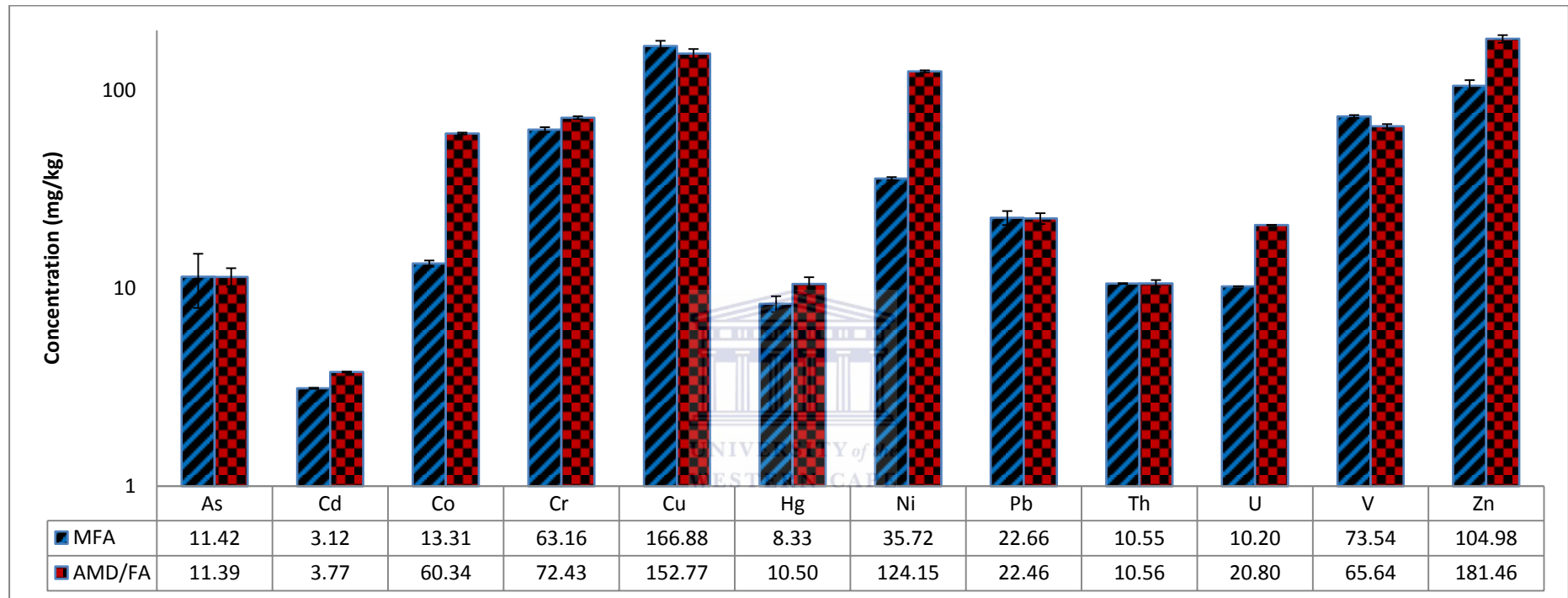


Figure 5.5: Concentrations of trace elements in Matla fly ash (MFA) and AMD fly ash residue (AMD/FA) as determined by LA ICP-MS [number of determinations for LA ICP-MS = 3]

## Chapter Five: Applications of fly ash for AMD treatment

---

Figure 5.5 presents and compares the trace elemental composition of the Matla fly ash with the AMD/FA residue determined by LA ICP-MS. Comparing the trace elemental content of the AMD/FA residue to the Matla fly ash (Figure 5.5) revealed a higher amount of Co, Cr, Ni, U, and Zn in the AMD/FA residue. The concentrations of Cu and V were observed to be slightly lower in the AMD/FA residue than in the Matla fly ash, however, the concentrations of As, Pb and Th were observed to be within the same range in the Matla fly ash and the AMD/FA residue. The removal of heavy metals and sulphates from AMD during treatment with fly ash is also accompanied with removal of trace elements in the AMD due to sorption capabilities of the surface of the metals hydroxides precipitated (Gitari, et al., 2008). This may account for the elevated concentrations of Co, Cr, Ni, U, and Zn in the AMD/FA residue. On the other hand the slightly lower concentrations of Cu and V in the AMD/FA residue may be attributed to the leaching of these elements from the Matla fly ash by the Carletonville AMD. The surface of coal fly ash particles are usually enriched with trace elements such as Sr, and V as a result of condensation reactions during combustion (Zandi and Russell, 2007). These surface associated elements usually dominate the leachate chemistry during the early stage of fly ash when in contact with water (Iyer, 2002). Studies of the leaching behaviour of elements in coal fly ash, shows that Cu exhibits some degree of mobility in an acidic environment, irrespective of the mode of occurrence (Izquierdo and Querol, 2012). The results also show that Matla fly ash and AMD/FA residue contains heavy metal (As, Cd, Cr, Hg, Ni and Pb) and radionuclides (Th and U) which are toxic and potentially harmful to human in excessive amounts. The presence of these toxic elements in AMD/FA residue raises concern over its safety as regards to its disposal since it is possible that these elements may leach out of AMD/FA residue when disposed (Wang et al., 1999).

### 5.4.4.3 Rare earth elements (RRE)

The results of the concentrations of the REE in the AMD/FA residue sample are compared to the REE concentrations of the Matla fly ash sample as determined by LA ICP-MS and presented in Figure 5.6 below.



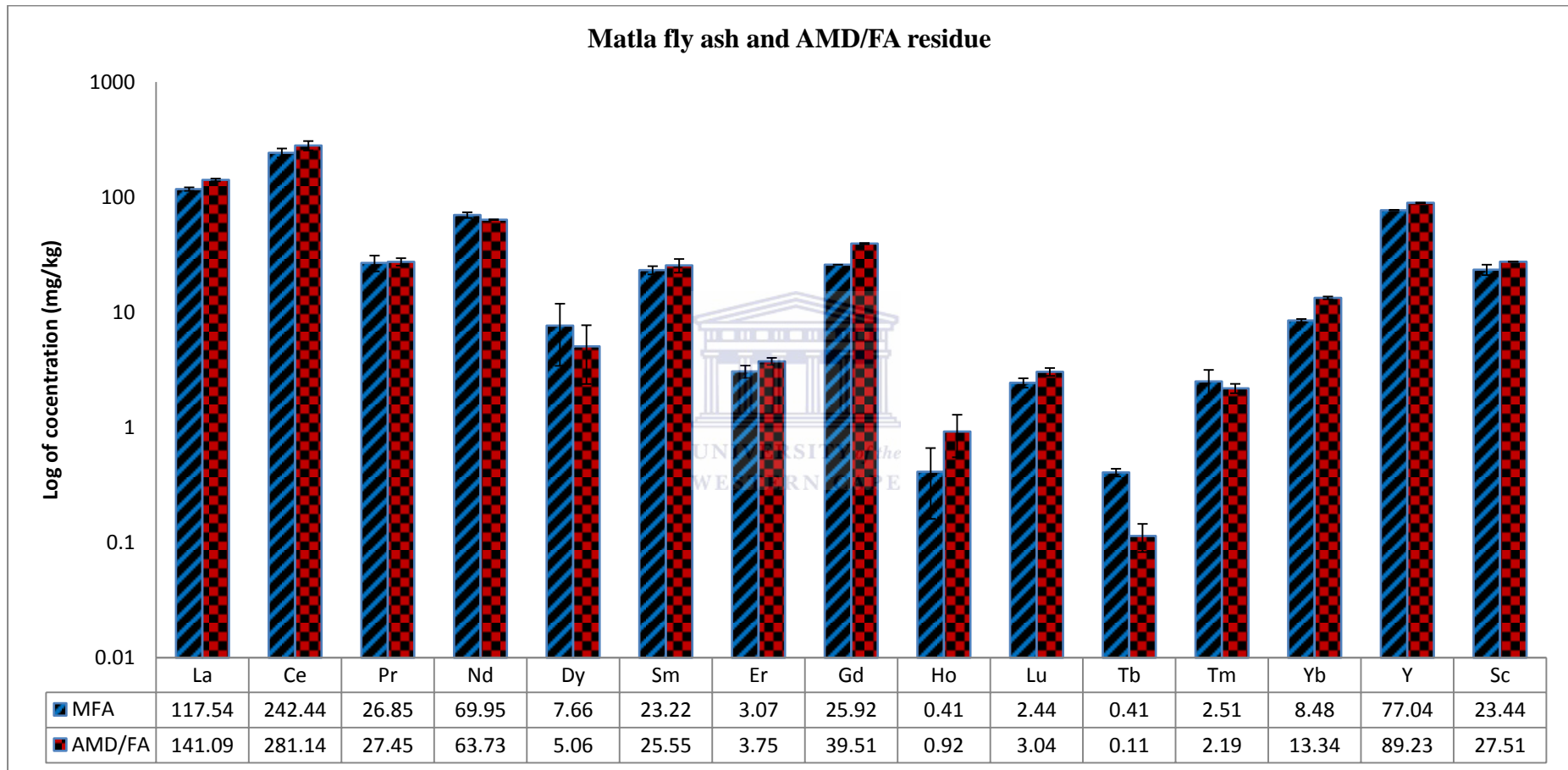


Figure 5.6: Concentrations of REE in Matla fly ash (MFA) and AMD/FA residue (AMD/FA) determined by LA ICP-MS [number of determinations for LA ICP-MS n = 3]

## Chapter Five: Applications of fly ash for AMD treatment

---

In Figure 5.6 the REE composition of the Matla fly ash and AMD/FA residue determined by LA-ICP-MS are compared. The concentration of REE La, Ce, Gd and Y, were found to be significantly higher in the AMD/FA residue than in the Matla fly ash. The concentration of other REE (Pr, Nd, Dy, Sm, Er, Gd, Ho, Lu, Tb, Tm, and Yb) detected were within the same range in both the Matla fly ash and AMD/FA residue. In the elemental composition of the untreated Carletonville mine water (Table 5.1) the concentrations of Ce and Y are  $3 \pm 0.27$  mg/L and  $2 \pm 0.07$  mg/L respectively. Whilst in the treated Carletonville mine water Ce and Y concentrations were  $0.06 \pm 0.03$  and  $0.02 \pm 0.00$  respectively. The lower amounts of Ce and Y in the treated Carletonville mine water indicates that these species might have accompanied the removal of heavy metal hydroxides and sulphates from the AMD as explained in section 5.4.3.2. The amounts of La, Ce, and Nd ( $117.54 \pm 4.16$  mg/kg;  $242.44 \pm 21.97$  mg/kg and  $69.95 \pm 3.93$  mg/kg, respectively) in Matla fly ash and ( $141.09 \pm 3.85$  mg/kg;  $281.14 \pm 26.28$  mg/kg and  $63.73 \pm 0.05$  mg/kg, respectively) in AMD/FA residue were found to be considerably higher than the average abundance in the earth crust which varies from 66 ppm in Ce and 40 ppm in Nd to 35 ppm in La (Tyler, 2004). La, Ce, and Nd have found wide applications in rechargeable LaNi metal hydride batteries, glass polishing and strong magnets respectively (Massari and Ruberti, 2013). Hence it is possible to investigate economical technologies to recover these elements from fly ash and the AMD/FA residue. This would not only reduce the release of these elements into the environment but also make the AMD/FA residue which has a significantly higher composition of La and Ce an available source of these valuable elements. This result is of utmost significance because this may be the first time the REE composition of the solid residue resulting from AMD treatment with fly was determined.

### 5.5 Radioactivity

The qualitative and quantitative analysis of the elemental composition of the Carletonville AMD before and after treatment, as well as Matla fly ash and the AMD/FA residue (section 5.4.3) revealed the presence of radionuclides such as Th and U in the Matla fly ash and Carletonville AMD before treatment (feedstock) and also in the AMD/FA residue (waste). Hence it is important to evaluate and understand the

## Chapter Five: Applications of fly ash for AMD treatment

---

radioactivity of the radionuclides present in the feedstock, product and waste. This is in order to ascertain that the radioactivity is not still in the product water and to understand the radioactivity of the Matla fly ash and AMD/FA residue with regards to its disposal or reuse. Hence the radioactivity of Carletonville AMD before and after treatment, Matla fly ash and the AMD/FA residue was undertaken using gamma spectrometric analysis as explained in Chapter 3, section 3.4.5. The results obtained from the gamma ray spectroscopy was used to determine the radioactivity of Carletonville goldmine water before and after treatment, the Matla fly ash and AMD/FA residue. The results of the radioactivity of the Carletonville goldmine water before and after treatment with Matla fly ash are presented discussed in section 5.5.1. While the results of the radioactivity of the Matla fly ash and AMD/FA residue are presented and discussed in section 5.5.2.

### 5.5.1 Activity of Carletonville goldmine water

Analysis of the Carletonville goldmine water before and after treatment with Matla fly ash for radioactivity was carried out using gamma spectrometry as outlined in section 3.4.5. Two samples were prepared for both the untreated and treated Carletonville goldmine water samples analysis and the results are presented in the Table 5.3. Only the radionuclides that were detected in the samples are reported in Table 5.3 Any other possible radionuclides (mainly naturally occurring radionuclides materials (NORM)) in the samples were below the detectable limits of the counting system used in this study.



## Chapter Five: Applications of fly ash for AMD treatment

Table 5:3: Activity concentrations (Bq/L) of radionuclides found in Carletonville goldmine Water samples (n=3)

Activity content in becquerels per liter (Bq/L)		
Sample	$^{238}\text{U}$	$^{226}\text{Ra}$
Carletonville goldmine Water	$38.4 \pm 2.0$	$14.3 \pm 4.7$
	$39.9 \pm 4.9$	$15.7 \pm 5.1$
Treated Carletonville goldmine water	< MDA	< MDA
	< MDA	< MDA

< MDA = Less than minimum detectable activity

Table 5.3 presents the results of the gamma spectrometry analysis of the Carletonville goldmine water before and after treatment with Matla fly ash. It was observed from the result that  $^{238}\text{U}$  concentration were calculated considering that the sample was not in secular equilibrium with the daughter nuclei after the decay of  $^{222}\text{Rn}$  because the  $^{238}\text{U}$  and  $^{226}\text{Ra}$  activity concentrations varied considerably. The results obtained indicated that the activities of the  $^{238}\text{U}$  ( $38.4 \pm 2.0$ ,  $39.9 \pm 4.9$  Bq/L) and  $^{226}\text{Ra}$  ( $14.3 \pm 4.7$ ,  $15.7 \pm 5.1$  Bq/L) in the Carletonville goldmine water were more than the required limit for potable water. The required limits of  $^{238}\text{U}$  and  $^{226}\text{Ra}$  activity for potable water are 10 Bq/litre and 1 Bq/litre respectively (WHO, 2011).

It was also observed from the result that after the treatment of the Carletonville goldmine water with Matla coal fly ash  $^{238}\text{U}$  and  $^{226}\text{Ra}$  activity of the mine water were below the minimum detection activity (MDA) of 7.8 Bq/L and 0.7 Bq/L respectively of the counting system used in this study. The result show that the treatment of the AMD with fly ash also leads to reduction in the radioactivity of the treated water and is in agreement with the elemental analysis of the treated Carletonville goldmine water in section 5.3. The elemental analysis of the Carletonville goldmine water before and after treatment with Matla fly ash showed that the concentration of the radionuclides U ( $3.65 \pm 0.36$  mg/L) and Th ( $0.23 \pm 0.11$  mg/L) in the untreated Carletonville goldmine water were reduced to U ( $1.40 \pm 0.24$  mg/L) and Th ( $0.15 \pm 0.04$  mg/L) after treatment with Matla fly ash.

## Chapter Five: Applications of fly ash for AMD treatment

### 5.5.2 Activity of Matla fly ash and AMD/FA residue

The radioactivity of Matla fly ash (feed stock) and the AMD/FA residue that was produced during the treatment of the Carletonville goldmine water with Matla fly ash in the jet loop reactor was analysed for radioactivity using gamma spectrometry as explained in Chapter 3, section 3.4.5. Two samples were prepared for the analysis of the AMD/FA residue. The results are presented and compared in Table 5.4. The activity concentrations of radionuclides found in AMD/FA residue and Matla fly ash are given in becquerels per kilogram (Bq/kg).

Table 5:4: Activity concentrations of radionuclides found in AMD/FA residue compared to the activity of Matla fly ash and Carletonville goldmine AMD (n=2)

Activity content in becquerels per liter (Bq/L)				
Sample	$^{238}\text{U}$	$^{226}\text{Ra}$	$^{232}\text{Th}$	$^{40}\text{K}$
Fly ash	$140.1 \pm 5.2$	$138.2 \pm 2.7$	$163.3 \pm 1.1$	$175.0 \pm 3.5$
AMD/FA residue	$357.8 \pm 21.2$	$239.1 \pm 8.6$	$173.0 \pm 2.6$	$183.5 \pm 5.1$
	$334.9 \pm 12.1$	$235.3 \pm 4.7$	$174.7 \pm 1.0$	$186.4 \pm 2.8$

The activity content of the Matla fly ash and AMD/FA residue are presented in Table 5.4 and the result reveals that anthropogenic (man-made) radionuclides were not detected in Matla coal fly ash and AMD/FA residue. Only U, Th, Ra, Pb and K, which are NORM were detected. From the results it was also observed that  $^{238}\text{U}$  concentration were calculated considering that the sample was in secular equilibrium with the daughter nuclei after the decay of  $^{226}\text{Ra}$ . This is because there is no significant variation in the activity of  $^{238}\text{U}$  and  $^{226}\text{Ra}$ . Also the result for  $^{232}\text{Th}$  assumes secular equilibrium with daughter nuclei  $^{228}\text{Ac}$ .

The activity concentrations of  $^{238}\text{U}$  and  $^{232}\text{Th}$ , in the Matla fly ash were also observed to be higher than the world-wide average concentrations of  $^{238}\text{U}$ , and  $^{232}\text{Th}$  in soil that are about 33 and 45 Bq kg<sup>-1</sup>, respectively (UNSCEAR 2000).

## Chapter Five: Applications of fly ash for AMD treatment

---

From Table 5.4 the activity measurement of the AMD/FA residue samples showed that the radionuclides in the  $^{238}\text{U}$  decay series are not in secular equilibrium because both the  $^{238}\text{U}$  and  $^{226}\text{Ra}$  activity concentrations varies considerably. However the result for  $^{232}\text{Th}$  assumes secular equilibrium with daughter nuclei. The activity content of  $^{238}\text{U}$  in the AMD/FA residue was observed to be much higher than in the Matla fly ash while there was no significant difference in the activity content of  $^{232}\text{Th}$  in the AMD/FA residue and the Fly ash. The elemental analysis of the Matla fly ash and AMD/FA residue in section 5.4.3.2 reveals that the concentration of U increased from  $10.24 \pm 0.32$  mg/kg in Matla fly ash to  $21.51 \pm 0.54$ . Whilst the concentration of Th was  $10.54 \pm 0.50$  and  $10.55 \pm 0.42$  in Matla fly ash and AMD/FA residue respectively. The observed higher activity content of  $^{238}\text{U}$  in the AMD/FA residue is in agreement with the increase in the U concentration in the AMD/FA residue. due to the removal of U from the Carletonville goldmine water during treatment with Matla fly ash. Hence the disposal or use of the AMD/FA residue should be monitored for environmental concerns since the activity content of  $^{238}\text{U}$  and  $^{232}\text{Th}$  in the AMD/FA residue is higher than world-wide average concentrations in soil and may require special handling because of the enhanced radioactivity which also shows that fly ash is effective as a medium to remove radioactivity from water.

### 5.6 DIN-S4 Leaching test

DIN-S4 leaching test was carried out according to the method specified in section 3.6.1 to assess the leachability of species in the water soluble fraction of the Matla fly ash and AMD/FA residue. This method was used to determine the elements that might be leached from the Matla fly ash and AMD/FA residue when it gets in contact with rainwater and is a measure of short term release of highly soluble species. The results of the DIN-S4 leaching tests that were carried out at different liquid/solid (L/S) ratios for the fly ash and AMD/FA residue are presented in below.

### 5.6.1 pH and EC

The pH and EC values of Matla fly ash and the AMD/FA residue were determined as specified in section 3.5.2. The results are presented in Figure 5.7 and 5.8 below.

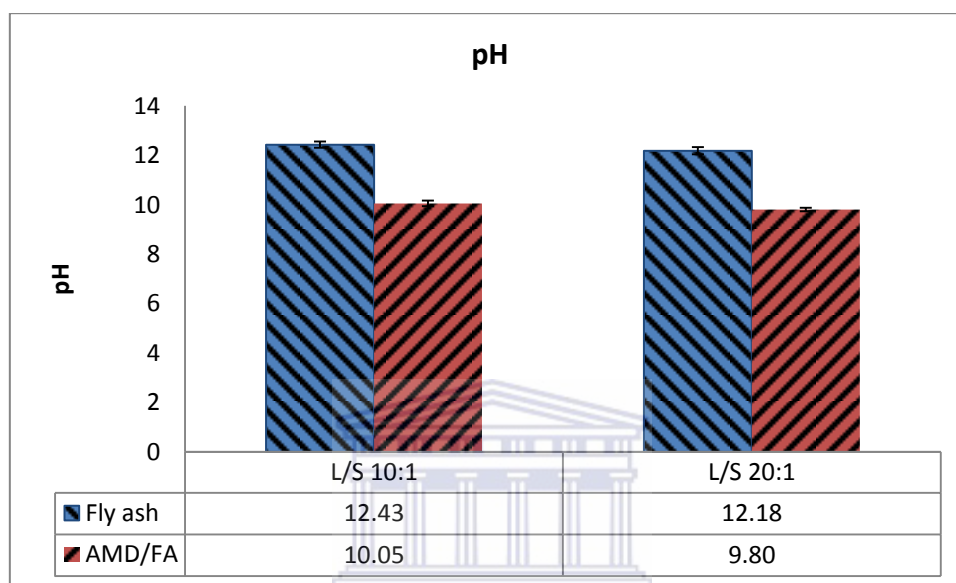


Figure 5.7: pH of Matla fly ash, AMD/FA residue and the synthesised geopolymer using different L/S ratios [number of determination = 3]

The pH of Matla fly ash and the AMD/FA residue at different (10:1 and 20:1) L/S ratios is shown in Figure 5.7. The pH values of Matla fly ash and the AMD/FA residue samples at different L/S ratios were found to be alkaline ranging between 9.80 and 12.43. It was observed that Matla fly ash had higher pH in the different L/S ratio than the AMD/FA residue. The observed higher pH of Matla fly ash compared to the AMD/FA residue may be attributed to the transformation of CaO to  $\text{CaSO}_4 \cdot 2\text{H}_2\text{O}$  during Matla fly ash interaction with the AMD in the jet loop reactor. The final pH value of fly ash usually depends on the relative contents and dissolutions of CaO and MgO present in the waste (Saikia et al., 2006). The pH of fly ash is either acidic or alkaline depending on its chemical constituents; alkaline fly ashes have significant CaO and MgO concentrations. In comparison it was observed that the pH values at the different L/S ratios were negligible in both the fly ash and AMD/FA residue after

## Chapter Five: Applications of fly ash for AMD treatment

leaching in the short term. The pH of fly ash plays a major role in aqueous media and influences the dissolution and leaching of mobile species from fly ash (Ward et al., 2009). As the Matla fly ash and AMD/FA residue alkalinity is reduced over time by natural weathering it can be expected that at elements that are immobile at the higher pH will become mobile at intermediate or lower pH,

Figure 5.8 below presents the EC of the Matla fly ash and the AMD/FA residue at the different L/S ratios.

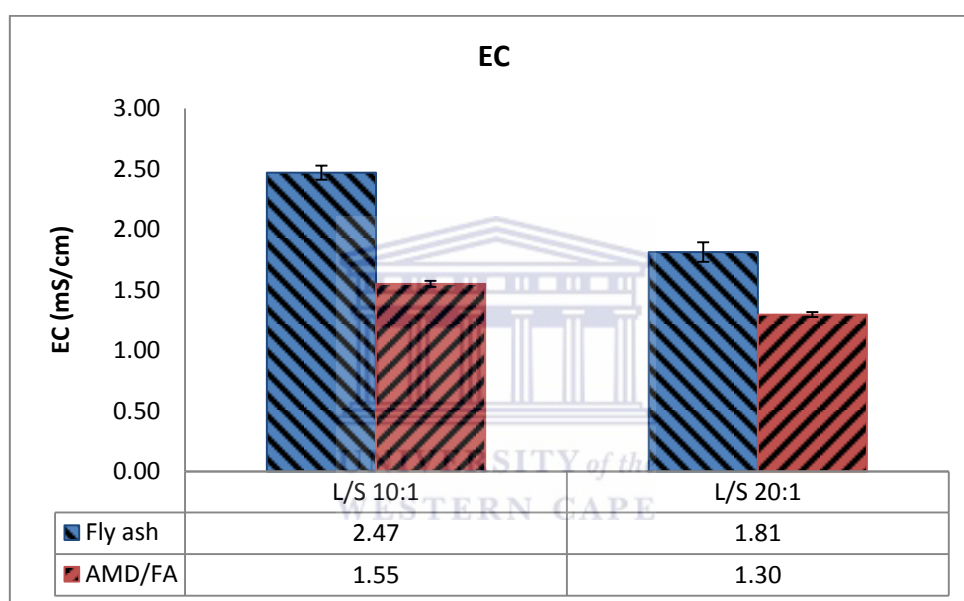


Figure 5.8: EC profile of Matla fly ash and AMD/FA residue using different L/S ratios [number of determination = 3]

The EC of Matla fly ash and AMD/FA residue using different L/S ratios is shown in Figure 5.8. EC values of the Matla fly ash and AMD/FA residue at the different L/S ratio ranged between 1.30 and 2.47 mS/cm. In comparison the EC value of Matla fly ash was observed to be slightly higher than the EC values of the AMD/FA residue at the different L/S ratio. The higher EC value of Matla fly ash is due to the presence of more ionic species in the fly ash than the AMD/FA residue because ionic species are responsible for high EC readings. This shows that contact with AMD during treatment in the jet loop reactor flushed out soluble specie. Also a significant change in EC values was observed in both Matla fly ash and AMD/FA residue samples as the L/S ratio

## Chapter Five: Applications of fly ash for AMD treatment

---

increases indicating that many species in both Matla fly ash and AMD/FA residue are soluble and easily released upon contact with water.

### 5.6.2 Results of DIN-S4 Leachate

The results of the ICP-OES analysis of the DIN-S4 leachates of Matla fly ash and the AMD/FA residue are shown in Table 5.3 and 5.4 below. The ICP analysis was carried out as described in section 3.4.3. The concentrations of the major and trace species in the DIN-S4 leachate at L/S 10:1 and 20:1 of Matla fly ash and the AMD/FA residue are presented in mg/kg and compared to their total elemental content (mg/kg). The percentages of the DIN-S4 leachates of Matla fly ash and the AMD/FA residue are also presented and compared in the tables.



## Chapter Five: Applications of fly ash for AMD treatment

Comparison of total metal content (mg/kg) and amount leached out in DIN-S4 from Matla fly ash and AMD/FA residue at L/S ratio 10:1

Element	Total metal content Matla fly ash (mg/kg)	Total metal content AMD/FA residue (mg/kg)	Matla fly ash L/S 10:1(mg/kg)	AMD/FA residue L/S 10:1(mg/kg)	% MFA leached out	% AMD/FA leached out
Si	254850 ± 444	244362 ± 1531	14.25 ± 0.26	0.20 ± 0.004	0.006	0.00008
Al	145387 ± 153	135369 ± 1631	4.41 ± 0.07	0.32 ± 0.002	0.003	0.0002
Fe	40262 ± 245	45461 ± 1236	9.76 ± 0.19	0.10 ± 0.002	0.02	0.0002
Ca	38498 ± 109	41310 ± 189	225.63 ± 2.12	93.78 ± 0.34	0.57	0.23
Mg	8405 ± 70	8445 ± 61	9.79 ± 0.07	0.06 ± 0.001	0.12	0.0007
K	6281 ± 127	5230 ± 48	21.98 ± 0.55	13.97 ± 0.32	0.35	0.28
Na	1484 ± 20	3858 ± 20	10.83 ± 0.09	1.85 ± 0.016	0.73	0.05
Sr	1272 ± 28.06	1097 ± 10.81	6.49 ± 0.12	0.55 ± 0.002	0.51	0.05
Ba	1014 ± 21.39	945 ± 11.38	6.49 ± 0.13	0.13 ± 0.002	0.64	0.01
Mn	387 ± 0	620 ± 45	4.18 ± 0.08	BDL	1.08	BDL
Zn	104.98 ± 7.25	181.46 ± 8.01	0.03 ± 0.002	0.14 ± 0.002	0.14	0.08
V	73.54 ± 1.18	65.64 ± 1.62	0.03 ± 0.0009	BDL	0.04	BDL
Cr	63.16 ± 1.75	72.43 ± 1.27	0.03 ± 0.001	0.005 ± 0.0001	0.05	0.007
Ni	35.72 ± 0.77	124.15 ± 1.6	0.02 ± 0.0018	BDL	0.06	BDL
As	23.90 ± 3.48	11.39 ± 1.21	0.069 ± 0.009	0.03 ± 0.0006	0.03	0.25
Pb	22.66 ± 1.85	22.46 ± 1.43	0.002 ± 0.0001	0.02 ± 0.00002	0.009	0.11
Co	13.31 ± 0.48	60.34 ± 0.64	0.005 ± 0.0001	0.004 ± 0.0001	0.04	0.007
U	10.20 ± 0.14	20.8 ± 0.012	0.01 ± 0.0025	0.14 ± 0.002	0.1	0.68
Hg	8.33 ± 0.21	10.5 ± 0.85	0.17 ± 0.029	0.04 ± 0.004	2.05	0.41
Cd	3.12 ± 0.21	3.77 ± 0.02	0.00.4 ± 0.0002	BDL	0.13	BDL

BDL = below detection limit

## Chapter Five: Applications of fly ash for AMD treatment

Comparison of total metal content (mg/kg) and amount leached out in DIN-S4 from Matla fly ash and AMD/FA residue at L/S ratio 20:1

Element	Total metal content Matla fly ash (mg/kg)	Total metal content AMD/FA residue (mg/kg)	Matla fly ash L/S 20:1(mg/kg)	AMD/FA residue L/S 20:1(mg/kg)	% MFA leached out	% AMD/FA leached out
Si	254850 ± 444	244362 ± 1530.76	2.12 ± 0.02	3.35 ± 0.02	0.0008	0.001
Al	145387 ± 153	135369 ± 1630.63	5.22 ± 0.01	0.52 ± 0.001	0.004	0.0004
Fe	40262 ± 245	45461 ± 1235.96	0.19 ± 0.0001	BDL	0.0005	BDL
Ca	38498 ± 109	41310 ± 189.36	1406.46 ± 1.10	1145.87 ± 0.23	3.65	2.77
Mg	8405 ± 70	8445 ± 60.50	46.4 ± 0.05	0.08 ± 0.0003	0.55	0.001
Na	1484 ± 20	3858 ± 20.49	42.22 ± 0.05	2.25 ± 0.009	2.85	0.06
K	6281 ± 127	5230 ± 47.92	84.57 ± 0.36	84.85 ± 0.43	1.35	1.62
Sr	959.36 ± 28.06	1097 ± 10.81	4.13 ± 0.003	0.793 ± 0.001	0.33	0.07
Ba	528.38 ± 21.39	945 ± 11.38	0.24 ± 0.0003	0.23 ± 0.0006	0.23	0.024
Zn	104.98 ± 7.25	181.46 ± 8.01	0.02 ± 0.00003	BDL	0.02	BDL
V	73.54 ± 1.18	65.64 ± 1.62	0.01 ± 0.00006	0.01 ± 0.00004	0.02	0.022
Cr	63.16 ± 1.75	72.43 ± 1.27	0.09 ± 0.0009	0.06 ± 0.0005	0.14	0.08
As	23.90 ± 3.48	11.39 ± 1.21	0.22 ± 0.001	0.02 ± 0.0001	0.91	0.2
Pb	22.66 ± 1.85	22.46 ± 1.43	0.02 ± 0.0002	0.04 ± 0.0002	0.11	0.17
Co	13.31 ± 0.48	60.34 ± 0.64	0.009 ± 0.00002	0.006 ± 0.00003	0.07	0.01
Hg	8.33 ± 0.21	10.5 ± 0.85	0.06 ± 0.003	0.03 ± 0.002	0.74	0.31

BDL = below detection limit



## Chapter Five: Applications of fly ash for AMD treatment

---

The major and trace elements ICP analysis of the DIN-S4 leachate for the Matla fly ash and the AMD/FA as shown in table 5.3, reveals that Pb, Mo, Ba, U, Al, Ca, Mg, Na, K, Hg, As, Pb, Fe, Cr, Co, Sr, U, Zn and Si were mobile in Matla fly ash and AMD/FA residue at L/S 10:1. The metals Cd, Mn, Ni and V were detected in the DIN-S4 leachate of the Matla fly ash but were not leached out of the AMD/FA residue at L/S 10:1. Whilst Table 5.3, shows that Ca, Mg, Al, Na, K, Si, Ba, Hg, As, Pb, Cr, Sr, V, and Co were leached out of Matla fly ash and AMD/FA at L/S 20:1. Zn and Fe were detected in the DIN-S4 leachate of the Matla fly ash but were not leached out of the AMD/FA residue at L/S 20:1.

Higher amount of species were leached out of Matla fly ash and AMD/FA residue at L/S 10:1 ratio than at L/S ratio 20:1 except for, Ca, Mg and Na that had higher amount leached out at L/S ratio 20:1. This shows that increasing the amount of water in the L/S ratio did not increase the amount of species leached out but rather dilutes the leached species. This was corroborated by the EC results in section 5.6.1 which showed higher EC readings at L/S ratios 10:1 than at L/S ratio 20:1 in both Matla fly ash and AMD/FA residue. It was also observed that higher amount of species were leached out of Matla fly ash when compared to the amount leached out of the AMD/FA residue at the different L/S ratios. Only U and Zn had higher amounts leached out in the AMD/FA residue at L/S ratio 10:1 (0.06 % and 1.62 % respectively) L/S ratio 10:1 (0.05 % and 0.28 % respectively). Both elements were below detection limit in the leachate of the AMD/FA residue. The observed higher amount of species leached from Matla fly ash compared to AMD/FA residue indicates that secondary minerals are entrapping or capturing the metals in the AMD/FA residue..

For Ca, the percentage leached out of Matla fly ash samples at the L/S ratios 10:1 and 20:1 were 0.57 % and 3.65 % respectively. Whilst for Mg, Na and K the percentages leached out of Matla fly ash at L/S ratios 10:1 were 0.12 %, 0.73 % and respectively and at L/S ratio 20:1 were 0.55 %, 2.85 % and 1.35 % respectively. Ca, Mg, Na and K are known to be associated with the surface of fly ash particles, as well as being incorporated in aluminosilicate phases of the fly ash

(Khanra et al., 1998; Rice et al., 1999). The amounts of Ca, Mg, Na and K that were leached out of the fly ash at both L/S ratios within a period of 24 h may be attributed to the easily soluble sublimates on the surface of fly ash particles. Though Ca is not considered as an element of concern in terms of environmental toxicity, however it does play a crucial role in the environmental quality of the ash. The pH of the fly ash-water system is influenced by Ca (Saikia et al., 2006), and the leachability of most trace elements in coal fly ash is pH-dependant (Jankowski et al., 2006). The existence of Ca is also vital for the precipitation of ettringite and other secondary Ca-hydrated phases that are less soluble and thus are likely to encompass and keep elements of environmental concern such as As, Cr or Se (Izquierdo and Querol, 2012). Hence, to a large extent the leachability of environmentally toxic heavy metal from fly ash are influenced by Ca. Thus the lesser amount of species leached from the AMD/FA residue in comparison to Matla fly ash show that the trace elements are more mobile in Matla fly ash than in the AMD/FA residue. This is because of the existence of secondary Ca-hydrated phases such as ettringite and gypsum. These secondary minerals to some extent control the leachability of trace elements from the AMD/FA residue by encompassing and keeping elements of environmental concern such as As, Cr or Se (Izquierdo and Querol, 2012)

### **5.7 Summary of characterisation of the Matla fly ash Carletonville AMD before and after treatment and AMD/FA residue**

The investigations provided significant insight into the molecular structure, morphology, mineralogy and chemical composition of the Matla fly ash, and the AMD/FA residue. The Carletonville goldmine water samples before and after treatment with Matla fly ash were also characterised. The characterisation results of the untreated Carletonville goldmine water sample classified it as an AMD. The results also showed that the Carletonville goldmine AMD contained elevated levels of toxic metals such as B, Cd, Cr, Hg, and Zn and radionuclide U than the WHO TWQR of portable water. The results also confirmed that the treatment of 80L of the Carletonville goldmine AMD with 16 kg of Matla coal fly ash, 200g of

## Chapter Five: Applications of fly ash for AMD treatment

---

$\text{Ca}(\text{OH})_2$  and 344.95 g of  $\text{Al}(\text{OH})_3$  resulted in the removal of sulphate ions to within the TWQR for potable water.

FT-IR analysis of the Matla fly ash feedstock and the resulting waste (AMD/FA residue) revealed that the fly ash and AMD interaction in the jet loop reactor did not result in the formation of new functional groups in the AMD/FA residue. Morphological studies (by SEM) of the Matla fly ash and AMD/FA residue show that the Matla fly ash and AMD/FA residue consists of irregular, spherically shaped and agglomerated particles. The outer surfaces of the Matla ash particles are smooth while the outer surface of the AMD/FA residue particles appeared encrusted an indication of the formation of new secondary mineral phases. SEM-EDS and XRD confirmed that the encrustations were due to the formation of new mineral phases in the AMD/FA residue. The mineralogical investigation of the Matla fly ash and the AMD/FA residue revealed that the only consistent major mineral components were quartz and mullite in Matla fly ash and AMD/FA residue and established the formation of new mineral phases during the AMD treatment with fly ash in the jet loop reactor.

The elemental content of Matla fly ash and AMD/FA, determined by LA ICP-MS analysis reveals that the toxic heavy metals (As, Cd, Co, Cr, Hg and Pb) and radionuclides (Th and U) were presents in both Matla fly ash and AMD/FA samples. The presence of these toxic elements in AMD/FA residue raises concern over its safety as regards to its disposal because of the possibility of these elements leaching from the AMD/FA residue when disposed. The Matla fly ash and AMD/FA sample were further shown to be class F and silico-aluminate. The AMD/FA residue also meets the requirements of Class F fly ash but has a higher LOI due to formation of new secondary minerals during the AMD treatment in the jet loop reactor. The result of the REE determined in Matla fly ash showed that the concentrations of La, Ce, and Nd in Matla fly ash were much higher than the average abundance in the earth crust. This result is of utmost significance because this is the first time the REE composition of the solid residue resulting from AMD

## Chapter Five: Applications of fly ash for AMD treatment

---

treatment with fly was determined. This, it is possible to investigate methods that can be used in recovering these elements AMD/FA residue.

Analysis of the Carletonville goldmine water before and after treatment for radioactivity revealed that the activities of the  $^{238}\text{U}$  and  $^{226}\text{Ra}$  in the Carletonville goldmine water were more than the required limit for potable water. It was also shown that after the treatment of the Carletonville goldmine water with Matla coal fly ash  $^{238}\text{U}$  and  $^{226}\text{Ra}$  activity of the mine water were observed to be below the minimum detection activity of the counting system used in this study. This indicates that the treatment of the AMD with fly ash also results in the reduction of the radioactivity of the treated water and is in agreement with the elemental analysis of the treated Carletonville goldmine water. The radioactivity studies of Matla fly ash (feed stock) and the AMD/FA residue revealed that only NORM was detected in Matla coal fly ash and AMD/FA residue samples. The activity concentrations of  $^{238}\text{U}$  ( $^{226}\text{Ra}$ ) and  $^{232}\text{Th}$ , in the Matla fly ash and AMD/FA residue were also observed to be higher than the world-wide average concentrations of  $^{238}\text{U}$ , and  $^{232}\text{Th}$  in soil thus, raising environmental concerns over the safety of their disposal and beneficiation.

The pH values of Matla fly ash and the AMD/FA residue samples at different L/S ratios were found to be alkaline. Also Matla fly ash had higher pH in the different L/S ratio than the AMD/FA residue due to transformation of  $\text{CaO}$  to  $\text{CaSO}_4 \cdot 2\text{H}_2\text{O}$  during interaction with the AMD in the jet loop reactor. The EC value of Matla fly ash was observed to be slightly higher than the EC values of the AMD/FA residue at the different L/S ratio and a significant change in EC values was observed in both Matla fly ash and AMD/FA residue samples as the L/S ratio increases due to dilution of the soluble species released from the samples due to the higher amount of water used. The analysis of the DIN- S4 leachates of Matla fly ash and the AMD/FA residue shows that a higher amount of species were leached out of Matla fly ash and AMD/FA residue at L/S 10:1 ratio than at L/S ratio 20:1 and that increasing the amount of water in the L/S ratio did not increase the amount of species leached out but rather dilutes the leached species. The DIN-S4 study also

## **Chapter Five: Applications of fly ash for AMD treatment**

---

revealed that higher amount of species were leached out of Matla fly ash when compared to the amount leached out of the AMD/FA residue at the different L/S ratios. This due to the incorporation of these species in the secondary mineral phases such as ettringite that were formed in the AMD/FA residue as a result of the fly ash AMD interaction in the jet loop reactor. Results from the leaching test provided valuable information on the relative availability of trace pollutants in the AMD/FA residue and, hence, on the extent of entrapment or encapsulation

.



### Chapter Six: Geopolymer from fly ash

#### 6 Introduction

This chapter presents and discusses the use of Matla fly ash in the synthesis of foamed geopolymer. It includes the results of the physical and chemical characterisation of Matla fly ash and synthesised geopolymer that were carried out using different analytical techniques such as LA ICP-MS, XRF, XRD, SEM-EDS and FTIR. This chapter also presents and discusses the results of the Gamma Spectroscopy of the Matla fly ash (feedstock) and the synthesised geopolymer (product) in order to determine the radioactivity of the process feedstock and product. Furthermore the results of the leaching tests (DIN-S4) of the Matla fly ash and the synthesised geopolymer, used to determine the solubility and leachability of the toxic components, are also presented and discussed.

This chapter starts with an overview of geopolymer materials and the aims and objectives of this chapter in section 6.1. Whilst a brief description of the materials and methods used is given in section 6.2 the results of the spectroscopic methods used in characterising the Matla fly ash and synthesised geopolymer samples are presented and discussed in section 6.3. The functional group characterisation studies for molecular structure identification (FTIR data) are presented and discussed in section 6.3.1 while the morphological analysis (SEM-EDS data) are presented and discussed in section 6.3.2. The mineralogical composition of the Matla fly ash and the synthesised geopolymer samples are presented and discussed in section 6.3.3.

In section 6.3.4 the bulk chemical composition of the Matla fly ash and the synthesised geopolymer (XRF and LA ICP-MS analysis) are presented and discussed. The results from the gamma spectrum analysis and the DIN-S4 leach test will be presented and discussed in section 6.4 and 6.5 respectively. This chapter will end with a summary of the major findings of the use of Matla fly ash in the synthesis of geopolymer. The results of the possibility of extracting REE from Matla fly ash will be presented and discussed in chapter seven.

### 6.1 Overview

The most abundant manmade material on earth is concrete. Portland cement is one of the main constituents in a regular concrete mixture. The production of ordinary Portland cement accounts for about 5% of the world's CO<sub>2</sub> emissions, hence the need to create and develop a greener building material. Geopolymer concrete is a high strength and lightweight inorganic polymer that can be used in place of normal concrete. Geopolymers were introduced by Davidovits in the early 1970s to describe inorganic materials formed by activating silica-aluminium rich feedstock with alkaline or alkaline-silicate solution at ambient or higher temperature level (Davidovits, 2001).

The hardened polymeric material has an amorphous, three-dimensional structure similar to that of an aluminosilicate glass (Satpute Manesh, et al., 2012). These materials represent a new order of cementitious products able to provide ceramic and polymeric properties not normally present in traditional cement materials. Unlike conventional organic polymers, glass, ceramic, or cement, geopolymers are non-combustible, heat-resistant, formed at low temperatures, and are fire/acid resistant.

Geopolymerisation is the process that describes the creation of a geopolymer. It is a very complex multiphase exothermic process, involving a series of dissolution-reorientation-solidification reaction analogous to zeolite synthesis. Hence the chemical composition of geopolymers is similar to that of natural zeolitic materials, but they are usually amorphous instead of crystalline (Palomo et al. 1999; Xu and van Deventer 2000; Al Bakri, et al., 2012; Takeda et al., 2010). The reactants needed to form a geopolymer are an alkali metal hydroxide/silicate solution (often referred to as the chemical activator) and an aluminosilicate fine binder.



## Chapter Six: Geopolymer from fly ash

---

The binder or feedstock needs to have a significant proportion of silicon and aluminium ions held in amorphous phases. Many industrial by-products or waste can be used as feed stocks for geopolymer production. Fly ash can be used as a cheap source material for making geopolymers because of its high aluminosilicate content, the main reactants in the geopolymerisation reaction. Hence several research studies have been focused on the utilization of coal fly ash in the development of geopolymers as a replacement for cement in the construction industry (Duxson et al. 2007; Lloyd et al., 2010). The production of geopolymer concrete allows fly ash to be recycled and eliminated from dump sites.

Fly ash is composed of multiple chemical compounds, including heavy metals (As, Pb, Cd, Hg) and radionuclides (U and Th) as well as other harmful elements. The potential toxicity of coal fly ash is an important factor that has to be investigated if it is to be used for geopolymer concrete in buildings. Thus the aim of this chapter is to evaluate and understand the toxicity of geopolymer synthesised from Matla fly ash. The objectives of this chapter are: a) to characterise the fly ash feedstock and synthesised geopolymer in order to understand the properties of the fly ash that are carried over to the geopolymer, b) to determine the toxicity of the synthesised geopolymer in terms of the radioactivity of the radionuclides present in the fly ash, and c) to investigate the leachability of potentially toxic elements from the geopolymer.

### 6.2 Materials and methods

The Matla fly ash sample used as feedstock for the synthesis of foamed geopolymer was collected directly from the hoppers at Matla power station located in Mpumalanga province of South Africa. The sodium hydroxide (NaOH) was analytical grade (98%) and the sodium hypochlorite (NaOCl) solution was 12%. Both NaOH and NaOCl were supplied by Merck. The foamed geopolymer was synthesised by the method proposed by Boke et al., (2014) and the synthesis procedure is described in detail in chapter 3, section 3.6.3.



The Matla fly ash and the synthesised geopolymer were characterised using different analytical techniques such as LA ICP-MS and XRF for determination of chemical composition; FTIR for structural analysis; XRD for analysis of the mineral phase composition; and SEM-EDS for morphological and elemental composition. The procedures for these analytical processes are outlined and detailed in Chapter 3 sections 3.4.2, 3.4.4, 3.4.6, 3.4.7 and 3.4.7 respectively. The radioactivity measurement of Matla fly ash and synthesised geopolymer were undertaken using gamma spectrometric analysis as explained in Chapter 3, section 3.4.5. The DIN-S4 leaching test was carried out to assess the concentrations of the species in the water soluble fraction of the Matla fly ash and synthesised geopolymer, according to the method specified in section 3.6.1.

### 6.3 Results of the characterisation of geopolymer

#### 6.3.1 FT-IR analysis of geopolymer from Matla fly ash

The geopolymer synthesised from the Matla fly ash was characterised using the FT-IR technique in order to obtain information about the structural configuration of the synthesised geopolymer. Figures 6.1 compare the FT-IR spectrum of the synthesised geopolymer to that of Matla fly ash.

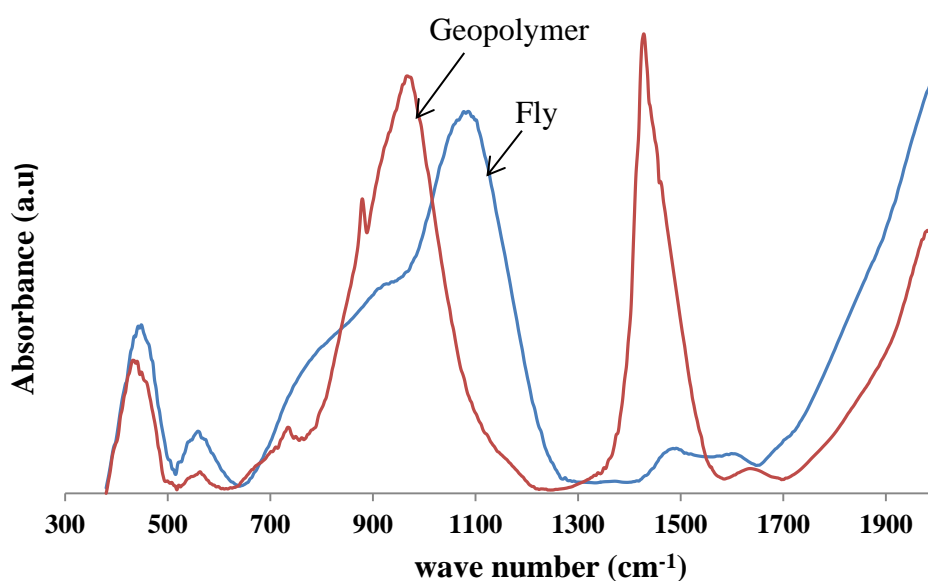


Figure 6.1: FTIR spectra of the Matla fly ash compared to the synthesised geopolymer

## Chapter Six: Geopolymer from fly ash

---

The transformation of the fly ash into geopolymer can be established by comparing the FT-IR spectrum of the Matla fly ash to the FT-IR spectrum of the synthesised geopolymer. In Figure 6.1 two distinctive features are observed that differ between the FT-IR spectrum of Matla fly ash and the FT-IR spectrum of the synthesised geopolymer. The first is the shift of the band attributed to the asymmetric stretching vibrations of Si-O-Si and Al-O-Si. This band, which appeared as a broad band at around  $1101\text{ cm}^{-1}$  in the FT-IR spectrum of the Matla fly ash, became sharper and shifted to a lower frequency at around  $977\text{ cm}^{-1}$  in the FT-IR spectrum of the synthesised geopolymer indicating the formation of a new product (the amorphous aluminosilicate gel phase) that is associated with the dissolution of the fly ash amorphous phase in the strong alkaline activating solutions (Fernández-Jiménez, and. Palomo, 2005) and polycondensation with alternating Si-O and Al-O bonds (Andini et al., 2008). The frequencies of the Si-O-Si bands are an indication of the overall degree of polymerization of the silica network. In general, a lower frequency corresponds to a lower degree of polymerization.

The second distinctive feature is the high intensity of the band at  $1432\text{ cm}^{-1}$  observed in the spectrum of the synthesised geopolymer. This high intensity is attributed to stretching vibrations of O-C-O bonds indicating the presence of sodium bicarbonate that is suggested to occur due to the atmospheric carbonation of the contained Na, which is incorporated into the geopolymer structures surface (Swanepoel and. Strydom, 2002).

The spectra of synthesised geopolymer also revealed vibration bands characteristic of aluminosilicates. These vibrations were observed at  $441\text{ cm}^{-1}$  which is a region associated with Si-O-Si and O-Si-O bending vibrations (Álvarez-Ayuso et al., 2008; Fernández-Jiménez & Palomo, 2005b). Barnes et al., (1999) reported that vibration bands between  $440\text{ cm}^{-1}$  and  $470\text{ cm}^{-1}$  may also be associated with Si-O bending vibrations of sodalite zeolite phase.

### 6.3.2 Morphological analysis of geopolymer from Matla fly ash

The scanning electron micrographs comparing the surface morphology of the geopolymer synthesised from Matla coal fly ash is to that of Matla fly ash is shown in Figure 6.2.



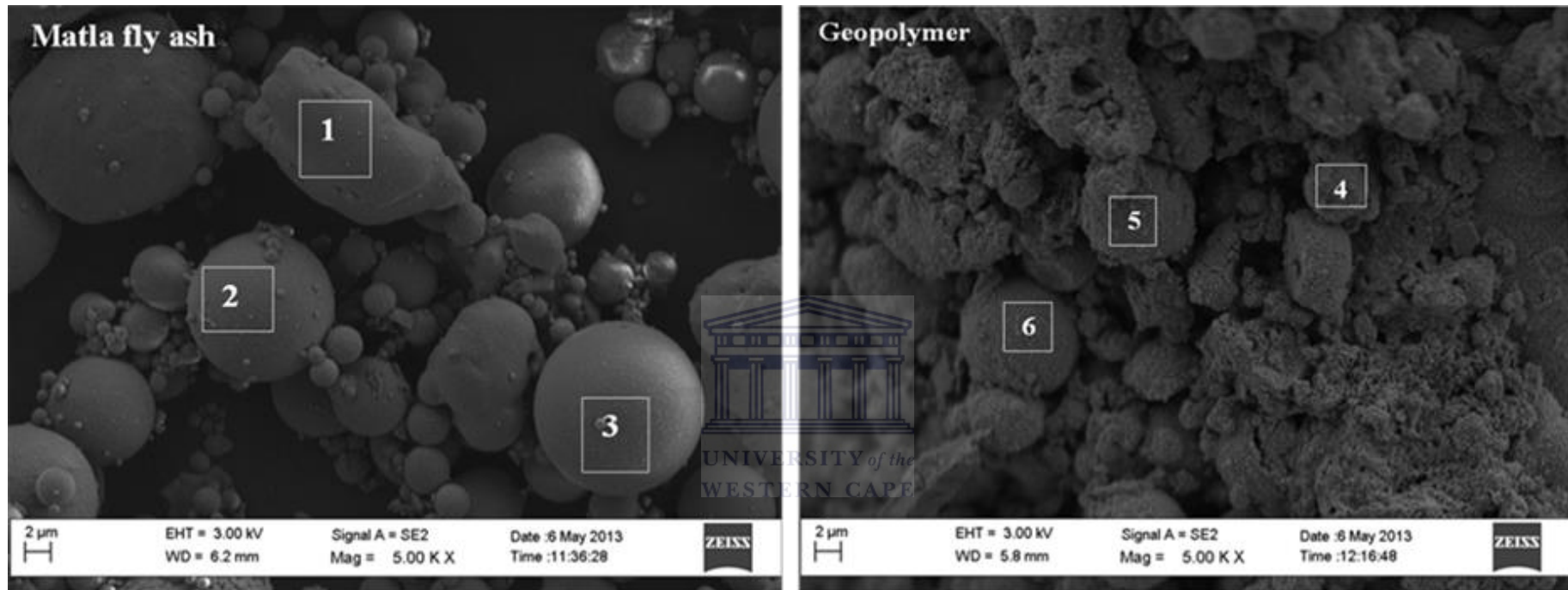


Figure 6.2: SEM Micrograph of Matla ash and the synthesised geopolymer showing the area chosen for EDS analysis

## Chapter Six: Geopolymer from fly ash

In Figure 6.2 the SEM image shows that Matla fly ash consisted mostly of irregular as well as spherically shaped and agglomerated particles with outer smooth surfaces. Whilst the synthesised geopolymer was comprised of mostly irregular shaped and agglomerated particles. Also the outer surfaces of the synthesised geopolymer particles appeared etched indicating dissolution of the glassy phase. The particles of the synthesised geopolymer were also observed to be agglomerated more than the Matla coal fly ash particles (Figure 6.2). The observed etched surface and the increase in agglomeration of the geopolymer particles results from the dissolution of  $\text{SiO}_2$  and  $\text{Al}_2\text{O}_3$  (aluminosilicate structure) in the alkaline solution leading to the formation of aluminosilicate gel (Chen-Tan et al., 2009)

Table 6.1 below shows the atomic % of elements in Matla fly ash and the synthesised geopolymer in the areas chosen for the EDS spot analysis.

Table 6:1: SEM-EDS (atomic %) of the synthesised geopolymer compared to Matla fly ash n = 3

Elements	Matla fly ash			Synthesised geopolymer		
	1	2	3	4	5	6
Al	18.50	5.27	45.22	22.38	12.45	39.98
Si	30.69	12.40	48.45	34.91	21.76	28.83
Ca	5.43	3.83	1.29	12.94	19.93	3.04
Ti	3.60	Nd	2.35	Nd	Nd	Nd
Fe	41.77	78.50	1.67	Nd	Nd	Nd
Cl	Nd	Nd	Nd	11.07	28.22	2.85
W	Nd	Nd	Nd	3.89	Nd	Nd
F	Nd	Nd	Nd	Nd	Nd	8.47
Na	Nd	Nd	Nd	14.84	17.69	16.82
K	Nd	Nd	1.02	Nd	Nd	Nd
Total	100	100	100	100	100	100

Nd = not detected

Table 6.1 compares the result of the SEM-EDS (atomic %) analyses of Matla fly ash to the synthesised geopolymer. The elemental composition of the analysed

spots shows that Al, Si, Ca, Ti, and Fe were the elements detected in the analysed areas of the Matla fly ash sample. C, Si, Al, Na, Cl, and Ca, were the elements detected in the three analysed areas of the synthesised geopolymer but in different atomic percentages. The table also shows that Na, Cl, F and Mg were detected in the synthesised geopolymer but were not detected in the Matla fly ash sample. The inconsistency in the atomic percentages of the detected elements in the analysed spots also highlights that the EDS is a qualitative method and cannot be relied on for quantitative analysis. This EDS spot analysis also emphasizes the heterogeneity of the Matla fly ash feed stock at micron scale.

### 6.3.3 Mineralogical analysis of geopolymer from Matla fly ash

Figure 6.3 shows the XRD patterns of the Matla fly ash and the synthesised geopolymer. The XRD patterns are compared in order to understand the transformation in the mineralogy of the synthesised geopolymer.

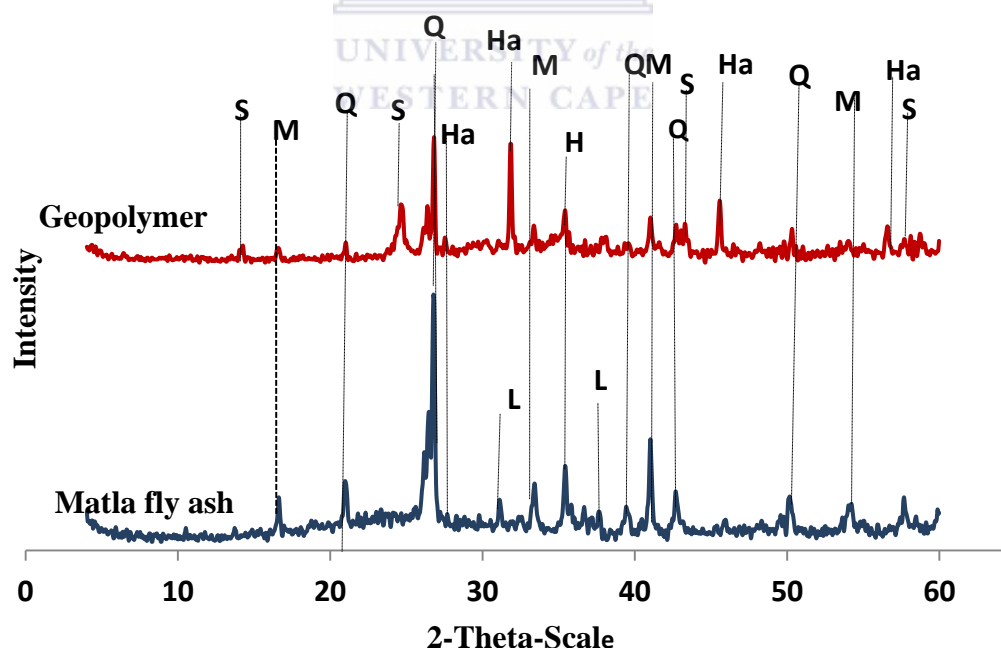
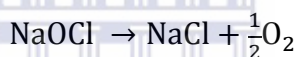


Figure 6.3: XRD patterns for Matla fly ash sample and the synthesised geopolymer [M = Mullite; Q = Quartz; S = Sodalite; Ha = Halite; L = Lime; H = Hematite]

## Chapter Six: Geopolymer from fly ash

---

In Figure 6.3, the XRD results of the geopolymer synthesised from Matla fly ash shows that quartz ( $\text{SiO}_2$ ), mullite ( $\text{Al}_6\text{Si}_2\text{O}_{13}$ ), halite ( $\text{NaCl}$ ) and sodalite ( $\text{Na}_8\text{Al}_6\text{Si}_6\text{O}_{24}\text{Cl}_2$ ) were the major crystalline peaks. In comparison, quartz and mullite are also the observed major crystalline peaks in the XRD result of the Matla fly ash. There were significant decreases in the peak intensities of the quartz and mullite mineral phases of the geopolymer spectrogram compared to the fly ash spectrogram. This indicates that the dissolution of these minerals play a substantial role in the geopolymerisation process of the Matla fly ash. This may be attributed to the demineralisation of the quartz and mullite mineral phases by the NaOH that was used in the alkaline activation of the fly ash. The halite mineral phase may have resulted from the chemical dissociation of the NaOCl that was used as the foaming agent during geopolymerisation. NaOCl decomposed to produce NaCl and  $\text{O}_2$  as shown in the following equation:



The sodalite phase reported in the geopolymer may have resulted from the geopolymerisation process. Sodalite is a type of zeolite and geopolymers are zeolite precursors (Fernández-Jiménez, and. Palomo, 2005). Hence the identified sodalite was due to the partial conversion of geopolymer gel into zeolite (Kumar and Kumar, 2011). The corroborate the FT-IR results of the synthesised geopolymer that showed vibration bands at  $441\text{ cm}^{-1}$  that are usually associated with Si-O bending vibrations of sodalite zeolite phase (Barnes et al., 1999).

Although, lime ( $\text{CaO}$ ) and hematite ( $\text{Fe}_2\text{O}_3$ ) phaseses were present in Matla fly ash these mineral phases were not presnt in the synthesised geopolymer indicating that Ca and Fe did not participate in the formation of the crystalline phases in the synthesised geopolymer. This maybe due to the conversion of  $\text{CaO}$  and  $\text{Fe}_2\text{O}_3$  crystalline structure to amorphous phases during the geopolymerisation process.

### 6.3.4 Bulk Chemical Composition Analysis

The elemental concentrations of the geopolymer synthesised from Matla fly ash samples were determined by XRF spectroscopy and LA ICP-MS. The results are presented and discussed in sections 6.3.4.1 to 6.3.4.3

#### 6.3.4.1 Major

The results of the concentrations of the major and minor elements in the geopolymer synthesised from Matla fly ash determined by XRF spectroscopy are presented in Figure 5.5 below. In the figure the major and minor elemental concentrations of the synthesised geopolymer are compared to the elemental composition of the Matla fly ash. The compositions of the elements are reported in mg/kg.





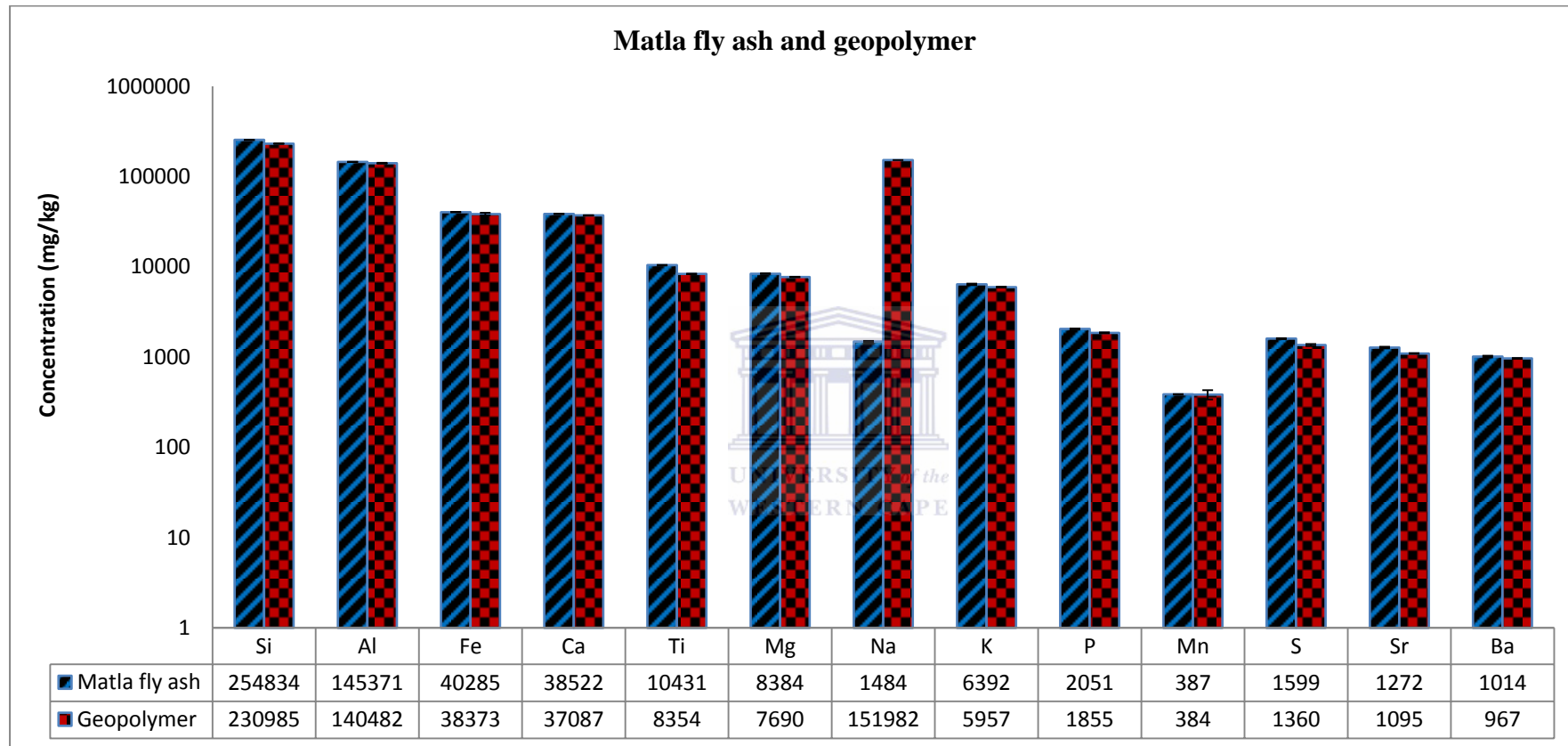


Figure 6.4: Concentrations of major elements in Matla fly ash and the synthesised geopolymer determined by XRF spectroscopy [number of determinations = 3]

Figure 6.4 presents and compares the elemental composition of the synthesised geopolymer and Matla fly ash determined by XRF spectroscopy. It was observed that Si and Al were the major elements in both Matla fly ash and the synthesised geopolymer. The concentration of Na (151982 mg/kg) obtained in the synthesised geopolymer was much higher than its concentration in the Matla fly ash (1484 mg/kg). The increase in the concentration of Na resulted from the NaOH and NaOCl that were used in the synthesis of the foamed geopolymer and corroborates the XRD result which revealed the presence of halite (NaCl) phase. On the other hand the concentrations of the major elements Si, Al, Fe, Ca, Ti, Mg, K, Mn and S in the Matla fly ash were observed to be higher than their concentrations in the synthesised geopolymer. The decrease in the concentrations of these species in the synthesised geopolymer could be attributed to the dilution effect of the NaOH and NaOCl during the geopolymer synthesis.

### 6.3.4.2 Trace elements

The results of the concentrations of the trace elements in the synthesised geopolymer sample and Matla fly ash determined by LA ICP-MS are presented in Figure 6.5 below. The compositions of the trace elements are reported in mg/kg and compared to the trace element concentrations of the Matla fly ash sample.

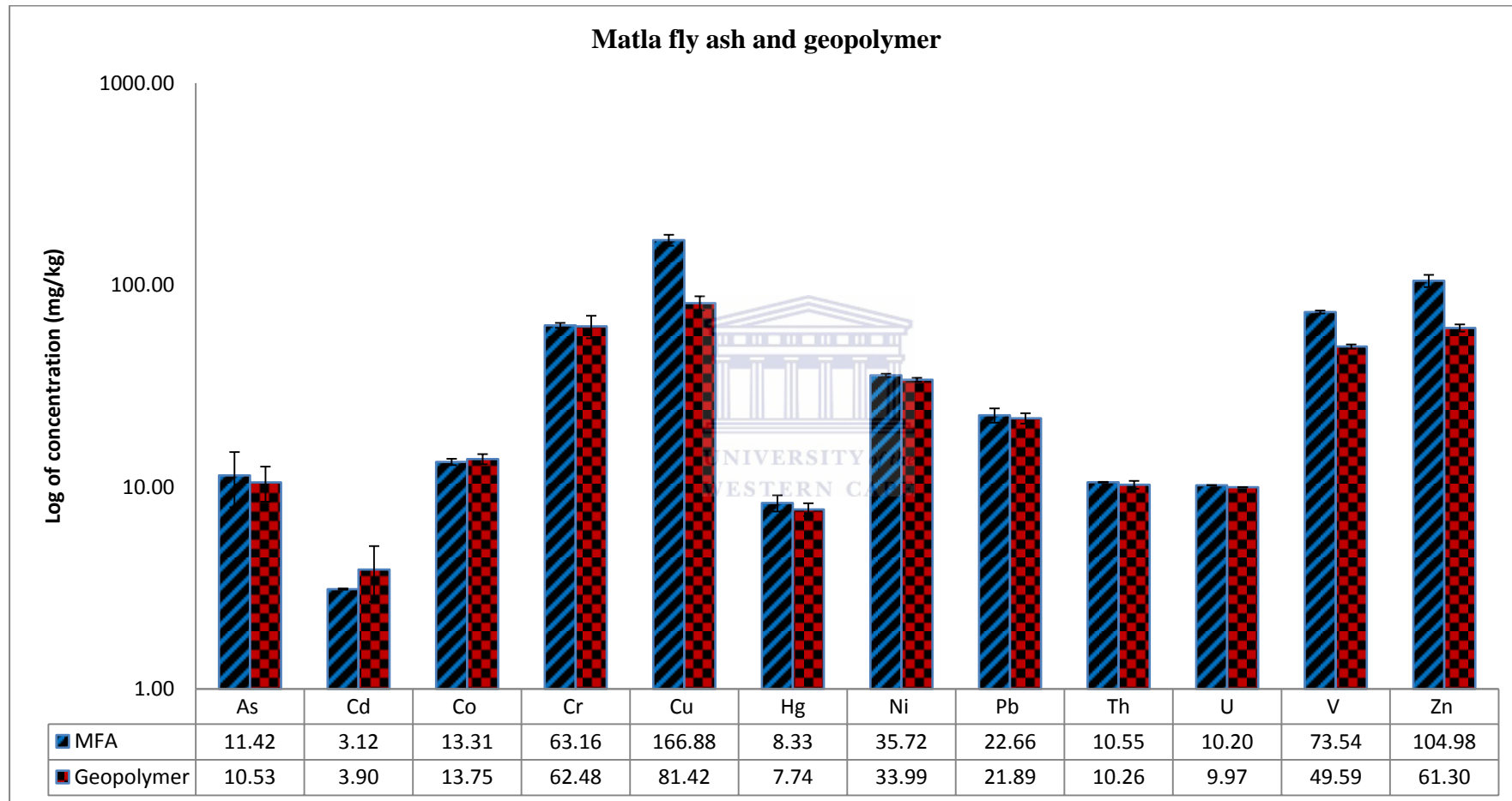


Figure 6.5: Concentrations of trace elements in Matla fly ash and the synthesised geopolymer determined by LA ICP-MS [number of determinations = 3]

The trace elemental concentrations of the synthesised geopolymer and the Matla fly ash are presented and compared in Figure 6.5. The heavy metals As, Cd, Cr, Hg, Ni, Pb and radio nuclides Th and U were detected in the geopolymer samples as well as in Matla fly ash. The result shows that the concentrations of the trace elements determined were within the same magnitude in Matla fly ash and the synthesised geopolymer. This indicates that the geopolymerisation process did not contribute to any increase or reduction of the trace elements concentration from the fly ash (feedstock) to the synthesised geopolymer (products). Generally, heavy metals such as As, Cd, Cr, Hg, Ni, and Pb; and radionuclides (Th and U) may be toxic (Järup, 2003; MacKenzie, 2000). Thus the presence of these elements in the synthesised geopolymer raises concerns over its safety with regard to its use as construction materials.

### 6.3.4.3 Rare earth elements (REE)

The results of the concentrations of the REE geopolymer synthesised from Matla fly ash determined by LA ICP-MS are presented in Figure 6.6 below. The REE concentrations of the synthesised geopolymer are compared to the REE concentration of the Matla fly ash and compositions of the elements are reported in mg/kg.

## Chapter Six: Geopolymer from fly ash

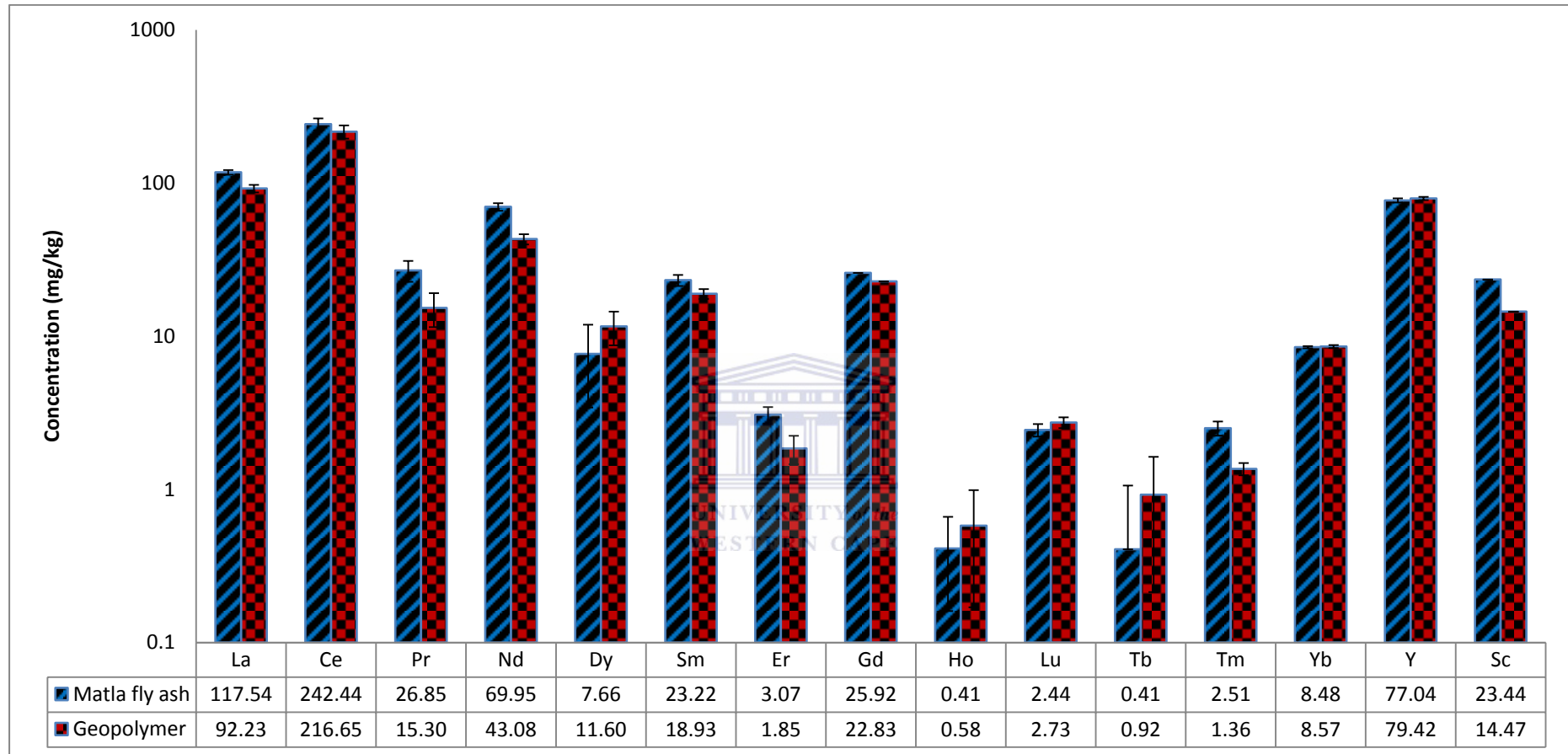


Figure 6.6: Concentrations of REE in Matla fly ash and the synthesised geopolymer determined by LA ICP-MS [number of determinations = 3]

## Chapter Six: Geopolymer from fly ash

In Figure 6.6 the REE composition of the synthesised geopolymer determined by LA-ICP-MS are presented. From the Figure it was observed that concentrations of the REE were higher in Matla fly ash when compared to the synthesised geopolymer. As in the case of the major and minor elements (section 5.5.3.2), the decrease in the concentrations of the REE in the synthesised geopolymer could be attributed to the dilution effect of the NaOH and NaOCl during the geopolymer synthesis. This was the first time the REE content of geopolymer synthesised from Matla fly ash has been determined and the results show that geopolymerisation process may not play any role in the valorisation of fly ash in terms of extracting the REE. This is because the reduction in the concentration of REEs in the synthesised geopolymer.

### 6.4 Activity of the synthesised geopolymer

The radioactivity of the geopolymer synthesised Matla fly ash was determined using gamma spectrometric analysis and the results are presented in Table 6.2. As observed in the activity measurement of the Matla fly ash (section 6.1) there were no anthropogenic (man-made) radionuclides detected in the synthesised Geopolymer. Only naturally occurring radionuclides materials (NORM) were detected, which were U, Th, Ra, Pb and K.

Table 6.2: Activity concentrations of radionuclides found in the synthesised geopolymer compared to the activity of Matla fly ash

Activity content in becquerels per kilogram (Bq/kg)				
Sample	$^{238}\text{U}$	$^{226}\text{Ra}$	$^{232}\text{Th}$	$^{40}\text{K}$
Geopolymer	$93.7 \pm 9.7$	$92.5 \pm 2.3$	$108.4 \pm 1.0$	$120.5 \pm 3.3$
Fly ash	$140.1 \pm 5.2$	$138.2 \pm 2.7$	$163.3 \pm 1.1$	$175.0 \pm 3.5$

Table 6.2 present the activity content of the geopolymer. It was observed from the result that  $^{238}\text{U}$  concentration of the synthesized geopolymer and Matla fly ash samples were calculated considering that the samples were in secular equilibrium with the daughter nuclei. This is because there was no significant variation in the

## Chapter Six: Geopolymer from fly ash

$^{238}\text{U}$  and  $^{226}\text{Ra}$  activity concentrations. The results show that the activity content of the synthesised geopolymer was lower than that of the Matla fly ash. The understanding of the activity concentrations of the synthesized geopolymer as a material to be used in building is important in the assessment of its possible radiological hazards to human health.

The radiological hazard due to the use of the synthesized geopolymer was calculated using the following indices

1. Radium equivalent index,  $Ra_{eq} = C_{Ra} + 1.43C_{Th} + 0.077C_K$

2. External hazard index,  $H_{ex} = \frac{C_{Ra}}{370} + \frac{C_{Th}}{259} + \frac{C_K}{4810}$

3. Activity index or gamma index,  $I_\gamma = \frac{C_{Ra}}{300} + \frac{C_{Th}}{200} + \frac{C_K}{3000}$

Where,  $C_{Ra}$ ,  $C_{Th}$  and  $C_K$  are the activity concentrations of  $^{226}\text{Ra}$ ,  $^{232}\text{Th}$  and  $^{40}\text{K}$  in Bq/kg respectively.

Table 6:3: Radiological hazard indices of the synthesized geopolymer and Matla fly ash

<b>Radiological hazard indices</b>			
<b>Sample</b>	<b><math>Ra_{eq}</math> (Bq/kg)</b>	<b><math>H_{ex}</math> (Bq/kg)</b>	<b><math>I_\gamma</math></b>
Geopolymer	256.79	0.7	0.89
Fly ash	385.19	1.0	1.34

Table 6.3 presents the results of the calculated values of radium equivalent index ( $Ra_{eq}$  in Bq/kg), external hazard index ( $H_{ex}$  in Bq/kg) and activity index or gamma index ( $I_\gamma$ ) of the synthesised geopolymer and Matla fly ash. The calculated  $Ra_{eq}$  value of the synthesised geopolymer was 256.79 Bq/kg and is less than 370 Bq/kg

that is estimated to keep the gamma-ray dose below  $1.5 \text{ mSv y}^{-1}$  in building material (UNSCEAR, 2000). Also the calculated  $H_{\text{ex}}$  value of the synthesised geopolymer was  $0.7 \text{ Bq/kg}$  ( $<1 \text{ Bq/kg}$ ).  $H_{\text{ex}}$  should be less than 1 for any material to be considered safe in the construction of buildings (Ademola, 2009). While the calculated  $I_{\gamma}$  value of the synthesised geopolymer, 0.89 was also  $<1$ . A material with  $I_{\gamma}$  of 1 or  $<1$  can be used as building material without restriction in terms of radioactivity (EC, 1999). On the other hand the calculated  $R_{\text{a}_{\text{eq}}}$ ,  $H_{\text{ex}}$  and  $I_{\gamma}$  values of the Matla fly ash ( $385.19 \text{ Bq/kg}$ ,  $1.0 \text{ Bq/kg}$  and  $1.34$ ) were above the recommended values and did not meet the requirements as a building material in terms of radioactivity.

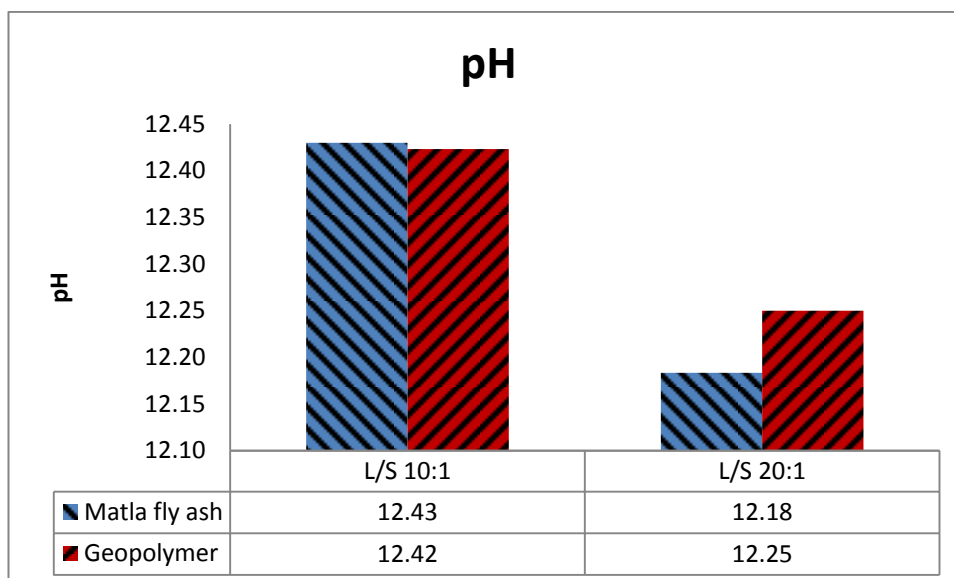
### 6.5 Leaching

DIN-S4 leaching test using different liquid/solid (L/S) ratios was carried out according to the method specified in section 3.6.1 to assess the leachability and the water soluble fraction of the Matla fly ash and synthesised geopolymer. This method was used to determine the elements that might be leached of the geopolymer when it is exposed to water and is a measure of short term release of highly soluble species. The results of the DIN-S4 leaching tests that were carried out at different liquid/solid (L/S) ratios for the fly ash and synthesised geopolymer are presented in section 6.5.1 and 6.5.2 below.

#### 6.5.1 pH and EC

The pH and EC values of leachates from Matla fly ash and the synthesised geopolymer were determined as specified in section 3.5.2. The results are presented below in Figure 6.7 and 6.8 respectively.



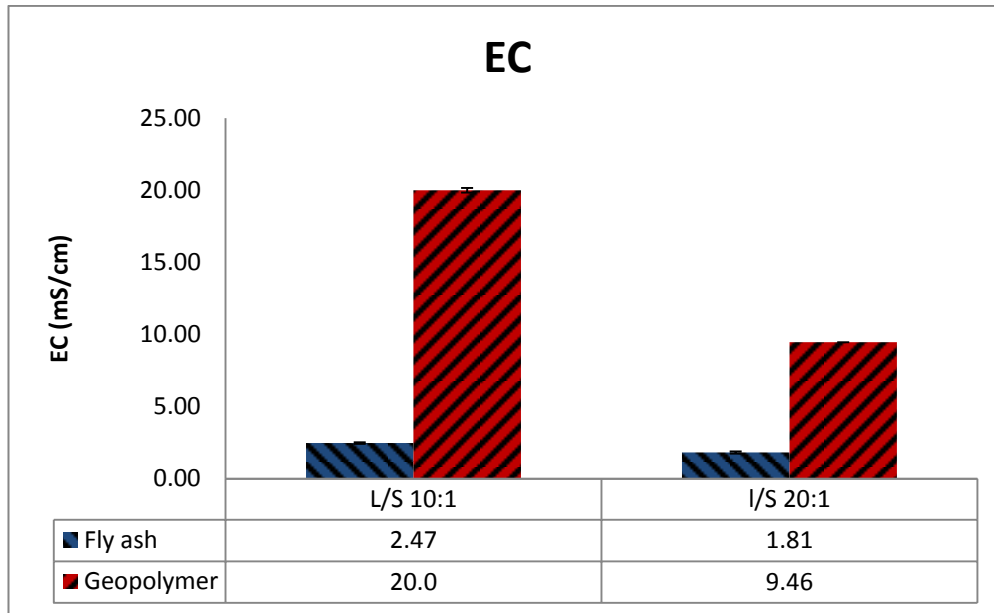


L/S = liquid to solid ratio

Figure 6.7: pH of leachates of Matla fly ash and the synthesised geopolymer using different L/S ratios [number of determinations = 3]

The pH of Matla fly ash and the synthesised geopolymer using different L/S ratios are shown in Figure 6.7. The pH values of the leachates of fly ash and the synthesised geopolymer samples at different L/S ratios were found to be alkaline ranging between 12.18 and 12.42. This may have an impact on the mobility of species with a strong pH dependent solubility. It was observed that there was no significant change in the pH of the leachates of synthesised geopolymer and Matla fly ash in the different L/S ratio. Thus the NaOH and NaOCl that were used in the synthesis of the geopolymer did not alter the pH of the synthesised geopolymer compared to the fly ash. It was also observed that the changes in pH values at the different L/S ratios were negligible in Matla fly ash and the synthesised geopolymer samples.

Figure 6.8 below presents the EC of Matla fly ash and the synthesised geopolymer at the different L/S ratios.



L/S = liquid to solid ratio

Figure 6.8: EC profile of leachates of Matla fly ash and the synthesised geopolymer using different L/S ratios [number of determinations = 3]

The EC of leachates of Matla fly ash and the synthesised geopolymer using different L/S ratios is shown in Figure 6.8. The EC values of the leachates of Matla fly ash at the different L/S ratio 10:1 and 20:1 were 2.47 and 1.81 mS/cm respectively whilst the EC of the synthesised geopolymer at L/S ratios 10:1 and 20:1 were 20.0 and 9.46 mS/cm respectively. The EC values of the leachates of synthesised geopolymer were significantly higher when compared to the EC values of leachates of the Matla fly ash at the different L/S ratio. The high EC values of leachates of the synthesised geopolymer indicate the release of more ionisable species and the presence of various soluble components present during the geopolymerisation process. Ionic species are responsible for high EC readings. Also a significant change in EC values of leachates of Matla fly ash and the synthesised geopolymer was observed as the L/S ratio increases because the solution becomes weaker due to lower solid content. This is attributed to the dilution of the soluble species released from samples due to the higher amount of water used.

### 6.5.2 Results of DIN-S4 Leachate

The results of the ICP analysis of the DIN-S4 leachates are shown in Table 6.4 and 6.5 below. In the tables the total concentration of the different elements in the fly ash and synthesised geopolymer are compared to the amount leached out during the DIN-S4 leaching test.



## Chapter Six: Geopolymer from fly ash

Table 6:4: Comparison of total elemental content and amount leached out in DIN-S4 from Matla fly ash and synthesised geopolymer at L/S 10:1 (n=3)

Element	Total elemental content Matla fly ash (mg/kg)	Total elemental content geopolymer (mg/kg)	Matla fly ash L/S 10:1(mg/kg)	Geopolymer L/S 10:1(mg/kg)	% Matla fly ash leached	% Geopolymer leached
Si	254850 ± 444	230985 ± 390	14.25 ± 0.26	42.97 ± 2.00	0.006	0.02
Al	145387 ± 153	140482 ± 267	4.41 ± 0.07	0.33 ± 0.003	0.003	0.0002
Fe	40262 ± 245	38373 ± 40	9.76 ± 0.19	BDL	0.02	BDL
Ca	38498 ± 109	37087 ± 124	225.63 ± 2.12	1.97 ± 0.01	0.59	0.005
Mg	8405 ± 70	7690 ± 35	9.79 ± 0.07	0.055 ± 0.003	0.12	0.0007
Na	1484 ± 20	151982 ± 30.81	10.83 ± 0.09	61.306 ± 31.14	0.73	0.04
K	6281 ± 127	5957 ± 127	21.98 ± 0.55	16.40 ± 0.26	0.17	0.27
Sr	1272 ± 28.06	1095 ± 16.60	6.49 ± 0.12	0.0067 ± 0.0001	0.51	0.0006
Ba	1014 ± 21.39	967 ± 13.80	4.54 ± 0.13	0.0029 ± 0.0001	0.45	0.0003
Mn	387 ± 0	384 ± 45	4.18 ± 0.08	BDL	1.09	BDL
Zn	104.98 ± 7.25	101.3 ± 2.49	0.03 ± 0.002	0.10 ± 0.003	0.04	0.1
V	73.54 ± 1.18	72.59 ± 1.20	0.03 ± 0.0009	0.15 ± 0.0012	0.05	0.21
Cr	63.16 ± 1.75	62.84 ± 5.79	0.03 ± 0.001	BDL	0.05	BDL
Ni	35.72 ± 0.77	33.99 ± 1.44	0.02 ± 0.0018	0.02 ± 0.002	0.05	0.05
As	23.90 ± 3.48	20.53 ± 2.08	0.069 ± 0.009	BDL	0.3	BDL
Pb	22.66 ± 1.85	21.89 ± 1.30	0.002 ± 0.0001	0.014 ± 0.0002	0.01	0.1
Co	13.31 ± 0.48	13.75 ± 0.55	0.005 ± 0.0001	BDL	0.04	BDL
U	10.20 ± 0.14	9.97 ± 0.21	0.01 ± 0.0025	BDL	0.08	BDL
Hg	8.33 ± 0.12	7.74 ± 0.03	0.17 ± 0.029	0.024 ± 0.004	2.05	0.3
Cd	3.12 ± 0.12	3.9 ± 0.05	0.004 ± 0.0002	BDL	0.13	BDL

BDL = below detection limit

## Chapter Six: Geopolymer from fly ash

Table 6:5; Comparison of total elemental content and amount leached out in DIN-S4 from Matla fly ash and synthesised geopolymer at L/S 20:1 (n=3)

Element	Total elemental content Matla fly ash (mg/kg)	Total elemental content Geopolymer (mg/kg)	Matla fly ash L/S 20:1(mg/kg)	Geopolymer L/S 20:1(mg/kg)	% Matla fly ash leached	% Geopolymer leached
Si	254850 ± 444	230985 ± 390	2.12 ± 0.02	8.21 ± 1.05	0.0008	0.004
Al	145387 ± 153	140482 ± 267	5.22 ± 0.01	1.42 ± 0.009	0.004	0.001
Fe	40262 ± 245	38373 ± 40	0.19 ± 0.0001	BDL	0.0005	BDL
Ca	38498 ± 109	37087 ± 124	1406.46 ± 1.10	6.42 ± 0.02	3.65	0.02
Mg	8405 ± 70	7690 ± 35	46.4 ± 0.05	0.1 ± 0.003	0.55	0.0014
Na	1484 ± 20	151982 ± 30.81	42.22 ± 0.05	30.81 ± 3.16	2.85	0.02
K	6281 ± 127	4957 ± 127	84.57 ± 0.36	71.54 ± 0.20	1.35	1.44
Sr	959.36 ± 28.06	1095 ± 16.60	4.13 ± 0.003	0.02 ± 5.90	0.33	0.002
Ba	528.38 ± 21.39	967 ± 13.80	0.24 ± 0.0003	0.009 ± 0.001	0.23	0.0009
Zn	104.98 ± 7.25	101.3 ± 2.49	0.02 ± 0.00003	0.058 ± 0.001	0.02	0.06
V	73.54 ± 1.18	72.59 ± 1.20	0.01 ± 0.00006	0.26 ± 0.001	0.02	0.36
Cr	63.16 ± 1.75	62.84 ± 5.79	0.09 ± 0.0009	BDL	0.14	BDL
As	23.90 ± 3.48	20.53 ± 2.08	0.22 ± 0.001	BDL	0.91	BDL
Pb	22.66 ± 1.85	21.89 ± 1.30	0.02 ± 0.0002	BDL	0.11	BDL
Co	13.31 ± 0.48	13.75 ± 0.55	0.009 ± 0.00002	0.01 ± 0.00005	0.07	0.11
Hg	8.33 ± 0.21	7.74 ± 0.03	0.62 ± 0.003	BDL	7.43	BDL

BDL = below detection limit

## Chapter Six: Geopolymer from fly ash

---

Table 6.4 and 6.5 presents the concentrations of the major and trace species in the DIN-S4 leachate (L/S ratios 10:1 and 20:1 respectively) of the Matla fly ash and synthesised geopolymer determined by ICP-OES. Table 6.4 reveals that Si, Al, Fe, Ca, Mg, Na, K, Sr, Ba, Mn, Zn, V, Ni, Cr, As, Pb, Co U Hg and Cd were mobile in Matla fly ash leachate at L/S ratio 10:1. It was observed from Table 6.4 that these elements were also mobile in the synthesised geopolymer except for Fe, Mn, Cr, As, Co, U and Cd. Whilst Table 6.5, shows that Si, Al, Ca, Mg, Na, K, Sr, Ba, Zn, V, and As were leached out of Matla fly ash and the synthesised geopolymer at L/S ratio 20:1. Fe, Cr, Pb, Co and Hg were also leached out of Matla fly ash but were not detected in the DIN-S4 leachate of the synthesised geopolymer at L/S ratio 20:1. It was also observed that higher amount of Si, Na, Zn, V and Pb were leached out of synthesised geopolymer compared to the amount leached out of the Matla fly ash at L/S ratio 10:1 While Si, Na, V and Co had higher amounts leached out of the synthesised geopolymer compared to the amount leached out of the Matla fly ash at L/S ratio 20:1.

The concentrations of Si and Na detected in the DIN-S4 leachate of the synthesised geopolymer at L/S ratio 10:1 were  $42.94 \pm 2.0$  mg/kg and  $61.31 \pm 31.14$  mg/kg respectively. Si and Na are of interest because they contribute largely to the total elemental content of the synthesised geopolymer ( $230985 \pm 390$  mg/kg and  $151982 \pm 30.81$  mg/kg for Si and Na respectively) Si may have been released from the amorphous phase during the geopolymer synthesis process. This is because during geopolymer synthesis from fly ash the first step in the geopolymerisation process is the alkali activation or the generation of silica and alumina reactive species. This step involves the conversion of the amorphous phases (e.g., aluminosilicates) by alkali (NaOH/KOH) to produce small reactive silica and alumina species (Buchwald et al., 2004; Duxson et al., 2005). XRD analysis of the synthesised geopolymer in section 6.3.3 revealed that halite (NaCl) was formed as a secondary mineral phase from the chemical dissociation of the NaOCl that was used as the foaming agent during geopolymerisation. Hence the Na released may have been liberated from the dissolution of this highly soluble mineral.

The amounts of Ca ( $6.42 \pm 0.02$  mg/kg), Sr ( $0.02 \pm 5.90$  mg/kg) and Ba released from the synthesised geopolymer at L/S ratio 10:1 were significantly lower compared to the amounts released from Matla fly ash ( $225.63 \pm 2.12$  mg/kg for Ca,  $6.49 \pm 0.12$  mg/kg for Sr and  $4.54 \pm 0.13$  mg/kg for Ba) at L/S ratio 10:1. A similar trend was observed for these elements at L/S 20:1. The lower amount of Ca, Sr and Ba leached out of the synthesised geopolymer is in line with the findings of Bankowski et al. (2004) and Izquierdo et al., (2009) who attributed the immobilization mechanism of the above elements in the synthesised geopolymer to changes in modes of occurrence in the geopolymer frame work and fly ash matrix.

The trace elements detected in the synthesised geopolymer leachate were Zn, V, Ni, Pb, and Hg at L/S ratio 10:1 whilst Zn, V and Co were the trace elements detected at L/S ratio 20:1. The amount of V released from the synthesised geopolymer increased from  $0.15 \pm 0.0012$  mg/kg at L/S ratio 10:1 to  $0.26 \pm 0.001$  mg/kg at L/S ratio 20:1. These amounts were also higher than the amount leached out of Matla fly at the same L/S ratios. There were no significant differences in the amounts of Zn, Ni, Pb and Co leached out from the synthesised geopolymer compared to the amounts leached out from Matla fly ash showing that geopolymerisation had no effect on the mobility of these elements. Though U was only detected in the leachate of Matla fly ash at L/S ratio 10:1 it was not detected in the leachate of the synthesised geopolymer at both L/S ratios. This indicates that the geopolymerisation process may have contributed to the stabilization of U in the synthesised geopolymer.

### **6.6 Summary of characterisations studies of the foamed geopolymer synthesised from Matla fly ash**

The Matla fly ash and the synthesised geopolymer were characterised using different analytical techniques such as FT-IR, SEM-EDS, XRD, XRF and LA ICP-MS in order to understand the properties of the fly ash that was transferred into the geopolymer. Gamma spectrometric analysis and DIN-S4 leaching test

## Chapter Six: Geopolymer from fly ash

---

were also used to investigate the radioactivity and leachability respectively, of the radionuclides and potentially toxic elements that were carried into the synthesised geopolymer. The investigations provided significant insight into the molecular structure, morphology, mineralogy, chemical composition and leaching behaviour of the Matla fly ash, and the synthesised geopolymer.

The transformation of Matla fly ash into geopolymer was established by two distinctive features that were observed when the FT-IR spectrum of the Matla fly ash was compared to the FT-IR spectrum of the synthesised geopolymer. The first was shift of the band attributed to the asymmetric stretching vibrations of Si-O-Si and Al-O-Si from  $1102\text{ cm}^{-1}$  in the FT-IR spectrum of the Matla fly ash to a lower frequency of  $977\text{ cm}^{-1}$  in the FT-IR spectrum of the synthesised geopolymer. The other distinctive feature observed in the synthesised geopolymer spectrum was the high intensity of the band attributed to stretching vibrations of O-C-O bonds at  $1432\text{ cm}^{-1}$ .

Morphological studies (by SEM) of the Matla fly ash show that it consists of irregular, spherically shaped and agglomerated particles. Whilst the SEM micrograph of the synthesised geopolymer shows that the geopolymer comprises of mostly irregular shaped and agglomerated particles. The outer surfaces of the Matla ash particles are smooth while the outer surfaces of the geopolymer particles appeared encrusted. SEM-EDS and XRD confirmed that the encrustations were due to the formation of new mineral phases in geopolymer particles. The XRD results established the formation of new mineral phases such as sodalite and halite during the geopolymerisation process of the fly ash. The mineralogical investigation of Matla fly ash and synthesised geopolymer also reveals that quartz and mullite were the only consistent major mineral components in Matla fly ash and the synthesised geopolymer. The XRD patterns agree with the results of the XRF of the Matla fly ash and synthesised geopolymer which reported high percentages of the oxides of Si and Al. The quartz and mullite phases correspond to the significant levels of Si and Al in the fly ash and synthesised geopolymer.



## Chapter Six: Geopolymer from fly ash

---

Elemental analysis reveals that heavy metals As, Cd, Cr, Hg, Ni, Pb and radionuclides Th and U were present in the synthesised geopolymer samples as well as in Matla fly ash. These heavy metals and radionuclides are potentially toxic and their presence in the synthesised geopolymer raises concern over its safety with regards to its use as construction materials. Hence the investigation of the leaching of heavy metals and radionuclides from the synthesised geopolymer is important to understand how these species are mobile in the synthesised geopolymer. Zn, V, Ni, Pb, Co and Hg were the trace elements detected in the leachate of the synthesised geopolymer. There were no significant differences in the amounts of Zn, Ni, Pb and Co leached out from the synthesised geopolymer compared to the amounts leached out from Matla fly ash showing that geopolymerisation had no effect on the mobility of these elements. Analysis of the DIN-S4 leachate of the synthesised geopolymer also reveals that elements such as Ca, Sr, Ba and the radionuclide U were immobilized in the synthesised geopolymer.

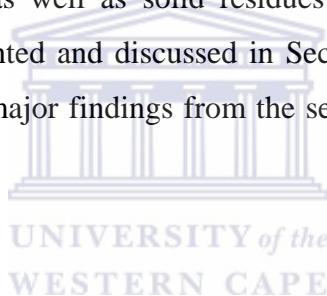
The radioactivity of the synthesised geopolymer and Matla fly ash was undertaken using gamma spectrometric analysis and the results revealed that the activity content of the synthesised geopolymer was lower than that of the Matla fly ash. The radiological hazard due to the use of the synthesized geopolymer was calculated using the radium equivalent index ( $Ra_{eq}$  in Bq/kg), external hazard index ( $H_{ex}$  in Bq/kg) and activity index or gamma index ( $I_\gamma$ ). The values obtained for the synthesised geopolymer were below the recommended values and meets the requirements as a building material in terms of radioactivity. This finding is of paramount importance because no research has previously been done to determine the radioactivity of geopolymers synthesised from coal fly ash that is has potential as a construction material.

### **Chapter Seven: Possibility of rare earth recovery from fly ash**

#### **7 Introduction**

This chapter presents and discusses the results of the sequential leaching studies of REE from Matla fly ash. The physical and chemical characterisation of Matla fly ash, resulting supernatant and the solid residue after each leaching step were carried out using different analytical techniques such as LA ICP-MS, ICP-MS, XRF and XRD. Section 7.1 gives an overview of REE, fly ash, and the aim and objectives of this chapter. Whilst a brief descriptions of the materials and methods used is given in Section 7.2. The results and discussion of this chapter is divided into two (2) (Sections 7.3 and 7.4). Section 7.3 presents and discusses the results of the magnetic separation of Fe from Matla fly ash. The elemental analysis of the leachate (supernatant), as well as solid residues produced from the sequential leaching steps are presented and discussed in Section 7.4. This chapter will end with a summary of the major findings from the sequential leaching of REE from Matla fly ash.

#### **7.1 Overview**



Products and devices such as hybrid vehicles, rechargeable batteries, mobile phones, plasma, LCD and LED screens, laptop computers, disk drives, catalytic converters and space-based satellites and communication systems forms part of our daily lives. What is not commonly known to us is that these products and devices, amongst many others, are dependent on the unique properties of REE. The REE is a group of seventeen chemically similar metallic elements including the 15 periodic elements of the lanthanide family, scandium and yttrium. Scandium and yttrium are also considered REE because they usually occur in the same ore deposits as the lanthanides and exhibit similar properties to the lanthanide family (REF). The lanthanides reside at the bottom of the periodic table in the top horizontal row of the f-block elements with atomic number spanning from 57 (lanthanum, La) to 71 (lutetium, Lu). These REE can be further classified as “light” or “heavy” based on their relative atomic weights. The light

## **Chapter Seven: Possibility of Rare earth recovery from fly ash**

---

REE include lanthanum, cerium, praseodymium, neodymium, promethium, samarium, and europium, while heavy REE describe gadolinium, terbium, dysprosium, holmium, erbium, thulium, ytterbium, lutetium, scandium, and yttrium (Moldoveanu and Papangelakis, 2012). Although, yttrium is the lightest REE, it is usually grouped with the heavy REE due to its similarity in chemical and physical properties (Kastori et al., 2010). The special properties of luminescence, magnetism and electronics of REE arising from their unsaturated 4f electronic structure are harnessed in the production of high tech products and devices. The elemental forms of REE are iron grey to silvery lustrous metals that are typically soft, malleable, and ductile and usually reactive, especially at elevated temperatures or when finely divided (USGS, 2012).

REE are not as "rare" as their name implies but are enriched in the earth's crust and usually occur together naturally due to their similar ionic radii and oxidation state. This similarity in their ionic radii and oxidation states allow for easy substitution of the REE for each other into various crystal lattices. This substitution accounts for their wide distribution in the earth's crust and the characteristic multiple occurrences of REE within a single mineral (Castor and Hedrick, 1986). REE are moderately abundant in the earth's crust, some even more abundant than copper, lead, gold, and platinum (Moldoveanu and Papangelakis, 2012), though most REE are not concentrated enough to make them easily exploitable economically. Most REE throughout the world are located in deposits of the minerals bastnaesite and monazite (Jiang et al., 2005; Nasab et al., 2011; USGS, 2011). Bastnaesite occurs as a primary mineral, while monazite is found in primary deposits of other ores. The lighter REE such as lanthanum, cerium, praseodymium, and neodymium are more abundant and concentrated and usually make up about 80% - 99% of the REE content of La deposit (Humphries, 2011). Also REE often occur with other elements, such as copper, gold, uranium, phosphates, and iron. Significant amounts of REE are produced in only a few countries. China is currently the dominant producer of REE and is believed to be responsible for over 97% of the world mine production on a rare earth oxide equivalent basis (USGS, 2012). Other countries with notable production in 2009

## **Chapter Seven: Possibility of Rare earth recovery from fly ash**

---

were: Brazil, India, Kyrgyzstan and Malaysia while minor production may have occurred in Indonesia, Commonwealth of Independent States, Nigeria, North Korea and Vietnam (USGS, 2011).

The separation and purification of these elements have gained considerable attention because of the ever-increasing demand for REE due to the increasing number of applications of REE in industry. This has led to a growing interest in the exploration and exploitation of new sources. Elemental analysis of various South Africa fly coal ashes shows that it contains several REE such as Ce, La and Y. Coal fly ash is a particulate waste product that results during the combustion of pulverised coal to generate electricity. In South Africa, millions of tons of coal fly ash are generated annually by coal-fired power plants in order to meet with the large demand for industrial and domestic energy. The management of this combustion waste is of major concern because of the huge amount that is produced annually and the environmental issues arising from its disposal (Gitari et al., 2008). The advantage of recovering REE from fly ash over minerals is in the availability of fly ash as already mined, fine powder that can be readily processed chemically. Thereby eliminating the cost of excavation, pulverization, and grinding of the minerals to a fine powder necessary for chemical processing. The ability to extract REE from coal fly ash is important in terms of economic and environmental issues because recovery can be used to produce value-added products from stored coal fly ash. Hence, the aim of this chapter is to develop a practical method to leach out the REE in Matla fly ash using a sequential leaching scheme. The objective of this chapter is to firstly systematically extract the major fly ash components such as Fe, Si, Al and Ca in order to concentrate the trace constituent such as the REE, in the residual fraction, or alternatively to find protocols to leach REE from the ash matrix.

### **7.2 Materials and methods**

The fresh fly ash samples used in this study were collected directly from the hoppers at Matla power station located in Mpumalanga province of South Africa

indicated by the red peg in Figure 3.1. The power stations are usually located within close proximity to the coal mines in South Africa. The fly ash samples were kept in plastic containers which were tightly closed to prevent ingress of air, and stored at room temperature for subsequent analysis. The sodium hydroxide (NaOH) and mineral acids ( $H_2SO_4$ , HCl and  $HNO_3$ ) used were supplied by Merck. The schematic leaching procedure used in this study was adopted from the extraction techniques that have been used in several studies of extraction and recovery of different components from fly ash. Detailed descriptions and explanations of the sequential leaching procedures are given in Section 3.6.5. The leached components (supernatant) after leaching with 8 M NaOH, 5 M  $H_2SO_4$ , 3 M HCl and 7 M  $HNO_3$ , respectively were analysed using ICP-MS whilst solid ash residues after each step were also analysed using XRF and LA ICP-MS for elemental composition. XRD studies were also carried out on the Matla fly ash, the separated magnetic and non-magnetic fractions, and the solid residue after each leaching step. The procedures for these analytical processes are described in Chapter 3. Sections 3.4.2 detailed the XRF technique, while Sections 3.4.3 and 3.4.4 dealt with ICP-MS/OES and LA ICP-MS, respectively.

### **7.3 The results of the magnetic separation of Fe from Matla fly ash**

In the first case it was considered necessary to establish to what extent REE might be associated with the magnetic fraction in the fly ash. The magnetic separation process involved the partitioning of magnetic iron contained in raw Matla fly ash through a wet separation technique involving magnetic stirring. Upon completion of the separation, the fly ash slurry was present as three fractions. These fractions included the magnetic portion of Matla fly ash indicated as granular iron, the solid residue which was essentially the non-magnetic portion of Matla fly ash, and the filtrate (supernatant) which was produced as a result of the filtering process.

## Chapter Seven: Possibility of Rare earth recovery from fly ash

### 7.3.1 Elemental composition of the fractions produced during the extraction of iron oxide from Matla fly ash

The elemental composition of the magnetically extracted granular iron oxide and the non-magnetic solid residue was determined both qualitatively and quantitatively using XRF as well as LA- ICP-MS. The XRF technique reports concentration as % oxides for major elements whilst the LA- ICP-MS reports concentration as ppm (mg/kg) for REE. Elements reported as % oxides were converted to element value in ppm (mg/kg) using element conversion software downloaded from <http://www.mariscigrp.org/oxtoel.html>. The elemental composition (in mg/kg) of the raw Matla fly ash, the non-magnetic and magnetic fraction was calculated based on the amount (% composition) of the element in each of the sample.

Table 7:1: Major element composition of Matla fly ash, the non-magnetic fraction and magnetic fraction reported in mg/kg

Elements	Raw Matla fly ash (mg/kg)	Non- magnetic fraction (mg/kg)	Magnetic fraction (mg/kg)
Si	254834 ± 444.22	161858 ± 282	92976 ± 254
Al	145371 ± 153	100690 ± 105	44681 ± 43
Fe	40285 ± 245	2338 ± 14	37947 ± 12
Ca	38522 ± 109	19199 ± 54	19323 ± 38
Mg	8384 ± 69	3867 ± 31	4517 ± 16
K	6392 ± 69	4883 ± 53	1509 ± 27
Na	1484 ± 27	1150 ± 21	334 ± 14
Ti	10431 ± 127	6711 ± 81	3720 ± 43
P	2051 ± 25	1165 ± 14	886 ± 20
Mn	387 ± 1.00	77 ± 0.00	310 ± 1.00

The XRF analysis of Matla fly ash, the non-magnetic fraction and magnetic fraction are presented and compared in Table 7.1. The table revealed that the Matla fly ash was mainly composed of Si (254834 mg/kg), Al (145371 mg/kg), and Fe (40285 mg/kg) whilst the non-magnetic fraction also has Si (161858 mg/kg) and Al (100690 mg/kg) as the major component. A significant decrease (37947 mg/kg) in the Fe content of the non-magnetic fraction was observed when

compared to the Fe content of Matla fly ash. Also, the amount of the other species (Si, Al, Ca, Mg, K, Na, Ti, P and Mn) detected in the magnetic fraction were significantly lower than the amounts detected in Matla fly ash. This can be attributed to the partitioning effect of the magnetic portion during the extraction process and establishes that the magnetic extraction process resulted in the extraction or removal of specific species such as Fe from Matla fly ash.

The magnetic fraction was composed primarily of Fe (37947 mg/kg), and significant amount of Mn (310 mg/kg) compared to Matla fly ash. This enrichment of Mn in the magnetic fraction extracted from Matla fly ash agrees with findings reported by Kukier et al., 2003 and Vassilev et al., 2006. The extracted magnetic fraction also contained significant amounts of Si and Al (92976 mg/kg and 44681 mg/kg, respectively) and moderate amounts of Ca (19323 mg/kg), Mg (4517 mg/kg) and Ti (3720 mg/kg). The detection of non-magnetic elements such as Si and Al may be attributed to the entrapment of Fe bearing phases within the aluminosilicate matrix of the fly ash during its formation at elevated temperatures (Molcan et al., 2009). The partitioning of elements and their surface association in fly ash is controlled by the extent of vaporisation during the coal combustion process (Choi et al., 2002). Fe is not volatile and is therefore not associated with the surface of the aluminosilicate but rather assimilated in the aluminosilicate matrix (Kukier et al., 2003; Kutchko and Kim 2006). The magnetic separation isolates these closely associated species (Si and Al) in the magnetic fraction Table 7:1: REE composition of Matla fly ash, the non-magnetic fraction and magnetic fraction

### **7.3.2 REE composition of Matla fly ash, the non-magnetic fraction and magnetic fraction**

The fractions produced during the magnetic separation process were also subjected to LA ICP-MS to analyse their REE composition. The results are presented in Table 7.2.



## Chapter Seven: Possibility of Rare earth recovery from fly ash

Table 7:2: REE composition of Matla fly ash, the non-magnetic fraction and magnetic fraction

Elements	Raw Matla fly ash (mg/kg)	Non-magnetic fraction (mg/kg)	Magnetic fraction (mg/kg)
La	117.54 ± 8.87	84.85 ± 2.85	37.99 ± 2.16
Ce	242.44 ± 10.44	215.64 ± 6.28	79.00 ± 2.97
Pr	26.85 ± 1.25	21.31 ± 1.18	20.90 ± 1.04
Nd	69.95 ± 1.09	45.87 ± 1.93	3.00 ± 0.05
Dy	7.66 ± 1.67	6.10 ± 0.23	7.46 ± 0.04
Sm	23.22 ± 1.32	13.45 ± 1.03	10.38 ± 1.44
Er	3.07 ± 0.18	3.60 ± 0.18	0.50 ± 0.02
Eu	3.75 ± 0.82	2.21 ± 0.2	Nd
Gd	25.92 ± 2.03	24.89 ± 0.47	10.15 ± 0.01
Ho	0.41 ± 0.07	4.88 ± 0.37	0.06 ± 0.02
Lu	2.44 ± 0.49	0.28 ± 0.2	Nd
Tb	0.41 ± 0.39	2.12 ± 0.21	6.13 ± 0.06
Tm	2.51 ± 0.01	Nd	7.25 ± 0.07
Yb	8.48 ± 0.87	7.81 ± 0.26	5.09 ± 0.14
Y	77.04 ± 1.48	55.30 ± 0.10	1.00 ± 0.01
Sc	23.44 ± 2.47	23.59 ± 0.01	9.29 ± 0.31

Nd = Not detected

In Table 7.2 the REE composition of Matla fly ash, the non-magnetic and magnetic fractions determined by LA-ICP-MS are presented and compared. Table 7.2 shows that REE such as La, Ce, Nd, Y and Sc were preferably gathered in the non-magnetic fractions, as indicated by their significantly higher amount of 84.85 ± 2.85 mg/kg; 215.64 ± 6.28 mg/kg; 45.87 ± 1.93 mg/kg; 55.30 ± 0.10 mg/kg and 23.59 ± 0.01 mg/kg, respectively than in the magnetic fraction (37.99 ± 2.16 mg/kg; 79.00 ± 2.97 mg/kg; 3.00 ± 0.05 mg/kg; 1.00 ± 0.01 mg/kg and 9.29 ± 0.31 mg/kg, respectively). This shows that these REE are present in forms that are closely associated with the non-magnetic fraction of Matla fly ash. Whilst REE such as Pr, Dy, Sm and Yb were 21.31 ± 1.18 mg/kg; 6.10 ± 0.23 mg/kg; 13.45 ± 1.03 mg/kg and 7.81 ± 0.26 mg/kg, respectively in the non-magnetic, and 20.90 ±



1.04 mg/kg;  $7.46 \pm 0.04$  mg/kg;  $10.38 \pm 1.44$  mg/kg and  $5.09 \pm 0.14$  mg/kg, respectively in the magnetic fraction. This shows that the proportions of these REE were evenly distributed between the magnetic and non-magnetic fractions of Matla fly ash. Eu and Lu were detected in the non-magnetic fraction but were not detected in the magnetic fraction, whilst Tm was detected in the magnetic fraction but was not detected in the non-magnetic fraction.

### 7.3.3 Mineralogical analysis of Matla fly ash, the magnetic and non-magnetic fractions

Figure 7.1 shows the XRD patterns of Matla fly ash, the extracted non-magnetic and magnetic fractions. The XRD patterns are compared in order to understand the transformation in the mineralogy of the separated fractions.

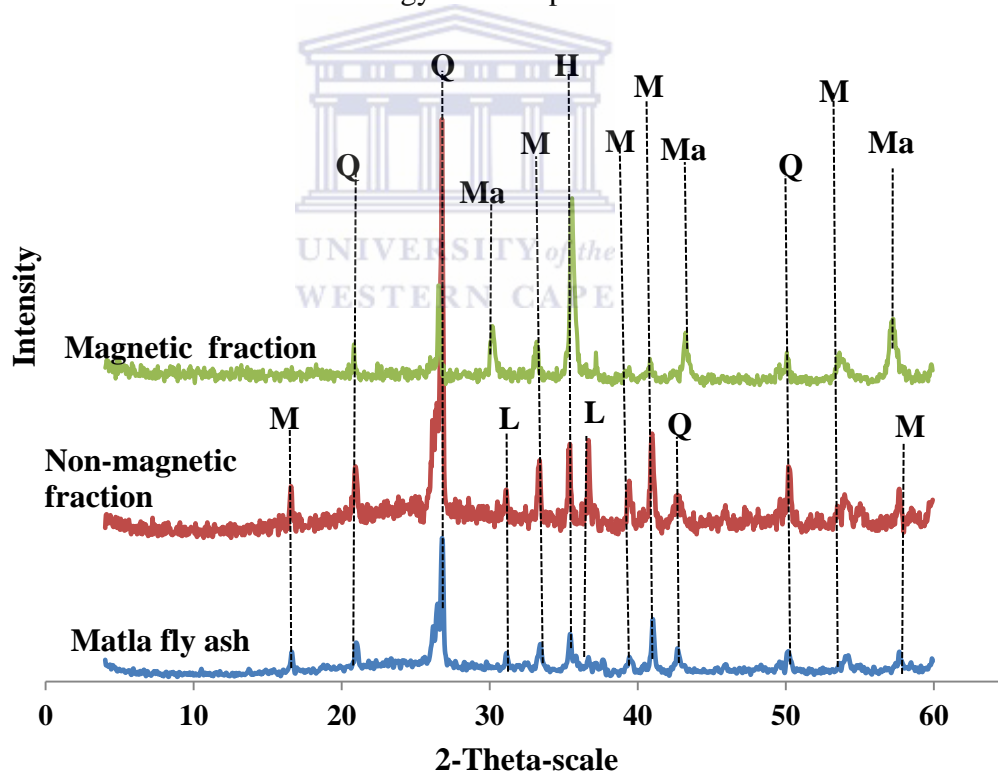


Figure 7.1: XRD patterns of the extracted Magnetic and non-magnetic fraction and Matla fly ash. (H = hematite, L = lime, M = mullite, Ma = magnetite, and Q = quartz)

In Figure 7.1 the XRD pattern of Matla fly ash is compared to that of the extracted magnetic and non-magnetic fractions. The XRD patterns of Matla fly ash and the extracted non-magnetic fraction showed that quartz ( $\text{SiO}_2$ ), mullite ( $\text{Al}_6\text{Si}_2\text{O}_{13}$ ) and lime ( $\text{CaO}$ ) were the major crystalline peaks present. A hematite ( $\text{Fe}_2\text{O}_3$ ) peak was also observed. The XRD revealed that the mineralogy of the non-magnetic fraction was very similar to that of Matla fly ash, however; the lime peaks had a higher intensity in the non-magnetic fraction than in Matla fly ash. The XRD pattern of the magnetic fraction revealed an iron rich material primarily composed of hematite and magnetite ( $\text{Fe}_3\text{O}_4$ ). Other minerals such as quartz and mullite were also present in the magnetic fraction. These results corroborate the XRF result above; which indicated iron as the major oxide extracted magnetically with traces of Al and Si due to the residual quartz in the magnetic fraction.

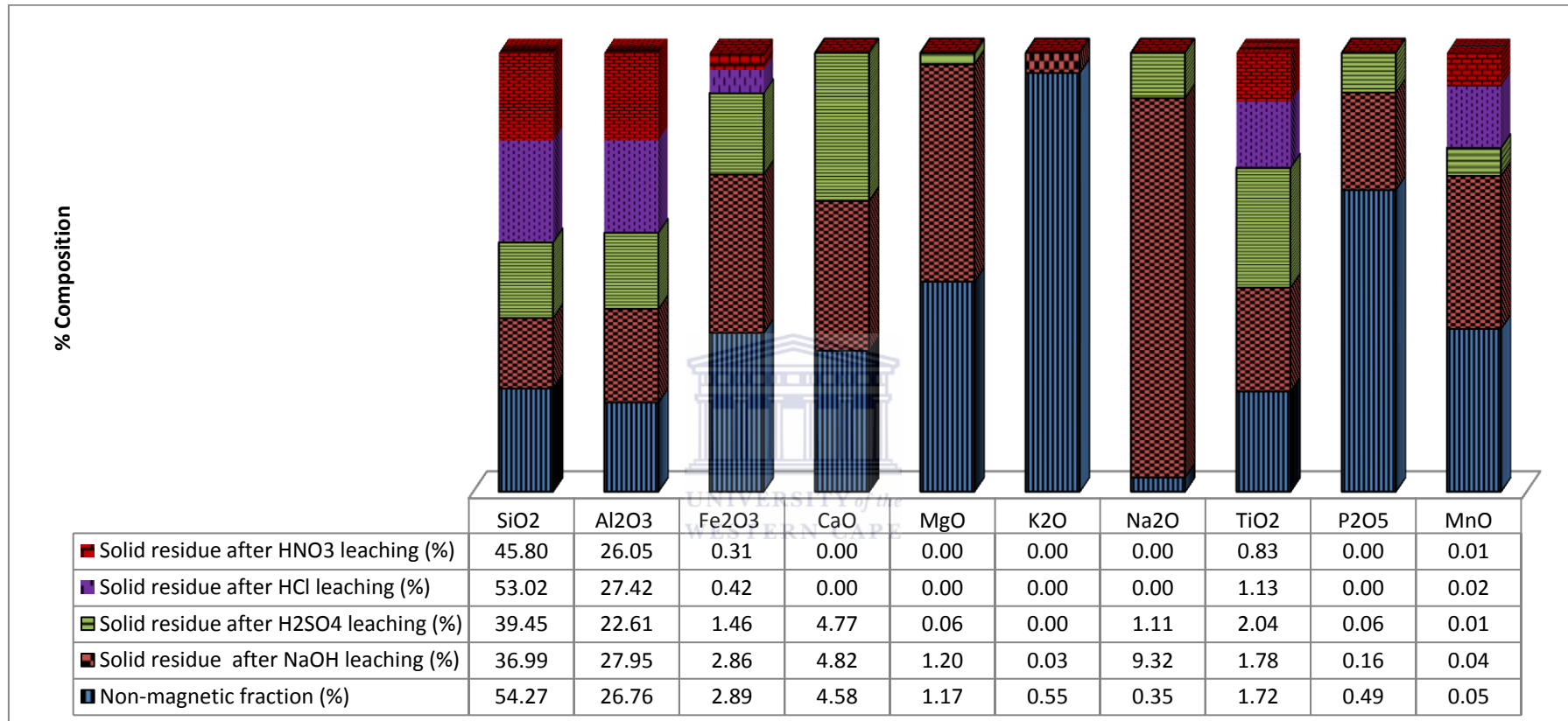
### **7.4 The results of the sequential leaching of non-magnetic fraction of Matla fly ash**

This sequential leaching procedure was carried out to extract the major components such as Si, Al and Ca from the non-magnetic fraction of Matla fly ash. Detailed descriptions and explanations of the sequential extraction scheme are given Section 3.6.5. The leachate (supernatant) from the different leaching steps was analysed using ICP-MS whilst solid residues were also analysed using XRF and LA ICP-MS/OES for elemental composition. XRD analysis was also carried out on the solid residue to determine the changes in the mineral phases if the solid residue.

#### **7.4.1 Composition of the major element in the solid residue produced during the sequential leaching of the non-magnetic fraction of Matla fly ash**

Figure 7.2 presents the composition of the major components that remained in the solid residue after the sequential leaching of the non-magnetic fraction of Matla fly ash with NaOH,  $\text{H}_2\text{SO}_4$ , HCl and  $\text{HNO}_3$ , respectively.

## Chapter Seven: Possibility of Rare earth recovery from fly ash



0.0 = below detection limit

Figure 7.2: Percentage composition of the major components major components that remained in the solid residue after the sequential leaching the non-magnetic fraction of Matla fly ash with NaOH, H<sub>2</sub>SO<sub>4</sub>, HCL and HNO<sub>3</sub>

## Chapter Seven: Possibility of Rare earth recovery from fly ash

---

The results presented in Figure 7.2 shows the amounts of the major elements (Si, Al, Fe, Ca, Mg, K, Na, Ti, P and Mn) that remained in the solid residue after the sequential leaching of the non-magnetic fraction of Matla fly ash. The results revealed that Fe, Ca, Mg, Na and Mn were strongly retained in the solid residue after leaching with NaOH leaching indicating that very small quantities of Fe, Ca, Mg, Na and Mn entered the leachate during the first leaching process whereas Si was leached. This is because the addition of NaOH to fly ash results in the dissolution of the aluminosilicate matrix of the fly ash particles (Swanepoel and Strydom, 2002), the reason for leaching the fly ash with 8 M NaOH was to remove silicate Si from the fly ash as reported by Su et al., 2011.

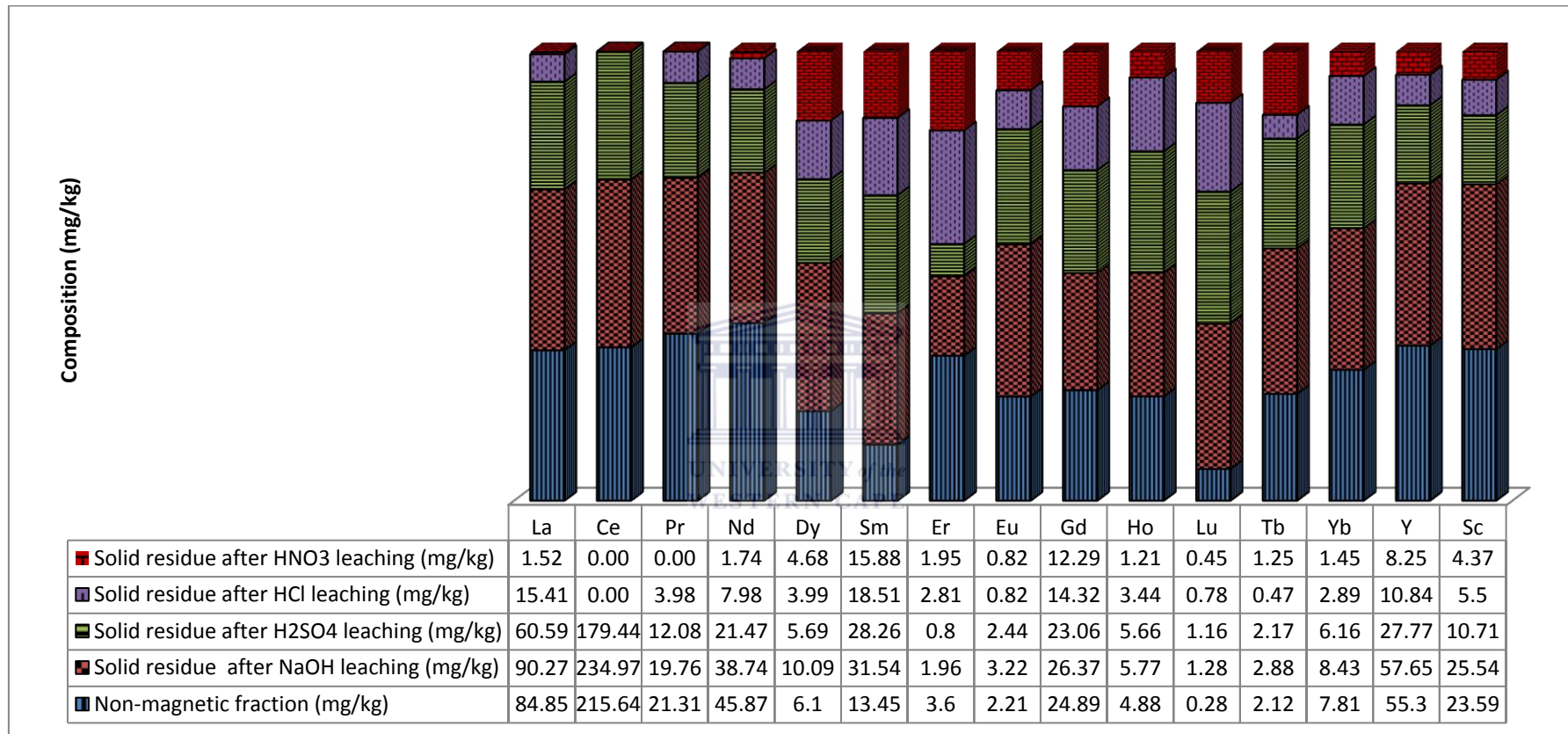
Si and Al exhibited the same leaching pattern with all the leaching reagents. These elements were strongly retained in each of the solid residue after the four leaching steps. This indicates that only a small quantity of the fly ash content of Si and Al was leached during the four leaching steps. For Si, the residue after NaOH leaching has the lowest composition of Si ( $36.99 \pm 4.80$  %) followed by the residue after  $H_2SO_4$  leaching ( $39.45 \pm 5.06$  %), while the residue from the HCl and  $HNO_3$  leaching steps had  $53.02 \pm 0.84$  % and  $45.08 \pm 0.03$  % Si, respectively. Thus, the leaching efficiency of Si with respect to each of the reagents can be ordered as:  $NaOH > H_2SO_4 > HNO_3 > HCl$ . For Al, the residues from the four leaching steps (NaOH,  $H_2SO_4$ , HCl and  $HNO_3$ ) were  $227.95 \pm 0.84$  %;  $22.61 \pm 1.71$  %;  $27.42 \pm 0.95$  % and  $26.05 \pm 0.03$  %, respectively, respectively and the leaching efficiency of Al with respect to each of the reagents can be ordered as:  $H_2SO_4 > HNO_3 > HCl > NaOH$ .

K was below the detection limit in the solid residue after leaching with  $H_2SO_4$ , while Ca, Mg, Na and P were also below the detection limit in the solid residue after leaching with HCl. Thus, the leaching efficiency of the major elements K, Ca, Mg, Na and P in the non-magnetic fraction of Matla fly ash, with respect to each of the reagents can be ordered as:  $HCl > H_2SO_4 > NaOH$ .

### **7.4.2 Elemental composition of the REE in the solid residue produced during the sequential leaching of the non-magnetic fraction of Matla fly ash**

Figure 7.3 presents the composition of the REE that were retained in the solid residue, after the sequential leaching the non-magnetic fraction of Matla fly ash with NaOH, H<sub>2</sub>SO<sub>4</sub>, HCl and HNO<sub>3</sub>, respectively.





0.0 = below detection limit

Figure 7.3: REE composition (mg/kg) in the solid residue after the sequential leaching the non-magnetic fraction of Matla fly ash with NaOH, H<sub>2</sub>SO<sub>4</sub>, HCL and HNO<sub>3</sub>

## Chapter Seven: Possibility of Rare earth recovery from fly ash

Figure 7.3 showed significant variations of the amounts of REE retained in the residue after leaching with NaOH, H<sub>2</sub>SO<sub>4</sub>, HCl, and HNO<sub>3</sub>. About 100 % (90.27 mg/kg), 71.41 % (60.59 mg/kg), 18.16 % (15.41mg/kg), and 1.79 % (1.52 mg/kg) La were retained in the non-magnetic fraction of the Matla fly ash residue after leaching with 8 M NaOH, 5 M H<sub>2</sub>SO<sub>4</sub>, 3 M HCl, and 7 M HNO<sub>3</sub>, respectively. Approximately 100 % (234.97 mg/kg) and 83.21 % (179.44mg/kg) Ce were left in the residue after NaOH and H<sub>2</sub>SO<sub>4</sub> leaching, respectively. However, total Ce leaching (100 %) was achieved using 3 M HCl, as no Ce was recorded after the HCl leaching. Approximately, 92.87 % (19.76 mg/kg), 56.69 % (12.08 mg/kg) and 18.68% (3.98 mg/kg) Pr were present in the non-magnetic fraction of the Matla fly ash residue after NaOH, H<sub>2</sub>SO<sub>4</sub>, and HCl leaching, respectively. No Pr was thus recorded after the HNO<sub>3</sub> leaching.

Moreover, a total of 84.46 %, 46.81 %, 17.40 %, and 3.79 % of Nd; 100 %, 93.28 %, 65.41 %, and 76.72 % of Dy; 54.44%, 22.22%, 78.08 %, and 54.17 % of Er; 100 %, 100 %, 37.10 %, and 37.10 % of Eu; 100 %, 92.65 %, 57.53 %, and 49.38 % of Gd; 100 % 100 %, 70.49 % , and 24.80 % of Ho; 100 % , 100 % , 22.17 % , and 58.96 % of Tb; 100 % , 78.87 % , 37.00 % , and 18.57 % of Yb; 100 % , 50.22 %, 19.60 % , and 14.92 % of Y, and 100 %, 45.40 % , 23.31 % , and 18.52 % of Sc were retained in the non-magnetic fraction of the Matla fly ash residue after successive leaching with 8 M NaOH, 5 M H<sub>2</sub>SO<sub>4</sub>, 3 M HCl, and 7 M HNO<sub>3</sub>, respectively.

It can therefore be deduced from the results that; all the REE (La, Ce, Dy, Gd, Yb, Y and Sc) were strongly retained in the solid residue after leaching with NaOH indicating that trace amount of REE entered the solution during the NaOH leaching process and hence, the leaching of REE with NaOH was found to be very low. The residue had approximately 100% of the quantity of Eu and Ho retained after NaOH and H<sub>2</sub>SO<sub>4</sub> leaching, moreover, Sm and Lu were not leached out in any of the four leaching steps. The acid leaching (with H<sub>2</sub>SO<sub>4</sub> and HCl) enhanced the percentage REE leached, while the four leaching steps (NaOH, H<sub>2</sub>SO<sub>4</sub>, HCl, and HNO<sub>3</sub>) were able to leach considerable amount of REE from the non-



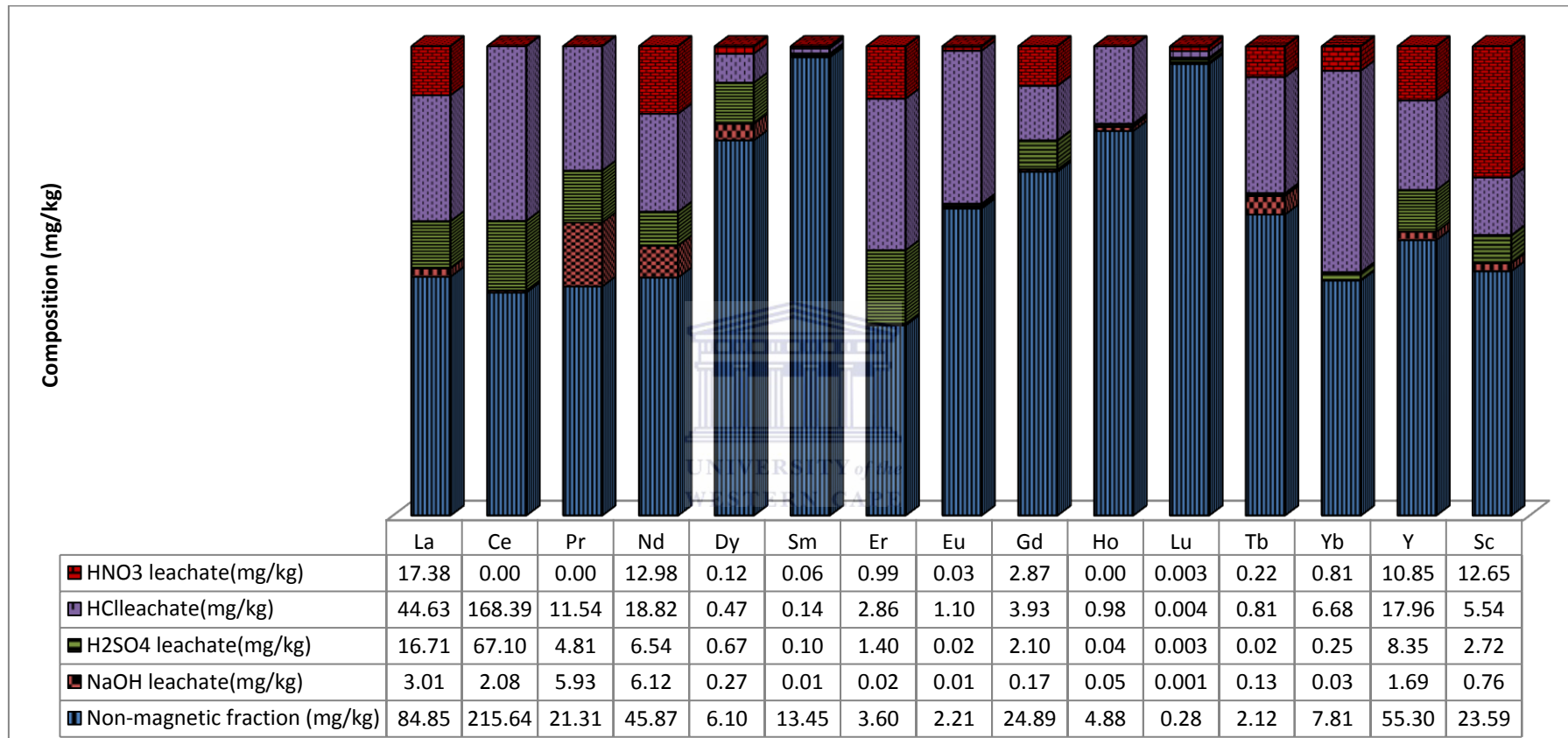
magnetic fraction of the Matla fly ash. These results showed that REE are better leached from the non-magnetic fraction of the Matla fly ash with acids (low pH) rather than with base (high pH). This is because it is difficult to dissolve REE in their hydroxide forms. Thus, the leaching efficiency of REE with respect to each of the reagents can be ordered as:  $\text{HCl} > \text{H}_2\text{SO}_4 > \text{HNO}_3 > \text{NaOH}$ .

The Figure 7.3 also indicated that the REE Nd – Sc are strongly held onto in the non-magnetic fraction of the Matla fly ash when compared to La, Ce, and Pr. This is because approx. 100% of La, Ce, and Pr were completely leaching within three leaching steps, whereas Nd – Sc were still noticeable in the non-magnetic fraction of the Matla fly ash residue after all the four leaching steps.

### **7.4.3 Elemental composition of the REE in the leachate (supernatant) produced during the sequential leaching of the non-magnetic fraction of Matla fly ash**

Figure 7.4 presents the composition of the REE determined using ICP-MS that was sequentially leached out of the non-magnetic fraction of Matla fly ash with 8NaOH, 5H<sub>2</sub>SO<sub>4</sub>, 3HCl and 7HNO<sub>3</sub>, respectively.



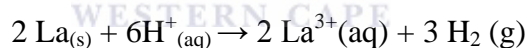


0 = Not detected

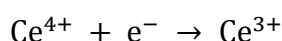
Figure 7.4: Elemental composition of the REE in the leachate (supernatant) produced during the sequential leaching of the non-magnetic fraction of Matla fly after the sequential leaching with NaOH, H<sub>2</sub>SO<sub>4</sub>, HCL and HNO<sub>3</sub>

## Chapter Seven: Possibility of Rare earth recovery from fly ash

The results (Figure 7.4) obtained showed that the amounts of REE in the different leachate varied widely. About 3.01 mg/kg, 16.71 mg/kg, 44.63 mg/kg, and 17.38mg/kg La were sequentially leached with NaOH, H<sub>2</sub>SO<sub>4</sub>, HCl and HNO<sub>3</sub>, respectively. Most of the La was extracted within the first three leaching steps (evident on Figure 7.4), the highest amount leached was observed with HCl (44.63 mg/kg; 52.60 %), while the lowest amount was witnessed with NaOH (3.01 mg/kg; 3.55 %). It is difficult to dissolve La in its hydroxide forms because most lanthanide hydroxides exist in ionic and basic form (Cotton et al., 1988) and are insoluble but rather precipitated by NaOH. Indicating that the hydroxides (La(OH)<sub>3</sub>) and/or hydroxy-complexes of La may be present during the OH<sup>-</sup> leaching. These hydroxides are almost insoluble in water but are sufficiently basic to dissolve readily in acids. This might be the reason for the observed amount 16.71mg/kg (19.70 %); 44.63 mg/kg (52.60 %); and 17.38 mg/kg (20.48 %) of La leached out with H<sub>2</sub>SO<sub>4</sub>, HCl and HNO<sub>3</sub>, respectively. The dissolved species in solution during the acid leaching might be La<sup>3+</sup> this is because La dissolves readily in dilute acid to form solutions containing the La<sup>3+</sup>, which exist as [La(OH<sub>2</sub>)<sub>9</sub>]<sup>3+</sup> complexes (Cotton et al., 1988).



All the Ce present in the non-magnetic fraction of the Matla fly ash was also extracted within the first three leaching steps with NaOH, H<sub>2</sub>SO<sub>4</sub> and HCl (≈ 100 %). The highest amount of Ce leached was observed with the HCl (168.39 mg/kg; 78.09%), 2.08mg/kg (0.97 %) and 67.1 mg/kg (31.12 %) Ce was leached with NaOH and H<sub>2</sub>SO<sub>4</sub>, respectively. Ce exhibits three oxidation states, +2, +3 and +4 but the +2 state is rare (Patnaik, 2003). The two oxidation states of Ce differ enormously in basicity. Ce<sup>3+</sup> is a strong base, comparable to the other trivalent lanthanides, but Ce<sup>4+</sup> is weak and unstable under alkaline conditions (Cotton et al., 1988).



Thus, the 0.46% of Ce leached out with the NaOH may exist in the +4 state.

## Chapter Seven: Possibility of Rare earth recovery from fly ash

---

The results obtained also showed that the amounts of Nd in the different leachate vary widely. About 6.12 mg/kg, 6.54mg/kg, 18.82 mg/kg, and 12.98 mg/kg Nd were sequentially leached with NaOH, H<sub>2</sub>SO<sub>4</sub>, HCl and HNO<sub>3</sub>, respectively. The highest amount of Nd leached was observed with the HCl and HNO<sub>3</sub> leaching, they are 18.82 mg/kg (41.03 %) and 12.98mg/kg (28.30 %), respectively, while the amount of Nd that was leached out with NaOH and H<sub>2</sub>SO<sub>4</sub> was 6.12 mg/kg (13.42 %) and 6.54 mg/kg (14.26 %), respectively. A total of and 1.66 %, 1.29 % and 20.09 % of Ho were sequentially leached with NaOH, H<sub>2</sub>SO<sub>4</sub>, HCl and HNO<sub>3</sub>, respectively. All the Pr and Ho were extracted within the first three leaching steps. Furthermore, a total of 27.85 %, 22.58% and 54.17 % of Pr; 13.34 %, 14.26%, 41.03 %, and 28.31 % of Nd; 7.72 %, 10.94 %, 7.70 %, and 1.97 % of Dy; 0.1 %, 0.74 %, 1.08 %, and 0.48 % of Sm; 0.67 %, 38.77 %, 79.35 %, and 27.49 % of Er; 0.52 %, 1.06 %, 49.73 %, and 1.48 % of Eu; 0.66 %, 8.45 %, 15.80 %, and 11.53 % of Gd; 0.36 %, 1.07 %, 1.43 %, and 1.07 % of Lu; 6.19 %, 0.92 %, 38.47 %, and 10.23 % of Tb; 0.38 %, 3.20 %, 85.54 %, and 10.38 % of Yb; 3.07 %, 15.09 %, 32.47 %, and 19.62 % of Y and 3.22 %, 11.53 %, 23.48 %, and 53.59 % of Sc were released from the non-magnetic fraction of the Matla fly ash residue after successive leaching with 8 M NaOH, 5 M H<sub>2</sub>SO<sub>4</sub>, 3 M HCl, and 7 M HNO<sub>3</sub>, respectively.

The leaching trend observed was similar to that of La. The highest amounts were leached with the HCl and the lowest amounts with NaOH. The lanthanides are all typically trivalent (+3) and almost identical in size due to lanthanide contraction. The chemical properties of an ion are mainly dependent on its size and charge (Sturza et al., 2008). The various REE ions exhibit similar chemical properties since their charge remains the same and the decrease in size is just minimal. Hence the similarities in the leaching pattern. Thus, the leaching efficiency of REE with respect to each of the reagents can be ordered as: HCl > H<sub>2</sub>SO<sub>4</sub> > HNO<sub>3</sub> > NaOH.

### 7.4.4 Mineralogical analysis of the solid residues from the leaching of the non-magnetic fraction of Matla fly

Figures XXX shows the XRD patterns the non-magnetic fraction of fly ash and the solid residue after the sequentially leaching with 8M NaOH, 5M.H<sub>2</sub>SO<sub>4</sub>, 3M HCl and 7M HNO<sub>3</sub> The XRD patterns are compared in order to understand the transformation in the mineralogy of the leached residues.

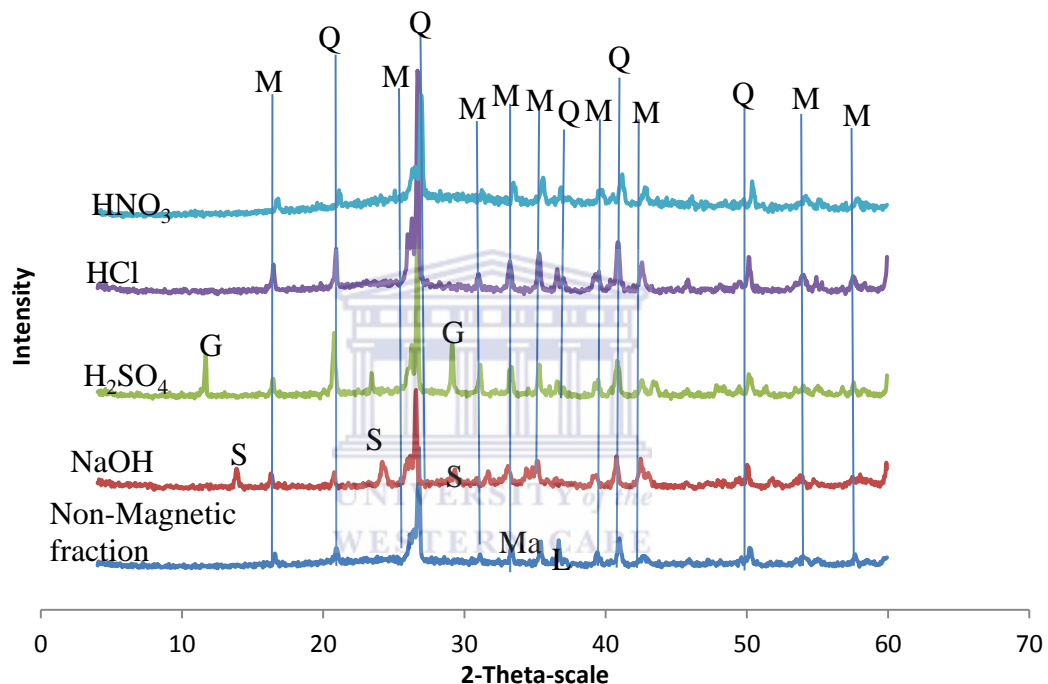


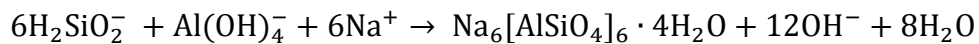
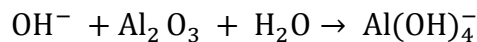
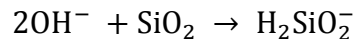
Figure 7.5: XRD patterns of the extracted Magnetic and non-magnetic fraction and Matla fly ash. (G = gypsum, L = lime, M = mullite, Mg = magnetite, Q = quartz and S = sodalite)

In Figure 7.5, the XRD pattern of the non-magnetic fractions is compared to that of the solid residues after each of the four leaching steps. The XRD patterns showed that quartz (SiO<sub>2</sub>) and mullite (3Al<sub>2</sub>O<sub>3</sub>·2SiO<sub>2</sub>) were the major crystalline peaks present in the non-magnetic fraction and the solid residues after the sequential leaching with NaOH, H<sub>2</sub>SO<sub>4</sub>, HCl and HNO<sub>3</sub>. Lime (CaO) and magnetite (Fe<sub>3</sub>O<sub>4</sub>) were present in the non-magnetic fraction but were not

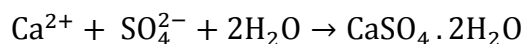
## Chapter Seven: Possibility of Rare earth recovery from fly ash

observed in any of the solid residues from the sequential leaching process. This XRD results corroborate the XRF result of the non-magnetic fraction and the solid residues presented in Section 7.4.1. The XRF results reported that the percentage composition of Ca and Fe, the major elements in these mineral phases, respectively decreased from 4.58 % (Ca) in the non-magnetic fraction to below the detection limit in the solid residue after the HCl and HNO<sub>3</sub> leaching steps. Whilst the percentage composition of Fe also decreased from 2.89 % in the non-magnetic fraction to 0.42 % and 0.31 % in the solid residue after the HCl and HNO<sub>3</sub> leaching steps, respectively.

The XRD patterns of the solid residues after the sequential leaching with NaOH, H<sub>2</sub>SO<sub>4</sub>, HCl and HNO<sub>3</sub> also revealed that the mineralogy of the solid residues from each of the leached steps were similar to one another. However, sodalite (Na<sub>8</sub>Al<sub>6</sub>Si<sub>6</sub>O<sub>24</sub>Cl<sub>2</sub>) and gypsum (CaSO<sub>4</sub>·2H<sub>2</sub>O) were identified in the solid residues after the NaOH and H<sub>2</sub>SO<sub>4</sub> leaching steps, respectively but not identified in the solid residues after the HCl and HNO<sub>3</sub> leaching steps. The sodalite mineral phase (a type of zeolite) present in the solid residue after the NaOH leaching step resulted from the dissolution of the silica and alumina in the fly ash by NaOH and can be represented by the equation below:



The gypsum phase may have resulted between the interaction of the fly ash and the H<sub>2</sub>SO<sub>4</sub>. Gypsum is formed through the following reaction:



### 7.5 Summary of the sequential leaching studies of the non-magnetic fraction of Matla fly ash

The aim of this study was to develop a practical method to leach REE from Matla fly ash using a sequential leaching scheme, by systematically leaching the major fly ash components such as Fe, Si, Al and Ca in order to concentrate or leach out the trace constituent such as the REE. The Matla fly ash was separated into magnetic and non-magnetic fractions through a wet separation technique involving magnetic stirring. The non-magnetic fraction was then sequentially leached with 8 M NaOH, 5 M H<sub>2</sub>SO<sub>4</sub>, 3 M HCl and 7 M HNO<sub>3</sub>. Chemical and physical characterisation were carried out using different analytical techniques such as XRF, LA ICP-MS and XRD in order to understand the major elements, REE and mineral phases, respectively present in the Matla fly ash; the separated magnetic and non-magnetic fractions; and the ensuing leachates and solid residues after the sequential leaching process.

The XRF results of the Matla fly ash and the separated non-magnetic fractions revealed a significant decrease in the Si, Al, Ca, Fe, Mg, K, Na, Ti, P and Mn content in the magnetic fraction when compared to their content in Matla fly ash due to the partitioning effect of the magnetic portion during the extraction process and establishes that the magnetic extraction process resulted in the selective extraction specific elements such as Fe from Matla fly ash. The XRF results also showed that the magnetic fraction was composed primarily of Fe and Mn. A significant amount of Si, Al and moderate amount of Ca were also reported in the magnetic fraction. The detection of non-magnetic elements such as Si, Al and Ca was attributed to the entrapment of Fe bearing phases within the aluminosilicate matrix of the fly ash. The magnetic separation isolated these closely associated species in the magnetic fraction. The LA ICP-MS analyses of the Matla fly ash, the magnetic and non-magnetic fractions showed that La, Ce, Nd, Y and Sc had significantly higher amount in the non-magnetic fraction than in the magnetic fraction indicating that these REE were preferably gathered in the non-magnetic fractions and not highly associated with the magnetic fraction. The mineralogical

## Chapter Seven: Possibility of Rare earth recovery from fly ash

---

investigation of the Matla fly ash, magnetic and non-magnetic fractions revealed that quartz ( $\text{SiO}_2$ ) and mullite ( $\text{Al}_6\text{Si}_2\text{O}_{13}$ ) were the only consistent major mineral components in their XRD patterns. The XRD pattern of the magnetic fraction also revealed an iron rich material primarily composed of hematite ( $\text{Fe}_2\text{O}_3$ ) and magnetite ( $\text{Fe}_3\text{O}_4$ ). This corroborates the XRF result which reported Fe as the major oxide extracted magnetically in the magnetic fraction.

The XRF results of the solid residue after the sequential leaching of the non-magnetic fraction of Matla fly ash with NaOH,  $\text{H}_2\text{SO}_4$ , HCl and  $\text{HNO}_3$  revealed that Si and Al exhibited the same leaching pattern with all the leaching reagents. These elements were strongly retained in each of the solid residue after the four leaching steps. The XRF results also showed that K was below the detection limit in the solid residue after leaching with  $\text{H}_2\text{SO}_4$ , while Ca, Mg, Na and P were also below the detection limit in the solid residue after leaching with HCl. From the XRF results, the leaching efficiency of Si and Al with respect to each of the reagents can be ordered as:  $\text{NaOH} > \text{H}_2\text{SO}_4 > \text{HNO}_3 > \text{HCl}$  and  $\text{H}_2\text{SO}_4 > \text{HNO}_3 > \text{HCl} > \text{NaOH}$ , respectively. Whilst for K, Ca, Mg, Na and P the leaching efficiency can be ordered as:  $\text{HCl} > \text{H}_2\text{SO}_4 > \text{NaOH}$ .

The LA ICP-MS analyses of the REE retained in the solid residue, after the sequential leaching revealed that the REE are better leached from the non-magnetic fraction of the Matla fly ash with acids rather than with base. This is because it is difficult to dissolve REE in their hydroxide forms. The leaching efficiency of the REE with respect to each of the reagents can be ordered as:  $\text{HCl} > \text{H}_2\text{SO}_4 > \text{HNO}_3 > \text{NaOH}$ .

The ICP-MS analyses of the REE in the leachates obtained revealed that the REE exhibited similar leaching pattern due to similarities in the chemical properties of REE. The leaching efficiency of the REE with respect to each of the reagents can be ordered as:  $\text{HCl} > \text{H}_2\text{SO}_4 > \text{HNO}_3 > \text{NaOH}$ .



### Chapter Eight: Conclusions and Recommendations

#### 8 Introduction

This chapter gives a summary of the discussions, significant findings and conclusions of the results presented in the previous chapters. Recommendations for further research on some aspects are outlined

##### 8.1 Overview

The aims and objectives of this study were to determine quantitatively, the full elemental composition of coal fly ash using different analytical techniques; to investigate and validate the application potentials of fly ash beneficiation processes in terms of their environmental safety; and to develop a sequential extraction scheme with a view of concentrating or leaching the REE in the coal fly ash. The ash beneficiation processes investigated were the treatment of Carletonville goldmine AMD with Matla fly ash following the same procedure reported by Madzivire, 2013; geopolymer synthesis from coal fly ash following the protocols and optimized conditions reported by Boke et al., 2014.; and the sequential leaching of Matla fly ash in order to concentrate or leach the REE. In order to achieve the aims and objectives of this study, several analytical techniques such as ENAA, FT-IR, XRD, XRF, HR-SEM/EDS, ICP-MS, LA ICP-MS and IC were applied to characterize the Matla fly ash, products and wastes recovered from the fly ash beneficiation processes. The results of these analyses were compared in order to give a conclusive statement on this study.

##### 8.2 Summary on the elemental composition of Matla fly ash using nuclear and related analytical techniques

The elemental composition of Matla fly ash was determined using ENAA, ICP-OES, LA ICP-MS, and XRF. The aim was to determine the analytical technique that was best suited in determining and quantifying the different categories of elements in fly ash. For the first time a total of 54 major, trace and REE were accurately determined in Matla fly ash by the four analytical techniques. It was



shown that the elemental content of Matla fly ash was of the same order as the SRM NIST coal fly ash 1633b. The concentration of the major elements in Matla fly ash as determined by ENAA and XRF was very similar, apart from Na and correlated well with that of the certified SRM NIST 1633b. Determination of trace and REE content obtained by the ENAA and LA ICP-MS techniques was more reliable than their determination by the XRF or ICP-OES techniques. Although ENAA is a sensitive and accurate method for the determination of many trace elements, this method has some shortcomings. Pb cannot be determined because of its nuclear characteristics. Moreover, the ENAA technique is not readily available in South Africa compared to XRF and LA ICP-MS making it difficult to use the method for routine application. Hence, this study focused on the use of XRF for the determination of the major and minor elements whilst the LA ICP-MS was used for trace elements and REE determination. The reliability of the XRF and LA ICP-MS in the major and trace elemental determination, respectively was confirmed by the results presented in this study.

### 8.3 Summary of the applications of fly ash for AMD treatment

The treatment of Carletonville goldmine AMD with Matla fly ash in a jet loop reactor was carried out in this study. The aim was to assess and understand the residual toxicity of treated water and of the solid waste residue generated from the AMD treatment with fly ash. The characterisation results obtained were used for comparative studies in order to understand the physiochemical changes in the feed stocks, products and waste from this fly ash beneficiation process.

The Carletonville goldmine water samples before and after treatment with Matla fly ash were characterised using ICP-OES and IC and the results obtained were compared. The characterisation results of the untreated Carletonville goldmine water sample classified it as an AMD. The results also showed that the Carletonville goldmine AMD contained elevated levels of toxic metals such as B ( $3.21 \pm 1.04$  mg/L), Cd ( $0.07 \pm 0.02$  mg/L), Cr ( $0.69 \pm 0.26$  mg/L), Hg ( $4.79 \pm 0.81$  mg/L), and Zn ( $23.87 \pm 1.50$  mg/L), and radionuclides U ( $3.65 \pm 0.36$  mg/L),

## Chapter Eight: Conclusions and Recommendations

---

which were higher than the WHO TWQR of potable water. Furthermore, the results also confirmed that the treatment of 80 L of the Carletonville goldmine AMD with 16 kg of Matla coal fly ash, 200 g of  $\text{Ca}(\text{OH})_2$  and 344.95 g of  $\text{Al}(\text{OH})_3$  resulted in the removal of sulphate ions to within the TWQR for potable water.

FT-IR analysis of the Matla fly ash (Feedstock) and the AMD/FA residue (waste) revealed that the fly ash and AMD interaction in the jet loop reactor did not result in any change of the functional groups in the AMD/FA residue. Morphological studies (by SEM) of the Matla fly ash and AMD/FA samples showed that the Matla fly ash and AMD/FA residue consists of irregular, spherically shaped and agglomerated particles. The outer surfaces of the Matla ash particles are smooth while the outer surface of the AMD/FA residue particles appeared encrusted an indication of the formation of new secondary mineral phases. SEM-EDS and XRD confirmed that the encrustations were due to the formation of new mineral phases in the AMD/FA residue.

The elemental content of Matla fly ash and AMD/FA, determined by the XRF and LA ICP-MS analysis revealed that the toxic heavy metals (As, Cd, Co, Cr, Hg and Pb) and radionuclides (Th and U) were present in both Matla fly ash and AMD/FA samples. The Matla fly ash and AMD/FA residues were further shown to be class F and silico-aluminate. The AMD/FA residue also meets the requirements of Class F fly ash but has a higher LOI due to formation of new secondary minerals during the AMD treatment in the jet loop reactor.

The mineralogical investigation of the Matla fly ash and the AMD/FA residue reveals that the only consistent major mineral components were quartz and mullite in Matla fly ash and AMD/FA residue. The XRD results also established the formation of new mineral phases such as gypsum and ettringite during the AMD treatment with fly ash in the jet loop reactor. The XRD patterns agree with the results of the XRF of the Matla fly ash and AMD/FA residue which reported high percentages of the oxides of Si (54.57 % and 52.27 %, respectively) and Al (27.47

## Chapter Eight: Conclusions and Recommendations

---

and 25.18 %, respectively). The quartz and mullite phases correspond to the significant levels of Si and Al in the fly ash and AMD/FA residue. The XRF result also reported higher percentages of Fe (6.50 %) in the AMD/FA residue compared to the Fe (5.76 %) content of the Matla fly ash. Hence, hematite peaks had a higher intensity in the AMD/FA spectrogram compared to the Matla fly ash.

Analysis of the Carletonville goldmine water before and after treatment with Matla fly ash for radioactivity revealed that  $^{238}\text{U}$  and  $^{226}\text{Ra}$  were below detection limit in the treated water indicating that the treatment of the AMD with fly ash also resulted in the reduction of the radioactivity of the treated water. This correlated with the elemental analysis of the Carletonville goldmine water before and after treatment. The Carletonville goldmine AMD had  $3.65 \pm 0.36$  mg/kg of U whilst, U was not detect in the treated water. The radioactivity studies of Matla fly ash and the AMD/FA residue raised environmental concerns over the safety of their disposal and beneficiation because the activity concentrations of  $^{238}\text{U}$  ( $140.1 \pm 5.2$  and  $357.8 \pm 21.2$  Bq/litre, respectively) and  $^{232}\text{Th}$  ( $163.3 \pm 1.1$  and  $174.7 \pm 1.0$  Bq/litre, respectively) were higher than the world-wide average concentrations.

The pH values of leachate solutions of Matla fly ash and of the AMD/FA residue samples were alkaline though, the pH of Matla fly ash (12.43 and 12.18) was higher than that of the AMD/FA residue (10.05 and 9.08) at L/S ratios 10:1 and 20:1 respectively. This was due to loss of CaO from Matla fly ash during neutralisation of the AMD in the jet loop reactor. Moreover, the EC value of leachate solutions of Matla fly ash (1.81 and 2.47 mS/cm) was slightly higher than the EC values of the AMD/FA residue (1.30 and 1.55 mS/cm) at L/S ratios 10:1 and 20:1 respectively. This indicates that many species in both Matla fly ash and AMD/FA residue are soluble and easily released upon contact with water. The analysis of the DIN-S4 leachates of Matla fly ash and the AMD/FA residue showed that increasing the amount of water in the L/S ratio did not increase the amount of species leached but rather diluted the leached species. These results also revealed that Pb, Mo, Ba, U, Al, Ca, Mg, Na, K, Hg, As, Pb, Fe, Cr, Co, Sr,

U, Zn and Si were mobile in Matla fly ash and AMD/FA residue at L/S 10:1. Though, Cd, Mn, Ni and V were detected in the DIN-S4 leachate of the Matla fly ash but were not leached from the AMD/FA residue at L/S 10:1 whilst Ca, Mg, Al, Na, K, Si, Ba, Hg, As, Pb, Cr, Sr, V, and Co were mobile at L/S 20:1. Which provided valuable information on the relative availability of trace pollutants in the AMD/FA residue and, hence, on the extent of entrapment or encapsulation of toxic metals in the residue

### **8.4 Summary of the application of Matla fly ash in the synthesis of foamed geopolymer**

Geopolymer was synthesised from Matla fly ash and the aim was to evaluate and understand the toxicity of the synthesised geopolymer. The synthesised geopolymer and Matla fly ash were characterised and the compared results were used to understand the chemical properties of the fly ash that were carried into the geopolymer. The investigations provided significant insight into the molecular structure, morphology, mineralogy, chemical composition and leaching behaviour of the Matla fly ash, and the synthesised geopolymer.

The transformation of Matla fly ash into geopolymer was characterised by two distinctive features that were observed when the FT-IR spectrum of the Matla fly ash was compared to the spectrum of the synthesised geopolymer. The first was shift of the band attributed to the asymmetric stretching vibrations of Si-O-Si and Al-O-Si from  $1102\text{ cm}^{-1}$  in the spectrum of the Matla fly ash to a lower frequency of  $977\text{ cm}^{-1}$  in the spectrum of the synthesised geopolymer. That is associated with the dissolution of the fly ash amorphous phase in the strong alkaline activating solutions and polycondensation with alternating Si-O and Al-O bonds. The other distinctive feature observed in the synthesised geopolymer spectrum was the high intensity of the band at  $1432\text{ cm}^{-1}$  attributed to stretching vibrations of O-C-O bonds indicating the presence of sodium bicarbonate which occurred due to the atmospheric carbonation of the contained Na that is incorporated into the geopolymer structures surface.

## Chapter Eight: Conclusions and Recommendations

---

The morphological studies (by SEM) revealed that the Matla fly ash consists of irregular spherically shaped and agglomerated particles with smooth outer surfaces. Whilst the synthesised geopolymer comprises of mostly irregular shaped and agglomerated particles with encrusted outer surfaces. SEM-EDS and XRD confirmed that the encrustations were due to the formation of new mineral phases in geopolymer particles. The XRD results also established the formation of new mineral phases such as sodalite and halite during the geopolymerisation process of the fly ash which are both soluble phases indicating the geopolymer would need to be kept away from water.

The elemental analysis revealed that potentially toxic heavy metals As ( $10.53 \pm 2.08$  mg/kg), Cd ( $3.90 \pm 1.2$  mg/kg), Cr ( $62.48 \pm 7.96$  mg/kg), Hg ( $7.74 \pm 0.56$  mg/kg), Ni ( $33.99 \pm 0.75$  mg/kg), Pb ( $21.89 \pm 1.3$  mg/kg), V ( $49.59 \pm 1.2$ ), Zn ( $61.30 \pm 2.49$  mg/kg) and radionuclides Th ( $10.26 \pm 0.46$  mg/kg) and U ( $9.97 \pm 0.01$  mg/kg) were present in the synthesised geopolymer as well as in Matla fly ash. The analysis of the DIN-S4 leachates of the synthesised geopolymer revealed that Zn ( $0.10 \pm 0.003$  mg/kg), V ( $0.15 \pm 0.0012$  mg/kg), Ni ( $0.02 \pm 0.002$  mg/kg), Pb ( $0.014 \pm 0.0002$  mg/kg), and Hg ( $0.024 \pm 0.004$  mg/kg) were leached. In comparison, the following amounts of Zn ( $0.03 \pm 0.002$  mg/kg), V ( $0.03 \pm 0.0009$  mg/kg), Ni ( $0.02 \pm 0.0018$  mg/kg), and Pb ( $0.002 \pm 0.0001$  mg/kg), were leached from Matla fly ash. This showed that geopolymerisation had no effect on the mobility of these elements. While, elements such as Fe ( $9.76 \pm 0.19$  mg/kg), Mn ( $4.18 \pm 0.08$  mg/kg), As ( $0.069 \pm 0.009$  mg/kg) and the radionuclide U ( $0.01 \pm 0.0025$  mg/kg) were detected in Matla fly ash leachates they were below detection limit in the synthesised geopolymer leachate indicating that these species were immobilized in the synthesised geopolymer.

Gamma spectrometric analysis revealed that the activity content of the synthesised geopolymer was lower than that of the Matla fly ash and meets the requirements as a building material in terms of radioactivity. The calculated  $R_{a_{eq}}$ ,  $H_{ex}$  and  $I_{\gamma}$  values of the Matla fly ash (385.19 Bq/kg, 1.0 Bq/kg and 1.34) were above the

recommended values and did not meet the requirements as a building material in terms of radioactivity. This finding is of paramount importance because no research has previously been done to determine the radioactivity of geopolymers synthesised from coal fly ash that has potential as a construction material.

### 8.5 Summary of the sequential leaching of REE from Matla fly ash

The sequential leaching studies of REE from Matla fly ash was undertaken with the aim to developing a practical method to leach the REE that are present in the Matla fly ash. The Matla fly ash was separated into magnetic and non-magnetic fractions through a wet separation technique involving magnetic stirring. The non-magnetic fraction was then sequentially leached with 8M NaOH, 5M H<sub>2</sub>SO<sub>4</sub>, 3M HCl and 7M HNO<sub>3</sub>. Chemical and physical characterisation were carried out in order to understand the major elements, REE and mineral phases present in the Matla fly ash; the separated magnetic and non-magnetic fractions; and the ensuing leachates and solid residues after the sequential leaching process.

The XRF results of the Matla fly ash and the separated non-magnetic fractions revealed a significant decrease in the Si, Al, Ca, Fe, Mg, K, Na, Ti, P and Mn content in the non-magnetic fraction due to the partitioning effect of the magnetic portion during the extraction process and established that the magnetic extraction process resulted in the extraction or removal of many species not just Fe from Matla fly ash. The XRF results also showed that the magnetic fraction was composed primarily of Fe and Mn. A significant amount of Si, Al and moderate amount of Ca were also reported in the magnetic fraction. The detection of non-magnetic elements such as Si, Al and Ca was attributed to the entrapment of Fe bearing phases within the aluminosilicate matrix of the fly ash. The magnetic separation isolated these closely associated species in the magnetic fraction. The LA ICP-MS analyses of the Matla fly ash, the magnetic and non-magnetic fractions showed that La, Ce, Nd, Y and Sc were significantly more concentrated in the non-magnetic fraction than in the magnetic fraction indicating that these REE were preferably associated with the non-magnetic fraction of the fly ash. The

## Chapter Eight: Conclusions and Recommendations

---

mineralogical investigation of the Matla fly ash, magnetic and non-magnetic fractions revealed that quartz ( $\text{SiO}_2$ ) and mullite ( $3\text{Al}_2\text{O}_3 \cdot 2\text{SiO}_2$ ) were the only consistent major mineral components in their XRD patterns. The XRD pattern of the magnetic fraction also revealed enrichment of an iron rich material primarily composed of hematite ( $\text{Fe}_2\text{O}_3$ ) and magnetite ( $\text{Fe}_3\text{O}_4$ ). This corroborates the XRF result which reported Fe as the major oxide extracted magnetically in the magnetic fraction.

The XRF results of the solid residues retained after the sequential leaching of the non-magnetic fraction of Matla fly ash with NaOH,  $\text{H}_2\text{SO}_4$ , HCl and  $\text{HNO}_3$ , respectively revealed that Si and Al exhibited the same leaching pattern with all the leaching reagents. These elements (>50 % of Si and Al) were strongly retained in each of the solid residue after the four leaching steps. The results also showed that K was below the detection limit in the solid residue after leaching with  $\text{H}_2\text{SO}_4$ , while Ca, Mg, Na and P were also below the detection limit in the solid residue after leaching with HCl. From the XRF results, the leaching efficiency of Si and Al with respect to each of the reagents can be ordered as:  $\text{NaOH} > \text{H}_2\text{SO}_4 > \text{HNO}_3 > \text{HCl}$  and  $\text{H}_2\text{SO}_4 > \text{HNO}_3 > \text{HCl} > \text{NaOH}$ , respectively. Whilst for K, Ca, Mg, Na and P the leaching efficiency can be ordered as:  $\text{HCl} > \text{H}_2\text{SO}_4 > \text{NaOH}$ .

The LA ICP-MS analyses of the REE retained in the solid residue after the sequential leaching, revealed that the REE are better leached from the non-magnetic fraction of the Matla fly ash with acids (low pH) rather than with base (high pH).. The residue after NaOH leaching had approximately 100 % of La, Ce, Dy, Gd, Yb, Y and Sc. This is because it is difficult to dissolve REE in their hydroxide forms. Approximately 100 % of Eu and Ho retained in the residue after NaOH and  $\text{H}_2\text{SO}_4$  leaching, whilst approximately 100 % of Sm and Lu were retained in each of the residue after leaching with NaOH,  $\text{H}_2\text{SO}_4$ , HCl and  $\text{HNO}_3$ , respectively. This indicates that Eu and Ho were not leached from fly ash by NaOH and  $\text{H}_2\text{SO}_4$  and sequential leaching scheme had no effect on Sm and Lu. Ce was not detected in the residues after HCl leaching and Pr was not detected



after  $\text{HNO}_3$  leaching indicating that these REE were completely leached from the fly ash. The leaching efficiency of the REE with respect to each of the reagents can be ordered as:  $\text{HCl} > \text{H}_2\text{SO}_4 > \text{HNO}_3 > \text{NaOH}$ .

The ICP-MS analyses of the REE in the leachates obtained after the sequential leaching of the non-magnetic fraction of Matla fly ash revealed that HCl leached 85.54 % of Yb, 79.35 % of Er, 78.09 % of Ce, 52.60 % of La, 54.17% of Pr, 49.73% of Eu, 41.03% of Nd and 38.47% of Tb. These high amounts of REE leached by HCl are due to the dissolution of REE in dilute acids to form solutions containing the trivalent (+3) ions. The REE also exhibited similar leaching pattern due to similarities in their chemical properties. The leaching efficiency of the REE with respect to each of the reagents can be ordered as:  $\text{HCl} > \text{H}_2\text{SO}_4 > \text{HNO}_3 > \text{NaOH}$ .

### 8.6 Significance of the study

The novel findings from this thesis are of importance to both the scientific and industrial community. The significance of the contributions from this research can be summarized as follows;

1. ENAA along with ICP-OES, LA ICP-MS, and XRF were used to determine the elemental composition of coal fly ash from the Malta coal power station in the Mpumalanga province of South Africa. For the first time a total of 54 major, trace and REE were accurately determined in the Matla fly ash by the four analytical techniques. The results showed that ENAA is a sensitive and accurate method for the determination of the major, minor and trace elements in coal fly ash. That XRF is best suited for the determination of the major and minor elements, whilst the LA ICP-MS is reliable for trace elements determination and equivalent to ENAA.
2. The results of the elemental composition revealed that after AMD neutralisation, the remaining AMD/FA residues contains toxic metal (As,



## Chapter Eight: Conclusions and Recommendations

---

Cd, Cr, Hg, Ni and Pb) and radionuclides (Th and U) which are potentially harmful to humans in excessive amounts. The results also showed that the amounts of La, Ce, and Nd in AMD/FA residues were found to be considerably higher than the in fly ash and average abundance in the earth crust

3. The DIN-S4 leaching test results showed that higher amount of species was leached from Matla fly ash when compared to the amount leached from the AMD/FA residue at the different L/S ratios. This provided valuable information on the relative availability of trace pollutants (Cr, Hg, Pb, Zn and U) in the AMD/FA residue and, hence, on the extent of entrapment or encapsulation of Cd, Mn, Ni, V and Th in the residue
4. The gamma spectrometric analysis revealed that the activity content of the synthesised geopolymer in terms of radiological hazard was lower than that of the Matla fly ash and meets the requirements as a building material in terms of radioactivity. This finding is of paramount importance because no research has previously been carried out to determine the radioactivity of geopolymers synthesised from coal fly ash for construction material.
5. The elemental analysis of separated fraction of Matla fly ash revealed that REE were evenly distributed between the magnetic and non-magnetic fractions of the Matla fly ash.
6. The sequential leaching scheme revealed that the REE are better leached from the non-magnetic fraction of the Matla fly ash with acids (low pH) rather than with base (high pH) and that REE in fly ash exhibited similar leaching pattern due to similarities in their chemical properties.

### 8.7 Recommendations

## Chapter Eight: Conclusions and Recommendations

---

The techniques used in the characterization of the fly ash beneficiation products and wastes in comparison with fly ash (feed stock) in this study proved to be effective, replicable and can therefore be applied in similar research studies. It also proved to be adequate for the defined purpose of investigating and validating the application potentials of fly ash beneficiation processes in terms of their environmental safety. The sequential leaching scheme proved successful in the leaching of the REE in the coal fly ash but could be optimized for better yield



## Reference

---

### References

Abbott, D.; Essington, M.; Mullen, M.; Ammons, J., 2001: Fly ash and lime-stabilized biosolid mixtures in mine spoil reclamation: Simulated weathering. *J. Environ. Qual.*, 30 (2), 608-616.

Ademola, J., 2009: Natural Radioactivity and Hazard Assessment of Imported Ceramic Tiles in Nigeria African. *Journal of Biomedical Research*, 12(3), 161-165.

Adriano, D. C.; Page, A. L.; Elsewi, A. A.; Chang, A. C.; Straughan, I., 1980: Utilization and Disposal of Fly Ash and other Coal Residues in Terrestrial Ecosystems: A Review. *J. Environ. Qual.* Volume & Issue 9,(3) 333 - 344

Ahmaruzzaman, M. 2010: A review on the utilization of fly ash. *Progress in Energy and Combustion Science*, 36(3), 327-363.

Alexander, M.; Smith, M.; Hartman, J.; Mendoza, A. and Koppelaar, D., 1998: Laser ablation inductively coupled plasma mass spectrometry, *Applied surface science*, 127, 255-261.

Akcil, A. and Koldas, S. 2006: Acid Mine Drainage (AMD): causes, treatment and case studies. *Journal of Cleaner Production*, 14(12), 1139-1145.

Akinyemi A, S.; Akinlua, A.; Gitari, W.; Nyale, S.; Akinyeye, R. and Petrik, L., 2012: An investigative study on the chemical, morphological and mineralogical alterations of dry disposed fly ash during sequential chemical extraction. *Energy Science and Technology*, 3(1), 28-37.

Al Bakri, A.; Kamarudin, H.; Bnhussain, M.; Nizar, I.; Rafiza, A. & Zarina, Y., 2012: The processing, characterization, and properties of fly ash based geopolymer concrete. *Rev. Adv. Mater. Sci*, 30, 90-97.

## Reference

---

Alonso, E.; Sherman, A.; Wallington, T.; Everson, M.; Field, F.; Roth, R., and Kirchain, R., 2012: Evaluating rare earth element availability: A case with revolutionary demand from clean technologies. *Environmental science & technology*, 46 (6), 3406-3414.

Álvarez-Ayuso, E.; Querol, X.; Plana, F.; Alastuey, A.; Moreno, N.; Izquierdo, M.; and Barra, M., 2008: Environmental, physical and structural characterisation of geopolymer matrixes synthesised from coal (co-) combustion fly ashes. *Journal of hazardous materials*, 154 (1) 175-183.

Åmand, L. and Tullin, C., 1999: The theory behind FT-IR analysis. *Dep. Of Energy Conversion, Chalmers University of Technology, Sweden*  
<http://www.fysik.lu.se/cecocost/pdf>, assessed 10<sup>th</sup> of April 2013

American society for testing and material 1993: ASTM C 618: Standard specification for fly ash and raw or calcined natural pozzolan for use as a mineral admixture in Portland cement concrete. *In: Annual book of ASTM Standards*. ASTM, Philadelphia, PA.

Andini, S.; Cioffi, R.; Colangelo, F.; Grieco, T.; Montagnaro, F. and Santoro, L., 2008: Coal fly ash as raw material for the manufacture of geopolymer-based products, *Waste management*, 28(2), 416-423.

Araripe, D.; Bellido, L.; Patchineelam, S.; Bellido, A.; Guimarães, M. and Vasconcellos, M., 2006: Trace and major elements in rock samples from Itinguassú River Basin, Coroa-Grande, Rio de Janeiro, *Journal of Radioanalytical and Nuclear Chemistry*, Vol. 270, No.1, pp103-109

Ashbaugh, C. 1982: Gamma-ray spectroscopy to measure radioactivity in gemstone, *Gems & Gemology*, Vol. 28, No. 2, pp. 104-111.

## Reference

---

Asokana, P.; Saxena, M.; Asolekar, S., 2005: Coal combustion residues - environmental implications and recycling potentials, *Resources, Conservation and Recycling*, 43:239-262. DOI: 10.1016/j.resconrec.2004.06.003.

Baba, A, Gurdal, G, Sengunalp, F and Ozay, O., 2008: Effects of leachant temperature and pH on leachability of metals from fly ash. A case study: Can thermal power plant, province of Canakkale, Turkey, *Environ Monit Assess*, 139:287–298. DOI 10.1007/s10661-007-9834-8

Bada, S. and Potgieter-Vermaak, S., 2008: Evaluation and Treatment of Coal Fly Ash for Adsorption Application, Leonardo Electronic *Journal of Practices and Technologies*, Issue 12, p. 37-48

Baeyens, W.; Monteny, F.; Leermakers, M.; Bouillon, S., 2003: Evaluation of Sequential Extractions on Dry and Wet Sediments, *Anal Bioanal Chem*, 376: 890–901

Bai, G.; Teng, W., Wang, X.; Qin, J.; Xu, P. and Li, P., 2010: Alkali desilicated coal fly ash as substitute of bauxite in lime-soda sintering process for aluminum production. *Transactions of Nonferrous Metals Society of China*, 20, s169-s175.

Bailey, A.; Luthert, P.; Dean, A.; Harding, B.; Janota, I., Montgomery, M.; Ru'iter, M. and Lantos, P., 1998: A Clinicopathological Study of Autism. *Brain* 121: 101-117.

Bailey, S.; Olin, T.; Bricka, R. and Adrian, D., 1999: A review of potentially low-cost sorbents for heavy metals. *Water research*, 33(11), 2469-2479

Baltakys, K.; Jauberthie, R.; Siauciunas, R. and Kaminskas, R., 2007: Influence of modification of SiO<sub>2</sub> on the formation of calcium silicate hydrate. *Materials Science-Poland*, 25(3), 663-670.

## Reference

---

Bankowski, P.; Zou, L.; Hodges, R., 2004: Reduction of metal leaching in brown coal fly ash using geopolymers, *J. Hazard. Mater.*, B114 59–67.

Barnes, M.; Addai-Mensah, J. and Gerson, A., 1999: The solubility of sodalite and cancrinite in synthetic spent Bayer liquor. *Colloids and Surfaces A: Physicochemical and Engineering Aspects*, 157(1), 101-116.

Basu, M.; Pande, M.; Bhadoria, P.; Mahapatra, S., 2009: Potential fly-ash utilization in agriculture: A global review, *Progress in Natural Science*, 19, 1173–1186

Batabyal D.; Sahu A.; Chaudhuri, S., 1995: Kinetics and mechanism of removal of 2,4- dimethyl phenol from aqueous solutions with coal fly ash, *Sep Technol*, 5, 179–86.

Baxter, M., 1993: Environmental radioactivity: A perspective on industrial contributions. *IAEA Bulletin*, 35(2), 33-38.

Bayati, B.; Babaluo, A.; and Karimi, R., 2008: Hydrothermal synthesis of nanostructure NaA zeolite: The effect of synthesis parameters on zeolite seed size and crystallinity *Journal of the European Ceramic Society*, Vol. 28, pp. 2653–2657.

Beeghly, J.; Bigham, J.; Dick, W.; Stehouwe, R.; Wolfe, W., 1995: The Impact of Weathering and Aging on a LIMB Ash Stockpile Material, 11th International Symposium on Use and Management of Coal Combustion By-products, *American Coal Ash Association & EPRI*, January 15-19, 1995, Orlando, Florida

Bend, S., 1992: The origin, formation and petrographic composition of coal, *Fuel*, Vol. 71, pp 851- 864

## Reference

---

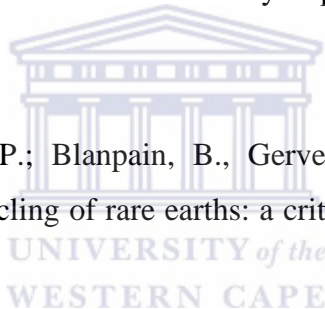
Beretka, J. and Mathew, P., 1985: Natural radioactivity of Australian building materials, industrial wastes and by-products. *Health physics*, 48(1), 87-95.

Berndt, H., 1991: Acidity: A Review of Fundamentals. *The Book and Paper Annual*, Vol. 10

Bhat, S. and Lovell, C., 1996: Use of Coal Combustion Residues and Foundry Sands in Flowable Fill. Publication FHWA/IN/JHRP-96/02., *Joint Highway Research Project*, Indiana Department of Transportation and Purdue University, West Lafayette, Indiana, 1996. doi: 10.5703/1288284313339

Bhattacharyya, S.; Donahoe, J.; Patel, D., 2009: Experimental study of chemical treatment of coal fly ash to reduce the mobility of priority trace elements, *Fuel* 88, 1173–1184.

Binnemans, K.; Jones, P.; Blanpain, B.; Gerven, T., Yang, Y., Walton, A.; Buchert, M., 2013: Recycling of rare earths: a critical review, *Journal of Cleaner Production* 51, 1-22



Blissett, R. and Rowson, N., 2012: A review of the multi-component utilisation of coal fly ash. *Fuel* 97:1-23. DOI: doi.org/10.1016/j.fuel.2012.03.024.

Bode, P.; Greenberg, R.; De Nadai Fernandes, E., 2009: Neutron activation analysis: a primary (ratio) method to determine SI-traceable values of element content in complex samples. *Chimia*, 63(10):678-680. DOI: <http://dx.doi.org/10.2533/chimia.2009.678>.

Böke, N.; Birch, G.; Nyale, S.; and Petrik, L., 2015: New synthesis method for the production of coal fly ash-based foamed geopolymers. *Construction and Building Materials*, 75, 189-199.

## Reference

---

Bose-O'Reilly, S.; McCarty, K.; Steckling, N. and Lettmeier, B., 2010: Mercury Exposure and Children's Health, *Curr. Probl. Pediatr. Adolesc. Health Care* 40, 186–215

Boss, C. and Fredeen, K., 1999: *Concepts, instrumentation and techniques in inductively coupled plasma optical emission spectrometry* (Vol. 997). Norwalk: Perkin Elmer.

Brigden K and Santillo D., 2002: Heavy metal and metalloid content of fly ash collected from the Sual, Mauban and Masinloc coal fired power plants in the Philippines. Exeter, UK: *Greenpeace Research Laboratories, Department of Biological Sciences, University of Exeter.*

Brouwers, H.; and. Van Eijk, R., 2003: Chemical Reaction of Fly Ash, Proceedings of the 11th International Congress on the Chemistry of Cement (ICCC) 11 - 16 May 2003, Durban, South Africa 'Cement's Contribution to the Development in the 21st Century' ISBN Number: 0-9584085-8-0

Browne E.; Firestone R.; Shirley V., 1986: Table of Radioactive Isotopes. *John Wiley & Sons*, New York

Brower, G., 1985: Solid wastes and water quality, *Journal (Water Pollution Control Federation)*, Vol. 57, No. 6, 625-629

Brown, R. and Milton, M., 2005: Analytical techniques for trace element analysis: an overview, *Trends in Analytical Chemistry*, Vol. 24, No. 3 pp.266-274

Bruder-Hubscher, V.; Lagarde, F.; Leroy, M.; Coughanowrb, C.; Enguehard, F., 2002: Application of a sequential extraction procedure to study the release of elements from municipal solid waste incineration bottom ash, *Analytica Chimica Acta*, 451, 285–295



## Reference

---

Buchwald, A.; Hohmann, M. and Kaps, C., 2004: Stabilization of foamed clay bodies with geopolymeric binders for the production of high thermal insulation bricks. In: Müller, W., Fischer, A. (Eds.), *Zi—Annual for the Brick and Tile, Structural Ceramics and Clay Pipe Industries*. Bauverlag, Güthersloh, pp. 104–114.

Carlsen, L. and Chrisliansrn, J., 1995: Flash pyrolysis of coals: A new approach of classification, *Journal of Analytical and Applied Pyrolysis* 35, 77 – 91

Castor, S. and Hedrick, J., 2006: Rare earth elements. *Industrial Minerals volume, 7th edition: Society for Mining, Metallurgy, and Exploration*, Littleton, Colorado, 769-792.

Cetin, C. and Pehlivan, E., 2007: The use of fly ash as a low cost, environmentally friendly alternative to activated carbon for the removal of heavy metals from aqueous solutions, *Colloids and Surfaces A: Physicochem. Eng. Aspects* 298, 83–87

Chakhmouradian, A. and Wall, F., 2012: Rare earth elements: Minerals, mines, magnets (and more), *Elements*, 8, 5, 333-340

Charro, E. and Peña, V. 2012: Environmental impact of natural radionuclides from a coal-fired power plant in Spain, *Radiation Protection Dosimetry* pp. 1–11

Chen, M. and Ma, L., 2001: Comparison of Three Aqua Regia Digestion Methods for Twenty Florida Soils, *Soil Sci. Soc. Am. J.* 65:491-499. DOI:10.2136/sssaj2001.652491x.

Chen, Y.; Shah, N.; Huggins, F.; Huffman, G. and Dozier, A., 2005: Characterization of ultrafine coal fly ash particles by energy-filtered TEM, *Journal of Microscopy*, Vol. 217, Pt 3 March 2005, pp. 225–234

## Reference

---

Cheng, S., 2003: Heavy Metal Pollution in China: Origin, Pattern and Control, *Environ Sci & Pollut Res* 10 (3) 192 - 198 (2003)

Choi, S.; Lee, S.; Song, Y.; Moon, H., 2002: Leaching characteristics of selected Korean fly ashes its implications for the ground water composition near the ash dump, *Fuel* 81, 1083-1090.

Chen-Tan, N.; Van Riessen, A.; Ly, C. and Southam, D., 2009: Determining the reactivity of a fly ash for production of geopolymer. *Journal of the American Ceramic Society*, 92(4), 881-887.

Cho, H.; Oh, D.; Kim, K., 2005: A study on removal characteristics of heavy metals from aqueous solution by fly ash, *Journal of Hazardous Materials B* 127, 187–195.

Clarke, L. and Sloss, L., 1992: Trace elements. In Zandi, M and Russell, N, 2007: Design of a Leaching Test Framework for Coal Fly Ash Accounting for Environmental Conditions, *Environ Monit Assess*, 131:509–526

Cooke, J. 2005: Spectroscopy in Inorganic Chemistry (Theory), Department of Chemistry, University of Alberta, [www.chem.ualberta.ca/~inorglab/specttheorypdf](http://www.chem.ualberta.ca/~inorglab/specttheorypdf)  
Assessed 10th of April 2013

Cotton, F.; and Wilkinson, G., 1988: Advanced Inorganic Chemistry, a Comprehensive Text, 4<sup>th</sup> Ed., New York.

Cundy, C. and Cox, P., 2005: The hydrothermal synthesis of zeolites: Precursors, intermediates and reaction mechanism. *Microporous and Mesoporous Materials*, 82(1), 1-78.

Daintith, J. 2004: A Dictionary of Chemistry, 5th Edition, *Oxford University Press*, Oxford OX2 6DP

## Reference

---

Davidovits, J. 1991: Geopolymers. *Journal of Thermal Analysis and calorimetry*, 37 (8), 1633-1656.

Davison, R.; Natusch, D.; Wallace, J. and Evans, C., 1974: Trace Elements in Fly Ash Dependence of Concentration on Particle Size, *Environ. Sci. Technol.* 8, (13) 1107-1113

Dellantonio A.; Fitz, W.; Custovic, H.; Repman, F.; Schneider, B.; Grünewald, H.; Gruber, V.; Zgorelec, Z.; Zerem, N.; Carter, N.;C.; Markovic, M.;Puschenreiter, M.; Wenzel, W., 2008: Environmental risks of farmed and barren alkaline coal ash landfills in Tuzla, Bosnia and Herzegovina. *Environmental Pollution* 153: 677-686

Djingova, R.; Ivanova, J.; Kuleff, I., 1998: Comparative Evaluation of the Possibilitéis of INAA, ED-XRF, ICP-AES and AAS in the Análisis of Plants, *Journal of Radioanalytical and Nuclear Chemistry*, 237(1-2), 25-34.

Dmitriev A and Pavlov S., 2013: Automation of quantitative determination of elemental content of samples by neutron activation analysis at the reactor IBR-2 in FLNP JINR, *Physics of Particles and Nuclei Letters*. 2013;10(178):58-64. DOI: 10.1134/S1547477113010056

Dudas, M., 1981: Long-Term Leachability of Selected Elements from Fly Ash, *Environmental Science & Technology*, *American Chemical Society*, Volume 15, 840 – 843

Duliu, O.; Culicov, O.; Rădulescu, I.; Cristea, C. and VasIU, T., 2005: Major, trace, and natural radioactive elements in bituminous coal from Australia, Romania, Russia, South Africa and Ukraine: *A comparative study*. *Journal of radioanalytical and nuclear chemistry*, 264(3), 525-534.

## Reference

---

Dutta, B.; Khanra, S.; Mallick, D., 2009: Leaching of Elements from Coal Fly Ash: Assessment of its Potential for Use in Filling Abandoned Coal Mines, *Fuel* 88 1314–1323

Ebaid, Y. 2010: Use of gamma-ray spectrometry for uranium isotopic analysis in environmental samples. *Rom Journ Phys*, 55(1-2), 69-74.

Eberhard, A. 2011: The future of South African Coal: market, investment, and policy challenges. PESD Working Paper 100, Stanford

Eckerman, F. and Ryman, C., 1993: *External Exposure to Radionuclides in Air, Water, and Soil*; Federal Guidance Report No.12. EPA 402-R-93e081; <http://ordose.ornl.gov/documents/fgr12.pdf>, U.S. Environmental Protection Agency, Washington, DC

Ehmann, W. and Vance, D., 1991: Radiochemistry and Nuclear Methods of Analysis, *John Wiley*, New York.

Enamorado-Báez, S.; Abril, L.; Gómez-Guzmán J.; 2013: Determination of 25 trace element concentrations in biological reference materials by icp-ms following different microwave-assisted acid digestion methods based on scaling masses of digested samples. *ISRN Analyt Chem.*, 1-14. DOI: 10.1155/2013/851713.

Environmental Concerns: <http://www.chemistryexplained.com/CeCo/Coal.html>. Web Page Retrieved 3rd September 2010.

European Commission Radiation protection 112, (1999) Radiological Protection Principles concerning the Natural Radioactivity of Building Materials, [ec.europa.eu/energy/nuclear/radiation\\_protection/doc/.../112.pdf](http://ec.europa.eu/energy/nuclear/radiation_protection/doc/.../112.pdf)

Falcon, R. and Ham, A., 1988: The characteristics of Southern African coals, *J. S. At. Inst. Min. Metal*, vol. 88, no. 5, 145-161.

## Reference

---

Fatoba, O, 2008: Chemical compositions and leaching behaviour of some South African fly ashes, *Unpublished M.Sc. thesis*, University of the Western Cape, Cape Town, South Africa.

Feng, D.; Aldrich, C. and Tan, H., 2000: Treatment of acid mine water by use of heavy metal precipitation and ion exchange, *Minerals Engineering*, 13(6): 623-642.

Fernández-Turie, J.; de Carvalho, W.; CabalSas, M.; Querol, X.; Lopez-Soler, A., 1994: Mobility of heavy metals from coal fly ash, *Environmental Geology*, 23:264-270

Fernández-Jiménez, A. and Palomo, A., 2005: Composition and microstructure of alkali activated fly ash binder: effect of the activator. *Cement and Concrete Research*, 35(10), 1984-1992.

Fisher, G. I. 1983: Biomedically Relevant Chemical and Physical Properties of Coal Combustion Products, *Environmental Health Perspectives*, Vol. 47, pp. 189-199.

Foner, H.; Robl, T.; Hower, J.; Graham, U., 1999: Characterization of fly ash from Israel with reference to its possible utilization, *Fuel* 78, 215–223.

Font, O.; Querol, X.; Juan, R.; Casado, R.; Ruiz, C. ; López-Soler, Á. and Peña, F., 2007: Recovery of gallium and vanadium from gasification fly ash. *Journal of hazardous materials*, 139(3), 413-423.

Fruchter, J.; Rai, D.; Zacchara, J., 1990: Identification of solubility controlling solid phases in a large fly ash field lysimeter. *Environ. Sci. Technol.*, 24, 1173–1179.

## Reference

---

Gaikwad, R. and Gupta, D., 2007. Acid Mine Drainage (AMD) Management. *Jr. of Industrial pollution control*, 23 (2), 285-297.

Garavaglia, R. and Caramuscio, P., 1994: Coal Fly-Ash Leaching Behaviour and Solubility Controlling Solids. In: J.J.J.M. Goumans, H.A. van der Sloot and Th.G. Aalbers, Editors, *Environmental Aspects of Construction with Waste Materials*, Elsevier Science, Amsterdam.

Gilbert, C. 2013: Synthesis and characterisation of iron nanoparticles by extraction from iron rich waste material for the remediation of acid mine drainage. *Unpublished M.Sc. thesis*, University of the Western Cape, Cape Town, South Africa

Gitari, W.; Petrik, L.; Etchebers, O.; Key, D.; Okujeni, C., 2008: Utilization of fly ash for treatment of coal mines wastewater: Solubility controls on major inorganic contaminants, *Fuel* 87, 2450–2462.

Gitari, W.; Petrik, L.; Etchebers, O.; Key, D.; Iwuoha, E.; Okujeni, C., 2008: Passive neutralisation of acid mine drainage by fly ash and its derivatives: A column leaching study, *Fuel* 87, 1637–1650.

Gitari, W.; Fatoba, O.; Petrik, L.; Vadapalli, V., 2009: Leaching characteristics of selected South African fly ashes: Effect of pH on the release of major and trace species. *Journal of Environ. Sci. and Health, Part A: Toxic/Hazardous Substances and Environmental Engineering*, 1532-4117, Volume 44, Issue 2, 206 – 220

Gitari, W.; Petrik, L.; Key, D. ; and Okujeni, C., 2010: Partitioning of major and trace inorganic contaminants in fly ash acid mine drainage derived solid residues. *International Journal of Environmental Science & Technology*, 7(3), 519-534.

Gitari, W.; Petrik, L.; Key, D. ; and Okujeni, C., 2011: Interaction of acid mine drainage with Ordinary Portland Cement blended solid residues generated from

## Reference

---

active treatment of acid mine drainage with coal fly ash, *Journal of Environmental Science and Health, Part A: Toxic/Hazardous Substances and Environmental Engineering*, 46:2, 117-137, DOI: 10.1080/10934529.2011.532423

Gluskoter, H. J., 1975: Mineral Matter and Trace Elements in Coal; In Trace Elements in Fuel; Babu, S.; *Advances in Chemistry*; American Chemical Society: Washington, DC, 1975.

Gómez, D.; Dos Santos, M.; Fujiwara, F.; Griselda, P.; Marrero, J.; Dawidowski, L. and Smichowski, P., 2007: Fractionation of Metals and Metalloids by Chemical Bonding from Particles Accumulated by Electrostatic Precipitation in an Argentine Thermal Power Plant, *Microchemical Journal* 85, 276–284

Goodarzi, F., 2006: Assessment of elemental content of milled coal, combustion residues, and stack emitted materials: Possible environmental effects for a Canadian pulverized coal-fired power plant, *International Journal of Coal Geology* 65, 17– 25

Gurdeep, S., 2005: Environmental Assessment of Fly Ash from some Thermal Power Stations for Reclamation of Mined Out Areas; *Fly Ash Utilization Programme* (FAUP), TIFAC, DST, New Delhi

Griepink, B.; Coline, E.; Guzzi, G.; Haemers, L. and Muntau, H. 1983: Certification of Trace Element Contents (As, Cd, Co, Cu, Fe, Mn, Hg, Na, Pb and Zn) in a Fly Ash Obtained from the Combustion of Pulverised Coal, *Fresenius Z Anal Chem*, 315:20-25

Gschneidner Jr, K. 2011: The rare earth crisis—the supply/demand situation for 2010–2015. *Material Matters*, 6(2).

## Reference

---

Guimaraes, J.; Ikingura J.; Akagi H., 2000: Methyl mercury production and distribution in river water-sediment systems investigated through radiochemical techniques, *Water Air Soil Pollut* 124(1–2):113–124.

Günther, D. 2002: Laser Ablation-Inductively Coupled Plasma Mass Spectrometry Trends *Journal of Analytical and Bioanalytical Chemistry*, 372/1, 31-32

Habashi, F., 1995: Bayer's process for alumina production--a historical perspective. *Cahiers d'Histoire de l'Aluminium*, 13.

Hannaker, P.; Haukka, M. and Sen, S., 1984: Comparative study of ICP-AES and XRF analysis of major and minor constituents on geological materials, *Chem Geol.*, 42:319-324.

Hansen Y.; Notten P.; Petrie G., 2002: A life cycle impact assessment indicator for ash management in coal-based power generation, *The Journal of the South African Institute of Mining and Metallurgy*, p. 299 -306.

Harwell, S., 1999: Overview of Current Leaching Approaches, Proceedings of the Environmental Protection Agency public meeting on waste leaching Session III - *Leaching Science* [www.epa.gov/osw/hazard/testmethods/pdfs/current.pdf](http://www.epa.gov/osw/hazard/testmethods/pdfs/current.pdf)

Haynes, R. J., 2009: Reclamation and revegetation of fly ash disposal sites – Challenges and research needs, *Journal of Environmental Management*, 90, 43-53.

Hibstie, A.; Chaubey, A.; Hailu, A. and Mamo, D., 2013: Thermal Neutron Activation Analysis Technique of Rock Samples from Choke Mountain Range, East Gojjam, Ethiopia. *Scope of Journal*, 694.



## Reference

---

Hind, A.; Bhargava, S.; and Grocott, S., 1999: The surface chemistry of Bayer process solids: a review. *Colloids and surfaces A: Physicochemical and engineering aspects*, 146(1), 359-374.

Holloway, P. and Vaidyanathan, P., 2010: *Characterization of Metals and Alloys*, Momentum Press, New York

Hou, X. and Jones, B., 2000: Inductively Coupled Plasma/Optical Emission Spectrometry. In: *Encyclopedia of Analytical Chemistry*. Meyers RA editor. Chichester: John Wiley & Sons Ltd; 9468-9485.

Howard, D.; Grobler, C.; Robinson, R. and Cole P., 2009: Sustainable Purification of Mine Water Using Ion Exchange Technology, *Abstracts of the International Mine Water Conference 19th – 23rd October 2009*, Pretoria, South Africa Proceedings ISBN Number: 978-0-9802623-5-3

Hsiang, J. and Díaz, E. 2011: Lead and developmental neurotoxicity of the central nervous system, *Current Neurobiology*, 2 (1): 35-42

Hsu, C., 1997: Infrared spectroscopy. *Handbook of instrumental techniques for analytical chemistry*, 249.

Huffman, G. and Huggins, F., 1986: Reactions and Transformations of Coal Mineral Matter at Elevated Temperatures. *ACS Symposium Series*, Vol. 301, 100–113

Hulett, L.; Weinberger, A.; Northcut, K.; Ferguson, M., 1980: Chemical species in fly ash from coal-burning power plants. *Science 210*: 1356-1358.

Humpries, M., 2013: Rare earth elements: The global supply chain. *BiblioGov*

## Reference

---

Hvistendahl, M. 2007: Coal ash is more radioactive than nuclear waste, *Scientific American*, 12 (13),

Institute Fur Normung, “DIN38414 S4: German standard procedure for water, waste water and sediment testing-group S (sludge and sediment); *Determination of leachability(S4)*” Berlin, Germany, 1984.

Iwashita, A.; Nakajima, T.; Takanashi H.; Akira Ohki A.; Yoshio Fujita Y.; Yamashita T., 2005: Effect of pretreatment conditions on the determination of major and trace elements in coal fly ash using ICP-AES, *Fuel*, 85:257-263. DOI:10.1016/j.fuel.2005.04.034.

Iwashita, A.; Sakaguchi, Y.; Nakajima, T.; Takanashi, H.; Ohki, A.; Kambara, S., 2005: Leaching characteristics of boron and selenium for various coal fly ashes, *Fuel* 84, 479-485.

Iyer, R., 2002: The surface chemistry of leaching coal fly ash, *Journal of Hazardous Materials B93*, 321-329.

Iyer, R. and Scott, J., 2001: Power station fly ash—a review of value-added utilization outside of the construction industry. *Resources, conservation and recycling*, 31(3), 217-228.

Izquierdo, M.; Querol, X.; Davidovits, J.; Antenucci, D.; Nugteren, H.; and Fernández-Pereira, C., 2009: Coal fly ash-slag-based geopolymers: microstructure and metal leaching. *Journal of hazardous materials*, 166(1), 561-566.

Jackson B.; Miller W., 1998: Arsenic and selenium speciation in coal fly ash extracts by ion chromatography-inductively coupled plasma mass spectrometry. *J Analyt Atomic Spectrometry*. 13:1107-1112. DOI: 10.1039/A806159I

## Reference

---

Jala, S. and Goyal, D., 2006: Fly ash as a soil ameliorant for improving crop production—a review. *Bioresource Technology*, 97(9), 1136-1147.

Janković, M.; Todorović, D.; Nikolić, J., 2011: Analysis of natural radionuclides in coal, slag and ash in coal-fired power plants in Serbia, *Journal of Mining and Metallurgy, Sect. B-Metall.* 47, 2 B, 149 - 155

Jankowski, J.; Ward, C.; French, D.; Groves, S., 2006: Mobility of trace elements from selected Australian fly ashes and its potential impact on aquatic ecosystems, *Fuel* 85, 243-256

Jaturapitakkul, C.; Kiattikomol, K.; Sata, V.; Leekeeratikul, T., 2004: Use of ground coarse fly ash as a replacement of condensed silica fume in producing high-strength concrete, *Cement and Concrete Research* 34, 549–555.

Järup, L., 2003: Hazards of heavy metal contamination, *British Medical Bulletin*, Vol. 68 167–182

Jegadeesan G.; Al-Abed S.; Patricio, P., 2008: Influence of trace metal distribution on its leachability from coal fly ash, *Fuel* 87, 1887–1893.

Johnson, C.; Brandenberger, S.; Baccini, P.; 1995: Acid neutralization capacity of municipal waste incinerator bottom ash. *Environmental Science Technology* 29, 142-147.

Jones, D. R., 1995: The Leaching of Major and Trace Elements from Coal Ash. In Swaine D.J., & Goodarzi, F, (Eds.), *Environmental aspects of trace elements in coal* (p. 221). Netherland: Kluwer.

Johnson, D. and Hallberg, B., 2005: Acid mine drainage remediation options: a review, *Science of the Total Environment*, 338, 3– 14

## Reference

---

Kastori, R.; Maksimović, I.; Zeremski-Škorić, T. and Putnik-Delić, M., 2010: Rare earth elements: Yttrium and higher plants, *Zbornik Matice srpske za prirodne nauke*, (118), 87-98.

Khale, D.; Chaudhary, R., 2007: Mechanism of Geopolymerization and Factors Influencing Its Development: A Review, *J Mater Sci* 42, pp.729-746, 2007.

Khanra, S., Mallick, D., Dutta, S., and Chaudhuri, S., 1998: Studies on the phase mineralogy and leaching characteristics of coal fly ash. *Water, Air, and Soil Pollution*, 107(1-4), 251-275.

Kim, A.; Kazonich, G. and Dahlberg, M., 2003: Relative solubility of cations in class F fly ash, *Environmental science & technology*, 37(19), 4507-4511

Kim, A. G. 2005: Leaching Methods Applied to the Characterization of Coal Utilization By-Products. ORISE Research Fellow, *National Energy Technology Laboratory*, US Department of Energy, Pittsburgh, Pennsylvania

Kim, A. and Hesbach, P., 2009: Comparison of fly ash leaching methods, *Fuel* 88, 926–937.

Kishor, P.; Ghosh, A. and Kumar, D., 2010: Use of fly ash in agriculture: A way to improve soil fertility and its productivity. *Asian J. Agric. Res.*, 4: 1-14.

Kola, H. and Perämäki, P. 2004: “The Study of the Selection of Emission Lines and Plasma Operating Conditions for Efficient Internal Standardization in Inductively Coupled Plasma Optical Emission Spectrometry”, *Spectrochimica Acta B*. No. 59, pp. 231-242

Koukouzas N.; Ward C.; Papanikolaou D.; Li, Z. and Ketikidis C., 2009: Quantitative evaluation of minerals in fly ashes of biomass, coal and biomass-coal

## Reference

---

mixture derived from circulating fluidised bed combustion technology, *Journal of Hazardous Materials* 169, 100- 107.

Krishnan, K. and Anirudhan, T. 2003: Removal Of Cadmium (II) from Aqueous Solutions by Steam Activated Sulphurised Carbon Prepared from Sugar-Cane Bagasse Pith: Kinetics and Equilibrium Studies, *Water SA* Vol. 29 No. 2 pp. 147-156

Kruger, R. A., 1997: Fly ash beneficiation in South Africa: creating new opportunities in the market-place, *Fuel* Vol. 76, No. 8, pp. 777-779

Kukier, U.; Ishak, C.; Sumner, M. and Miller, W..2003:. Composition and element solubility of magnetic and non-magnetic fly ash fractions. *Environmental Pollution*, 123(2), 255-266.

Kumar, S. and Kumar, R., 2011: Mechanical activation of fly ash: Effect on reaction, structure and properties of resulting geopolymer. *Ceramics International*, 37(2), 533-541.

Kutchko, B. and Kim, A., 2006: Fly ash characterization by SEM–EDS, *Fuel* 85, 2537–2544.

Lehn, S.; Warner, K.; Huang, M. and Hieftje, G., 2003: Effect of sample matrix on the fundamental properties of the inductively coupled plasma. *Spectrochimica Acta Part B: Atomic Spectroscopy*, 58(10), 1785-1806.

Lee, S. and Spears, D., 1977: Natural Weathering of Pulverized Fuel Ash and Porewater Evolution, *Applied Geochemistry*, Vol. 12, pp. 367-376,

Levandowski, J. and Kalkreut, W., 2009; Chemical and petrographical characterization of feed coal, fly ash and bottom ash from the Figueira Power Plant, Paraná, Brazil, *International Journal of Coal Geology* 77, 269–281

## Reference

---

Lidsky, T. and Schneider, J. 2003: Lead neurotoxicity in children: basic mechanisms and clinical correlates, *Brain*, 126, 5-19

Lloyd, N. and Rangan, B., 2010: Geopolymer Concrete: A Review of Development and Opportunities. In *35th Conference on Our World in Concrete & Structures*. <http://cipremier.com/100035037>

MacKenzie, A., 2000: Environmental radioactivity: experience from the 20th century—trends and issues for the 21st century, *Science of the Total Environment*, 249(1), 313-329.

Madzivire, G.; Maleka, P.; Vadapalli, V.; Gitari, W.; Lindsay, R. and Petrik, L., 2013: Fate of the naturally occurring radioactive materials during treatment of acid mine drainage with coal fly ash and aluminium hydroxide, *Journal of environmental management*, 133, 12-17.

Madzivire, G., 2012: Chemistry and speciation of potentially toxic and radioactive elements during mine water treatment. Unpublished PhD thesis, University of the Western Cape, Cape Town, South Africa

Madzivire, G.; Petrik, L.; Gitari, W.; Ojumu, T. and Balfour, G., 2010: Application of coal fly ash to circumneutral mine waters for the removal of sulphates as gypsum and ettringite, *Mineral Engineering*, 23, pp. 252-257.

Mahlaba, S.; Kearsley, P. and Kruger, R., 2011: Physical, chemical and mineralogical characterisation of hydraulically disposed fine coal ash from SASOL Synfuels. *Fuel* (2011), doi:10.1016/j.fuel.2011.03.022

## Reference

---

Makreski, P. ; Jovanovski, G. ; Runčevski, T. and Jaćimović, R., 2011: Simple and efficient method for detection of traces of rare earth elements in minerals by raman spectroscopy instrumentation. *Macedonian Journal of Chemistry and Chemical Engineering*, 30(2), 241-250.

Manz, O. E., 1997: Worldwide production of coal ash and utilization in concrete and other products, *Fuel* Vol. 76, No. 8, pp. 691-696.

Martinez-Tarazona, M. and Spears, D., 1996: The fate of trace elements and bulk minerals in pulverized coal combustion in a power station, *Fuel Processing Technology* 47, 79-92

Massari, S. and Ruberti, M., 2013: Rare earth elements as critical raw materials: Focus on international markets and future strategies, *Resources Policy*, 38, 36–43

Matjie, R.; Bunt, J. and Van Heerden, J., 2005: Extraction of alumina from coal fly ash generated from a selected low rank bituminous South African coal. *Minerals Engineering*, 18(3), 299-310.

Mattigod, S.; Dhanpat R.; Eary, L.; Ainsworth, C., 1990: Geochemical Factors Controlling the Mobilization of Inorganic Constituents from Fossil Fuel Combustion Residues: I. Review of the Major Elements, *J. Environ. Qual.* Volume & Issue 19 (2) 188-201.

McCarthy, T., 2011: The impact of acid mine drainage in South Africa. *South African Journal of Science*, 107(5-6), 01-07.

McCarthy G., 1987: X-ray powder diffraction for studying the mineralogy of fly ash. *MRS Proceedings*, 113:75-86. DOI: 10.1557/PROC-113-75.

## Reference

---

- McNally, D.; Crowley-Parmentier, J.; Whitman, B., 2012: Trace metal leaching and bioavailability of coal-generated fly ash, *Int Res J Environment Sci.*, 1(5):76-80.
- Mehra, R., 2009: Use of gamma ray spectroscopy measurements for assessment of the average effective dose from the analysis of  $^{226}\text{Ra}$ ,  $^{232}\text{Th}$ , and  $^{40}\text{K}$  in soil samples. *Indoor and Built Environment*, 18(3), 270-275.
- Mehra, A.; Farago, M. and Banerjee, D., 1998: Impact of Fly Ash from Coal fired Power Stations in Delhi, with Particular Reference to Metal Contamination, *Environmental Monitoring and Assessment* 50: 15–35
- Mester, Z.; Angelone, M.; Brunori, C.; Cremisini, C.; Muntau, H.; Morabito, R., 1999: Digestion methods for analysis of fly ash samples by atomic absorption spectrometry, *Anal. Chim. Acta* 395:157-163.
- Meynen, V.; Cool, P. and Vansant, E., 2009: Verified Syntheses of Mesoporous Materials, *Microporous and Mesoporous Materials* 125, 170–223
- Mickley, M.; Hamilton, R.; Gallegos, L. and Truesdall, J., 1993: Membrane Concentrate Disposal, *AWWA Research Foundation and American Water Works Association*, USA, 1993, 242
- Misra, N., 2011: Total reflection X-ray fluorescence and energy-dispersive X-ray fluorescence characterizations of nuclear materials. *Pramana journal physics*, Vol. 76, No. 2, pp. 201–212
- Mljač, L. and Križman, M., 1996: Radioactive contamination of surface waters from a fly-ash depository at Velenje (Slovenia), *Environment International*, 22, 339-345



## Reference

---

Molcan, P.; Lu, G.; Bris, T.; Yan, Y.; Taupin, B. and Caillat, S., 2009: Characterisation of biomass and coal co-firing on a 3MWth combustion test facility using flame imaging and gas/ash sampling techniques. *Fuel*, 88(12), 2328-2334.

Mohan, S. and Gandhimathi, R., 2009: Removal of heavy metal ions from municipal solid waste leachate using coal fly ash as an adsorbent. *Journal of Hazardous Materials*, 169(1), 351-359

Mohapatra, R., and Rao, J., 2001 Some aspects of characterisation, utilisation and environmental effects of fly ash. *Journal of Chemical Technology & Biotechnology*, 76(1), 9-26.

Moldoveanu, G.; Papangelakis, V., Recovery of rare earth elements elements from a low grade ore, *Minerals Engineering*, Vol. 39, 2012

Moreno, N.; Querol, X.; Andre´s, J.; Stanton, K.; Towler, M.; Nugteren, H.; Janssen-Jurkovicova´d, M.; Jones, R., 2005: Physico-chemical characteristics of European pulverized coal combustion fly ashes, *Fuel* 84, 1351-1363

Morin, K.A. and Hutt, N.M., 1997: Environmental Geochemistry of Minesite Drainage: Practical, *Theory and Case Studies*. Vancouver, Canada: MDAG

Murayama, N.; Yamamoto, H. and Shibata, J., 2002: Mechanism of zeolite synthesis from fly ash by alkali hydrothermal reaction, *International Journal Mineral Processing*, Vol. 64, pp. 1–17.

Muhammad, M.; Idris, I.; Simon P. and Arabi S., 2010: “Distribution of Gamma-Emitting Radionuclides in Soil around the Center for Energy Research and Training (CERT) Ahmadu Bello University, Zaria, Zaria-Nigeria,” *Journal of American Science*, Vol. 6, No. 12, pp. 995-1001.

## Reference

---

Muriithi, G., 2012: Re-use of South African fly ash for CO<sub>2</sub> capture and brine remediation *Unpublished PhD. thesis*, University of the Western Cape, Cape Town, South Africa.

Musyoka, N., 2013: Zeolite A, X and Cancrinite from South African coal fly ash: mechanism of crystallization, routes to rapid synthesis and new morphology. Unpublished PhD thesis, University of the Western Cape, Cape Town, South Africa

Nasab, M.; Sam, A. and Milani, S., 2011: Determination of optimum process conditions for the separation of thorium and rare earth elements by solvent extraction, *Hydrometallurgy*, 106(3), 141-147.

Nathan, Y.; Dvorachek, M.; Pelly, I.; Mimran, U., 1999: Characterization of coal fly ash from Israel, *Fuel* 78 (1999) 205–213

National Institute of Standards and Technology (NIST). *Certificate of Analysis, Standard Reference Material*, 1633. 2008.

Neupane, G., and Donahoe, R., 2013: Leachability of elements in alkaline and acidic coal fly ash samples during batch and column leaching tests. *Fuel*, 104, 758-770.

Nisnevich, M.; Sirotnin, G.; Schlesinger, T.; Eshel, Y., 2008: Radiological safety aspects of utilizing coal ashes for production of lightweight concrete, *Fuel* 87, 1610–1616

Olesik, J. 1991 Elemental Analysis Using ICP-OES and ICP/MS. *Analytical Chemistry*, 63(1), 12A-21A.

Orvini, E. and Speziali. M., 1998: Applicability and limits of instrumental neutron activation analysis: State of the art in the year 2000. *Microchem. J.* 59: 160–172.

## Reference

---

Palomo, A.; Grutzeck, M. and Blanco M., 1999: Alkali-activated fly ashes, a cement for the future, *Cem. Concr. Res.*, 29, 1323– 1329

Pandey, V.; Singh, J.; Singh, R.; Singh, N.; Yunus, M., 2011: Arsenic hazards in coal fly ash and its fate in Indian scenario, Resources, *Conservation and Recycling* 55, p 819–835

Papastefanou, C. 2008: Radioactivity of coals and fly ashes *Journal of Radioanalytical and Nuclear Chemistry*, 275(1), 29-35.

Patel, D. 2011: Matrix Effect in a View of LC-MS/MS: An overview. *International Journal of Pharma and Bio Sciences*, Vol2, Issue1, 559-564.

Patnaik, P., (2003). Handbook of Inorganic Chemical Compounds. *McGraw-Hill*. p. 199-200.

Pérez-López, R.; Nieto, J.; Almodóvar, G., 2007a: Utilization of fly ash to improve the quality of the acid mine drainage generated by oxidation of a sulphide-rich mining waste: Column experiments. *Chemosphere*, 67 (8), 1637-1646.

Pérez-López, R.; Cama, J.; Nieto, J.; Ayora, C., 2007b: The iron-coating role on the oxidation kinetics of a pyritic sludge doped with fly ash. *Geochim. Cosmochim. Acta.*, 71 (7), 1921-1934 (14 pages).

Pérez-López, R.; Álvarez-Valero, A.; Nieto, J.; Almodóvar, G, 2007c: Mineralogy of the hardpan formation processes in the interface between sulphiderich sludge and fly ash: Applications for acid mine drainage mitigation. *Am. Mineralog.*, 92 (11-12), 1966-1977 (12 pages).

## Reference

---

Pickles, C.; McLean, A.; Alcock, C. and Nikolic, R.,1990: Plasma recovery of metal values from flyash. *Canadian Metallurgical Quarterly*, 29(3), 193-200.

Petrik L.; White R.; Klink M.; Somerset V.; Burgers C.; Frey M., 2003: Utilisation of South African fly ash to treat acid mine drainage, and production of high quality zeolites from the residual solids. In: *Proceedings of the International Ash Utilisation Symposium*, University of Kentucky, USA, Paper no. 61. <http://www.flyash.info>.

Popovic, A.; Djordjevic,D.; Polic, P, 2001: Trace and major element pollution originating from coal ash suspension and transport processes, *Environment International* 26, 251-255.

Potgieter-Vermaak, S., Potgieter, J.; Kruger, R.; .Spolink, Z.; Van Grieken, R., 2005: A characterisation of the surface properties of ultra fine fly ash (UFFA) used in the polymer industry, *Fuel* 84, 2295-2300.

Praharaj, T.; Powell, M.; Hart, B.; Tripathy, S., 2001: Leachability of elements from sub-bituminous coal fly ash from India, *Environment International* 27, 609–615.

Prakash, S.; Mohanty, J.; Das, B., and Venugopal, R., 2001: Characterisation and removal of iron from fly ash of talcher area, Orissa, India. *Minerals engineering*, 14(1), 123-126.

Querol, X.; Alastuey, A.; Lopez-Soler, A.; Mantillai, E and Plana, F., 1996: Mineral Composition of Atmospheric Particulates Around a Large Coal-Fired Power Station, *Atmospheric Environment* Vol 30, No. 21, pp. 3557-3572,

Querol, X.; Juan, R.; Lopez-Soler, A.; Fernandez-Turiel, J. and Ruiz, C., 1996: Mobility of trace elements from coal and combustion wastes, *Fuel* Vol. 75, No. 7, 821 838.

## Reference

---

Querol, X.; Fernhdez-Turiel, J. and López-Soler, A., 1995: Trace elements in coal and their behaviour during combustion in a large power station, *Fuel* Vol 74 No. 3, pp. 331-343.

Rademaker, J.; Kleijn, R. and Yang, Y., 2013: Recycling as a strategy against Rare Earth Element Criticality: A systemic evaluation of the potential yield of NdFeB magnet recycling, *Environmental science & technology*, 47(18), 10129-10136.

Ramesh, A. and Kozinski, J., 2001: Investigations of ash topography/morphology and their relationship with heavy metals leachability, *Environmental Pollution*, vol. 111, no. 2, pp. 255-262.

Rice, C.; Breit, G.; Fishman, N.; Bullock, J., 1999: Leachability of trace elements in coal and coal combustion wastes. Proceedings of 24th International Technical Conference on Coal Utilization and Fuel Systems, Clearwater, Florida, March 8–11, 1999. *Coal Slurry Technology Assn*, Washington, DC, pp. 355–366.

Richardson, D.; Shore, M.; Hartee, R. and Richardson, R.; 1995: The use of X-ray fluorescence spectrometry for the analysis of plants, especially lichens, employed in biological monitoring. *The Science of the Total Environment*, 176, 97–105.

Rose, P. 2013: Long-term sustainability in the management of acid mine drainage wastewaters-development of the Rhodes BioSURE Process. *Water SA*, 39(5), 583-592.

Rowbotham, A.; Levy, L.; Shuker, L. 2000: Chromium in the environment: an evaluation of exposure of the uk general population and possible adverse health effects, *Journal of Toxicology and Environmental Health, Part B*, 3:145-178

## Reference

---

Saikia, N.; Kato, S.; Kojima, T., 2006: Composition and leaching behaviour of combustion residues. *Fuel* 85, 264-271.

Satpute Manesh, B.; Wakchaure Madhukar, R. and Patankar Subhash, V., 2012: Effect of Duration and Temperature of Curing on Compressive Strength of Geopolymer Concrete.

Scrivenera, K.; Füllmann, T.; Galluccia, E.; Walentab, G.; Bermejo, E., 2004: Quantitative Study of Portland Cement Hydration by X-ray Diffraction/Rietveld Analysis and Independent Methods, *Cement and Concrete Research* 34, 1541–1547

Scott, J.; Guang, D.; Naeramitmarnsuk, K.; Thabuot, M. and Amal, R., 2002: Zeolite synthesis from coal fly ash for the removal of lead ions from aqueous solution, *Journal of Chemical Technology and Biotechnology*, 77(1), 63-69.

Seames, W., 2003: An initial study of the fine fragmentation fly ash particle mode generated during pulverized coal combustion, *Fuel Processing Technology* 81 109– 125

Senneca, O, 2008: Burning and Physico-Chemical Characteristics of Carbon in Ash from a Coal Fired Power Plant, *Fuel* 87, 1207–1216.

Senapati M., 2011: Fly ash from thermal power plants - waste management and overview. *Current Science*. 100 (12):1791-1974.

Shin, B.; Lee, S.; and Kook, N., 1995: Preparation of zeolitic adsorbents from waste coal fly ash, *Korean Journal of Chemical Engineering*, 12(3), 352-357.

Shoval, S., 2003: Using FTIR spectroscopy for study of calcareous ancient ceramics, *Optical Materials* 24 117–122.

## Reference

---

- Singh, N.; Kumar, D. and Sahu, A. 2007: Arsenic in the environment : Effects on human health and possible prevention, *Journal of Environmental Biology*, 28(2) 359-365
- Singh, D. and Kolay, P., 2002: Simulation of ash water interaction and its influence on ash characteristics, *Progress in Energy and Combustion Science*, 28, 267-299.
- Smith, A.; Hopenhayn-Rich, C.; Bates, M.; Goeden, H.; Hertz-Picciotto, I.; Duggan, H.; Wood, R.; Kosnett, M.; Smith, M., 1992: Cancer risks from arsenic in drinking water. *Environ. Health Perspect.* 97, 259–267
- Smolka-Danielowska, D. 2006: Heavy Metals in Fly Ash from a Coal-Fired Power Station in Poland, *Polish J. of Environ. Stud.* Vol. 15, No. 6, 943-946
- Sočo, E. and Kalembkiewicz, J., 2009: Investigations on Cr mobility from coal fly ash, *Fuel* 88, 1513–1519.
- Somerset, V.; Petrik, L.; White, R.; Klink, M.; Key.; D, Iwuoha, E., 2005: Alkaline hydrothermal zeolites synthesized from high SiO<sub>2</sub> and Al<sub>2</sub>O<sub>3</sub> co-disposal fly ash filtrates, *Fuel* 84, 2324–2329.
- Sorini, S. and Jackson, L. 1988: Evaluation of Toxicity Characteristic Leaching Procedure (TCLP) on Utility Waste. *Nuclear and Chemical Waste Management* 8: 217-223.
- Spears D. 2004: The use of laser ablation inductively coupled plasma-mass spectrometry (LA ICP-MS) for the analysis of fly ash. *Fuel*. 83(13):1765-1770.
- Srinivasan, K., and Sivakumar, A., 2013: Geopolymer Binders: A Need for Future Concrete Construction. *International Scholarly Research Notices*, 2013.

## Reference

---

- Sushil, S. and Batra, S., 2006: Analysis of fly ash heavy metal content and disposal in three thermal power plants in India. *Fuel* 85:2676-2679. DOI: 10.1016/j.fuel.2006.04.031
- Stas, J.; Ajaj D. and Omar A., 2007: Recovery of vanadium, nickel and molybdenum from fly ash of heavy oil-fired electrical power station. *Chemical Engineering* 51.2: 67-70.
- STUK (Radiation and Nuclear Safety Authority) (2003): The radioactivity of building materials and ash. Regulatory Guides on Radiation Safety (ST Guides) ST 12.2 (Finland)
- Sturza, C.; Boscencu, R. and Nacea, V., 2008: The lanthanides: physico-chemical properties relevant for their biomedical applications. *FARMACIA-BUCURESTI*, 56(3), 326.
- Styszko-Grochowiaka, K.; Gołaś, J.; Jankowski, H. and Kozinski, S., 2004: Characterization of the Coal Fly Ash for the Purpose of Improvement of Industrial On-line Measurement of Unburned Carbon Content, *Fuel* 83, 1847–1853
- Su, S.; Yang, J.; Ma, H.; Jiang, F.; Liu, Y. and Li, G., 2011., Preparation of ultrafine aluminum hydroxide from coal fly ash by alkali dissolution process, *Integrated Ferroelectrics*, 128(1), 155-162.
- Sukandar S.; Yasuda K.; Tanaka, M.; Aoyama, I. 2006: Metals leachability from medical waste incinerator fly ash: A case study on particle size comparison, *Environmental Pollution* 144, 726 – 735
- Swanepoel, J. and Strydom, C. 2002: Utilisation of fly ash in a geopolymeric material. *Applied Geochemistry*, 17(8), 1143-1148.



## Reference

---

Tadmor, J. 1986: Radioactivity from Coal-Fired Power Plants: A Review, *J. Environ. Radioactivity* 4, 177-204

Takeda, H.; Hashimoto, S.; Honda, S. and Iwamoto, Y., 2010: In-situ formation of novel geopolymer-zeolite hybrid bulk materials from coal fly ash powder. *Journal of the Ceramic Society of Japan*, 118(1380), 771-774.

Taylor, J.; Pape, S. and Murphy, N. 2005: A Summary of Passive and Active Treatment Technologies for Acid and Metalliferous Drainage (AMD). *In Proceeding of the Fifth Australian Workshop on Acid Drainage* (Eds LC Bell and RW McLean) pp (pp. 151-191).

Thomas, J. and Gai, P., 2004: Electron Microscopy and the Materials Chemistry of Solid Catalysts, *Advances in Catalysis*, Vol. 48 pp.171-227

Todoli, J. and Mermet, J., 1999: "Acid Interferences in Atomic Spectrometry,: Analyte Signal Effects and Subsequent Reduction", *Spectrochimica Acta B*. No. 54, pp. 895-929

Todoli, J.; Gras, L.; Hernandis, V.; Mora, J., 2002: "Elemental Matrix Effects", *Journal of Analytical Atomic Spectrometry*, No.17, pp. 142-169.

Trasande,L.; Landrigan,P. and Schechter, C. 2005; Public Health and Economic Consequences of Methyl Mercury Toxicity to the Developing Brain, *Environmental Health Perspectives*, volume 113 | number 5

Tyler, G. 2004: Rare earth elements in soil and plant systems-A review. *Plant and soil*, 267(1-2), 191-206.

Ugurlu, A. 2004: Leaching characteristics of fly ash. *Environ. Geol.*, 46, 890–895

## Reference

---

United States Geological Survey, October 1997, 1997-last update, Radioactive Elements in Coal and Fly Ash: Abundance, Forms, and Environmental Significance [Homepage of USGS],[Online].Available :<http://pubs.usgs.gov/fs/1997/fs163-97/FS-163-97.pdf> assessed [November, 2013]

UNSCEAR: Sources and Effects of Ionizing Radiation, United Nations Scientific Committee on the Effect of Atomic Radiation, United Nations, New York, 1998

Van der Sloot, H. A.1998: Quick techniques for evaluating the leaching properties of waste materials: their relation to decisions on utilization and disposal. *TrAC Trends in Analytical Chemistry*, 17(5), 298-310.

Ural, S., 2005: Comparison of Fly Ash Properties from Afsin–Elbistan Coal Basin, Turkey, *Journal of Hazardous Materials* B119, 85–92. <http://www.fhwa.dot.gov/>

U.S. Geological Survey, Reston, Virginia: 2012. [minerals.usgs.gov/minerals/pubs/mcs/2012/mcs2012.pdf](http://minerals.usgs.gov/minerals/pubs/mcs/2012/mcs2012.pdf)

U.S. Geological Survey, Reston, Virginia: 2011. [pubs.usgs.gov/of/2011/1189/of2011-1189.pdf](http://pubs.usgs.gov/of/2011/1189/of2011-1189.pdf)

Vassilev, S.; Menendez, R.; Borrego, A.; Diaz-Somoano, M.; and Rosa Martinez-Tarazona, M. 2004: Phase-mineral and chemical composition of coal fly ashes as a basis for their multicomponent utilization. 3. Characterization of magnetic and char concentrates. *Fuel*, 83(11), 1563-1583.

Vassilev, S, and Vassileva, C. 2005: Methods for Characterization of Composition of Fly Ashes from Coal-Fired Power Stations: A Critical Overview, *Energy & Fuel*, 19, 1084-1098

## Reference

---

Vassilev, S. and Vassileva, C., 2005: Methods for Characterization of Composition of Fly Ashes from Coal-Fired Power Stations: A Critical Overview, *Energy & Fuels*, 19, 108

Vassilev, S. and Vassileva, C., 1996: Mineralogy of combustion wastes from coal-fired power stations, *Fuel Processing Technology* 47, 261-280

Vassilev, S. and Vassileva, C., 2007: A new approach for the classification of coal fly ashes based on their origin, composition, properties, and behaviour, *Fuel* 86, 1490–1512.

Vassilev, S. and Vassileva, C., 2006: Behaviour of inorganic matter during heating of Bulgarian coals 2. Subbituminous and bituminous coals, *Fuel Processing Technology* 87, 1095–1116

Vijayan, V.; Behera, S.; Ramamurthy, V.; Puri, S.; Shahi, J., and Singh, N., 1997: Elemental composition of fly ash from a coal-fired thermal power plant: A study using PIXE and EDXRF. *X-Ray Spectrometry*, 26(2), 65-68.

Wang, Y.; Ren, D.; Zhao, F., 1999: Comparative leaching experiments for trace elements in raw coal, laboratory ash, fly ash and bottom ash, *International Journal of Coal Geology* 40, 103–108.

Wang, J.; Wang, T.; Mallhi, H.; Liu, Y.; Ban, H.; Ladwig, K. 2007: The role of ammonia on mercury leaching from coal fly ash, *Chemosphere* 69, 1586–1592

Ward, C.; French, D.; Jankowski, J.; Dubikova, M.; Li, Z.; Riley, K., 2009: Element mobility from fresh and long-stored acidic fly ashes associated with an Australian power station; *International Journal of Coal Geology* 80 224–236

## Reference

---

Welna M; Szymczycha-Madeja A.; Pohl P., 2011 Quality of the trace element analysis: sample preparation steps, [www.intechopen.com](http://www.intechopen.com) Pdf assessed 8<sup>th</sup> February 2013

Weltje, G.; Tjallingii, R., 2008: Calibration of XRF core scanners for quantitative geochemical logging of sediment cores: Theory and application, *Earth and Planetary Science Letters*, 274, 423 - 438.

White, S. and Case, E., 1990: Characterization of fly ash from coal-fired power plants, *J. of Mat. Sci.*, 25, pp. 5215–5219.

Wicks, F.; Corbeil, M.; Back, M. and Ramik, R., 1995: Microbeam X-Ray Diffraction in the Analysis of Minerals and Materials, *The Canadian Mineralogist*, vol. 33, pp.313-322

Windom, B. and Hahn, D., 2009: Laser ablation—laser induced breakdown spectroscopy (LA-LIBS): A means for overcoming matrix effects leading to improved analyte response. *Journal of Analytical Atomic Spectrometry*, 24(12), 1665-1675.

World Energy Council, 2013: *World Energy Resources 2013 Survey*, [www.worldenergy.org](http://www.worldenergy.org)

World Health Organization, 2011: Guidelines for drinking-water quality, third edition, incorporating first and second addenda Volume 1 - Recommendations. Geneva: WHO Press.

Wu, G.; Yang, C.; Guo, L.; Wang, Z. 2013: *Cadmium contamination in Tianjin agricultural soils and sediments: relative importance of atmospheric deposition from coal combustion*, *Environ Geochem Health*, 35:405–416

[http://www.eskom.co.za/AboutElectricity/FactsFigures/Pages/Facts\\_Figures.aspx](http://www.eskom.co.za/AboutElectricity/FactsFigures/Pages/Facts_Figures.aspx)

## Reference

---

<http://www.fhwa.dot.gov/pavement/recycling/fach01.cfm>

<http://www.files.chem.vt.edu/chem-ed/sep/lc/ion-chro.html>

[http://www.deldot.gov/information/pubs\\_forms/manuals/mat\\_research/pdfs/doh\\_2.pdf](http://www.deldot.gov/information/pubs_forms/manuals/mat_research/pdfs/doh_2.pdf)

<http://www.epa.gov/osw/nonhaz/define/pdfs/coal-combust.pdf>

[www.eskom.co.za/live/content.php?category\\_id=121](http://www.eskom.co.za/live/content.php?category_id=121)

[http://www.eskom.co.za/annreport09/ar\\_2009/downloads/eskom\\_ar\\_2009.pdf](http://www.eskom.co.za/annreport09/ar_2009/downloads/eskom_ar_2009.pdf)

[http://www.iea.org/papers/2010/power\\_generation\\_from\\_coal.pdf](http://www.iea.org/papers/2010/power_generation_from_coal.pdf)

<http://www.lycos.com/info/ion.html>

Xenidis, A.; Evangelia, M.; Ioannis P., 2002. Potential use of lignite fly ash for the control of acid generation from sulphidic wastes. *Waste Manage.*, 22 (6), 631-641 (11 pages).

Xinwei, L., 2004: Natural radioactivity in some building materials and by-products of Shaanxi, China, *Journal of radioanalytical and nuclear chemistry*, 262(3), 775-777.

Xu, H. and Van Deventer, J., 2002: Geopolymerisation of aluminosilicates: Relevance to the minerals industry, *AusIMM Bulletin*, no. 1

Xu, M.; Yan,R.; Zheng, C.; Qiao, Y.; Han, J.; Sheng, C. 2003: Status of trace element emission in a coal combustion process: a review, *Fuel Processing Technology* 85, 215– 237

## Reference

---

Yan, J., 1998: Major leaching processes of combustion residues: characterisation, modelling and experimental investigation *Ph.D. thesis*, Division of Chemical Engineering, Royal Institute of Technology, Stockholm, Sweden

Yan, J. and Neretnieks, I., 1995: Is the glass phase dissolution rate always a limiting factor in the leaching processes of combustion residues?, *The Science of the Total Environment* 172, 95-118

Yao, Z.; Xia, M.; Sarker, P.; and Chen, T. 2014: A review of the alumina recovery from coal fly ash, with a focus in China, *Fuel*, 120, 74-85.

Zandi, M. and Russell, N., 2007: Design of a leaching test framework for coal fly ash accounting for environmental conditions, *Environ Monit Assess.*, 131:509–526

Zhang, Y.; Jiang, Z.; He, M.; Hu, B., 2007: Determination of trace rare earth elements in coal fly ash and atmospheric particulates by electrothermal vaporization inductively coupled plasma mass spectrometry with slurry sampling, *Environmental Pollution* 148, 459-467

## Appendix

Concentrations of major and trace elements in Matla fly ash determined by XRF  
[number of determinations = 3]

	Sample 1	Sample 2	Sample 3	Mean
<b>Majors (wt %)</b>				
SiO <sub>2</sub>	48.30	48.22	48.30	48.27
Al <sub>2</sub> O <sub>3</sub>	30.67	30.91	31.11	30.89
Fe <sub>2</sub> O <sub>3</sub>	2.79	2.84	2.81	2.81
MnO	0.02	0.02	0.02	0.02
MgO	2.17	2.12	2.09	2.12
CaO	6.79	6.73	6.62	6.71
Na <sub>2</sub> O	0.56	0.55	0.54	0.55
K <sub>2</sub> O	0.85	0.84	0.83	0.84
TiO <sub>2</sub>	1.27	1.26	1.24	1.26
P <sub>2</sub> O <sub>5</sub>	0.90	0.88	0.88	0.89
SO <sub>3</sub>	0.20	0.19	0.19	0.19
LOI	5.24	5.24	5.24	5.24
Sum	99.75	99.81	99.88	99.81
<b>Traces (mg/kg)</b>				
Ba	2064.53	2086.81	2086.60	2079.31
Ce	247.86	197.26	232.94	226.02
Co	23.79	10.53	13.92	16.08
Cr	91.90	87.45	88.72	89.36
Cu	115.60	115.04	121.15	117.26
Mo	2.28	2.26	2.30	2.28
Nb	52.70	49.43	52.37	51.50
Ni	82.12	89.98	94.82	88.97
Pb	104.52	96.53	99.72	100.25
Rb	72.84	73.13	71.46	72.48
Sr	3496.27	3500.79	3489.60	3495.55
Th	50.33	43.94	45.54	46.60
U	64.54	60.48	64.82	63.28
V	64.20	59.05	71.47	64.91
Y	102.42	103.42	105.30	103.71
Zn	68.65	65.28	59.90	64.61
Zr	784.75	791.35	787.10	787.73

## Appendix

Concentrations of trace elements and REE in Matla CFA determined by LA ICP-MS [number of determinations = 3]

Elements (mg/kg)	Sample 1	Sample 2	Sample 3	Mean
V	155.11	157.33	150.49	154.31
Cr	185.77	181.89	181.36	183.01
Co	16.77	17.37	17.75	17.30
Ni	47.47	50.75	50.41	49.54
Cu	61.37	61.21	62.95	61.84
Zn	45.12	47.98	42.64	45.25
Rb	53.61	54.87	57.89	55.46
Sr	2163.50	2202.20	2045.37	2137.02
Zr	320.90	329.08	291.85	313.94
Nb	43.43	44.02	41.45	42.97
Mo	10.07	10.68	10.60	10.45
Cs	13.51	13.69	13.72	13.64
Ba	2370.00	2405.12	2341.20	2372.11
Sc	25.31	26.19	23.33	24.94
Y	53.45	55.04	48.40	52.30
La	82.84	85.26	76.89	81.66
Ce	189.93	193.83	185.58	189.78
Pr	18.35	18.95	17.76	18.35
Nd	63.93	65.02	61.54	63.50
Sm	12.11	12.37	11.30	11.93
Eu	2.39	2.46	2.20	2.35
Gd	10.68	11.05	9.48	10.40
Tb	1.69	1.65	1.46	1.60
Dy	9.45	10.08	8.97	9.50
Ho	1.99	2.15	1.77	1.97
Er	5.47	5.61	5.07	5.38
Tm	0.82	0.78	0.70	0.77



## Appendix

Concentrations of Major elements, trace elements and REE in Matla CFA  
determined by ENAA [number of determinations = 3]

Elements (mg/kg)	Sample 1	Sample 2	Sample 3	Mean
Na	2640	2510	2460	2537
Mg	37900	38800	38000	38233
Al	127000	129000	130000	128667
Si	10100	184000	168000	120700
S	1040	1270	1950	1420
Cl	78.60	67.00	72.00	72.53
K	7010	6120	6790	6640
Ca	34600	31700	33000	33100
Sc	34.70	33.50	33.20	33.80
Ti	9730	9610	8810	9383
V	114	126	120	120
Cr	163	170	199	177
Mn	279	298	292	290
Fe	29300	29700	28700	29233
Ni	75.70	70.40	70.70	72.27
Co	26.00	25.90	25.80	25.90
Zn	409	227	115	250
As	27.10	21.40	17.40	21.97
Se	2.06	0.78	1.47	1.44
Br	0.57	0.60	0.50	0.55
Rb	46	47	47	46.67
Sr	1940	1880	1880	1900
Ag	1.43	1.00	0.71	1.04
Cd	3.15	7.61	5.93	5.56
In	0.43	0.25	0.47	0.39
Sb	3.65	2.21	1.66	2.51
Cs	10.60	10.40	10.50	10.50
Ba	1890	1820	1760	1823
La	82	126	69	92.23
Ce	255	244	243	247
Nd	89	93	83	88.40
Sm	18.00	18.00	18.00	18.00
Eu	3.01	3.07	3.25	3.11
Gd	27.60	28.00	27.10	27.57
Tb	2.18	2.47	2.12	2.26
Dy	36.40	33.20	36.10	35.23
Tm	1.48	2.73	1.47	1.89
Yb	5.43	8.34	9.16	7.64
Lu	1.84	1.06	0.89	1.26
Hf	14.40	14.50	14.70	14.53
Ta	3.48	3.47	3.44	3.46
W	9.04	9.18	8.80	9.01
Au	0.012	0.009	0.004	0.01
Th	49.80	50.50	49.70	50.00
U	12.00	12.00	12.00	12.00

## Appendix

Concentrations of Major elements, trace elements and REE in Matla CFA  
determined by ICP-OES [number of determinations = 3]

Elements (mg/kg)	Sample 1	Sample 2	Sample 3	Mean
Si	176761	176759.019	176761.96	176761
Al	62041	620340	62041	62040
Fe	9201.664	9201.516	9201.738	9202
Ca	17211.77	17211.672	17211.816	17212
Mg	896.213	896.167	896.236	896
Na	21033.37	21031.652	21034.226	21033
K	116.4036	116.3876	116.4116	116
P	2539.105	2539.055	2539.13	2539
Ti	9558.226	9558.094	9558.292	9558
Mn	132.414	132.41	132.416	132
Cr	76.099	76.081	76.108	76.10
Ni	169.644	169.596	169.668	169.64
Co	2.365	2.363	2.366	2.36
Zn	26.562	26.558	26.564	26.56
As	64.231	64.209	64.242	64.23
Nb	519.791	519.709	519.832	520
Se	20.158	20.082	20.196	20.15
Rb	0.240003	0.23999671	0.2400066	0.24
Sr	110.227	110.213	110.234	110.22
Cd	0.11005	0.10995	0.1101	0.11
U	11.4432	11.4168	11.4564	11.44
Cu	44.4526	44.4474	44.4552	44.45
Mo	4.8101	4.8099	4.8102	4.81
Pb	22.456	22.444	22.462	22.45
Zr	258.952	258.908	258.974	258.94
Sc	0.8301	0.8299	0.8302	0.83
La	0.196	0.196	0.196	0.20
Ce	20.314	20.306	20.318	20.31
Sm	3.723	3.717	3.726	3.72
Eu	1.2386	1.2374	1.2392	1.24
Gd	1.164	1.162	1.165	1.16
Dy	0.441	0.439	0.442	0.44
Lu	0.3002	0.2998	0.3004	0.30
Pr	9.534	9.526	9.538	9.53
Er	4.304	4.296	4.308	4.30

## Appendix

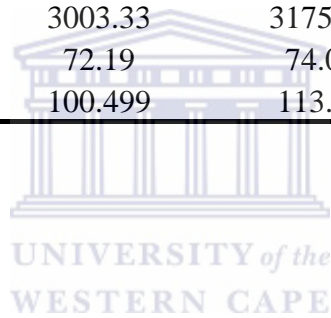
Concentrations of major in Matla fly ash determined by XRF [number of determinations = 3]

Majors (wt. %)	Sample 1	Sample 2	Sample 3	Mean
SiO <sub>2</sub>	54.50	54.61	54.42	54.51
Al <sub>2</sub> O <sub>3</sub>	27.49	27.44	27.49	27.47
Fe <sub>2</sub> O <sub>3</sub>	5.76	5.72	5.79	5.76
CaO	5.40	5.37	5.39	5.39
MgO	1.40	1.38	1.40	1.39
Na <sub>2</sub> O	0.00	0.00	0.00	0.00
K <sub>2</sub> O	0.78	0.78	0.74	0.77
TiO <sub>2</sub>	1.76	1.74	1.74	1.74
P <sub>2</sub> O <sub>5</sub>	0.48	0.47	0.46	0.47
MnO	0.05	0.05	0.05	0.05
SO <sub>3</sub>	0.40	0.39	0.39	0.39
LOI	5.11	5.09	5.13	5.11
Total	103.13	103.03	103.00	103.05

## Appendix

Concentrations of trace elements in Matla fly ash determined by LA ICP-MS  
[number of determinations = 3]

Traces (mg/kg)	Sample 1	Sample 2	Sample 3	Mean
As	11.424	11.738	11.1	11.42067
Ba	504.965	533.277	546.893	528.3783
Cd	3.06574	3.17199	3.19383	3.143853
Co	12.808	13.351	13.764	13.30767
Cr	61.355	63.269	64.856	63.16
Cu	288.0252	133.6684	78.9588	166.8841
Mo	84.886	11.15	5.776	33.93733
Ni	34.839	36.003	36.307	35.71633
Pb	23.56	23.89265	20.5326	22.661
Sr	927.54	969.954	980.574	959.3555
Th	9.992	10.963	10.685	10.54667
Ti	3003.33	3175.975	3223.575	3134.292
V	72.19	74.046	74.378	73.53933
Zn	100.499	113.345	101.096	104.98



## Appendix

Concentrations of REE in Matla fly ash determined by LA ICP-MS [number of determinations = 3]

REE (mg/kg)	Sample 1	Sample 2	Sample 3	Mean
La	117.73	117.68	117.17	117.53
Ce	243.25	246.38	243.59	244.41
Pr	25.55	30.42	24.59	26.85
Nd	68.81	67.97	72.92	69.90
Dy	8.37	7.13	7.49	7.66
Sm	22.75	23.70	23.21	23.22
Er	3.29	3.43	2.51	3.08
Gd	26.41	24.78	26.56	25.92
Ho	0.45	0.41	0.41	0.42
Lu	3.06	2.04	2.24	2.45
Tb	0.45	0.42	0.35	0.41
Tm	2.70	2.35	2.49	2.51
Yb	8.49	8.36	8.63	8.49
Y	77.04	76.04	78.05	77.04
Sc	22.408	24.691	23.231	23.44

WESTERN CAPE

## Appendix

Concentrations of major in AMD/FA residue determined by XRF [number of determinations = 3]

Majors (wt. %)	Sample 1	Sample 2	Sample 3	Mean
SiO <sub>2</sub>	52.53	51.90	52.37	52.27
Al <sub>2</sub> O <sub>3</sub>	25.46	25.93	25.35	25.58
Fe <sub>2</sub> O <sub>3</sub>	6.59	6.30	6.62	6.50
CaO	5.80	5.79	5.75	5.78
MgO	1.40	1.39	1.41	1.40
Na <sub>2</sub> O	0.20	0.21	0.20	0.20
K <sub>2</sub> O	0.64	0.63	0.64	0.63
TiO <sub>2</sub>	1.66	1.65	1.64	1.65
P <sub>2</sub> O <sub>5</sub>	0.46	0.47	0.47	0.47
MnO	0.07	0.08	0.08	0.08
SO <sub>3</sub>	0.04	0.03	0.04	0.03
LOI	7.61	7.98	7.71	7.77



## Appendix

Concentrations of trace elements in AMD/FA residue determined by LA ICP-MS  
[number of determinations = 3]

	Sample1	Sample 2	Sample 3	Mean
As	11.476	12.552	10.128	11.38533
Ba	520.307	529.993	542.979	531.093
Cd	3.8759	3.68756	3.75499	3.772817
Co	60.094	61.066	59.856	60.33867
Cr	70.993	72.908	73.395	72.432
Cu	184.8614	187.9038	85.54572	152.7703
Hg	9.314	12.928	9.342	10.528
Ni	124.001	125.823	122.639	124.1543
Pb	24.08135	21.9266	21.3792	22.46238
Sr	911.1375	921.258	932.7465	921.714
Th	10.657	10.101	10.915	10.55767
U	20.7508	21.1138	20.1458	20.67013
V	65.216	67.427	64.276	65.63967
Zn	188.979	182.356	173.039	181.458

UNIVERSITY of the  
WESTERN CAPE

## Appendix

Concentrations of REE in AMD/FA residue determined by LA ICP-MS [number of determinations = 3]

Elements (mg/kg)	Sample 1	Sample 2	Sample 3	Mean
La	141.1964	141.3984	140.5982	141.06
Ce	269.86	293.96	279.60	281.14
Pr	29.33	27.16	25.85	27.45
Nd	63.22	65.427	62.556	63.73
Dy	5.02	5.25	4.90	5.06
Sm	25.85	27.93	22.86	25.55
Er	3.72	4.13	3.41	3.75
Gd	38.50	40.01	40.04	39.52
Ho	0.90	0.97	0.89	0.92
Lu	3.10	3.03	3.01	3.05
Tb	0.01	0.11	0.20	0.11
Tm	2.21	2.26	2.12	2.19
Yb	13.22	13.37	13.44	13.34
Y	89.32	89.26	89.10	89.23
Sc	27.10	28.01	27.41	27.51



## Appendix

Concentrations of major in synthesised geopolymer determined by XRF [number of determinations = 3]

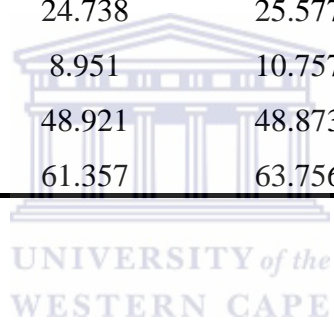
	Sample 1	Sample 2	Sample 3	Mean
SiO <sub>2</sub>	38.62	38.74	38.78	38.71
Al <sub>2</sub> O <sub>3</sub>	19.69	19.79	19.75	19.74
Fe <sub>2</sub> O <sub>3</sub>	4.06	4.06	4.05	4.06
CaO	3.78	3.81	3.78	3.79
MgO	0.94	0.94	0.95	0.94
Na <sub>2</sub> O	20.68	20.77	20.01	20.49
K <sub>2</sub> O	0.49	0.46	0.48	0.48
TiO <sub>2</sub>	1.23	1.24	1.21	1.23
P <sub>2</sub> O <sub>5</sub>	0.33	0.34	0.33	0.33
MnO	0.03	0.04	0.04	0.03
SO <sub>3</sub>	0.03	0.02	0.03	0.02
LOI	10.75	10.47	10.70	10.59
Total	100.62	100.66	100.10	100.46

UNIVERSITY of the  
WESTERN CAPE

## Appendix

Concentrations of trace elements in synthesised geopolymer determined by LA ICP-MS [number of determinations = 3]

Elements (mg/kg)	Sample1	Sample 2	Sample 3	Mean
As	9.314	12.928	9.342	10.53
Cd	4.828076	3.412832	3.504108	3.92
Co	23.128	23.927	24.191	23.75
Cr	52.001	41.219	50.292	47.84
Cu	165.5878	21.87108	56.79504	81.42
Hg	7.353864	8.477416	7.388452	7.74
Ni	48.174	49.121	49.661	48.99
Pb	43.19955	41.87015	40.60875	41.89
Th	24.738	25.577	25.467	25.26
U	8.951	10.757	10.19	9.97
V	48.921	48.873	50.969	49.59
Zn	61.357	63.756	58.776	61.30



## Appendix

Concentrations of REE in synthesised geopolymer determined by LA ICP-MS  
[number of determinations = 3]

Elements (mg/kg)	Sample 1	Sample 2	Sample 3	Mean
La	93.91	91.86	90.93	92.23
Ce	216.59	216.97	216.40	216.65
Pr	15.05	15.85	15.10	15.33
Nd	43.14	44.01	42.11	43.09
Dy	11.09	12.06	11.67	11.61
Sm	19.93	18.98	20.87	19.93
Er	1.75	1.84	1.95	1.85
Gd	23.60	22.95	21.94	22.83
Ho	0.39	0.38	0.96	0.58
Lu	2.60	2.50	3.10	2.74
Tb	0.94	0.92	0.91	0.92
Tm	1.31	1.37	1.39	1.36
Yb	8.50	8.69	8.52	8.57
Y	79.27	79.59	79.40	79.42
Sc	14.81	13.35	15.26	14.47

## Appendix

Composition of the major components that remained in the solid residue after the sequential leaching the non-magnetic fraction of Matla fly ash with NaOH, H<sub>2</sub>SO<sub>4</sub>, HCL and HNO<sub>3</sub> determined by XRF [number of determinations = 2]

Major (wt %)	Non-magnetic fraction		8M NaOH		5M H <sub>2</sub> SO <sub>4</sub>		3M HCl		7M HNO <sub>3</sub>	
Fe <sub>2</sub> O <sub>3</sub>	2.89	2.86	2.88	2.86	1.46	1.37	0.42	1.30	0.32	0.31
MnO	0.05	0.05	0.04	0.04	0.02	0.02	0.02	0.02	0.01	0.01
Cr <sub>2</sub> O <sub>3</sub>	0.03	0.03	0.04	0.03	0.02	0.02	0.04	0.04	0.03	0.03
TiO <sub>2</sub>	1.72	1.71	1.75	1.78	2.04	1.45	1.13	1.55	0.83	0.82
CaO	4.58	4.48	4.82	4.82	4.77	5.55	0.00	0.47	0.00	0.00
K <sub>2</sub> O	0.55	0.54	0.03	0.03	0.00	0.33	0.00	0.38	0.00	0.00
SO <sub>3</sub>	0.32	0.31	0.33	0.34	8.04	7.75	0.14	0.00	0.00	0.00
P <sub>2</sub> O <sub>5</sub>	0.48	0.49	0.17	0.16	0.06	0.09	0.00	0.05	0.00	0.00
SiO <sub>2</sub>	54.27	54.28	37.03	36.99	39.45	46.60	53.02	54.21	45.77	45.80
Al <sub>2</sub> O <sub>3</sub>	26.74	26.76	27.99	27.95	22.61	25.02	27.42	28.76	26.05	26.15
MgO	1.17	1.16	1.16	1.20	0.06	0.18	0.00	0.16	0.00	0.00
Na <sub>2</sub> O	0.34	0.35	9.35	9.32	1.11	0.03	0.00	0.00	0.00	0.00
LOI %	5.90	5.91	13.83	13.83	19.97	10.12	15.42	10.25	24.22	24.23
Total	99.03	98.93	99.43	99.35	99.62	98.51	97.61	97.19	97.22	97.34

## Appendix

Composition of the REE that remained in the solid residue after the sequential leaching the non-magnetic fraction of Matla fly ash with NaOH, H<sub>2</sub>SO<sub>4</sub>, HCl and HNO<sub>3</sub> determined by LA ICP-MS [number of determinations = 2]

REE (mg/kg)	NaOH leaching		H <sub>2</sub> SO <sub>4</sub>		HCl		HNO <sub>3</sub>	
La	90.27	90.27	60.59	60.59	15.41	15.41	1.52	1.52
Ce	234.97	234.97	179.44	179.44	0.00	0	0.00	0
Pr	19.76	19.76	12.08	12.08	3.98	3.98	0.00	0
Nd	38.74	38.74	21.47	21.47	7.98	7.98	1.74	1.74
Dy	10.09	10.09	5.69	5.69	3.99	3.99	4.68	4.68
Sm	31.54	31.54	28.26	28.26	18.51	18.51	15.88	15.88
Er	1.96	1.96	0.80	0.8	2.81	2.81	1.95	1.95
Eu	3.22	3.22	2.44	2.44	0.82	0.82	0.82	0.82
Gd	26.37	26.37	23.06	23.06	14.32	14.32	12.29	12.29
Ho	5.77	5.77	5.66	5.66	3.44	3.44	1.21	1.21
Lu	1.28	1.28	1.16	1.16	0.78	0.78	0.45	0.45
Tb	2.88	2.88	2.17	2.17	0.47	0.47	1.25	1.25
Tm	0.83	0.83	0.69	0.69	1.33	1.33	0.16	0.16
Yb	8.43	8.43	6.16	6.16	2.89	2.89	1.45	1.45
Y	57.65	57.65	27.77	27.77	10.84	10.84	8.25	8.25
Sc	25.54	25.54	10.71	10.71	5.50	5.5	4.37	4.37

## Appendix

Composition REE in the leachate the non-magnetic fraction of Matla fly after the sequential leaching with NaOH, H<sub>2</sub>SO<sub>4</sub>, HCL and HNO<sub>3</sub> determined by LA ICP-MS [number of determinations = 2]

REE (mg/kg)	NaOH		H <sub>2</sub> SO <sub>4</sub>		HCl		HNO <sub>3</sub>	
La	3.01	3.00	16.71	16.36	44.63	44.93	17.38	17.38
Ce	2.08	2.07	67.10	67.55	168.39	167.68	0.00	0.00
Pr	5.93	5.98	4.81	4.41	11.54	11.31	0.00	0.00
Nd	6.12	6.04	6.54	6.27	18.82	13.16	12.98	12.50
Dy	0.27	0.29	0.67	0.83	0.47	0.39	0.12	0.17
Sm	0.01	0.02	0.10	0.13	0.14	0.13	0.06	0.06
Er	0.02	0.01	1.40	1.40	2.86	2.72	0.99	0.90
Eu	0.01	0.04	0.02	0.01	1.10	1.10	0.03	0.03
Gd	0.17	0.22	2.10	2.15	3.93	3.86	2.87	2.49
Ho	0.05	0.06	0.04	0.04	0.98	0.88	0.00	0.00
Lu	0.001	0.00	0.003	0.00	0.004	0.01	0.003	0.01
Tb	0.13	0.10	0.02	0.02	0.81	0.83	0.22	0.20
Yb	0.03	0.01	0.25	0.27	6.68	6.34	0.81	0.08
Y	1.69	1.68	8.35	8.17	17.96	17.59	10.85	10.85
Sc	0.76	0.82	2.72	2.81	5.54	5.91	12.65	12.64

0 = Not detected